ISSN 1007-9327 (print)
ISSN 2219-2840 (online)

World Journal of *Gastroenterology*

World J Gastroenterol 2020 July 14; 26(26): 3712-3850

Published by Baishideng Publishing Group Inc

World Journal of Gastroenterology

Contents

Weekly Volume 26 Number 26 July 14, 2020

Observational Study

ABOUT COVER

Editorial board member of *World Journal of Gastroenterology*, Dr. Niu is an Associate Professor of Department of Pathology, Medical College of Qingdao University, China. His ongoing research interests are precancerous lesions of hepatocellular carcinoma (HCC) and the molecular mechanism of HCC pathogenesis. He is a reviewer and a part-time editor of *Journal of Qingdao University (Medical Edition)*, as well as an editorial board member and a reviewer of several scientific journals. He has published more than 30 peer-reviewed articles as the first author and coordinated/participated in seven research projects, five of which were sponsored by the Shandong Provincial Government. In addition, Dr. Niu is the Project Leader of five research projects in Qingdao University. Currently, Dr. Niu is the Deputy Director of Laboratory of Micromorphology, School of Basic Medicine, Medical College of Qingdao University.

AIMS AND SCOPE

The primary aim of *World Journal of Gastroenterology* (*WJG*, *World J Gastroenterol*) is to provide scholars and readers from various fields of gastroenterology and hepatology with a platform to publish high-quality basic and clinical research articles and communicate their research findings online. *WJG* mainly publishes articles reporting research results and findings obtained in the field of gastroenterology and hepatology and covering a wide range of topics including gastroenterology, hepatology, gastrointestinal endoscopy, gastrointestinal surgery, gastrointestinal oncology, and pediatric gastroenterology.

INDEXING/ABSTRACTING

The *WJG* is now indexed in Current Contents®/Clinical Medicine, Science Citation Index Expanded (also known as SciSearch®), Journal Citation Reports®, Index Medicus, MEDLINE, PubMed, PubMed Central, and Scopus. The 2020 edition of Journal Citation Report® cites the 2019 impact factor (IF) for *WJG* as 3.665; IF without journal self cites: 3.534; 5-year IF: 4.048; Ranking: 35 among 88 journals in gastroenterology and hepatology; and Quartile category: Q2.

NAME OF JOURNAL
World Journal of Gastroenterology

ISSN
ISSN 1007-9327 (print) ISSN 2219-2840 (online)

LAUNCH DATE
October 1, 1995

FREQUENCY
Weekly

EDITORS-IN-CHIEF
Andrzej S Tarnawski, Subrata Ghosh

EDITORIAL BOARD MEMBERS
http://www.wjgnet.com/1007-9327/editorialboard.htm

PUBLICATION DATE
July 14, 2020

INSTRUCTIONS TO AUTHORS
https://www.wjgnet.com/bpg/gerinfo/204

GUIDELINES FOR ETHICS DOCUMENTS
https://www.wjgnet.com/bpg/GerInfo/287

GUIDELINES FOR NON-NATIVE SPEAKERS OF ENGLISH
https://www.wjgnet.com/bpg/gerinfo/240

PUBLICATION ETHICS
https://www.wjgnet.com/bpg/GerInfo/288

PUBLICATION MISCONDUCT
https://www.wjgnet.com/bpg/gerinfo/208

ARTICLE PROCESSING CHARGE
https://www.wjgnet.com/bpg/gerinfo/242

STEPS FOR SUBMITTING MANUSCRIPTS
https://www.wjgnet.com/bpg/GerInfo/239

ONLINE SUBMISSION
https://www.f6publishing.com

E-mail: bpgoffice@wjgnet.com https://www.wjgnet.com

World Journal of Gastroenterology

Submit a Manuscript: https://www.f6publishing.com

World J Gastroenterol 2020 July 14; 26(26): 3712-3719

DOI: 10.3748/wjg.v26.i26.3712

ISSN 1007-9327 (print) ISSN 2219-2840 (online)

OPINION REVIEW

Functional gastrointestinal disorders in inflammatory bowel disease: Time for a paradigm shift?

Dipesh H Vasant, Alexander C Ford

ORCID number: Dipesh H Vasant 0000-0002-2329-0616; Alexander C Ford 0000-0001-6371-4359.

Author contributions: Vasant DH and Ford AC both reviewed the literature; Vasant DH wrote the paper; Ford AC reviewed and helped write the paper, and provided important intellectual input.

Conflict-of-interest statement: The authors declare that they have no conflict of interest.

Manuscript source: Invited manuscript

Received: March 28, 2020
Peer-review started: March 28, 2020
First decision: April 18, 2020

Dipesh H Vasant, Gastroenterology, Manchester University NHS Foundation Trust, Wythenshawe Hospital, Manchester M23 9LT, United Kingdom

Dipesh H Vasant, Division of Diabetes, Endocrinology and Gastroenterology, University of Manchester, Manchester M23 9LT, United Kingdom

Alexander C Ford, Leeds Institute of Medical Research at St. James's, University of Leeds, Leeds LS9 7TF, United Kingdom

Alexander C Ford, Leeds Gastroenterology Institute, Leeds Teaching Hospitals NHS Trust, Leeds LS9 7TF, United Kingdom

Corresponding author: Dipesh H Vasant, MBChB, MRCP, PhD, Senior Lecturer, Gastroenterology, Manchester University NHS Foundation Trust, Wythenshawe Hospital, Southmoor Road, Manchester M23 9LT, United Kingdom. dipesh.vasant@mft.nhs.uk

Abstract

Recent advances in biological therapies have revolutionalised and redefined treatment targets in inflammatory bowel disease (IBD). There is now a stronger emphasis on achieving the more stringent therapeutic goals of mucosal and histological healing, rather than clinical remission alone. Consequently, the treatment of refractory "functional" gastrointestinal symptoms, often attributed as the aftermath of previous inflammation, has recently become more prominent in quiescent disease. With further expected advances in anti-inflammatory treatments on the horizon, the burden of such symptoms in quiescent disease, which have been relatively neglected, is set to become an even bigger problem. In this article, we highlight the current state of research and understanding in this field, including recent developments and clinical practice guidelines on the diagnosis and management of functional gastrointestinal symptoms, such as irritable bowel syndrome and functional anorectal and pelvic floor disorders, in patients with quiescent IBD. These disorders are not only highly prevalent in these patients, they are often misdiagnosed, and are difficult to treat, with very few evidence-based therapies. Moreover, they are associated with substantial impairment in quality-of-life, considerable morbidity, and psychological distress. There is therefore an urgent need for a change in emphasis towards earlier recognition, positive diagnosis, and targeted treatment for patients with ongoing functional gastrointestinal symptoms in the absence of active IBD. This article also highlights the need for further research to develop much needed evidence-based

Revised: April 23, 2020
Accepted: July 1, 2020
Article in press: July 1, 2020
Published online: July 14, 2020

P-Reviewer: Chiba T, Lipták P
S-Editor: Ma YJ
L-Editor: A
E-Editor: Ma YJ

therapies.

Key words: Irritable bowel syndrome; Inflammatory bowel disease; Functional gastrointestinal disorders; Faecal incontinence; Pelvic floor dyssynergia

Core tip: Functional gastrointestinal symptoms, in the absence of inflammation, affect around one-third of inflammatory bowel disease (IBD) patients in remission, causing significant psychological distress and impairment of quality of life. As IBD therapies continue to advance, functional gastrointestinal symptoms, as a consequence of previous inflammation, are set to become a bigger problem. Here, we review the current evidence base, highlight a recently proposed diagnostic algorithm, and discuss empirical treatment guidance for functional gastrointestinal symptoms in quiescent IBD. We also discuss future considerations and areas of unmet need to stimulate further research.

Citation: Vasant DH, Ford AC. Functional gastrointestinal disorders in inflammatory bowel disease: Time for a paradigm shift? *World J Gastroenterol* 2020; 26(26): 3712-3719
URL: https://www.wjgnet.com/1007-9327/full/v26/i26/3712.htm
DOI: https://dx.doi.org/10.3748/wjg.v26.i26.3712

INTRODUCTION

Recent advances in medical therapies for both ulcerative colitis (UC) and Crohn's disease (CD) have improved the frequency and depth of remission in patients with inflammatory bowel disease (IBD)[1]. With the current availability of biological agents targeting multiple disease mechanisms including anti-tumour necrosis factor-α, anti-integrin, and anti-interleukin 12/23 drugs, as well as janus kinase inhibitors, the goals of IBD treatment have changed dramatically in recent years. Moreover, the introduction of several, more cost-effective, biosimilar drugs, have also improved access to some biological agents[2].

As a result of these developments, complete mucosal and histological healing, which appears to lead to improved outcomes for patients[3-5], has become a realistic therapeutic target. Consequently, clinical remission is no longer the recommended standard of care, and a more aggressive, "treat to target approach" , has been advocated[6-8]. This change in emphasis, together with the use of biochemical and endoscopic measures of subclinical inflammation to assess disease activity, has led to increasing awareness of a group of patients with IBD who have refractory gastrointestinal symptoms, in the absence of objective inflammation[9]. Indeed, recent data have shown that there is often a poor correlation between symptoms and mucosal inflammation in IBD[10]. Although the potential for co-existence of "functional" gastrointestinal symptoms in a proportion of patients with quiescent IBD was first described over 30 years ago[11], this group of patients has received minimal attention in the medical literature until relatively recently.

The pathophysiology of functional gastrointestinal disturbances in quiescent IBD is likely to be multifactorial, with numerous experimental studies demonstrating post-inflammatory changes in gut motility[12-17], permeability[18,19], impaired colorectal function (abnormal colonic tone, rectal compliance and impaired anal sphincter function)[14], and visceral hypersensitivity[20-23]. With further progress in controlling inflammation successfully in patients with IBD anticipated, it is likely that there will be an even higher burden of refractory functional symptoms in IBD clinics in the future. However, despite overlap of functional symptoms being common in patients with IBD, there are limited evidence-based treatment options. This article discusses recent developments in this field, to highlight areas of unmet need, and suggest future directions and treatment paradigms.

The importance of early recognition and a positive diagnosis of functional overlap

Functional gastrointestinal disorders (FGIDs), are the most common disorders seen by gastroenterologists[24], affecting around 35% of the general population[25]. Based on their putative pathophysiology, these disorders have recently been re-defined as disorders

of gut-brain interaction, and there is now an increased emphasis on making a positive diagnosis of the majority of these conditions, using symptom-based criteria, in the absence of red flag symptoms[26,27]. In the general population, functional bowel disorders are the most common of these disorders of gut-brain interaction, affecting almost 30% of people[25] and, interestingly, these conditions have a similar, or even higher, prevalence in the IBD clinic[9,11]. Indeed, pooled prevalence data from a 2012 meta-analysis suggested a prevalence of symptoms compatible with irritable bowel syndrome (IBS) of 35% in quiescent IBD, with a higher prevalence in CD compared with UC[28].

The majority of studies included in this meta-analysis pre-dated the availability of faecal calprotectin (FC) as a non-invasive biochemical marker of gut inflammation and therefore reported the frequency of IBS-type symptoms in patients in clinical remission. However, even in subsequent studies that have used markers of biochemical remission, such as FC, mucosal remission, or histological remission the proportion of patients with IBD reporting these symptoms remains in the region of 25% to 30%[29-31]. Importantly, and consistently, these functional bowel symptoms in IBD are associated with significant psychological distress, and impair quality of life to a similar extent to that seen in patients with IBD with confirmed active gastrointestinal inflammation[29,32-37]. Similarly, although even less well studied, functional anorectal disorders[38] including evacuatory disorders[39] and faecal incontinence[40,41], are often reported in patients with quiescent disease[32]. In the absence of active inflammation, escalation of IBD therapy, including potentially inappropriate use of corticosteroids or immunosuppressive drugs is likely to be futile[42], leading to further patient dissatisfaction, costly, and carries the risk of serious adverse effects[43-47]. This underlines the importance of early recognition of functional gastrointestinal symptoms in patients with IBD.

Unlike the diagnosis of FGIDs in a non-IBD population, the diagnosis of overlapping FGIDs in IBD first requires some investigation, in order to exclude active inflammation. As recommended in a recently proposed diagnostic algorithm, a stepwise approach using biochemical tests including FC, followed by endoscopy and biopsies, or cross sectional imaging, should be followed[48]. Although not the focus of the current paper, it is also important to consider and, where appropriate, exclude treatable mimics of FGIDs, such as bile acid diarrhoea, small intestinal bacterial overgrowth, or pancreatic insufficiency, particularly where there are risk factors such as ileal disease or a history of predisposing surgical intervention[49].

Following the exclusion of active inflammation and important potential mimics, careful consideration should be given to the likely mechanism of symptoms, based upon the predominant clinical features, and recognising that there are likely to be several perturbations contributing to the pathophysiology. In addition to the traditional IBD-focused clinical history, particularly in the absence of active inflammation and structural pathology, screening questions for positive diagnostic features of FGIDs and risk factors for pelvic floor dysfunction are important[38]. These include IBS symptoms (abdominal pain, bloating, and altered bowel habit or stool form), obstructive defaecatory symptoms, including incomplete emptying, straining, features of overflow diarrhoea or impaction, and rectal digitation. The latter is an important clinical feature, which appears to be predictive of response to pelvic floor biofeedback[50,51]. Faecal incontinence should also be specifically screened, for as it has been shown to be highly prevalent in patients with IBD[52], but may be underreported due to embarrassment on the part of patients[53]. This approach will help identify those in whom pelvic floor and anorectal physiology investigations are appropriate.

Current strategies for management of functional gastrointestinal disorders in IBD

One of the most important steps in managing overlapping FGIDs in this context is optimising the patient-provider relationship, providing clear, understandable explanations, and a positive diagnosis. This is likely to improve acceptance of the diagnosis, engagement with treatment, and also helps manage expectations, all of which are important in achieving a positive clinical outcome.

As highlighted in a recent expert review[48], there are very few randomised controlled trials or prospective studies on the management of functional gastrointestinal symptoms in IBD. Current practice is therefore largely empirical, and often based upon the central tenets of IBS management using dietary, pharmacological, or psychological approaches (Table 1). One of the interventions with some evidence in clinical trials, as well as in a blinded re-challenge study in quiescent IBD, is a diet low in fermentable oligo-, di-, or mono-saccharides, and polyols (FODMAPs)[54-56]. Further evidence for the low FODMAP diet in patients with quiescent IBD and co-existent functional gastrointestinal symptoms comes from recent

Table 1 Therapies empirically used to treat functional gastrointestinal symptoms in inflammatory bowel disease requiring validation in future clinical trials

Treatment	Gastrointestinal symptom(s) targeted
Low FODMAPs diet	Bloating, visceral pain, diarrhoea
Anti-motility agents (*e.g.*, loperamide, ondansetron)	Exaggerated gastro-colic reflex, faecal urgency, diarrhoea, faecal incontinence
Laxatives and pro-motility agents (*e.g.*, prucalopride, linaclotide)	Slow colonic transit, constipation
Antispasmodics	Visceral pain, bloating
Gut-brain neuromodulators (*e.g.*, antidepressants)	Visceral pain, faecal urgency, diarrhoea
Probiotics	Bloating, altered bowel habit
Pelvic floor biofeedback	Evacuatory dysfunction, faecal urgency, faecal incontinence
Psychological interventions (*e.g.*, hypnotherapy, cognitive behavioural therapy)	Visceral pain, bloating, altered bowel habit, non-colonic symptoms

FODMAPs: Fermentable oligo-, di-, or mono-saccharides, and polyols.

trial data demonstrating a significantly greater improvement in gastrointestinal symptom scores and significantly higher rates of symptom relief after 4 wk of a low FODMAP diet, compared with a sham exclusion diet[57].

Unfortunately, there remains very little evidence for the efficacy of specific pharmacological therapies in this patient group. Current approaches include the use of laxatives, prokinetics, such as prucalopride in those with chronic constipation (often those with distal colonic disease or proctitis), antispasmodics, anti-diarrhoeal drugs, such as loperamide, or central neuromodulators, such as antidepressants[48]. Although the latter class of drugs are one of the mainstays for the treatment of abdominal symptoms in IBS[58], to date there has been only one randomised controlled trial in CD, which did not show any benefit of fluoxetine in preventing relapse of disease activity in patients with quiescent disease[59]. In another retrospective study, using tricyclic antidepressants, the authors demonstrated moderate improvement of residual symptoms despite "optimal" medical therapy, particularly in those with UC[60]. Despite the fact that certain probiotics appear beneficial in the induction and maintenance of UC in particular[61], their efficacy in patients with overlapping FGIDs and quiescent disease has not been evaluated specifically, and should be assessed in future clinical studies.

In patients with anorectal dysfunction, or pelvic floor dyssynergia confirmed on anorectal physiology, targeted pelvic floor physiotherapy and biofeedback therapy appear to be of benefit in several small uncontrolled studies[39,62-64], underlining the importance of screening for these conditions in the IBD clinic. Several psychological interventions have been shown to be of benefit in patients with IBS, including gut-directed hypnotherapy[65] and cognitive behavioural therapy (CBT)[58]. Although these interventions may also benefit some patients with IBD, there have been few studies to date, most of which have not been conducted in patients with co-existent functional gastrointestinal symptoms[66]. Although the long-term benefits are unclear, CBT may have a short-term role in improving depression and quality of life in patients with IBD, and hypnotherapy has been shown to be of benefit in only two small studies[66,67].

CONCLUSION

Co-existent FGIDs are common in IBD, and are often under recognised and difficult to treat. Clinicians specialising in IBD are likely to soon become victims of their own success; as treatments targeting inflammation continue to improve they are likely to see more functional gastrointestinal symptoms, as a consequence of prior inflammation, in their clinics. There is therefore the need for a paradigm shift in the approach to some patients with IBD. Previously, in the absence of active inflammation as a cause for their symptoms, patients were often given reassurance that their disease was quiescent, but little else in the way of explanation as to why they were experiencing these symptoms, or how they should be managed. With improvements in our understanding of FGIDs in quiescent IBD, it is essential that clinicians have a

positive, structured, approach to managing these patients. The recent American Gastroenterological Association clinical practice update and diagnostic algorithm has helped raise awareness of these issues, and provided some much needed recommendations as to how to approach this group of patients[48]. There remains, however, an urgent need for evidence-based therapies, as most of the pharmacological treatment of these symptoms is empirical, and extrapolated from the IBS literature. At present, the key to successful management of FGIDs in IBD is recognition, early diagnosis, clear communication, avoidance of inappropriate escalation of IBD-related medications, and a careful and holistic clinical assessment to select appropriate patients for a low-FODMAP diet, and pelvic floor and physiology investigations. The latter, in the appropriate setting, may lead to targeted interventions such as biofeedback, which can improve symptoms as well as quality of life.

Future research should focus on developing specific evidence-based treatments for quiescent symptoms in IBD, based on the results of well-designed clinical trials. A forthcoming randomised study in the United Kingdom, funded by the National Institute for Health Research, has been designed to study the effectiveness of both dietary and pharmacological interventions in this setting. The study, a multi-arm multi-stage trial of a low FODMAP diet, amitriptyline, ondansetron, or loperamide, will include almost 500 patients with UC with ongoing diarrhoea, despite a FC < 250 mcg/g[68]. It is anticipated that this trial will provide much needed evidence as to how best to manage this group of patients. In addition to identifying effective medical therapies, there is also a need to develop a better evidence-base for psychological and behavioural therapies, as well as pelvic floor interventions, with larger clinical trials in patients with quiescent IBD. An improved understanding of the mechanism of pelvic floor dysfunction in quiescent disease as a prelude to potential neuromodulatory therapies is also required.

REFERENCES

1 **Kim DH**, Cheon JH. Pathogenesis of Inflammatory Bowel Disease and Recent Advances in Biologic Therapies. *Immune Netw* 2017; **17**: 25-40 [PMID: 28261018 DOI: 10.4110/in.2017.17.1.25]

2 **Gulacsi L**, Pentek M, Rencz F, Brodszky V, Baji P, Vegh Z, Gecse KB, Danese S, Peyrin-Biroulet L, Lakatos PL. Biosimilars for the Management of Inflammatory Bowel Diseases: Economic Considerations. *Curr Med Chem* 2019; **26**: 259-269 [PMID: 28393687 DOI: 10.2174/0929867324666170406112304]

3 **Bryant RV**, Burger DC, Delo J, Walsh AJ, Thomas S, von Herbay A, Buchel OC, White L, Brain O, Keshav S, Warren BF, Travis SP. Beyond endoscopic mucosal healing in UC: histological remission better predicts corticosteroid use and hospitalisation over 6 years of follow-up. *Gut* 2016; **65**: 408-414 [PMID: 25986946 DOI: 10.1136/gutjnl-2015-309598]

4 **Barreiro-de Acosta M**, Vallejo N, de la Iglesia D, Uribarri L, Bastón I, Ferreiro-Iglesias R, Lorenzo A, Domínguez-Muñoz JE. Evaluation of the Risk of Relapse in Ulcerative Colitis According to the Degree of Mucosal Healing (Mayo 0 vs 1): A Longitudinal Cohort Study. *J Crohns Colitis* 2016; **10**: 13-19 [PMID: 26351390 DOI: 10.1093/ecco-jcc/jjv158]

5 **Colombel JF**, Panaccione R, Bossuyt P, Lukas M, Baert F, Vaňásek T, Danalioglu A, Novacek G, Armuzzi A, Hébuterne X, Travis S, Danese S, Reinisch W, Sandborn WJ, Rutgeerts P, Hommes D, Schreiber S, Neimark E, Huang B, Zhou Q, Mendez P, Petersson J, Wallace K, Robinson AM, Thakkar RB, D'Haens G. Effect of tight control management on Crohn's disease (CALM): a multicentre, randomised, controlled phase 3 trial. *Lancet* 2018; **390**: 2779-2789 [PMID: 29096949 DOI: 10.1016/S0140-6736(17)32641-7]

6 **Colombel JF**, D'haens G, Lee WJ, Petersson J, Panaccione R. Outcomes and Strategies to Support a Treat-to-target Approach in Inflammatory Bowel Disease: A Systematic Review. *J Crohns Colitis* 2020; **14**: 254-266 [PMID: 31403666 DOI: 10.1093/ecco-jcc/jjz131]

7 **Peyrin-Biroulet L**, Sandborn W, Sands BE, Reinisch W, Bemelman W, Bryant RV, D'Haens G, Dotan I, Dubinsky M, Feagan B, Fiorino G, Gearry R, Krishnareddy S, Lakatos PL, Loftus EV Jr, Marteau P, Munkholm P, Murdoch TB, Ordás I, Panaccione R, Riddell RH, Ruel J, Rubin DT, Samaan M, Siegel CA, Silverberg MS, Stoker J, Schreiber S, Travis S, Van Assche G, Danese S, Panes J, Bouguen G, O'Donnell S, Pariente B, Winer S, Hanauer S, Colombel JF. Selecting Therapeutic Targets in Inflammatory Bowel Disease (STRIDE): Determining Therapeutic Goals for Treat-to-Target. *Am J Gastroenterol* 2015; **110**: 1324-1338 [PMID: 26303131 DOI: 10.1038/ajg.2015.233]

8 **Ungaro R**, Colombel JF, Lissoos T, Peyrin-Biroulet L. A Treat-to-Target Update in Ulcerative Colitis: A Systematic Review. *Am J Gastroenterol* 2019; **114**: 874-883 [PMID: 30908297 DOI: 10.14309/ajg.0000000000000183]

9 **Meng J**, Agrawal A, Whorwell PJ. Refractory inflammatory bowel disease-could it be an irritable bowel? *Nat Rev Gastroenterol Hepatol* 2013; **10**: 58-61 [PMID: 22965430 DOI: 10.1038/nrgastro.2012.173]

10 **Gracie DJ**, Williams CJ, Sood R, Mumtaz S, Bholah MH, Hamlin PJ, Ford AC. Poor Correlation Between Clinical Disease Activity and Mucosal Inflammation, and the Role of Psychological Comorbidity, in Inflammatory Bowel Disease. *Am J Gastroenterol* 2016; **111**: 541-551 [PMID: 27002800 DOI: 10.1038/ajg.2016.59]

11 **Isgar B**, Harman M, Kaye MD, Whorwell PJ. Symptoms of irritable bowel syndrome in ulcerative colitis in remission. *Gut* 1983; **24**: 190-192 [PMID: 6826101 DOI: 10.1136/gut.24.3.190]

12 **Mawe GM**. Colitis-induced neuroplasticity disrupts motility in the inflamed and post-inflamed colon. *J Clin*

Invest 2015; **125**: 949-955 [PMID: 25729851 DOI: 10.1172/JCI76306]
13 **Villanacci V**, Bassotti G, Nascimbeni R, Antonelli E, Cadei M, Fisogni S, Salerni B, Geboes K. Enteric nervous system abnormalities in inflammatory bowel diseases. *Neurogastroenterol Motil* 2008; **20**: 1009-1016 [PMID: 18492026 DOI: 10.1111/j.1365-2982.2008.01146.x]
14 **Bassotti G**, Antonelli E, Villanacci V, Salemme M, Coppola M, Annese V. Gastrointestinal motility disorders in inflammatory bowel diseases. *World J Gastroenterol* 2014; **20**: 37-44 [PMID: 24415856 DOI: 10.3748/wjg.v20.i1.37]
15 **Annese V**, Bassotti G, Napolitano G, Usai P, Andriulli A, Vantrappen G. Gastrointestinal motility disorders in patients with inactive Crohn's disease. *Scand J Gastroenterol* 1997; **32**: 1107-1117 [PMID: 9399391 DOI: 10.3109/00365529709002989]
16 **Peuhkuri K**, Vapaatalo H, Korpela R. Even low-grade inflammation impacts on small intestinal function. *World J Gastroenterol* 2010; **16**: 1057-1062 [PMID: 20205274 DOI: 10.3748/wjg.v16.i9.1057]
17 **Bassotti G**, Villanacci V, Nascimbeni R, Cadei M, Fisogni S, Antonelli E, Corazzi N, Salerni B. Enteric neuroglial apoptosis in inflammatory bowel diseases. *J Crohns Colitis* 2009; **3**: 264-270 [PMID: 21172285 DOI: 10.1016/j.crohns.2009.06.004]
18 **Vivinus-Nébot M**, Frin-Mathy G, Bzioueche H, Dainese R, Bernard G, Anty R, Filippi J, Saint-Paul MC, Tulic MK, Verhasselt V, Hébuterne X, Piche T. Functional bowel symptoms in quiescent inflammatory bowel diseases: role of epithelial barrier disruption and low-grade inflammation. *Gut* 2014; **63**: 744-752 [PMID: 23878165 DOI: 10.1136/gutjnl-2012-304066]
19 **Chang J**, Leong RW, Wasinger VC, Ip M, Yang M, Phan TG. Impaired Intestinal Permeability Contributes to Ongoing Bowel Symptoms in Patients With Inflammatory Bowel Disease and Mucosal Healing. *Gastroenterology* 2017; **153**: 723-731.e1 [PMID: 28601482 DOI: 10.1053/j.gastro.2017.05.056]
20 **Mueller MH**, Kreis ME, Gross ML, Becker HD, Zittel TT, Jehle EC. Anorectal functional disorders in the absence of anorectal inflammation in patients with Crohn's disease. *Br J Surg* 2002; **89**: 1027-1031 [PMID: 12153630 DOI: 10.1046/j.1365-2168.2002.02173.x]
21 **Andersson P**, Olaison G, Hallböök O, Boeryd B, Sjödahl R. Increased anal resting pressure and rectal sensitivity in Crohn's disease. *Dis Colon Rectum* 2003; **46**: 1685-1689 [PMID: 14668596 DOI: 10.1007/BF02660776]
22 **Brochard C**, Siproudhis L, Ropert A, Mallak A, Bretagne JF, Bouguen G. Anorectal dysfunction in patients with ulcerative colitis: impaired adaptation or enhanced perception? *Neurogastroenterol Motil* 2015; **27**: 1032-1037 [PMID: 25940976 DOI: 10.1111/nmo.12580]
23 **Loening-Baucke V**, Metcalf AM, Shirazi S. Anorectal manometry in active and quiescent ulcerative colitis. *Am J Gastroenterol* 1989; **84**: 892-897 [PMID: 2756980]
24 **Shivaji UN**, Ford AC. Prevalence of functional gastrointestinal disorders among consecutive new patient referrals to a gastroenterology clinic. *Frontline Gastroenterol* 2014; **5**: 266-271 [PMID: 28839783 DOI: 10.1136/flgastro-2013-100426]
25 **Aziz I**, Palsson OS, Törnblom H, Sperber AD, Whitehead WE, Simrén M. The Prevalence and Impact of Overlapping Rome IV-Diagnosed Functional Gastrointestinal Disorders on Somatization, Quality of Life, and Healthcare Utilization: A Cross-Sectional General Population Study in Three Countries. *Am J Gastroenterol* 2018; **113**: 86-96 [PMID: 29134969 DOI: 10.1038/ajg.2017.421]
26 **Drossman DA**. Functional Gastrointestinal Disorders: History, Pathophysiology, Clinical Features and Rome IV. *Gastroenterology* 2016 [PMID: 27144617 DOI: 10.1053/j.gastro.2016.02.032]
27 **Moayyedi P**, Mearin F, Azpiroz F, Andresen V, Barbara G, Corsetti M, Emmanuel A, Hungin APS, Layer P, Stanghellini V, Whorwell P, Zerbib F, Tack J. Irritable bowel syndrome diagnosis and management: A simplified algorithm for clinical practice. *United European Gastroenterol J* 2017; **5**: 773-788 [PMID: 29026591 DOI: 10.1177/2050640617731968]
28 **Halpin SJ**, Ford AC. Prevalence of symptoms meeting criteria for irritable bowel syndrome in inflammatory bowel disease: systematic review and meta-analysis. *Am J Gastroenterol* 2012; **107**: 1474-1482 [PMID: 22929759 DOI: 10.1038/ajg.2012.260]
29 **Gracie DJ**, Williams CJ, Sood R, Mumtaz S, Bholah MH, Hamlin PJ, Ford AC. Negative Effects on Psychological Health and Quality of Life of Genuine Irritable Bowel Syndrome-type Symptoms in Patients With Inflammatory Bowel Disease. *Clin Gastroenterol Hepatol* 2017; **15**: 376-384.e5 [PMID: 27189912 DOI: 10.1016/j.cgh.2016.05.012]
30 **Henriksen M**, Høivik ML, Jelsness-Jørgensen LP, Moum B; IBSEN Study Group. Irritable Bowel-like Symptoms in Ulcerative Colitis are as Common in Patients in Deep Remission as in Inflammation: Results From a Population-based Study [the IBSEN Study]. *J Crohns Colitis* 2018; **12**: 389-393 [PMID: 29186372 DOI: 10.1093/ecco-jcc/jjx152]
31 **Fukuba N**, Ishihara S, Tada Y, Oshima N, Moriyama I, Yuki T, Kawashima K, Kushiyama Y, Fujishiro H, Kinoshita Y. Prevalence of irritable bowel syndrome-like symptoms in ulcerative colitis patients with clinical and endoscopic evidence of remission: prospective multicenter study. *Scand J Gastroenterol* 2014; **49**: 674-680 [PMID: 24646420 DOI: 10.3109/00365521.2014.898084]
32 **Nigam GB**, Limdi JK, Hamdy S, Vasant DH. OWE-11 The prevalence and burden of Rome IV functional colorectal disorders in ulcerative colitis. *Gut* 2019; **68**: A203-A204 [DOI: 10.1136/gutjnl-2019-BSGAbstracts.390]
33 **Gracie DJ**, Ford AC. Ongoing Symptoms in Ulcerative Colitis Patients in Remission: Irritable Bowel Syndrome or Gastrointestinal Symptoms in the Absence of Inflammation? *Inflamm Bowel Dis* 2017; **23**: E4-E5 [PMID: 27930410 DOI: 10.1097/MIB.0000000000000984]
34 **Berrill JW**, Green JT, Hood K, Campbell AK. Symptoms of irritable bowel syndrome in patients with inflammatory bowel disease: examining the role of sub-clinical inflammation and the impact on clinical assessment of disease activity. *Aliment Pharmacol Ther* 2013; **38**: 44-51 [PMID: 23668698 DOI: 10.1111/apt.12335]
35 **Barratt SM**, Leeds JS, Robinson K, Shah PJ, Lobo AJ, McAlindon ME, Sanders DS. Reflux and irritable bowel syndrome are negative predictors of quality of life in coeliac disease and inflammatory bowel disease. *Eur J Gastroenterol Hepatol* 2011; **23**: 159-165 [PMID: 21178777 DOI: 10.1097/MEG.0b013e328342a547]

36 **Perera LP**, Radigan M, Guilday C, Banerjee I, Eastwood D, Babygirija R, Massey BT. Presence of Irritable Bowel Syndrome Symptoms in Quiescent Inflammatory Bowel Disease Is Associated with High Rate of Anxiety and Depression. *Dig Dis Sci* 2019; **64**: 1923-1928 [PMID: 30725303 DOI: 10.1007/s10620-019-05488-8]

37 **Mavroudis G**, Simren M, Jonefjäll B, Öhman L, Strid H. Symptoms compatible with functional bowel disorders are common in patients with quiescent ulcerative colitis and influence the quality of life but not the course of the disease. *Therap Adv Gastroenterol* 2019; **12**: 1756284819827689 [PMID: 30815033 DOI: 10.1177/1756284819827689]

38 **Nigam GB**, Limdi JK, Vasant DH. Current perspectives on the diagnosis and management of functional anorectal disorders in patients with inflammatory bowel disease. *Therap Adv Gastroenterol* 2018; **11**: 1756284818816956 [PMID: 30574193 DOI: 10.1177/1756284818816956]

39 **Rezaie A**, Gu P, Kaplan GG, Pimentel M, Al-Darmaki AK. Dyssynergic Defecation in Inflammatory Bowel Disease: A Systematic Review and Meta-Analysis. *Inflamm Bowel Dis* 2018; **24**: 1065-1073 [PMID: 29529194 DOI: 10.1093/ibd/izx095]

40 **Nigam GB**, Limdi JK, Hamdy S, Vasant DH. PTH-108 The hidden burden of faecal incontinence in active and quiescent ulcerative colitis: an underestimated problem? *Gut* 2019; **68**: A87-A87 [DOI: 10.1136/gutjnl-2019-BSGAbstracts.167]

41 **Gu P**, Kuenzig ME, Kaplan GG, Pimentel M, Rezaie A. Fecal Incontinence in Inflammatory Bowel Disease: A Systematic Review and Meta-Analysis. *Inflamm Bowel Dis* 2018; **24**: 1280-1290 [PMID: 29617820 DOI: 10.1093/ibd/izx109]

42 **Limdi JK**, Vasant DH. Anorectal Dysfunction in Distal Ulcerative Colitis: Challenges and Opportunities for Topical Therapy. *J Crohns Colitis* 2016; **10**: 503 [PMID: 26619892 DOI: 10.1093/ecco-jcc/jjv217]

43 **Williams CJ**, Peyrin-Biroulet L, Ford AC. Systematic review with meta-analysis: malignancies with anti-tumour necrosis factor-α therapy in inflammatory bowel disease. *Aliment Pharmacol Ther* 2014; **39**: 447-458 [PMID: 24444171 DOI: 10.1111/apt.12624]

44 **Ford AC**, Peyrin-Biroulet L. Opportunistic infections with anti-tumor necrosis factor-α therapy in inflammatory bowel disease: meta-analysis of randomized controlled trials. *Am J Gastroenterol* 2013; **108**: 1268-1276 [PMID: 23649185 DOI: 10.1038/ajg.2013.138]

45 **Lichtenstein GR**, Rutgeerts P, Sandborn WJ, Sands BE, Diamond RH, Blank M, Montello J, Tang L, Cornillie F, Colombel JF. A pooled analysis of infections, malignancy, and mortality in infliximab- and immunomodulator-treated adult patients with inflammatory bowel disease. *Am J Gastroenterol* 2012; **107**: 1051-1063 [PMID: 22613901 DOI: 10.1038/ajg.2012.89]

46 **Beaugerie L**, Brousse N, Bouvier AM, Colombel JF, Lémann M, Cosnes J, Hébuterne X, Cortot A, Bouhnik Y, Gendre JP, Simon T, Maynadié M, Hermine O, Faivre J, Carrat F; CESAME Study Group. Lymphoproliferative disorders in patients receiving thiopurines for inflammatory bowel disease: a prospective observational cohort study. *Lancet* 2009; **374**: 1617-1625 [PMID: 19837455 DOI: 10.1016/S0140-6736(09)61302-7]

47 **Lewis JD**, Scott FI, Brensinger CM, Roy JA, Osterman MT, Mamtani R, Bewtra M, Chen L, Yun H, Xie F, Curtis JR. Increased Mortality Rates With Prolonged Corticosteroid Therapy When Compared With Antitumor Necrosis Factor-α-Directed Therapy for Inflammatory Bowel Disease. *Am J Gastroenterol* 2018; **113**: 405-417 [PMID: 29336432 DOI: 10.1038/ajg.2017.479]

48 **Colombel JF**, Shin A, Gibson PR. AGA Clinical Practice Update on Functional Gastrointestinal Symptoms in Patients With Inflammatory Bowel Disease: Expert Review. *Clin Gastroenterol Hepatol* 2019; **17**: 380-390.e1 [PMID: 30099108 DOI: 10.1016/j.cgh.2018.08.001]

49 **Barros LL**, Farias AQ, Rezaie A. Gastrointestinal motility and absorptive disorders in patients with inflammatory bowel diseases: Prevalence, diagnosis and treatment. *World J Gastroenterol* 2019; **25**: 4414-4426 [PMID: 31496621 DOI: 10.3748/wjg.v25.i31.4414]

50 **Patcharatrakul T**, Valestin J, Schmeltz A, Schulze K, Rao SSC. Factors Associated With Response to Biofeedback Therapy for Dyssynergic Defecation. *Clin Gastroenterol Hepatol* 2018; **16**: 715-721 [PMID: 29111136 DOI: 10.1016/j.cgh.2017.10.027]

51 **Vasant DH**, Solanki K, Radhakrishnan NV. Rectal Digital Maneuvers May Predict Outcomes and Help Customize Treatment Intensity of Biofeedback in Chronic Constipation and Dyssynergic Defecation. *Dis Colon Rectum* 2017; **60**: e2 [PMID: 27926570 DOI: 10.1097/DCR.0000000000000725]

52 **Norton C**, Dibley LB, Bassett P. Faecal incontinence in inflammatory bowel disease: associations and effect on quality of life. *J Crohns Colitis* 2013; **7**: e302-e311 [PMID: 23228710 DOI: 10.1016/j.crohns.2012.11.004]

53 **Bartlett L**, Nowak M, Ho YH. Reasons for non-disclosure of faecal incontinence: a comparison between two survey methods. *Tech Coloproctol* 2007; **11**: 251-257 [PMID: 17676265 DOI: 10.1007/s10151-007-0360-z]

54 **Halmos EP**, Christophersen CT, Bird AR, Shepherd SJ, Muir JG, Gibson PR. Consistent Prebiotic Effect on Gut Microbiota With Altered FODMAP Intake in Patients with Crohn's Disease: A Randomised, Controlled Cross-Over Trial of Well-Defined Diets. *Clin Transl Gastroenterol* 2016; **7**: e164 [PMID: 27077959 DOI: 10.1038/ctg.2016.22]

55 **Gibson PR**. Use of the low-FODMAP diet in inflammatory bowel disease. *J Gastroenterol Hepatol* 2017; **32** Suppl 1: 40-42 [PMID: 28244679 DOI: 10.1111/jgh.13695]

56 **Cox SR**, Prince AC, Myers CE, Irving PM, Lindsay JO, Lomer MC, Whelan K. Fermentable Carbohydrates [FODMAPs] Exacerbate Functional Gastrointestinal Symptoms in Patients With Inflammatory Bowel Disease: A Randomised, Double-blind, Placebo-controlled, Cross-over, Re-challenge Trial. *J Crohns Colitis* 2017; **11**: 1420-1429 [PMID: 28525543 DOI: 10.1093/ecco-jcc/jjx073]

57 **Cox SR**, Lindsay JO, Fromentin S, Stagg AJ, McCarthy NE, Galleron N, Ibraim SB, Roume H, Levenez F, Pons N, Maziers N, Lomer MC, Ehrlich SD, Irving PM, Whelan K. Effects of Low FODMAP Diet on Symptoms, Fecal Microbiome, and Markers of Inflammation in Patients With Quiescent Inflammatory Bowel Disease in a Randomized Trial. *Gastroenterology* 2020; **158**: 176-188.e7 [PMID: 31586453 DOI: 10.1053/j.gastro.2019.09.024]

58 **Ford AC**, Lacy BE, Harris LA, Quigley EMM, Moayyedi P. Effect of Antidepressants and Psychological Therapies in Irritable Bowel Syndrome: An Updated Systematic Review and Meta-Analysis. *Am J Gastroenterol* 2019; **114**: 21-39 [PMID: 30177784 DOI: 10.1038/s41395-018-0222-5]

59 **Mikocka-Walus A**, Hughes PA, Bampton P, Gordon A, Campaniello MA, Mavrangelos C, Stewart BJ, Esterman A, Andrews JM. Fluoxetine for Maintenance of Remission and to Improve Quality of Life in Patients with Crohn's Disease: a Pilot Randomized Placebo-Controlled Trial. *J Crohns Colitis* 2017; **11**: 509-514 [PMID: 27664274 DOI: 10.1093/ecco-jcc/jjw165]

60 **Iskandar HN**, Cassell B, Kanuri N, Gyawali CP, Gutierrez A, Dassopoulos T, Ciorba MA, Sayuk GS. Tricyclic antidepressants for management of residual symptoms in inflammatory bowel disease. *J Clin Gastroenterol* 2014; **48**: 423-429 [PMID: 24406434 DOI: 10.1097/MCG.0000000000000049]

61 **Derwa Y**, Gracie DJ, Hamlin PJ, Ford AC. Systematic review with meta-analysis: the efficacy of probiotics in inflammatory bowel disease. *Aliment Pharmacol Ther* 2017; **46**: 389-400 [PMID: 28653751 DOI: 10.1111/apt.14203]

62 **Vasant DH**, Limdi JK, Solanki K, Radhakrishnan NV. Biofeedback therapy improves continence in quiescent inflammatory bowel disease patients with anorectal dysfunction. *J Gastroenterol Pancreatol Liver Disord* 2016; **3**: 1-4 [DOI: 10.15226/2374-815X/3/2/00153]

63 **Perera LP**, Ananthakrishnan AN, Guilday C, Remshak K, Zadvornova Y, Naik AS, Stein DJ, Massey BT. Dyssynergic defecation: a treatable cause of persistent symptoms when inflammatory bowel disease is in remission. *Dig Dis Sci* 2013; **58**: 3600-3605 [PMID: 24026401 DOI: 10.1007/s10620-013-2850-3]

64 **Khera AJ**, Chase JW, Salzberg M, Thompson AJV, Kamm MA. Gut-Directed Pelvic Floor Behavioral Treatment for Fecal Incontinence and Constipation in Patients with Inflammatory Bowel Disease. *Inflamm Bowel Dis* 2019; **25**: 620-626 [PMID: 30452638 DOI: 10.1093/ibd/izy344]

65 **Vasant DH**, Whorwell PJ. Gut-focused hypnotherapy for Functional Gastrointestinal Disorders: Evidence-base, practical aspects, and the Manchester Protocol. *Neurogastroenterol Motil* 2019; **31**: e13573 [PMID: 30815936 DOI: 10.1111/nmo.13573]

66 **Gracie DJ**, Irvine AJ, Sood R, Mikocka-Walus A, Hamlin PJ, Ford AC. Effect of psychological therapy on disease activity, psychological comorbidity, and quality of life in inflammatory bowel disease: a systematic review and meta-analysis. *Lancet Gastroenterol Hepatol* 2017; **2**: 189-199 [PMID: 28404134 DOI: 10.1016/S2468-1253(16)30206-0]

67 **Ballou S**, Keefer L. Psychological Interventions for Irritable Bowel Syndrome and Inflammatory Bowel Diseases. *Clin Transl Gastroenterol* 2017; **8**: e214 [PMID: 28102860 DOI: 10.1038/ctg.2016.69]

68 **Gracie DJ**, Ford AC. Functional Gastrointestinal Symptoms in Inflammatory Bowel Disease: Rising to the Challenge. *Clin Gastroenterol Hepatol* 2019; **17**: 572-573 [PMID: 30678841 DOI: 10.1016/j.cgh.2018.08.039]

World Journal of Gastroenterology

Submit a Manuscript: https://www.f6publishing.com

World J Gastroenterol 2020 July 14; 26(26): 3720-3736

DOI: 10.3748/wjg.v26.i26.3720

ISSN 1007-9327 (print) ISSN 2219-2840 (online)

REVIEW

Intratumoral heterogeneity of hepatocellular carcinoma: From single-cell to population-based studies

Qi Zhang, Yu Lou, Xue-Li Bai, Ting-Bo Liang

ORCID number: Qi Zhang 0000-0002-6096-0690; Yu Lou 0000-0003-2862-423X; Xue-Li Bai 0000-0001-6005-8384; Ting-Bo Liang 0000-0003-0143-3353.

Author contributions: Zhang Q and Lou Y contributed equally to this work; Zhang Q conceived the idea; Lou Y performed the search; Liang T and Bai X interpreted the clinical significance; Zhang Q and Lou Y drafted the manuscript; all authors made critical revision and approved the final version of the manuscript.

Supported by the National Natural Science Foundation of China, No. 81871320 and No. 81830089; and Zhejiang Provincial Natural Science Foundation of China, No. LR20H160002.

Conflict-of-interest statement: The authors declare no conflict of interests for this article.

Qi Zhang, Yu Lou, Xue-Li Bai, Ting-Bo Liang, Department of Hepatobiliary and Pancreatic Surgery, the First Affiliated Hospital, Zhejiang University School of Medicine, Hangzhou 310003, Zhejiang Province, China

Qi Zhang, Yu Lou, Xue-Li Bai, Ting-Bo Liang, Key Laboratory of Pancreatic Disease of Zhejiang Province, Hangzhou 310003, Zhejiang Province, China

Qi Zhang, Xue-Li Bai, Ting-Bo Liang, Innovation Center for the Study of Pancreatic Diseases of Zhejiang Province, Hangzhou 310003, Zhejiang Province, China

Qi Zhang, Xue-Li Bai, Ting-Bo Liang, Zhejiang Clinical Research Center of Hepatobiliary and Pancreatic Diseases, Hangzhou 310003, Zhejiang Province, China

Corresponding author: Ting-Bo Liang, MD, PhD, FACS, Chief Doctor, Professor, Research Fellow, Surgeon, Department of Hepatobiliary and Pancreatic Surgery, the First Affiliated Hospital, Zhejiang University School of Medicine, No. 79, Qingchun Road, Hangzhou 310003, Zhejiang Province, China. liangtingbo@zju.edu.cn

Abstract

Hepatocellular carcinoma (HCC) is characterized by high heterogeneity in both intratumoral and interpatient manners. While interpatient heterogeneity is related to personalized therapy, intratumoral heterogeneity (ITH) largely influences the efficacy of therapies in individuals. ITH contributes to tumor growth, metastasis, recurrence, and drug resistance and consequently limits the prognosis of patients with HCC. There is an urgent need to understand the causes, characteristics, and consequences of tumor heterogeneity in HCC for the purposes of guiding clinical practice and improving survival. Here, we summarize the studies and technologies that describe ITH in HCC to gain insight into the origin and evolutionary process of heterogeneity. In parallel, evidence is collected to delineate the dynamic relationship between ITH and the tumor ecosystem. We suggest that conducting comprehensive studies of ITH using single-cell approaches in temporal and spatial dimensions, combined with population-based clinical trials, will help to clarify the clinical implications of ITH, develop novel intervention strategies, and improve patient prognosis.

Key words: Hepatocellular carcinoma; Tumor heterogeneity; Tumor microenvironment; Single-cell analysis; Local immunity

Manuscript source: Invited manuscript

Received: February 27, 2020
Peer-review started: February 27, 2020
First decision: May 21, 2020
Revised: June 2, 2020
Accepted: June 18, 2020
Article in press: June 18, 2020
Published online: July 14, 2020

P-Reviewer: Capasso R, Grassi G, Link A
S-Editor: Gong ZM
L-Editor: Wang TQ
E-Editor: Zhang YL

Core tip: We summarize the comprehensive studies of intratumoral heterogeneity (ITH) of hepatocellular carcinoma, including the different aspects, various dimensions, and clinical significance of ITH.

Citation: Zhang Q, Lou Y, Bai XL, Liang TB. Intratumoral heterogeneity of hepatocellular carcinoma: From single-cell to population-based studies. *World J Gastroenterol* 2020; 26(26): 3720-3736
URL: https://www.wjgnet.com/1007-9327/full/v26/i26/3720.htm
DOI: https://dx.doi.org/10.3748/wjg.v26.i26.3720

INTRODUCTION

Liver cancer is one of the leading causes of cancer-related death worldwide, and approximately 90% of these deaths are attributed to hepatocellular carcinoma (HCC)[1]. With several non-surgical therapeutic options (*e.g.*, transcatheter arterial chemoembolization, radiofrequency ablation, stereotactic body radiation therapy, and systemic therapy) available, liver resection and liver transplantation remain the mainstay of cure of HCC. However, less than 30% of patients are eligible for surgery, and a considerable number of them will succumb to rapid tumor recurrence or metastasis[2]. Furthermore, HCC can demonstrate primary or secondary resistance to other interventions, including chemotherapy, targeted therapy, and immune checkpoint blockade. However, despite many cellular and molecular mechanisms revealed, the refractory nature of HCC to treatments is still far from understood. Thus, new perspectives are warranted to decode this intractable issue.

Intratumoral heterogeneity (ITH), first described in the 1830s by German physiologists Johannes Muller and Rudolf Virchow[3], is now found to be ubiquitous in all types of tumors and accounts for nearly all aspects of tumor progression[4]. Currently, people have realized that heterogeneity is not only a distinct morphological profile but also implicates genetics, epigenetics, transcriptomics, proteomics, posttranslational modification (PTM)-omics, metabolomics, and diverse tumor microenvironments (TMEs). Systematic ITH causes a wide functional divergence, providing a platform to perform natural selection in the particular TME and promoting the malignant phenotypes of HCC. Fortunately, the rapid development of next-generation sequencing (NGS) and mass spectrometry techniques has made elegant analysis of ITH a reality in recent years. Several advances in HCC have been achieved to help us gain in-depth insight into the evolutionary mode of tumorigenesis and development, the regulatory pattern of the signaling network, and the interaction between tumor cells and their microenvironment. Nevertheless, how to integrate the discoveries and implications of ITH into clinical practice is rarely discussed.

In this review, we provide an overview of ITH in HCC from microscopic to macrocosmic approaches to explore the clinical implications of ITH. Based on a systemic search of relevant studies from single-cell to population-based designs, we summarize the common patterns of ITH in HCC and propose a practicable way to guide the clinical management of this deadly disease.

CELLULAR HETEROGENEITY AND CANCER STEM CELL

Although heterogeneity at the DNA, RNA, and protein levels is frequently investigated, cells are actually the fundamental element of tumor heterogeneity that may impact tumor progression. Heterogeneity itself does not have a malignancy-specific implication since all healthy, transformed, and cancerous cells sustain heterogeneity to some extent. In the liver, hepatocytes are organized from the central vein to the portal node, showing a strong regularity of the gene expression profile[5,6]. For example, the expression of Alb, Glul, Cyp2e1, Cyp2f2, and other hepatocyte markers in different locations can be extremely different. Such cellular heterogeneity presented by highly regulated gene expression and exquisite cell spatial distribution is required for the normal physiological function of the liver. When hepatic cells

transform, precancerous nodules show heterogeneous genetic and epigenetic patterns as well[7].

For cancer, pathologists first used microscopes to identify the diversity among tumor cells. Due to the limitation of observational technologies, it took more than a century to describe and explore cellular heterogeneity through pathological sections and immunohistological staining[3], by which ITH cannot be quantitatively evaluated. Thanks to the emergence of single-cell analytic approaches (*e.g.*, single-cell sequencing, single-cell immunoblotting, single-cell mass spectrometry, and single-cell multiomic techniques) in the last decade, it is currently possible to establish a clear panorama of cellular heterogeneity[8-11]. Hou *et al*[12] developed scTrio-seq, a single-cell triple omics sequencing technique, and provided the first piece of evidence regarding the genetic heterogeneity in HCC at a single-cell level. Two subpopulations with distinct biological functions were observed by unsupervised hierarchical clustering based on genomic copy-number variations (CNVs), although the cells in the same subset were also not identical[12]. Since then, cellular heterogeneity has been repeatedly corroborated in HCC from genomic, transcriptomic, and other dimensions[13-16] (Table 1).

Since cellular heterogeneity varies greatly among individuals[14,17], it is of great value to find the key subpopulations of cancer cells with greater influence on ITH for further studies. Hence, a subset of cancer cells with stemness features, also known as cancer stem cells (CSCs), has attracted much attention[18-21]. Hepatic CSCs can be identified by various cell surface markers. For instance, EpCAM[22-25], CD90 (THY-1)[25-27], CD24[14,25,28], CD133 (Prominin-1)[14,25,28,29], CD13 (ANPEP)[29,30], CD44[16,25,30], CD47[30,31], and others have been identified in HCC in independent studies using single-cell sequencing[14,16]. More importantly, single-cell transcriptomic profiling indicated that stemness gene expression seemed to be consistent with the cancer diversity score based on principal component analysis and was significantly related to clinical outcomes[16,17,26]. These findings coincide with the "cancer stem cell model", which is favored to explain the origin of ITH recently[32,33] (Figure 1). Predominantly, this model demonstrates that only CSCs possess the capability of self-renewal, differentiation, and maintenance of tumor growth[34-36]. Similar to the normal tissue hierarchy, the hierarchical organization in cancer results from the punctuated proliferation of CSCs and consequently shapes.

Accumulating evidence likely reflects the fact that, even as an extremely tiny subset, CSCs can still be divided into various subpopulations with distinct cell membrane markers, molecular makeups, and functional phenotypes. Recently, elegant studies by Zheng *et al*[14] and Ma *et al*[17] provided direct evidence of hepatic CSC heterogeneity and its clinical implications at a single-cell resolution. CSC sorting by CD24, CD133, and/or EpCAM proliferated divergently in both normoxia and hypoxia and showed a distinctive spatial distribution within HCC[14]. These findings demonstrated the uneven distribution of functionally diverse CSC subpopulations across different regions, and the current understanding of CSCs may only reflect the features of specific subgroups[26,37-42]. Moreover, CSC identity is not immutable[14,19]. Under the influence of genetic stochastic mutation and recombination, epigenetic modifications, and field effects in the TME, reversible transformation can occur between CSCs and non-CSCs, which establishes new hierarchical CSC clones to enrich ITH tremendously[32,43,44]. This ability to reconstruct heterogeneity cautions against therapies targeting CSC-related membrane epitopes and increases the difficulty of ITH management.

However, CSCs are not an undruggable subset. Growing evidence suggests that plenty of environmental factors, such as hypoxia, inflammation, and DNA damage, play crucial roles in CSC phenotypes mediating in various cancers[45,46]. As an illustration, hypoxia has received considerable attention in recent years[47]. Similar to oxygen gradients between arteries and veins in liver lobules, abnormal vascular perfusion in HCC induces differential activities of the HIF signaling pathway in an oxygen-dependent manner, and consequently stemness. Hence, it is a promising therapeutic strategy for treatment of CSCs and heterogeneity.

Further identification of CSC subpopulations and the regulatory mechanism of the CSC transformation process is of paramount importance to clarify the roles of CSCs in the development and management of ITH. An advanced understanding of CSCs may create new opportunities for overcoming cellular heterogeneity.

CLONAL HETEROGENEITY REVEALS TUMOR EVOLUTION

In addition to single-cell technologies, multiregional sampling, the method to sample biopsies from multiple regions within a single tumor, is the most common

Table 1 Summary of studies on intra-tumoral heterogeneity in hepatocellular carcinoma using single-cell sequencing

No	Time	Patients (*n*)	Cells (*n*)	Methods	Findings	Ref.
Studies on cancer cells						
1	2016	1	25 T	scTrio-seq (DNA, DNA methylation, mRNA)	Two subpopulations were identified based on CNVs, DNA methylome, or mRNA.	[12]
2	2018	3	96 T + 15 N	Single-cell WGS	HCCs can be of monoclonal or polyclonal origins. Models of late dissemination and early seeding have a role in HCC progression.	[13]
3	2018	1	118 CSCs + 860 unsorted	mRNA (SMART-Seq +10X)	Different CSC subsets contain distinct molecular signatures, and are associated with prognosis.	[14]
4	2019	1	139 T	mRNA (C1)	EPCAM+ cells had upregulated expression of multiple oncogenes and sustain CSC property.	[16]
Studies on immune cells						
5	2017	6	5063 T cells	mRNA (Smart-Seq2)	11 T cell subsets were identified based on their molecular and functional properties.	[80]
6	2019	16	CD45+ cells (66187 + 11134)	mRNA (10X + Smart-Seq2)	40 immune cell subsets were identified, as well as their distinct roles in HCC development.	[81]
Studies on both						
7	2019	set1: 13 set2: 6	set1: 5115set2: 4831	mRNA (10X)	Tumors with higher transcriptomic diversity were associated with higher VEGFA expression, lower cytolytic activities, and worse outcome.	[17]
8	2019	4	19625	mRNA (microwell-seq)	The extent of heterogeneity in both tumor and immune cells varies among patients.	[72]
9	2020	2	38553	mRNA (10X)	Cancer cells from the same tumor were divided into different Hoshida subclasses and had different effects on immune infiltration.	[64]

T: Tumor cells; N: Normal cells; HCC: Hepatocellular carcinoma; WGS: Whole-genome sequencing; CSCs: Cancer stem cells; CNVs: Copy-number variations.

investigational strategy to determine the extent of ITH[48-50]. This strategy is based on the "clonal evolution model", which was first proposed by Nowell[51] in 1976, and became the most accepted hypothesis to depict the process of ITH in addition to the "CSC model". In this theory, carcinogenesis is considered to be a stochastic process. Numerous random genetic alterations created by genomic instability and continuous stimulation of carcinogens results in the emergence of subclones. The subclones with a survival advantage in a spatiotemporally specific microenvironment will establish dominance, while the non-adaptive subclones will be eliminated. Upon the selective pressure of the TME, the complex architecture of ITH is preserved and dynamically reorganized[52,53] (Figure 2).

Using a multiregional sampling strategy, spatially neighboring clones that are supposed to be genetically more similar can be pooled and compared with bulk samples from other regions. In early studies, ITH in morphology and genomics was poorly described[54-56]. Subsequently, bulk whole-genome sequencing (WGS)[57-59], whole-exome sequencing (WES)[59-62], targeted sequencing[63], single-cell sequencing[13,64], and DNA methylation profiling[61,65] were introduced into heterogeneity studies to quantify genetic alterations and provide a more comprehensive blueprint of hepatic ITH. Public, shared, and private genetic changes were defined to construct an evolutionary tree of tumor subclones[66]. As expected, the variable extent of ITH and the branch evolutionary model are well recapitulated[13,57-59], and subclonal populations that are spatially closer tend to be genetically more similar in both planar and solid models[59,65], which suggests the existence of a common ancestral clone and a continuous clonal expansion pattern with the accumulation of mutations. In the meantime, the time when potential driver mutations formed can be estimated. Similar to the mutation profile of HCC, the most common alterations, such as key driver mutations (*e.g.*, *TP53*, *CTNNB1*, and *TERT*) and CNVs (*e.g.*, amplification in 1q and deletions in 4q and 16q), are mostly identified in the trunks[57-59,61,63], revealing that they may represent an early event in HCC progression. However, an uneven distribution of driver mutations in *TP53* and *CTNNB1* across different regions was also observed in a minority of patients[58,62,63,65,67,68]. These findings indicated that this heterogeneous disease can be either monoclonal or polyclonal in origin. Additional mutations in

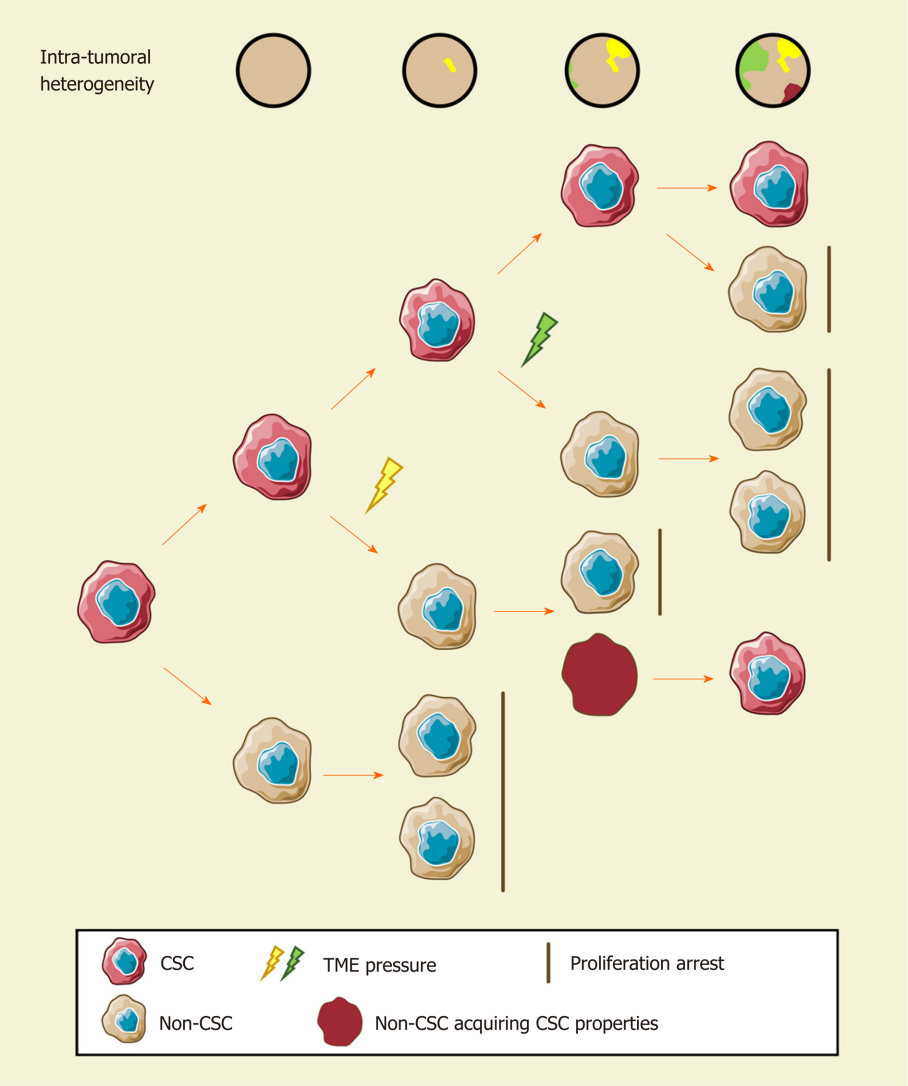

Figure 1 The cancer stem cell model and intratumoral heterogeneity. The cancer stem cell (CSC) model assumes that only CSCs possess robust self-renewal characteristics and the ability to differentiate. Different stimuli of CSCs induce distinct functional phenotypes to adapt to certain environmental stresses. Non-CSCs can spontaneously convert to a stem-like state and establish a new hierarchical CSC clone under certain circumstances. Consequently, the extent of ITH in hepatocellular carcinoma increase gradually. CSC: Cancer stem cell.

AXIN1, *RB1*, *KIT1*, *FAT4*, and other HCC-related genes involved in clonal evolution could dramatically change marker expression (*e.g.*, CK7, β-catenin, and GS) and functional phenotypes[60-62,65,67,68]. It is the functional diversity that promotes tumor development and, more importantly, worsens clinical outcome[60]. Unlike genetic alterations, ITH of genomic methylation appears prior to tumor initiation and forms clonal expansions in nonmalignant tissues[7,63]. In regard to cancer, regulation of DNA-methylated heterogeneity acts in a conservative manner, largely driven by the tumor itself and significantly related to tumor progression[13].

Clearly, clonal diversity changes dynamically with tumor evolution, but ITH is not necessarily correlated with positive changes. In support of this hypothesis, the findings of several studies have suggested that various genetic alterations in the single key gene across regions (*e.g.*, loss-of-function and stop-gain mutations in *CTNNB1*) embody convergent evolution of HCC under microenvironmental stress[57,65]. However, one size does not fit all in regard to clonal evolution. A study collected 286 samples on a plane of a single HCC and drew the most elaborate clonal map of HCC to date[69]. More than 100 million mutations are defined, illustrating astonishing genetic heterogeneity and a non-Darwinian mode during HCC development. In addition, another work using single-cell genome sequencing likely demonstrated the punctuated pattern[13], which is characterized by the early occurrence of numerous genetic alterations[70].

Another focus in ITH studies based on multiregional sampling is tracking the origins of different nodules to clarify the significance of ITH in invasion and

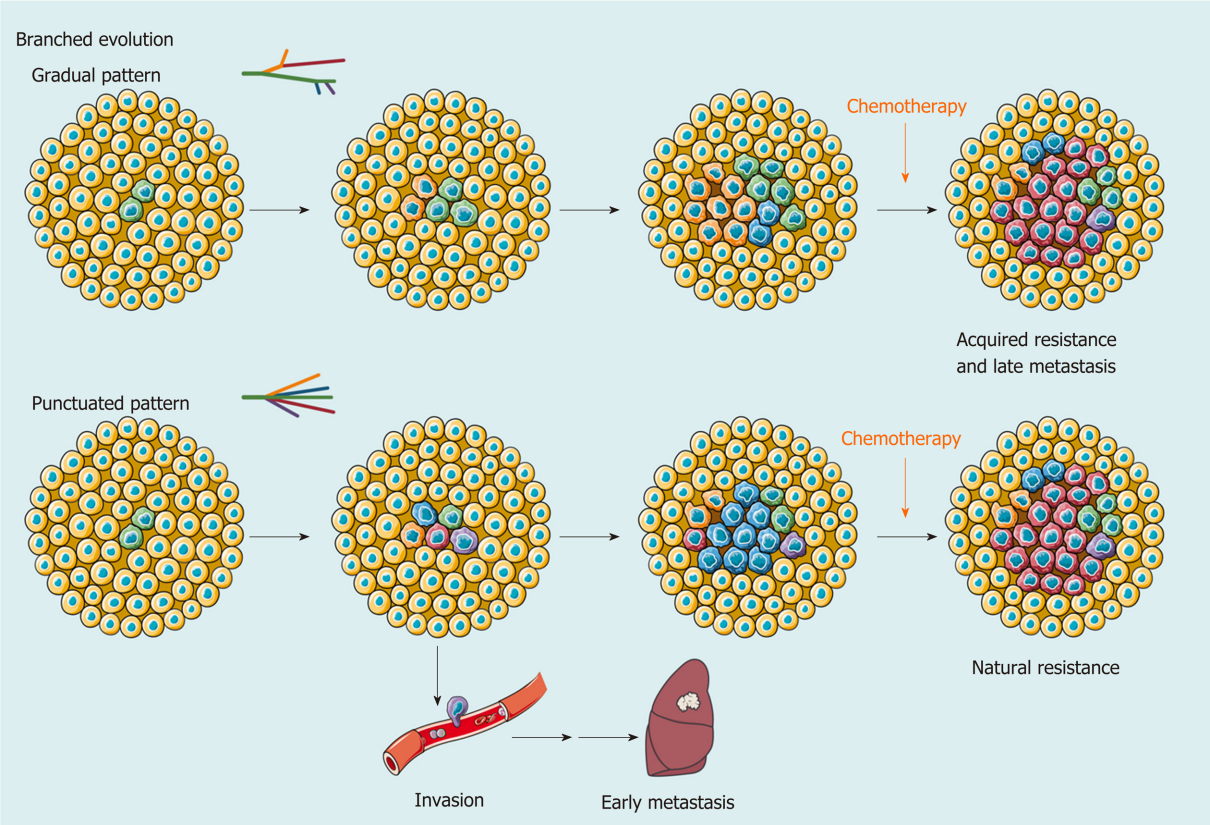

Figure 2 Branched evolution shapes intratumoral heterogeneity. As a result of branched evolution, the genetic heterogeneous subclones may be generated through two different trajectories. In the gradual pattern, subclones increase gradually due to genomic instability or microenvironment changes, such as acquired drug resistance and metastasis caused by systemic therapy. However, the punctuated pattern, also known as big bang mode, supposes that all subclones already exist in early development of hepatocellular carcinoma (HCC). Different subclones obtain a survival advantage in spatiotemporally specific microenvironment and change the extent of intratumoral heterogeneity at a clonal level. This model provides an explanation for early metastasis and natural resistance of HCC in clinic.

metastasis. Comparing the primary lesions with intrahepatic metastases, tumor thrombi, and satellite nodules found that migration is likely to occur either at the early or late stage of HCC development, while satellite nodules appear at the late stage[57,59,65]. Multicentral lesions, regarded as a unique subtype of HCC, share few common driver mutations, which implies a parallel evolutionary pattern[57,62,63]. These findings provide a theoretical basis for accurate differentiation between intrahepatic metastases and multicentric lesions in clinical practice[58,63].

Generally, a multiregional sampling strategy improves the ability to explore the symbiotic relationship between clonal heterogeneity and tumor evolution and enriches the value of ITH investigations in precision medicine. However, it can be impractical to obtain multiregional samples from an advanced tumor in clinical practice due to the high risk of bleeding after biopsy. A clinically friendly approach for ITH investigation is urgently needed.

FUNCTIONAL HETEROGENEITY ORCHESTRATES THE TUMOR ECOSYSTEM

Although studies of genetic and epigenetic heterogeneity reflect the life history of tumors, functional diversity is the factor affecting clinical outcome directly. The concept of "functional heterogeneity" was proposed in 2018 to integrate information on genomics, nongenomics, stemness, and TME heterogeneity[71]. Here, we adopt this concept to summarize the functional and microenvironmental characteristics of ITH and discuss its significance in tumor progression and treatment.

Transcriptomic[58,62,72] and proteomic profilings[72,73] take the lead in describing functional heterogeneity. Unsurprisingly, ITH at the RNA and protein levels is apparent. However, the gene expression profile does not seem to strictly follow the law of genetic alterations[58,62,72,73] and has poor relevance to tumor geometry[73]. Due to the distinct gene expression profiles across regions, neither the origin of metastatic

clones[58] nor the potential targets for clinical intervention[72,73] can be distinguished; however, the pivotal role of TME in functional heterogeneity is still reflected[62,72,73].

Owing to the breakthrough of immunotherapy, local immunity in HCC has attracted growing attention. Multiplex immunohistological staining was first used to decipher tumor infiltrating immune cells (TICs) in solid tumors[74]. Apparently, ITH of the microenvironment is neatly illustrated by the density, distribution, and composition of TICs and is likely correlated with tumor differentiation[74], which reveals the coordination of the tumoral functional phenotype and immune infiltration. To deeply explore the interaction between TICs and ITH, various algorithms have been developed to quantify the composition of immune infiltration using sequencing data[75-78] and expand the effectiveness of immune function assessment enormously[62,79]. Coincidentally, the latest two studies integrated DNA-seq, RNA-seq, T-cell receptor (TCR)-seq, neoantigen analysis, and other methods to uncover the role of functional heterogeneity in immune evasion[64,79]. Cancer cells across different regions present different immunogenicity and escape immune surveillance in distinct ways, such as a decrease in immune cell infiltration, loss of heterozygosity of human leukocyte antigen, low TCR clonality, and immunoediting[64]. This finding suggested that the coevolution of tumor and local immunity is quite ubiquitous in HCC and could partially explain the low response rate of immune checkpoint blockade monotherapy in HCC.

Similar to previous studies on clonal evolution[58,63], ITH in intrahepatic metastases and multicentral lesions was compared at an immunological resolution to evaluate the potential effect of immunotherapy[79]. Uneven composition of immune cell infiltration was observed, such as abundant TAM infiltration in intrahepatic metastases and rich CD8+ T-cell infiltration with a higher level of inhibitory immune checkpoint expression in multicentral lesions, which suggested that patients with multicentric HCC could be more likely to benefit from immune checkpoint blockade[79].

In addition, single-cell sequencing is also applied to TME research for a better understanding of immunological heterogeneity. Systematic works completed by Zemin Zhang's group provided a dynamic atlas of the immune landscape of HCC[80,81]. When integrating tumoral single-cell transcriptome data, the HCC cells of different Hoshida subclasses in a single tumor induced regional variance in the antitumoral immune response[64]. More importantly, the extent of ITH was responsible for hypoxia adaptation, VEGF expression, and drug resistance[17], which may be considered in the choice of transarterial (chemo)embolization, sorafenib, lenvatinib, or other antivascular therapies.

Our group also made some efforts to provide a comprehensive landscape of ITH of HCC in multiple dimensions[72]. The research integrating genomic, transcriptomic, proteomic, metabolomic, and immunomic (mass cytometry) data together demonstrated a heterogeneous interactive network of HCC cells, metabolites, and TICs and proposed a novel clinically friendly immunophenotypic classification to improve the clinical management of patients with HCC. We found that tumor cell heterogeneity and microenvironmental heterogeneity, which included diverse TICs, were closely related to each other and showed coevolution. Thus, the evaluation of the functional heterogeneity of HCC requires comprehensive investigation and currently lacks accurate and practical biomarkers.

ITH FROM THE PERSPECTIVE OF POPULATION

The significance of heterogeneity has been demonstrated in accumulating studies, but large-scale population-based studies are still needed to verify the effectiveness of ITH investigation in clinical practice (Table 2). A well-known prospective cohort study on non–small cell lung cancer (NSCLC) included 100 patients with NSCLC and validated the feasibility of predicting clinical outcome and recurrence with ITH[82]. ITH may also play a prognostic role in HCC since genome instability is a common feature of cancer[59]. A clinical trial aiming to investigate the clinical trajectories of HCC during its progression (NCT03267641) is critical to understand the dynamic change and clinical relevance of ITH. However, it is still ongoing with limited information to disclose. Current limited evidence reveals that heterogeneity evaluation of recurrent and primary tumors may serve as a predictor of clinical outcome[65,83].

To clarify the clinical implication of heterogeneity, researchers have developed different methods to quantify ITH with single bulk sequencing data from public databases to predict survival and recurrence. With single-region bulk DNA data, the heterogeneity score (or diversity score) calculated by mutant allele tumor

Table 2 Summary of studies on intra-tumoral heterogeneity in hepatocellular carcinoma using multiregional sampling

No	Time	Patients (*n*)	Samples(*n*)	Methods	Findings	Ref.
Studies on cancer cells						
1	2001	11	29 T + 11 N	IHC and *TP53*/*CTNNB1* sequencing	Heterogeneity existed in small HCC, accompanied by increased proliferative activity.	[68]
2	2015	23	120 T	IHC and *TP53*/*CTNNB1* sequencing	Intratumor heterogeneity may contribute to treatment failure and drug resistance in many cases of HCC.	[67]
3	2015	1	286 T	WES/Genotyping	20 unique cell clones were defined by WES. The size distribution of the clones revealed a non-Darwinian evolution model.	[69]
4	2016	1	8 HCC + 3 ICC +N	WES	IM showed similarity to a primary nodule and indicated that it could be an early event in HCC.	[60]
5	2016	10	43 T + 10 N	WGS/WES	Ubiquitous mutations ranged from 8% to over90%. Satellite nodules occurred late in HCC.	[57]
6	2017	11	52 T + 6 N + 11 B	WES + DNA methylation	29% of putative driver mutations were present in the branches. DNA methylation heterogeneity was largely driven by the cancer self.	[61]
7	2017	9	51 T + 9 N	WGS/WES	Tumor physically closer tend to be genetically more similar. HCC arose from ancestral clones and genetic lineages diverged as tumor grew.	[59]
8	2017	23	49 T	WGS + RNA-seq	Genetic diagnosis is good for an effective choice of therapeutic strategy and IM/MC determination.	[58]
9	2017	59	31 N + 120 T	TDS	Trunk events in early stages (*TERT*, *TP53*, and *CTNNB1* mutations) were ubiquitous across different regions.	[63]
10	2017	5	32 T + 5 N + cfDNA	WES + TDS	Single region TDS identified 70% of the total mutations, while the cfDNA covered 47.2% of total.	[116]
11	2017	10	55 T	WES	53.8% of oncogenic alterations varied among subclones. Targetable alterations were identified in subregions from 4 HCCs.	[121]
12	2018	5	15 T + 5 N	Proteomics	Diagnostic outcome may drastically differ if different sectors of tumor are analyzed.	[73]
13	2019	6	34 T + 5 N	WES + RNA-seq	Largest tumor contained higher proportion of ancestral clones. RNA expression pattern was associated with E-S grade	[62]
14	2019	5	36	WES + RNA-seq + proteomics + metabolomics + CyTOF	Comprehensive intratumoral heterogeneity exists in all dimensions, and the novel immunoclassification of HCC facilitates prognostic prediction and may guide therapy.	[72]
15	2019	113	356 (T + N)	WGS/WES/TDS + DNA methylation	Intratumoral heterogeneity revealed interactions between genomic and epigenomic features associated with tumor progression and recurrence.	[65]
16	2019	88	230 T	IHC and *TERT* promoter sequencing	Distinct marker expression in different nodules. Limited heterogeneity in metastasis compared to primary sites.	[83]
Studies on immune cells						
17	2018	124	919 T	Multiplex IHC	Varying degrees of intratumor heterogeneity of the immune microenvironment were observed.	[74]
18	2019	13	79 T	IHC + RNA-seq	A single-region sample might be reliable for the evaluation of tumor immune infiltration in approximately 60%-70% of patients with HCC.	[117]
19	2019	15	47 T	WES + RNA-seq + TCR-seq + IHC + immunopeptidomes	Genetic structure, neoepitope landscape, T cell profile and immunoediting status collectively shape tumor evolution.	[79]

20	2020	14	51 T + 20 N	WES + RNA-seq + TCR-seq + SNP array + immunofluorescence	The different components of the tumor ecosystem interact during cancer evolution, and promote heterogeneity in liver cancer.	[64]

HCC: Hepatocellular carcinoma; T: Tumor tissues; N: Adjacent tissues; WGS: Whole-genome sequencing; WES: Whole-exome sequencing; cfDNA: Cell-free DNA; IHC: Immunohistochemistry; TDS: Targeted deep sequencing.

heterogeneity and clonality approaches significantly distinguished patients with a higher ITH signature and poor prognosis[61,64]. It is remarkable that tumor clonality outperforms mutational burden in predicting prognosis in the TCGA-HCC dataset[64], indicating the crucial value of ITH in HCC. Other methods, such as the mITH method for DNA methylation data[61], the ITH gene signature algorithm for RNA data[17,64], and ITH-related models of CSCs and immune evasion[79], shared similar results that a higher level of ITH was associated with limited survival, which is also observed in many other types of cancer[84-86]. Moreover, evidence across a wide range of cancer types illustrated that ITH fostered resistance to various treatments[82,87-89]. In HCC, sorafenib-targeted genetic alterations have been constantly validated as a subclonal change[62], which may explain the low objective response rate to sorafenib in the clinic[90,91]. Furthermore, the response to immunotherapy is also manifested by functional heterogeneity. Tumors with higher ITH tend to secrete more VEGFA to promote immune suppression and limit the clinical efficacy of immune checkpoint blockade[17]. Similar phenomena were also observed in other tumors[92,93].

In the future, more stable, practicable, and cost-effective techniques should be introduced to large-scale population-based studies to broaden the scope of the clinical application of ITH. Based on current evidence, liquid biopsy and advanced imaging are promising candidates. Cell-free DNA (cfDNA) is one of the most notable minimally invasive examinations for cancer in recent years and is used to evaluate tumor load, tumor mutational burden, tumor recurrence, drug resistance, and patient survival[94-96]. There is evidence suggesting that cfDNA can reflect ITH in HCC and offer some insight into tumor evolution[97,98]. Using cfDNA sequencing, practical genetic heterogeneity assessment in advanced HCCs with a large size or multiple lesions becomes possible, although many technical and clinical confirmations are warranted before it can be accepted by physicians. cfDNA sequencing also creates the possibility for dynamic observation of ITH either combined with or even substitute sequential sampling[99]. By tracking the dynamic evolution of HCC, people can make more precise interventions for this heterogeneous disease and may obtain better efficacy. In addition, multiparametric magnetic resonance imaging and computed tomography have been proven effective in reflecting the histologic and genomic features and prognosis of HCC[100,101]. In lung cancer, breast cancer, and esophageal cancer, a quantitative ultrasound system and positron emission tomography/computed tomography are qualified to image ITH[102-105]. Combined with liver-specific contrast agents and radiomic analysis, the digital imaging system may bring ITH assessment into a new chapter[106-109]. However, more clinical trials are expected to test the potential role of these approaches in benefit-gain for HCC patients.

MANAGEMENT OF ITH IN HCC

Here, we take ITH into clinical consideration and discuss how to embody the implication of functional heterogeneity in HCC patient management. At present, only a few traditional indicators are well accepted and widely adopted by clinicians in HCC. Tumoral macrovascular invasion (MVI)[110-112] and TNM classification[113,114] systems, for example, are normally used for disease staging, therapy decision making, and prediction of prognosis. However, the demand for precision medicine forces clinicians to biopsy every tumor to obtain a molecular makeup for individual treatment. How to ensure the representativeness of biopsy samples under the influence of heterogeneity becomes an important and unavoidable problem. A study on renal cancer proposed that at least three distinct regions of the tumor should be sampled to detect five key genes with an accuracy of 90% or above[115]. In HCC, researchers carried out WES, targeted deep sequencing, and cfDNA sequencing to identify the effects of sampling strategy on genetic mutation detection[116]. The results indicated that targeted sequencing with single sampling could identify approximately 70% of the total genetic mutations, while cfDNA had merely 47.2%. Another study revealed that 60%-70% of patients with HCC obtained reliable results of immune cell infiltration with a single sample[117]. Altogether, these results suggested that ITH did affect clinical examination at least to some extent, and multiregional sampling might diminish or even eliminate such influence. Considering the clinical risk of the sampling strategy, it is of great value to find more effective methods for patients with advanced HCC.

ITH may also act as a novel measure combined with other indicators to establish a more comprehensive and effective system for several clinical scenarios. ITH quantification can be performed *in silico*, as mentioned above, using high-throughput sequencing data and radiomic data. Acquiring data from cfDNA or imaging can not only provide information on the entire tumor but is also minimally invasive or noninvasive, cost-effective, and temporally dynamic, which brings infinite possibility to clinical practice. In support of this strategy, the findings of a previous study highlighted the positive correlation between VEGFA expression and ITH, which leads to severe immune exhaustion in more heterogeneous tumors. This phenomenon indeed provides an explanation for the combination therapy of immune checkpoint inhibitors and anti-VEGF molecules to improve therapeutic efficacies (NCT03434379, NCT03006926, NCT03418922)[118,119], suggesting that ITH investigation may screen out HCC patients who benefit from anti-VEGF therapies.

The use of ITH to propose effective intervention strategies is the most attractive aim of the translational study of ITH. Pan-cancer therapeutic strategies targeting CSCs or clonal evolution have been fully described in previous reviews. The former includes inhibition of CSC signaling pathways, CSC ablation using antibody-drug conjugates, and epigenetic therapies[43]; the latter includes clonal events targeting therapies, attenuating or exploiting genome instability, and exploiting evolutionary constraints[66]. To provide a model for drug sensitivity assessment of heterogeneous clones, Nuciforo *et al*[120] established an organoid system with needle biopsies and succeeded in preserving the heterogeneity of original cancers. In another study, WES of 55 samples from multiple regions of ten HCC patients indicated that 40% of patients could be targeted by existing pharmacologic agents, and the significance was verified *in vitro*[121]. Our group developed a potential intervention strategy based on a novel immunoclassification according to ITH; however, the validity still needs to be verified in clinical trials[72]. Indeed, there are few treatments against ITH currently published regarding HCC and other types of liver cancer, and more research is thus urgently needed to explore the feasible strategy for HCC treatment and determine the roles of ITH in HCC management (Figure 3).

CONCLUSION

In general, ITH is a crucial issue that cannot be avoided in HCC progression and management. Although great efforts have been made to obtain a more comprehensive understanding of heterogeneity, the field of hepatic ITH-targeting therapeutics is still in its infancy. Heterogeneous clones and relevant ecosystems are spatially distinct and dynamically change over time, which poses many challenges to clinicians and scientists. Therefore, particular attention should be paid to several aspects in further research. First, integrative analysis of multi-omics data should be performed to establish a systematic relationship between genetic evolution and immune evasion in

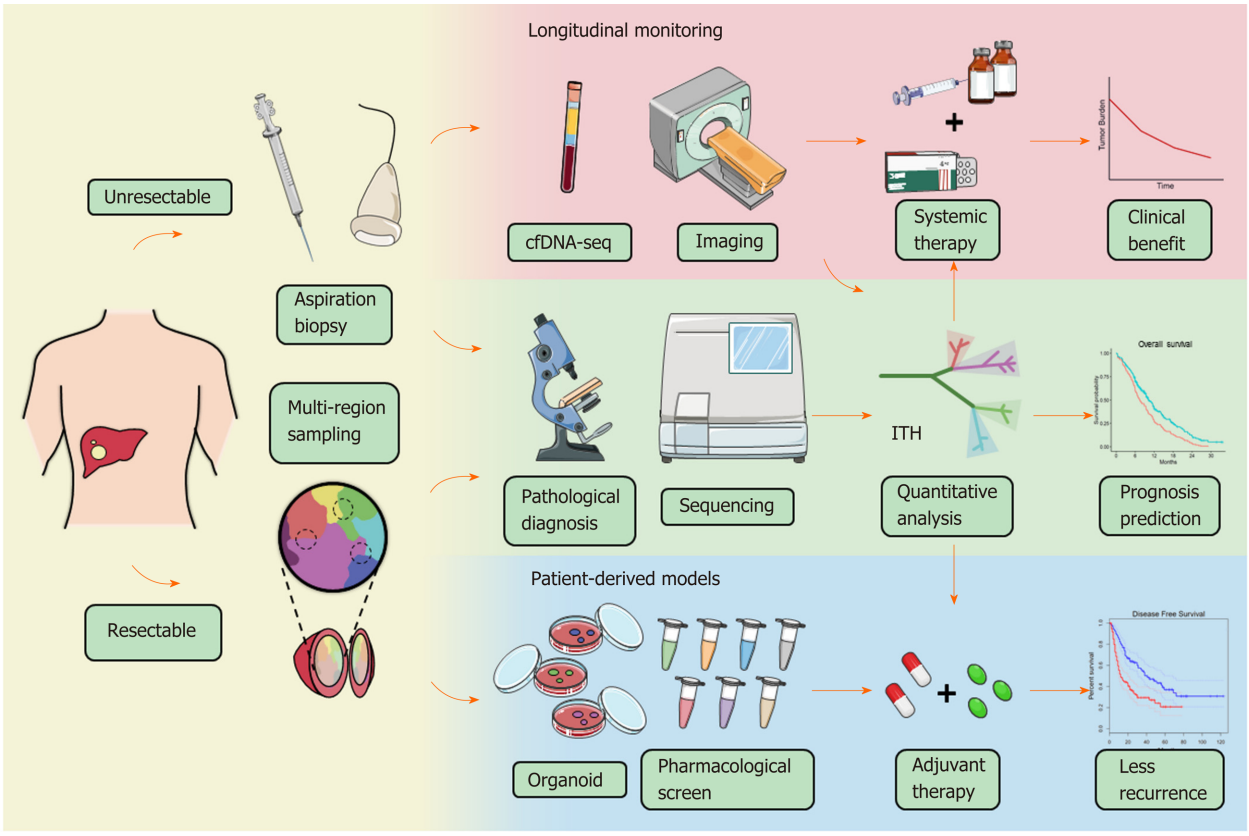

Figure 3 Schematic diagram of potential workflow for intratumoral heterogeneity clinical applications. For the patients with resectable liver cancer, intratumoral heterogeneity (ITH) can be evaluated by multiregional sampling of surgical samples, and in the meantime, patient-derived organoid model can be constructed for drug screening. The individualized treatment strategy will be determined according to the heterogeneity evaluation and the pharmacological results. For the patients with advanced hepatocellular carcinoma, biopsies will be used for both pathological diagnosis and ITH investigation. Moreover, ITH evaluation based on cell-free DNA and advanced imaging should be carried out to monitor ITH dynamically and guide medication adjustment. ITH: Intratumoral heterogeneity; cfDNA: Cell-free DNA.

HCC. Second, longitudinal monitoring of ITH alterations should be conducted for a high-resolution trajectory of clonal evolution. Finally, prospective population-based studies on HCC should be performed to accelerate the translation of ITH assessment into clinical practice. With an improved understanding of ITH, the evolutionary trajectory of HCC is likely to be predictable in the near future. Through the entire process of tracking tumor development, people may rewrite the clinical management of HCC and ultimately find solutions to completely change the outcome of HCC patients.

REFERENCES

1 **Siegel RL**, Miller KD, Jemal A. Cancer statistics, 2020. *CA Cancer J Clin* 2020; **70**: 7-30 [PMID: 31912902 DOI: 10.3322/caac.21590]
2 **Belghiti J**, Kianmanesh R. Surgical treatment of hepatocellular carcinoma. *HPB (Oxford)* 2005; **7**: 42-49 [PMID: 18333160 DOI: 10.1080/13651820410024067]
3 **Zellmer VR**, Zhang S. Evolving concepts of tumor heterogeneity. *Cell Biosci* 2014; **4**: 69 [PMID: 25937891 DOI: 10.1186/2045-3701-4-69]
4 **Greaves M**. Evolutionary determinants of cancer. *Cancer Discov* 2015; **5**: 806-820 [PMID: 26193902 DOI: 10.1158/2159-8290.CD-15-0439]
5 **Treyer A**, Müsch A. Hepatocyte polarity. *Compr Physiol* 2013; **3**: 243-287 [PMID: 23720287 DOI: 10.1002/cphy.c120009]
6 **Halpern KB**, Shenhav R, Matcovitch-Natan O, Toth B, Lemze D, Golan M, Massasa EE, Baydatch S, Landen S, Moor AE, Brandis A, Giladi A, Avihail AS, David E, Amit I, Itzkovitz S. Single-cell spatial reconstruction reveals global division of labour in the mammalian liver. *Nature* 2017; **542**: 352-356 [PMID: 28166538 DOI: 10.1038/nature21065]
7 **Hlady RA**, Zhou D, Puszyk W, Roberts LR, Liu C, Robertson KD. Initiation of aberrant DNA methylation patterns and heterogeneity in precancerous lesions of human hepatocellular cancer. *Epigenetics* 2017; **12**: 215-225 [PMID: 28059585 DOI: 10.1080/15592294.2016.1277297]
8 **Navin NE**. The first five years of single-cell cancer genomics and beyond. *Genome Res* 2015;

25: 1499-1507 [PMID: 26430160 DOI: 10.1101/gr.191098.115]
9 **Packer J**, Trapnell C. Single-Cell Multi-omics: An Engine for New Quantitative Models of Gene Regulation. *Trends Genet* 2018; **34**: 653-665 [PMID: 30007833 DOI: 10.1016/j.tig.2018.06.001]
10 **Liu L**, Liu C, Quintero A, Wu L, Yuan Y, Wang M, Cheng M, Leng L, Xu L, Dong G, Li R, Liu Y, Wei X, Xu J, Chen X, Lu H, Chen D, Wang Q, Zhou Q, Lin X, Li G, Liu S, Wang Q, Wang H, Fink JL, Gao Z, Liu X, Hou Y, Zhu S, Yang H, Ye Y, Lin G, Chen F, Herrmann C, Eils R, Shang Z, Xu X. Deconvolution of single-cell multi-omics layers reveals regulatory heterogeneity. *Nat Commun* 2019; **10**: 470 [PMID: 30692544 DOI: 10.1038/s41467-018-08205-7]
11 **Kang CC**, Lin JM, Xu Z, Kumar S, Herr AE. Single-cell Western blotting after whole-cell imaging to assess cancer chemotherapeutic response. *Anal Chem* 2014; **86**: 10429-10436 [PMID: 25226230 DOI: 10.1021/ac502932t]
12 **Hou Y**, Guo H, Cao C, Li X, Hu B, Zhu P, Wu X, Wen L, Tang F, Huang Y, Peng J. Single-cell triple omics sequencing reveals genetic, epigenetic, and transcriptomic heterogeneity in hepatocellular carcinomas. *Cell Res* 2016; **26**: 304-319 [PMID: 26902283 DOI: 10.1038/cr.2016.23]
13 **Duan M**, Hao J, Cui S, Worthley DL, Zhang S, Wang Z, Shi J, Liu L, Wang X, Ke A, Cao Y, Xi R, Zhang X, Zhou J, Fan J, Li C, Gao Q. Diverse modes of clonal evolution in HBV-related hepatocellular carcinoma revealed by single-cell genome sequencing. *Cell Res* 2018; **28**: 359-373 [PMID: 29327728 DOI: 10.1038/cr.2018.11]
14 **Zheng H**, Pomyen Y, Hernandez MO, Li C, Livak F, Tang W, Dang H, Greten TF, Davis JL, Zhao Y, Mehta M, Levin Y, Shetty J, Tran B, Budhu A, Wang XW. Single-cell analysis reveals cancer stem cell heterogeneity in hepatocellular carcinoma. *Hepatology* 2018; **68**: 127-140 [PMID: 29315726 DOI: 10.1002/hep.29778]
15 **Yan P**, Zhou B, Ma Y, Wang A, Hu X, Luo Y, Yuan Y, Wei Y, Pang P, Mao J. Tracking the important role of *JUNB* in hepatocellular carcinoma by single-cell sequencing analysis. *Oncol Lett* 2020; **19**: 1478-1486 [PMID: 31966074 DOI: 10.3892/ol.2019.11235]
16 **Ho DW**, Tsui YM, Sze KM, Chan LK, Cheung TT, Lee E, Sham PC, Tsui SK, Lee TK, Ng IO. Single-cell transcriptomics reveals the landscape of intra-tumoral heterogeneity and stemness-related subpopulations in liver cancer. *Cancer Lett* 2019; **459**: 176-185 [PMID: 31195060 DOI: 10.1016/j.canlet.2019.06.002]
17 **Ma L**, Hernandez MO, Zhao Y, Mehta M, Tran B, Kelly M, Rae Z, Hernandez JM, Davis JL, Martin SP, Kleiner DE, Hewitt SM, Ylaya K, Wood BJ, Greten TF, Wang XW. Tumor Cell Biodiversity Drives Microenvironmental Reprogramming in Liver Cancer. *Cancer Cell* 2019; **36**: 418-430.e6 [PMID: 31588021 DOI: 10.1016/j.ccell.2019.08.007]
18 **Brown HK**, Tellez-Gabriel M, Heymann D. Cancer stem cells in osteosarcoma. *Cancer Lett* 2017; **386**: 189-195 [PMID: 27894960 DOI: 10.1016/j.canlet.2016.11.019]
19 **Dirkse A**, Golebiewska A, Buder T, Nazarov PV, Muller A, Poovathingal S, Brons NHC, Leite S, Sauvageot N, Sarkisjan D, Seyfrid M, Fritah S, Stieber D, Michelucci A, Hertel F, Herold-Mende C, Azuaje F, Skupin A, Bjerkvig R, Deutsch A, Voss-Böhme A, Niclou SP. Stem cell-associated heterogeneity in Glioblastoma results from intrinsic tumor plasticity shaped by the microenvironment. *Nat Commun* 2019; **10**: 1787 [PMID: 30992437 DOI: 10.1038/s41467-019-09853-z]
20 **MacDonagh L**, Gray SG, Breen E, Cuffe S, Finn SP, O'Byrne KJ, Barr MP. Lung cancer stem cells: The root of resistance. *Cancer Lett* 2016; **372**: 147-156 [PMID: 26797015 DOI: 10.1016/j.canlet.2016.01.012]
21 **Zhang M**, Lee AV, Rosen JM. The Cellular Origin and Evolution of Breast Cancer. *Cold Spring Harb Perspect Med* 2017; **7** [PMID: 28062556 DOI: 10.1101/cshperspect.a027128]
22 **Ji J**, Yamashita T, Budhu A, Forgues M, Jia HL, Li C, Deng C, Wauthier E, Reid LM, Ye QH, Qin LX, Yang W, Wang HY, Tang ZY, Croce CM, Wang XW. Identification of microRNA-181 by genome-wide screening as a critical player in EpCAM-positive hepatic cancer stem cells. *Hepatology* 2009; **50**: 472-480 [PMID: 19585654 DOI: 10.1002/hep.22989]
23 **Zhao X**, Parpart S, Takai A, Roessler S, Budhu A, Yu Z, Blank M, Zhang YE, Jia HL, Ye QH, Qin LX, Tang ZY, Thorgeirsson SS, Wang XW. Integrative genomics identifies YY1AP1 as an oncogenic driver in EpCAM(+) AFP(+) hepatocellular carcinoma. *Oncogene* 2015; **34**: 5095-5104 [PMID: 25597408 DOI: 10.1038/onc.2014.438]
24 **Yamashita T**, Budhu A, Forgues M, Wang XW. Activation of hepatic stem cell marker EpCAM by Wnt-beta-catenin signaling in hepatocellular carcinoma. *Cancer Res* 2007; **67**: 10831-10839 [PMID: 18006828 DOI: 10.1158/0008-5472.CAN-07-0908]
25 **Gu Y**, Wei X, Sun Y, Gao H, Zheng X, Wong LL, Jin L, Liu N, Hernandez B, Peplowska K, Zhao X, Zhan QM, Feng XH, Tang ZY, Ji J. miR-192-5p Silencing by Genetic Aberrations Is a Key Event in Hepatocellular Carcinomas with Cancer Stem Cell Features. *Cancer Res* 2019; **79**: 941-953 [PMID: 30530815 DOI: 10.1158/0008-5472.CAN-18-1675]
26 **Yamashita T**, Honda M, Nakamoto Y, Baba M, Nio K, Hara Y, Zeng SS, Hayashi T, Kondo M, Takatori H, Yamashita T, Mizukoshi E, Ikeda H, Zen Y, Takamura H, Wang XW, Kaneko S. Discrete nature of EpCAM+ and CD90+ cancer stem cells in human hepatocellular carcinoma. *Hepatology* 2013; **57**: 1484-1497 [PMID: 23174907 DOI: 10.1002/hep.26168]
27 **Yang ZF**, Ho DW, Ng MN, Lau CK, Yu WC, Ngai P, Chu PW, Lam CT, Poon RT, Fan ST. Significance of CD90+ cancer stem cells in human liver cancer. *Cancer Cell* 2008; **13**: 153-166 [PMID: 18242515 DOI: 10.1016/j.ccr.2008.01.013]
28 **Wang R**, Li Y, Tsung A, Huang H, Du Q, Yang M, Deng M, Xiong S, Wang X, Zhang L, Geller DA, Cheng B, Billiar TR. iNOS promotes $CD24^{+}CD133^{+}$ liver cancer stem cell phenotype through a TACE/ADAM17-dependent Notch signaling pathway. *Proc Natl Acad Sci USA* 2018; **115**: E10127-E10136 [PMID: 30297396 DOI: 10.1073/pnas.1722100115]
29 **Wu J**, Zhu P, Lu T, Du Y, Wang Y, He L, Ye B, Liu B, Yang L, Wang J, Gu Y, Lan J, Hao Y, He L, Fan Z. The long non-coding RNA LncHDAC2 drives the self-renewal of liver cancer stem cells via activation of Hedgehog signaling. *J Hepatol* 2019; **70**: 918-929 [PMID: 30582981 DOI: 10.1016/j.jhep.2018.12.015]
30 **Rodríguez MM**, Fiore E, Bayo J, Atorrasagasti C, García M, Onorato A, Domínguez L, Malvicini M, Mazzolini G. 4Mu Decreases CD47 Expression on Hepatic Cancer Stem Cells and Primes a Potent

Antitumor T Cell Response Induced by Interleukin-12. *Mol Ther* 2018; **26**: 2738-2750 [PMID: 30301668 DOI: 10.1016/j.ymthe.2018.09.012]
31 **Lee TK**, Cheung VC, Lu P, Lau EY, Ma S, Tang KH, Tong M, Lo J, Ng IO. Blockade of CD47-mediated cathepsin S/protease-activated receptor 2 signaling provides a therapeutic target for hepatocellular carcinoma. *Hepatology* 2014; **60**: 179-191 [PMID: 24523067 DOI: 10.1002/hep.27070]
32 **Clevers H**. The cancer stem cell: premises, promises and challenges. *Nat Med* 2011; **17**: 313-319 [PMID: 21386835 DOI: 10.1038/nm.2304]
33 **Meacham CE**, Morrison SJ. Tumour heterogeneity and cancer cell plasticity. *Nature* 2013; **501**: 328-337 [PMID: 24048065 DOI: 10.1038/nature12624]
34 **Merlos-Suárez A**, Barriga FM, Jung P, Iglesias M, Céspedes MV, Rossell D, Sevillano M, Hernando-Momblona X, da Silva-Diz V, Muñoz P, Clevers H, Sancho E, Mangues R, Batlle E. The intestinal stem cell signature identifies colorectal cancer stem cells and predicts disease relapse. *Cell Stem Cell* 2011; **8**: 511-524 [PMID: 21419747 DOI: 10.1016/j.stem.2011.02.020]
35 **Dalerba P**, Kalisky T, Sahoo D, Rajendran PS, Rothenberg ME, Leyrat AA, Sim S, Okamoto J, Johnston DM, Qian D, Zabala M, Bueno J, Neff NF, Wang J, Shelton AA, Visser B, Hisamori S, Shimono Y, van de Wetering M, Clevers H, Clarke MF, Quake SR. Single-cell dissection of transcriptional heterogeneity in human colon tumors. *Nat Biotechnol* 2011; **29**: 1120-1127 [PMID: 22081019 DOI: 10.1038/nbt.2038]
36 **Zomer A**, Ellenbroek SI, Ritsma L, Beerling E, Vrisekoop N, Van Rheenen J. Intravital imaging of cancer stem cell plasticity in mammary tumors. *Stem Cells* 2013; **31**: 602-606 [PMID: 23225641 DOI: 10.1002/stem.1296]
37 **Cairo S**, Wang Y, de Reyniès A, Duroure K, Dahan J, Redon MJ, Fabre M, McClelland M, Wang XW, Croce CM, Buendia MA. Stem cell-like micro-RNA signature driven by Myc in aggressive liver cancer. *Proc Natl Acad Sci USA* 2010; **107**: 20471-20476 [PMID: 21059911 DOI: 10.1073/pnas.1009009107]
38 **Wang T**, Qin ZY, Wen LZ, Guo Y, Liu Q, Lei ZJ, Pan W, Liu KJ, Wang XW, Lai SJ, Sun WJ, Wei YL, Liu L, Guo L, Chen YQ, Wang J, Xiao HL, Bian XW, Chen DF, Wang B. Epigenetic restriction of Hippo signaling by MORC2 underlies stemness of hepatocellular carcinoma cells. *Cell Death Differ* 2018; **25**: 2086-2100 [PMID: 29555977 DOI: 10.1038/s41418-018-0095-6]
39 **Li L**, Liu Y, Guo Y, Liu B, Zhao Y, Li P, Song F, Zheng H, Yu J, Song T, Niu R, Li Q, Wang XW, Zhang W, Chen K. Regulatory MiR-148a-ACVR1/BMP circuit defines a cancer stem cell-like aggressive subtype of hepatocellular carcinoma. *Hepatology* 2015; **61**: 574-584 [PMID: 25271001 DOI: 10.1002/hep.27543]
40 **Yamashita T**, Ji J, Budhu A, Forgues M, Yang W, Wang HY, Jia H, Ye Q, Qin LX, Wauthier E, Reid LM, Minato H, Honda M, Kaneko S, Tang ZY, Wang XW. EpCAM-positive hepatocellular carcinoma cells are tumor-initiating cells with stem/progenitor cell features. *Gastroenterology* 2009; **136**: 1012-1024 [PMID: 19150350 DOI: 10.1053/j.gastro.2008.12.004]
41 **Sia D**, Villanueva A, Friedman SL, Llovet JM. Liver Cancer Cell of Origin, Molecular Class, and Effects on Patient Prognosis. *Gastroenterology* 2017; **152**: 745-761 [PMID: 28043904 DOI: 10.1053/j.gastro.2016.11.048]
42 **Shimada S**, Mogushi K, Akiyama Y, Furuyama T, Watanabe S, Ogura T, Ogawa K, Ono H, Mitsunori Y, Ban D, Kudo A, Arii S, Tanabe M, Wands JR, Tanaka S. Comprehensive molecular and immunological characterization of hepatocellular carcinoma. *EBioMedicine* 2019; **40**: 457-470 [PMID: 30598371 DOI: 10.1016/j.ebiom.2018.12.058]
43 **Batlle E**, Clevers H. Cancer stem cells revisited. *Nat Med* 2017; **23**: 1124-1134 [PMID: 28985214 DOI: 10.1038/nm.4409]
44 **Matak A**, Lahiri P, Ford E, Pabst D, Kashofer K, Stellas D, Thanos D, Zatloukal K. Stochastic phenotype switching leads to intratumor heterogeneity in human liver cancer. *Hepatology* 2018; **68**: 933-948 [PMID: 29171037 DOI: 10.1002/hep.29679]
45 **Saygin C**, Matei D, Majeti R, Reizes O, Lathia JD. Targeting Cancer Stemness in the Clinic: From Hype to Hope. *Cell Stem Cell* 2019; **24**: 25-40 [PMID: 30595497 DOI: 10.1016/j.stem.2018.11.017]
46 **Yuan H**, Yan M, Zhang G, Liu W, Deng C, Liao G, Xu L, Luo T, Yan H, Long Z, Shi A, Zhao T, Xiao Y, Li X. CancerSEA: a cancer single-cell state atlas. *Nucleic Acids Res* 2019; **47**: D900-D908 [PMID: 30329142 DOI: 10.1093/nar/gky939]
47 **Qian J**, Rankin EB. Hypoxia-Induced Phenotypes that Mediate Tumor Heterogeneity. *Adv Exp Med Biol* 2019; **1136**: 43-55 [PMID: 31201715 DOI: 10.1007/978-3-030-12734-3_3]
48 **Gerlinger M**, Horswell S, Larkin J, Rowan AJ, Salm MP, Varela I, Fisher R, McGranahan N, Matthews N, Santos CR, Martinez P, Phillimore B, Begum S, Rabinowitz A, Spencer-Dene B, Gulati S, Bates PA, Stamp G, Pickering L, Gore M, Nicol DL, Hazell S, Futreal PA, Stewart A, Swanton C. Genomic architecture and evolution of clear cell renal cell carcinomas defined by multiregion sequencing. *Nat Genet* 2014; **46**: 225-233 [PMID: 24487277 DOI: 10.1038/ng.2891]
49 **Gerlinger M**, Rowan AJ, Horswell S, Math M, Larkin J, Endesfelder D, Gronroos E, Martinez P, Matthews N, Stewart A, Tarpey P, Varela I, Phillimore B, Begum S, McDonald NQ, Butler A, Jones D, Raine K, Latimer C, Santos CR, Nohadani M, Eklund AC, Spencer-Dene B, Clark G, Pickering L, Stamp G, Gore M, Szallasi Z, Downward J, Futreal PA, Swanton C. Intratumor heterogeneity and branched evolution revealed by multiregion sequencing. *N Engl J Med* 2012; **366**: 883-892 [PMID: 22397650 DOI: 10.1056/NEJMoa1113205]
50 **Yates LR**, Gerstung M, Knappskog S, Desmedt C, Gundem G, Van Loo P, Aas T, Alexandrov LB, Larsimont D, Davies H, Li Y, Ju YS, Ramakrishna M, Haugland HK, Lilleng PK, Nik-Zainal S, McLaren S, Butler A, Martin S, Glodzik D, Menzies A, Raine K, Hinton J, Jones D, Mudie LJ, Jiang B, Vincent D, Greene-Colozzi A, Adnet PY, Fatima A, Maetens M, Ignatiadis M, Stratton MR, Sotiriou C, Richardson AL, Lønning PE, Wedge DC, Campbell PJ. Subclonal diversification of primary breast cancer revealed by multiregion sequencing. *Nat Med* 2015; **21**: 751-759 [PMID: 26099045 DOI: 10.1038/nm.3886]
51 **Nowell PC**. The clonal evolution of tumor cell populations. *Science* 1976; **194**: 23-28 [PMID: 959840 DOI: 10.1126/science.959840]
52 **Merlo LM**, Pepper JW, Reid BJ, Maley CC. Cancer as an evolutionary and ecological process. *Nat Rev Cancer* 2006; **6**: 924-935 [PMID: 17109012 DOI: 10.1038/nrc2013]

53 **Craig AJ**, von Felden J, Garcia-Lezana T, Sarcognato S, Villanueva A. Tumour evolution in hepatocellular carcinoma. *Nat Rev Gastroenterol Hepatol* 2020; **17**: 139-152 [PMID: 31792430 DOI: 10.1038/s41575-019-0229-4]

54 **Okada S**, Ishii H, Nose H, Okusaka T, Kyogoku A, Yoshimori M, Sakamoto M, Hirohashi S. Intratumoral DNA heterogeneity of small hepatocellular carcinoma. *Cancer* 1995; **75**: 444-450 [PMID: 7812914 DOI: 10.1002/1097-0142(19950115)75:2<444::aid-cncr2820750206>3.0.co;2-p]

55 **Saeki R**, Nagai H, Kaneko S, Unoura M, Yamanaka N, Okamoto E, Kobayashi K, Matsubara K. Intratumoral genomic heterogeneity in human hepatocellular carcinoma detected by restriction landmark genomic scanning. *J Hepatol* 2000; **33**: 99-105 [PMID: 10905592 DOI: 10.1016/s0168-8278(00)80165-8]

56 **Sirivatanauksorn Y**, Sirivatanauksorn V, Bhattacharya S, Davidson BR, Dhillon AP, Kakkar AK, Williamson RC, Lemoine NR. Genomic heterogeneity in synchronous hepatocellular carcinomas. *Gut* 1999; **45**: 761-765 [PMID: 10517917 DOI: 10.1136/gut.45.5.761]

57 **Xue R**, Li R, Guo H, Guo L, Su Z, Ni X, Qi L, Zhang T, Li Q, Zhang Z, Xie XS, Bai F, Zhang N. Variable Intra-Tumor Genomic Heterogeneity of Multiple Lesions in Patients With Hepatocellular Carcinoma. *Gastroenterology* 2016; **150**: 998-1008 [PMID: 26752112 DOI: 10.1053/j.gastro.2015.12.033]

58 **Furuta M**, Ueno M, Fujimoto A, Hayami S, Yasukawa S, Kojima F, Arihiro K, Kawakami Y, Wardell CP, Shiraishi Y, Tanaka H, Nakano K, Maejima K, Sasaki-Oku A, Tokunaga N, Boroevich KA, Abe T, Aikata H, Ohdan H, Gotoh K, Kubo M, Tsunoda T, Miyano S, Chayama K, Yamaue H, Nakagawa H. Whole genome sequencing discriminates hepatocellular carcinoma with intrahepatic metastasis from multi-centric tumors. *J Hepatol* 2017; **66**: 363-373 [PMID: 27742377 DOI: 10.1016/j.jhep.2016.09.021]

59 **Zhai W**, Lim TK, Zhang T, Phang ST, Tiang Z, Guan P, Ng MH, Lim JQ, Yao F, Li Z, Ng PY, Yan J, Goh BK, Chung AY, Choo SP, Khor CC, Soon WW, Sung KW, Foo RS, Chow PK. The spatial organization of intra-tumour heterogeneity and evolutionary trajectories of metastases in hepatocellular carcinoma. *Nat Commun* 2017; **8**: 4565 [PMID: 28240289 DOI: 10.1038/ncomms14565]

60 **Shi JY**, Xing Q, Duan M, Wang ZC, Yang LX, Zhao YJ, Wang XY, Liu Y, Deng M, Ding ZB, Ke AW, Zhou J, Fan J, Cao Y, Wang J, Xi R, Gao Q. Inferring the progression of multifocal liver cancer from spatial and temporal genomic heterogeneity. *Oncotarget* 2016; **7**: 2867-2877 [PMID: 26672766 DOI: 10.18632/oncotarget.6558]

61 **Lin DC**, Mayakonda A, Dinh HQ, Huang P, Lin L, Liu X, Ding LW, Wang J, Berman BP, Song EW, Yin D, Koeffler HP. Genomic and Epigenomic Heterogeneity of Hepatocellular Carcinoma. *Cancer Res* 2017; **77**: 2255-2265 [PMID: 28302680 DOI: 10.1158/0008-5472.CAN-16-2822]

62 **Xu LX**, He MH, Dai ZH, Yu J, Wang JG, Li XC, Jiang BB, Ke ZF, Su TH, Peng ZW, Guo Y, Chen ZB, Chen SL, Peng S, Kuang M. Genomic and transcriptional heterogeneity of multifocal hepatocellular carcinoma. *Ann Oncol* 2019; **30**: 990-997 [PMID: 30916311 DOI: 10.1093/annonc/mdz103]

63 **Torrecilla S**, Sia D, Harrington AN, Zhang Z, Cabellos L, Cornella H, Moeini A, Camprecios G, Leow WQ, Fiel MI, Hao K, Bassaganyas L, Mahajan M, Thung SN, Villanueva A, Florman S, Schwartz ME, Llovet JM. Trunk mutational events present minimal intra- and inter-tumoral heterogeneity in hepatocellular carcinoma. *J Hepatol* 2017; **67**: 1222-1231 [PMID: 28843658 DOI: 10.1016/j.jhep.2017.08.013]

64 **Losic B**, Craig AJ, Villacorta-Martin C, Martins-Filho SN, Akers N, Chen X, Ahsen ME, von Felden J, Labgaa I, D'Avola D, Allette K, Lira SA, Furtado GC, Garcia-Lezana T, Restrepo P, Stueck A, Ward SC, Fiel MI, Hiotis SP, Gunasekaran G, Sia D, Schadt EE, Sebra R, Schwartz M, Llovet JM, Thung S, Stolovitzky G, Villanueva A. Intratumoral heterogeneity and clonal evolution in liver cancer. *Nat Commun* 2020; **11**: 291 [PMID: 31941899 DOI: 10.1038/s41467-019-14050-z]

65 **Ding X**, He M, Chan AWH, Song QX, Sze SC, Chen H, Man MKH, Man K, Chan SL, Lai PBS, Wang X, Wong N. Genomic and Epigenomic Features of Primary and Recurrent Hepatocellular Carcinomas. *Gastroenterology* 2019; **157**: 1630-1645.e6 [PMID: 31560893 DOI: 10.1053/j.gastro.2019.09.005]

66 **McGranahan N**, Swanton C. Clonal Heterogeneity and Tumor Evolution: Past, Present, and the Future. *Cell* 2017; **168**: 613-628 [PMID: 28187284 DOI: 10.1016/j.cell.2017.01.018]

67 **Friemel J**, Rechsteiner M, Frick L, Böhm F, Struckmann K, Egger M, Moch H, Heikenwalder M, Weber A. Intratumor heterogeneity in hepatocellular carcinoma. *Clin Cancer Res* 2015; **21**: 1951-1961 [PMID: 25248380 DOI: 10.1158/1078-0432.CCR-14-0122]

68 **An FQ**, Matsuda M, Fujii H, Tang RF, Amemiya H, Dai YM, Matsumoto Y. Tumor heterogeneity in small hepatocellular carcinoma: analysis of tumor cell proliferation, expression and mutation of p53 AND beta-catenin. *Int J Cancer* 2001; **93**: 468-474 [PMID: 11477549 DOI: 10.1002/ijc.1367]

69 **Ling S**, Hu Z, Yang Z, Yang F, Li Y, Lin P, Chen K, Dong L, Cao L, Tao Y, Hao L, Chen Q, Gong Q, Wu D, Li W, Zhao W, Tian X, Hao C, Hungate EA, Catenacci DV, Hudson RR, Li WH, Lu X, Wu CI. Extremely high genetic diversity in a single tumor points to prevalence of non-Darwinian cell evolution. *Proc Natl Acad Sci USA* 2015; **112**: E6496-E6505 [PMID: 26561581 DOI: 10.1073/pnas.1519556112]

70 **Sottoriva A**, Kang H, Ma Z, Graham TA, Salomon MP, Zhao J, Marjoram P, Siegmund K, Press MF, Shibata D, Curtis C. A Big Bang model of human colorectal tumor growth. *Nat Genet* 2015; **47**: 209-216 [PMID: 25665006 DOI: 10.1038/ng.3214]

71 **Liu J**, Dang H, Wang XW. The significance of intertumor and intratumor heterogeneity in liver cancer. *Exp Mol Med* 2018; **50**: e416 [PMID: 29303512 DOI: 10.1038/emm.2017.165]

72 **Zhang Q**, Lou Y, Yang J, Wang J, Feng J, Zhao Y, Wang L, Huang X, Fu Q, Ye M, Zhang X, Chen Y, Ma C, Ge H, Wang J, Wu J, Wei T, Chen Q, Wu J, Yu C, Xiao Y, Feng X, Guo G, Liang T, Bai X. Integrated multiomic analysis reveals comprehensive tumour heterogeneity and novel immunophenotypic classification in hepatocellular carcinomas. *Gut* 2019; **68**: 2019-2031 [PMID: 31227589 DOI: 10.1136/gutjnl-2019-318912]

73 **Buczak K**, Ori A, Kirkpatrick JM, Holzer K, Dauch D, Roessler S, Endris V, Lasitschka F, Parca L, Schmidt A, Zender L, Schirmacher P, Krijgsveld J, Singer S, Beck M. Spatial Tissue Proteomics Quantifies Inter- and Intratumor Heterogeneity in Hepatocellular Carcinoma (HCC). *Mol Cell Proteomics* 2018; **17**: 810-825 [PMID: 29363612 DOI: 10.1074/mcp.RA117.000189]

74 **Kurebayashi Y**, Ojima H, Tsujikawa H, Kubota N, Maehara J, Abe Y, Kitago M, Shinoda M, Kitagawa Y, Sakamoto M. Landscape of immune microenvironment in hepatocellular carcinoma and its additional

impact on histological and molecular classification. *Hepatology* 2018; **68**: 1025-1041 [PMID: 29603348 DOI: 10.1002/hep.29904]

75 **Charoentong P**, Finotello F, Angelova M, Mayer C, Efremova M, Rieder D, Hackl H, Trajanoski Z. Pan-cancer Immunogenomic Analyses Reveal Genotype-Immunophenotype Relationships and Predictors of Response to Checkpoint Blockade. *Cell Rep* 2017; **18**: 248-262 [PMID: 28052254 DOI: 10.1016/j.celrep.2016.12.019]

76 **Aran D**, Hu Z, Butte AJ. xCell: digitally portraying the tissue cellular heterogeneity landscape. *Genome Biol* 2017; **18**: 220 [PMID: 29141660 DOI: 10.1186/s13059-017-1349-1]

77 **Gentles AJ**, Newman AM, Liu CL, Bratman SV, Feng W, Kim D, Nair VS, Xu Y, Khuong A, Hoang CD, Diehn M, West RB, Plevritis SK, Alizadeh AA. The prognostic landscape of genes and infiltrating immune cells across human cancers. *Nat Med* 2015; **21**: 938-945 [PMID: 26193342 DOI: 10.1038/nm.3909]

78 **Racle J**, de Jonge K, Baumgaertner P, Speiser DE, Gfeller D. Simultaneous enumeration of cancer and immune cell types from bulk tumor gene expression data. *Elife* 2017; **6** [PMID: 29130882 DOI: 10.7554/eLife.26476]

79 **Dong LQ**, Peng LH, Ma LJ, Liu DB, Zhang S, Luo SZ, Rao JH, Zhu HW, Yang SX, Xi SJ, Chen M, Xie FF, Li FQ, Li WH, Ye C, Lin LY, Wang YJ, Wang XY, Gao DM, Zhou H, Yang HM, Wang J, Zhu SD, Wang XD, Cao Y, Zhou J, Fan J, Wu K, Gao Q. Heterogeneous immunogenomic features and distinct escape mechanisms in multifocal hepatocellular carcinoma. *J Hepatol* 2020; **72**: 896-908 [PMID: 31887370 DOI: 10.1016/j.jhep.2019.12.014]

80 **Zheng C**, Zheng L, Yoo JK, Guo H, Zhang Y, Guo X, Kang B, Hu R, Huang JY, Zhang Q, Liu Z, Dong M, Hu X, Ouyang W, Peng J, Zhang Z. Landscape of Infiltrating T Cells in Liver Cancer Revealed by Single-Cell Sequencing. *Cell* 2017; **169**: 1342-1356.e16 [PMID: 28622514 DOI: 10.1016/j.cell.2017.05.035]

81 **Zhang Q**, He Y, Luo N, Patel SJ, Han Y, Gao R, Modak M, Carotta S, Haslinger C, Kind D, Peet GW, Zhong G, Lu S, Zhu W, Mao Y, Xiao M, Bergmann M, Hu X, Kerkar SP, Vogt AB, Pflanz S, Liu K, Peng J, Ren X, Zhang Z. Landscape and Dynamics of Single Immune Cells in Hepatocellular Carcinoma. *Cell* 2019; **179**: 829-845.e20 [PMID: 31675496 DOI: 10.1016/j.cell.2019.10.003]

82 **Jamal-Hanjani M**, Wilson GA, McGranahan N, Birkbak NJ, Watkins TBK, Veeriah S, Shafi S, Johnson DH, Mitter R, Rosenthal R, Salm M, Horswell S, Escudero M, Matthews N, Rowan A, Chambers T, Moore DA, Turajlic S, Xu H, Lee SM, Forster MD, Ahmad T, Hiley CT, Abbosh C, Falzon M, Borg E, Marafioti T, Lawrence D, Hayward M, Kolvekar S, Panagiotopoulos N, Janes SM, Thakrar R, Ahmed A, Blackhall F, Summers Y, Shah R, Joseph L, Quinn AM, Crosbie PA, Naidu B, Middleton G, Langman G, Trotter S, Nicolson M, Remmen H, Kerr K, Chetty M, Gomersall L, Fennell DA, Nakas A, Rathinam S, Anand G, Khan S, Russell P, Ezhil V, Ismail B, Irvin-Sellers M, Prakash V, Lester JF, Kornaszewska M, Attanoos R, Adams H, Davies H, Dentro S, Taniere P, O'Sullivan B, Lowe HL, Hartley JA, Iles N, Bell H, Ngai Y, Shaw JA, Herrero J, Szallasi Z, Schwarz RF, Stewart A, Quezada SA, Le Quesne J, Van Loo P, Dive C, Hackshaw A, Swanton C; TRACERx Consortium. Tracking the Evolution of Non-Small-Cell Lung Cancer. *N Engl J Med* 2017; **376**: 2109-2121 [PMID: 28445112 DOI: 10.1056/NEJMoa1616288]

83 **Martins-Filho SN**, Alves VAF, Wakamatsu A, Maeda M, Craig AJ, Assato AK, Villacorta-Martin C, D'Avola D, Labgaa I, Carrilho FJ, Thung SN, Villanueva A. A phenotypical map of disseminated hepatocellular carcinoma suggests clonal constraints in metastatic sites. *Histopathology* 2019; **74**: 718-730 [PMID: 30636011 DOI: 10.1111/his.13809]

84 **Andor N**, Graham TA, Jansen M, Xia LC, Aktipis CA, Petritsch C, Ji HP, Maley CC. Pan-cancer analysis of the extent and consequences of intratumor heterogeneity. *Nat Med* 2016; **22**: 105-113 [PMID: 26618723 DOI: 10.1038/nm.3984]

85 **Zhang J**, Fujimoto J, Zhang J, Wedge DC, Song X, Zhang J, Seth S, Chow CW, Cao Y, Gumbs C, Gold KA, Kalhor N, Little L, Mahadeshwar H, Moran C, Protopopov A, Sun H, Tang J, Wu X, Ye Y, William WN, Lee JJ, Heymach JV, Hong WK, Swisher S, Wistuba II, Futreal PA. Intratumor heterogeneity in localized lung adenocarcinomas delineated by multiregion sequencing. *Science* 2014; **346**: 256-259 [PMID: 25301631 DOI: 10.1126/science.1256930]

86 **Harbst K**, Lauss M, Cirenajwis H, Isaksson K, Rosengren F, Törngren T, Kvist A, Johansson MC, Vallon-Christersson J, Baldetorp B, Borg Å, Olsson H, Ingvar C, Carneiro A, Jönsson G. Multiregion Whole-Exome Sequencing Uncovers the Genetic Evolution and Mutational Heterogeneity of Early-Stage Metastatic Melanoma. *Cancer Res* 2016; **76**: 4765-4774 [PMID: 27216186 DOI: 10.1158/0008-5472.CAN-15-3476]

87 **Juric D**, Castel P, Griffith M, Griffith OL, Won HH, Ellis H, Ebbesen SH, Ainscough BJ, Ramu A, Iyer G, Shah RH, Huynh T, Mino-Kenudson M, Sgroi D, Isakoff S, Thabet A, Elamine L, Solit DB, Lowe SW, Quadt C, Peters M, Derti A, Schegel R, Huang A, Mardis ER, Berger MF, Baselga J, Scaltriti M. Convergent loss of PTEN leads to clinical resistance to a PI(3)Kα inhibitor. *Nature* 2015; **518**: 240-244 [PMID: 25409150 DOI: 10.1038/nature13948]

88 **Kwak EL**, Ahronian LG, Siravegna G, Mussolin B, Borger DR, Godfrey JT, Jessop NA, Clark JW, Blaszkowsky LS, Ryan DP, Lennerz JK, Iafrate AJ, Bardelli A, Hong TS, Corcoran RB. Molecular Heterogeneity and Receptor Coamplification Drive Resistance to Targeted Therapy in MET-Amplified Esophagogastric Cancer. *Cancer Discov* 2015; **5**: 1271-1281 [PMID: 26432108 DOI: 10.1158/2159-8290.CD-15-0748]

89 **Russo M**, Siravegna G, Blaszkowsky LS, Corti G, Crisafulli G, Ahronian LG, Mussolin B, Kwak EL, Buscarino M, Lazzari L, Valtorta E, Truini M, Jessop NA, Robinson HE, Hong TS, Mino-Kenudson M, Di Nicolantonio F, Thabet A, Sartore-Bianchi A, Siena S, Iafrate AJ, Bardelli A, Corcoran RB. Tumor Heterogeneity and Lesion-Specific Response to Targeted Therapy in Colorectal Cancer. *Cancer Discov* 2016; **6**: 147-153 [PMID: 26644315 DOI: 10.1158/2159-8290.CD-15-1283]

90 **Llovet JM**, Montal R, Sia D, Finn RS. Molecular therapies and precision medicine for hepatocellular carcinoma. *Nat Rev Clin Oncol* 2018; **15**: 599-616 [PMID: 30061739 DOI: 10.1038/s41571-018-0073-4]

91 **Zhu AX**, Finn RS, Edeline J, Cattan S, Ogasawara S, Palmer D, Verslype C, Zagonel V, Fartoux L, Vogel A, Sarker D, Verset G, Chan SL, Knox J, Daniele B, Webber AL, Ebbinghaus SW, Ma J, Siegel AB, Cheng AL, Kudo M; KEYNOTE-224 investigators. Pembrolizumab in patients with advanced hepatocellular carcinoma previously treated with sorafenib (KEYNOTE-224): a non-randomised, open-label phase 2 trial.

Lancet Oncol 2018; **19**: 940-952 [PMID: 29875066 DOI: 10.1016/S1470-2045(18)30351-6]

92 **Li J**, Byrne KT, Yan F, Yamazoe T, Chen Z, Baslan T, Richman LP, Lin JH, Sun YH, Rech AJ, Balli D, Hay CA, Sela Y, Merrell AJ, Liudahl SM, Gordon N, Norgard RJ, Yuan S, Yu S, Chao T, Ye S, Eisinger-Mathason TSK, Faryabi RB, Tobias JW, Lowe SW, Coussens LM, Wherry EJ, Vonderheide RH, Stanger BZ. Tumor Cell-Intrinsic Factors Underlie Heterogeneity of Immune Cell Infiltration and Response to Immunotherapy. *Immunity* 2018; **49**: 178-193.e7 [PMID: 29958801 DOI: 10.1016/j.immuni.2018.06.006]

93 **Wolf Y**, Bartok O, Patkar S, Eli GB, Cohen S, Litchfield K, Levy R, Jiménez-Sánchez A, Trabish S, Lee JS, Karathia H, Barnea E, Day CP, Cinnamon E, Stein I, Solomon A, Bitton L, Pérez-Guijarro E, Dubovik T, Shen-Orr SS, Miller ML, Merlino G, Levin Y, Pikarsky E, Eisenbach L, Admon A, Swanton C, Ruppin E, Samuels Y. UVB-Induced Tumor Heterogeneity Diminishes Immune Response in Melanoma. *Cell* 2019; **179**: 219-235.e21 [PMID: 31522890 DOI: 10.1016/j.cell.2019.08.032]

94 **Corcoran RB**, Chabner BA. Application of Cell-free DNA Analysis to Cancer Treatment. *N Engl J Med* 2018; **379**: 1754-1765 [PMID: 30380390 DOI: 10.1056/NEJMra1706174]

95 **Georgiadis A**, Durham JN, Keefer LA, Bartlett BR, Zielonka M, Murphy D, White JR, Lu S, Verner EL, Ruan F, Riley D, Anders RA, Gedvilaite E, Angiuoli S, Jones S, Velculescu VE, Le DT, Diaz LA Jr, Sausen M. Noninvasive Detection of Microsatellite Instability and High Tumor Mutation Burden in Cancer Patients Treated with PD-1 Blockade. *Clin Cancer Res* 2019; **25**: 7024-7034 [PMID: 31506389 DOI: 10.1158/1078-0432.CCR-19-1372]

96 **Okajima W**, Komatsu S, Ichikawa D, Miyamae M, Ohashi T, Imamura T, Kiuchi J, Nishibeppu K, Arita T, Konishi H, Shiozaki A, Morimura R, Ikoma H, Okamoto K, Otsuji E. Liquid biopsy in patients with hepatocellular carcinoma: Circulating tumor cells and cell-free nucleic acids. *World J Gastroenterol* 2017; **23**: 5650-5668 [PMID: 28883691 DOI: 10.3748/wjg.v23.i31.5650]

97 **Cai ZX**, Chen G, Zeng YY, Dong XQ, Lin MJ, Huang XH, Zhang D, Liu XL, Liu JF. Circulating tumor DNA profiling reveals clonal evolution and real-time disease progression in advanced hepatocellular carcinoma. *Int J Cancer* 2017; **141**: 977-985 [PMID: 28543104 DOI: 10.1002/ijc.30798]

98 **Huang A**, Zhang X, Zhou SL, Cao Y, Huang XW, Fan J, Yang XR, Zhou J. Detecting Circulating Tumor DNA in Hepatocellular Carcinoma Patients Using Droplet Digital PCR Is Feasible and Reflects Intratumoral Heterogeneity. *J Cancer* 2016; **7**: 1907-1914 [PMID: 27698932 DOI: 10.7150/jca.15823]

99 **Dagogo-Jack I**, Shaw AT. Tumour heterogeneity and resistance to cancer therapies. *Nat Rev Clin Oncol* 2018; **15**: 81-94 [PMID: 29115304 DOI: 10.1038/nrclinonc.2017.166]

100 **Hectors SJ**, Wagner M, Bane O, Besa C, Lewis S, Remark R, Chen N, Fiel MI, Zhu H, Gnjatic S, Merad M, Hoshida Y, Taouli B. Quantification of hepatocellular carcinoma heterogeneity with multiparametric magnetic resonance imaging. *Sci Rep* 2017; **7**: 2452 [PMID: 28550313 DOI: 10.1038/s41598-017-02706-z]

101 **Kiryu S**, Akai H, Nojima M, Hasegawa K, Shinkawa H, Kokudo N, Yasaka K, Ohtomo K. Impact of hepatocellular carcinoma heterogeneity on computed tomography as a prognostic indicator. *Sci Rep* 2017; **7**: 12689 [PMID: 28978930 DOI: 10.1038/s41598-017-12688-7]

102 **Sadeghi-Naini A**, Sannachi L, Tadayyon H, Tran WT, Slodkowska E, Trudeau M, Gandhi S, Pritchard K, Kolios MC, Czarnota GJ. Chemotherapy-Response Monitoring of Breast Cancer Patients Using Quantitative Ultrasound-Based Intra-Tumour Heterogeneities. *Sci Rep* 2017; **7**: 10352 [PMID: 28871171 DOI: 10.1038/s41598-017-09678-0]

103 **Dong X**, Wu P, Sun X, Li W, Wan H, Yu J, Xing L. Intra-tumour 18F-FDG uptake heterogeneity decreases the reliability on target volume definition with positron emission tomography/computed tomography imaging. *J Med Imaging Radiat Oncol* 2015; **59**: 338-345 [PMID: 25708154 DOI: 10.1111/1754-9485.12289]

104 **van Baardwijk A**, Bosmans G, van Suylen RJ, van Kroonenburgh M, Hochstenbag M, Geskes G, Lambin P, De Ruysscher D. Correlation of intra-tumour heterogeneity on 18F-FDG PET with pathologic features in non-small cell lung cancer: a feasibility study. *Radiother Oncol* 2008; **87**: 55-58 [PMID: 18328584 DOI: 10.1016/j.radonc.2008.02.002]

105 **Willaime JM**, Turkheimer FE, Kenny LM, Aboagye EO. Quantification of intra-tumour cell proliferation heterogeneity using imaging descriptors of 18F fluorothymidine-positron emission tomography. *Phys Med Biol* 2013; **58**: 187-203 [PMID: 23257054 DOI: 10.1088/0031-9155/58/2/187]

106 **Rimola J**. Heterogeneity of Hepatocellular Carcinoma on Imaging. *Semin Liver Dis* 2020; **40**: 61-69 [PMID: 31266063 DOI: 10.1055/s-0039-1693512]

107 **Lambin P**, Leijenaar RTH, Deist TM, Peerlings J, de Jong EEC, van Timmeren J, Sanduleanu S, Larue RTHM, Even AJG, Jochems A, van Wijk Y, Woodruff H, van Soest J, Lustberg T, Roelofs E, van Elmpt W, Dekker A, Mottaghy FM, Wildberger JE, Walsh S. Radiomics: the bridge between medical imaging and personalized medicine. *Nat Rev Clin Oncol* 2017; **14**: 749-762 [PMID: 28975929 DOI: 10.1038/nrclinonc.2017.141]

108 **Saini A**, Breen I, Pershad Y, Naidu S, Knuttinen MG, Alzubaidi S, Sheth R, Albadawi H, Kuo M, Oklu R. Radiogenomics and Radiomics in Liver Cancers. *Diagnostics (Basel)* 2018; **9** [PMID: 30591628 DOI: 10.3390/diagnostics9010004]

109 **O'Connor JP**, Rose CJ, Waterton JC, Carano RA, Parker GJ, Jackson A. Imaging intratumor heterogeneity: role in therapy response, resistance, and clinical outcome. *Clin Cancer Res* 2015; **21**: 249-257 [PMID: 25421725 DOI: 10.1158/1078-0432.CCR-14-0990]

110 **Lee S**, Kang TW, Song KD, Lee MW, Rhim H, Lim HK, Kim SY, Sinn DH, Kim JM, Kim K, Ha SY. Effect of Microvascular Invasion Risk on Early Recurrence of Hepatocellular Carcinoma After Surgery and Radiofrequency Ablation. *Ann Surg* 2019; Online ahead of print [PMID: 31058694 DOI: 10.1097/SLA.0000000000003268]

111 **Lei Z**, Li J, Wu D, Xia Y, Wang Q, Si A, Wang K, Wan X, Lau WY, Wu M, Shen F. Nomogram for Preoperative Estimation of Microvascular Invasion Risk in Hepatitis B Virus-Related Hepatocellular Carcinoma Within the Milan Criteria. *JAMA Surg* 2016; **151**: 356-363 [PMID: 26579636 DOI: 10.1001/jamasurg.2015.4257]

112 **Xu X**, Zhang HL, Liu QP, Sun SW, Zhang J, Zhu FP, Yang G, Yan X, Zhang YD, Liu XS. Radiomic analysis of contrast-enhanced CT predicts microvascular invasion and outcome in hepatocellular carcinoma. *J Hepatol* 2019;

70: 1133-1144 [PMID: 30876945 DOI: 10.1016/j.jhep.2019.02.023]
113 **Abdel-Rahman O**. Assessment of the discriminating value of the 8th AJCC stage grouping for hepatocellular carcinoma. *HPB (Oxford)* 2018; **20**: 41-48 [PMID: 28882455 DOI: 10.1016/j.hpb.2017.08.017]
114 **Minagawa M**, Ikai I, Matsuyama Y, Yamaoka Y, Makuuchi M. Staging of hepatocellular carcinoma: assessment of the Japanese TNM and AJCC/UICC TNM systems in a cohort of 13,772 patients in Japan. *Ann Surg* 2007; **245**: 909-922 [PMID: 17522517 DOI: 10.1097/01.sla.0000254368.65878.da]
115 **Sankin A**, Hakimi AA, Mikkilineni N, Ostrovnaya I, Silk MT, Liang Y, Mano R, Chevinsky M, Motzer RJ, Solomon SB, Cheng EH, Durack JC, Coleman JA, Russo P, Hsieh JJ. The impact of genetic heterogeneity on biomarker development in kidney cancer assessed by multiregional sampling. *Cancer Med* 2014; **3**: 1485-1492 [PMID: 25124064 DOI: 10.1002/cam4.293]
116 **Huang A**, Zhao X, Yang XR, Li FQ, Zhou XL, Wu K, Zhang X, Sun QM, Cao Y, Zhu HM, Wang XD, Yang HM, Wang J, Tang ZY, Hou Y, Fan J, Zhou J. Circumventing intratumoral heterogeneity to identify potential therapeutic targets in hepatocellular carcinoma. *J Hepatol* 2017; **67**: 293-301 [PMID: 28323123 DOI: 10.1016/j.jhep.2017.03.005]
117 **Shen YC**, Hsu CL, Jeng YM, Ho MC, Ho CM, Yeh CP, Yeh CY, Hsu MC, Hu RH, Cheng AL. Reliability of a single-region sample to evaluate tumor immune microenvironment in hepatocellular carcinoma. *J Hepatol* 2020; **72**: 489-497 [PMID: 31634533 DOI: 10.1016/j.jhep.2019.09.032]
118 **Kudo M**, Ikeda M, Motomura K, Okusaka T, Kato N, Dutcus CE, Hisai T, Suzuki M, Ikezawa H, Iwata T, Kumada H, Kobayashi M. A phase Ib study of lenvatinib (LEN) plus nivolumab (NIV) in patients (pts) with unresectable hepatocellular carcinoma (uHCC): Study 117. *J Clin Oncol* 2020; **38**: 513-513 [DOI: 10.1200/JCO.2020.38.4_suppl.513]
119 **Llovet JM**, Kudo M, Cheng AL, Finn RS, Galle PR, Kaneko S, Meyer T, Qin S, Dutcus CE, Chen E, Dubrovsky L, Zhu AX. Lenvatinib (len) plus pembrolizumab (pembro) for the first-line treatment of patients (pts) with advanced hepatocellular carcinoma (HCC): Phase 3 LEAP-002 study. *J Clin Oncol* 2019; **37**: TPS4152-TPS4152 [DOI: 10.1200/JCO.2019.37.15_suppl.TPS4152]
120 **Nuciforo S**, Fofana I, Matter MS, Blumer T, Calabrese D, Boldanova T, Piscuoglio S, Wieland S, Ringnalda F, Schwank G, Terracciano LM, Ng CKY, Heim MH. Organoid Models of Human Liver Cancers Derived from Tumor Needle Biopsies. *Cell Rep* 2018; **24**: 1363-1376 [PMID: 30067989 DOI: 10.1016/j.celrep.2018.07.001]
121 **Gao Q**, Wang ZC, Duan M, Lin YH, Zhou XY, Worthley DL, Wang XY, Niu G, Xia Y, Deng M, Liu LZ, Shi JY, Yang LX, Zhang S, Ding ZB, Zhou J, Liang CM, Cao Y, Xiong L, Xi R, Shi YY, Fan J. Cell Culture System for Analysis of Genetic Heterogeneity Within Hepatocellular Carcinomas and Response to Pharmacologic Agents. *Gastroenterology* 2017; **152**: 232-242.e4 [PMID: 27639803 DOI: 10.1053/j.gastro.2016.09.008]

World Journal of Gastroenterology

Submit a Manuscript: https://www.f6publishing.com

World J Gastroenterol 2020 July 14; 26(26): 3737-3749

DOI: 10.3748/wjg.v26.i26.3737

ISSN 1007-9327 (print) ISSN 2219-2840 (online)

ORIGINAL ARTICLE

Basic Study

Combining protein arginine methyltransferase inhibitor and anti-programmed death-ligand-1 inhibits pancreatic cancer progression

Nan-Nan Zheng, Min Zhou, Fang Sun, Man-Xiu Huai, Yi Zhang, Chun-Ying Qu, Feng Shen, Lei-Ming Xu

ORCID number: Nan-Nan Zheng 0000-0002-5628-406X; Min Zhou 0000-0002-5371-1098; Fang Sun 0000-0002-6688-4676; Man-Xiu Huai 0000-0002-3283-4152; Yi Zhang 0000-0002-1363-3291; Chun-Ying Qu 0000-0003-1846-1924; Feng Shen 0000-0001-7782-2211; Lei-Ming Xu 0000-0002-6735-4853.

Author contributions: Zheng NN and Zhou M contributed equally to this work; Zheng NN and Zhou M performed the majority of the experiments and wrote the paper; Sun F and Huai MX analyzed the data; Zhang Y, Qu CY, and Shen F edited the manuscript; Xu LM designed and supervised the study; all authors have read and approved the final manuscript.

Supported by the National Natural Science Foundation of China, No. 81472844.

Institutional review board statement: This study was reviewed and approved by the Ethics Committee of Xinhua Hospital Affiliated to Shanghai Jiao Tong University School of Medicine.

Institutional animal care and use committee statement: This study was reviewed and approved by the Ethics Committee of Xinhua Hospital Affiliated to Shanghai Jiao

Nan-Nan Zheng, Min Zhou, Fang Sun, Man-Xiu Huai, Yi Zhang, Chun-Ying Qu, Feng Shen, Lei-Ming Xu, Department of Gastroenterology, Xinhua Hospital Affiliated to Shanghai Jiao Tong University School of Medicine, Shanghai 200092, China

Corresponding author: Lei-Ming Xu, MD, PhD, Chief Doctor, Department of Gastroenterology, Xinhua Hospital Affiliated to Shanghai Jiao Tong University School of Medicine, No. 1665, Kongjiang Road, Yangpu District, Shanghai 200092, China. xuleiming@xinhuamed.com.cn

Abstract

BACKGROUND

Immunotherapy targeting programmed death-1 (PD-1) or programmed death-ligand-1 (PD-L1) has been shown to be effective in a variety of malignancies but has poor efficacy in pancreatic ductal adenocarcinoma (PDAC). Studies have shown that PD-L1 expression in tumors is an important indicator of the efficacy of immunotherapy. Tumor cells usually evade chemotherapy and host immune surveillance by epigenetic changes. Protein arginine methylation is a common posttranslational modification. Protein arginine methyltransferase (PRMT) 1 is deregulated in a wide variety of cancer types, whose biological role in tumor immunity is undefined.

AIM

To investigate the combined effects and underlying mechanisms of anti-PD-L1 and type I PRMT inhibitor in pancreatic cancer *in vivo*.

METHODS

PT1001B is a novel type I PRMT inhibitor with strong activity and good selectivity. A mouse model of subcutaneous Panc02-derived tumors was used to evaluate drug efficacy, toxic and side effects, and tumor growth *in vivo*. By flow cytometry, we determined the expression of key immune checkpoint proteins, detected the apoptosis in tumor tissues, and analyzed the immune cells. Immunohistochemistry staining for cellular proliferation-associated nuclear protein Ki67, TUNEL assay, and PRMT1/PD-L1 immunofluorescence were used to elucidate the underlying molecular mechanism of the antitumor effect.

RESULTS

Cultured Panc02 cells did not express PD-L1 *in vitro*, but tumor cells derived from Panc02 transplanted tumors expressed PD-L1. The therapeutic efficacy of anti-PD-

Tong University School of Medicine (XHEC-F- 2018-062).

Conflict-of-interest statement: The authors declare that there are no conflicts of interest related to this study.

Data sharing statement: No additional data are available.

ARRIVE guidelines statement: The authors have read the ARRIVE guidelines, and the manuscript was prepared and revised according to the ARRIVE guidelines.

Manuscript source: Unsolicited manuscript

Received: January 19, 2020
Peer-review started: January 19, 2020
First decision: May 1, 2019
Revised: June 2, 2020
Accepted: June 20, 2020
Article in press: June 20, 2020
Published online: July 14, 2020

P-Reviewer: Katuchova J, Tanase C
S-Editor: Dou Y
L-Editor: Wang TQ
E-Editor: Zhang YL

L1 mAb was significantly enhanced by the addition of PT1001B as measured by tumor volume (1054.00 ± 61.37 mm^3 *vs* 555.80 ± 74.42 mm^3, $P < 0.01$) and tumor weight (0.83 ± 0.06 g *vs* 0.38 ± 0.02 g, $P < 0.05$). PT1001B improved antitumor immunity by inhibiting PD-L1 expression on tumor cells (32.74% ± 5.89% *vs* 17.95% ± 1.92%, $P < 0.05$). The combination therapy upregulated tumor-infiltrating CD8+ T lymphocytes (23.75% ± 3.20% *vs* 73.34% ± 4.35%, $P < 0.01$) and decreased PD-1+ leukocytes (35.77% ± 3.30% *vs* 6.48% ± 1.08%, $P < 0.001$) in tumor tissue compared to the control. In addition, PT1001B amplified the inhibitory effect of anti-PD-L1 on tumor cell proliferation and enhanced the induction of tumor cell apoptosis. PRMT1 downregulation was correlated with PD-L1 downregulation.

CONCLUSION

PT1001B enhances antitumor immunity and combining it with anti-PD-L1 checkpoint inhibitors provides a potential strategy to overcome anti-PD-L1 resistance in PDAC.

Key words: Protein arginine methyltransferase; Programmed death-ligand-1 blockade; Pancreatic ductal adenocarcinoma; Combination therapy; Tumor microenvironment

Core tip: Pancreatic ductal adenocarcinoma exhibits marginal responses to immune checkpoint inhibitors targeting programmed death-ligand-1 (PD-L1), and the underlying mechanism remains poorly understood. PT1001B, an inhibitor of type I protein arginine methyltransferases (PRMTs), significantly enhanced the therapeutic efficacy of anti-PD-L1 mAb. PT1001B improved antitumor immunity by inhibiting PD-L1 expression on tumor cells, upregulating tumor infiltrating CD8+ T lymphocytes, and decreasing PD-1+ leukocytes. In addition, PT1001B amplified the inhibitory effect of anti-PD-L1 on tumor cell proliferation and enhanced the induction of tumor cell apoptosis. PRMT1 downregulation was correlated with PD-L1 downregulation. Thus, PRMT1 is a potential therapeutic target.

Citation: Zheng NN, Zhou M, Sun F, Huai MX, Zhang Y, Qu CY, Shen F, Xu LM. Combining protein arginine methyltransferase inhibitor and anti-programmed death-ligand-1 inhibits pancreatic cancer progression. *World J Gastroenterol* 2020; 26(26): 3737-3749
URL: https://www.wjgnet.com/1007-9327/full/v26/i26/3737.htm
DOI: https://dx.doi.org/10.3748/wjg.v26.i26.3737

INTRODUCTION

Pancreatic ductal adenocarcinoma (PDAC) is the seventh leading cause of cancer-related death worldwide and the fourth leading cause of cancer-related death in the United States[1,2]. Most cases of PDAC are diagnosed at the metastatic stage, and the median survival of these patients is less than one year[2]. Many factors are associated with the poor survival of PDAC patients and the treatment challenges, including the lack of early detection, high risk of relapse after curative surgery, and poor response to chemotherapy, radiation, molecular targeted therapy, and immunotherapy[3]. Programmed death-ligand-1 (PD-L1), also known as B7-H1, is a cell surface protein and one of two ligands for programmed death-1 (PD-1), a costimulatory molecule that negatively regulates T cell responses[4]. Ligation of PD-L1 on cancer cells to PD-1 on T cells suppresses T cell activation and proliferation. While immunotherapy using anti-PD-1/PD-L1 antibodies has been shown to be effective for many types of malignancies[5,6], its activity is limited in PDAC[7]. The mechanism underlying pancreatic cancer resistance to anti-PD-1/PD-L1 immunotherapy is poorly understood, but it has been suggested that PD-L1 expression in tumors is an important indicator of checkpoint immunotherapy efficacy[8,9].

Protein arginine methylation is a common posttranslational modification that plays a role in multiple pathways, including cell cycle control, RNA processing, and DNA replication[10]. Protein arginine methyltransferases (PRMTs) are enzymes that catalyze

the transfer of a methyl group from S-adenosylmethionine to arginine[10]. PRMT family members are classified into PRMT types I, II, and III based on the nature of the catalyzed methylation reaction[11]. PRMT1 is the predominant type I methyltransferase responsible for approximately 85% of all cellular arginine methylation events. PRMT1 is deregulated in a wide variety of cancer types, *e.g.*, pancreatic adenocarcinoma[12,13], gastric cancer[14], and lung cancer[15]. This enzyme controls epithelial-mesenchymal transition in cancer cells[16]. PRMT1 can catalyze arginine methylation on histones and other proteins, such as Axin and epidermal growth factor receptor[17,18]. PRMT1 is upregulated in pancreatic cancer and exerts an oncogenic role by regulating the β-catenin protein level[13].

The aim of the present study was to evaluate the effect of type I PRMT inhibitor against PDAC in mice and to investigate the influence of PRMT1 on PD-L1 expression.

MATERIALS AND METHODS

Cell culture

The murine PDAC cell line Panc02, which is syngeneic to C57BL/6 mice, was obtained from the cell bank of the Type Culture Collection of the Chinese Academy of Sciences (Shanghai, China). Panc02 cells were cultured in DMEM (Gibco, Grand Island, NY, United States) with 10% fetal bovine serum (Gibco) at 37°C in a 5% CO_2 atmosphere.

Mice and reagents

Female C57BL/6 mice (specific pathogen-free grade) aged 5 wk were obtained from Shanghai Jihui Experimental Animal Feeding Co., Ltd and housed in a specific pathogen-free facility (23°C, 12 h/12 h light/dark cycle, 50% humidity, and ad libitum access to food and water). All experimental procedures were approved by the ethics committee of Xinhua Hospital Affiliated to Shanghai Jiao Tong University School of Medicine, and the protocols adhered to approved institutional protocols set by the China Association of Laboratory Animal Care. Panc02 cells (5×10^6) suspended in 100 μL cold PBS were subcutaneously injected into the lower back region of each mouse. The tumor volume was calculated using the following formula: $0.52 \times \text{length} \times \text{width}^2$. When the tumors reached approximately 100 mm^3, the tumor-bearing mice were randomly divided into four groups ($n = 4$) that were treated with control solvent (PBS, once daily), PT1001B (30 mg/kg, once daily, synthesized by Wang *et al*[19]), anti-PD-L1 mAb (200 μg/mouse, every 2 d for 5 intervals, Clone No. 10F.9G2, BioXcell), or PT1001B + anti-PD-L1 mAb *via* intraperitoneal injection. Mice were sacrificed at 37 d following the initial injection, and tumors were removed and weighed.

Flow cytometry analysis

Immunophenotypic analyses of splenocytes and single-cell suspensions from tumors were assessed by flow cytometry (FCM). All primary antibodies used in this study were purchased from BioLegend (CA, United States). Cells were stained with antibodies specific for CD45-APC-Cy7 (Clone 30-F11), CD4-PE-Cy7 (Clone RM4-4), CD8-FITC (Clone 53-6.7), PD-L1-APC (Clone 10F.9G2), and PD-1-PE (Clone RMP1-30). For the apoptosis analysis, the cells were stained with annexin V-fluorescein isothiocyanate (FITC) and propidium iodide (PI) (BD apoptosis assay kit, BD Pharmingen, CA, United States) according to the manufacturer's protocol. Fresh PDAC tumor tissues from the mouse model were minced into small pieces and then digested with collagenase type IV to generate a single-cell suspension. After being filtered and washed with cold PBS, the cells were incubated with the primary antibodies on ice for 30 min, washed, fixed in PBS containing 1% formalin, and analyzed on a flow cytometer (CyAn ADP, Beckman). Data were visualized using FlowJo software.

Immunohistochemistry

The tumor tissues isolated from sacrificed mice were immediately fixed in 4% paraformaldehyde for 24 h and embedded in paraffin. The embedded sections were sliced into 5-μm sections for staining. The deparaffinized and rehydrated sections were boiled in a high-pressure pot with sodium citrate antigen retrieval solution for 3 min. After three washes in PBS, the sections were incubated with 3% hydrogen peroxide in methanol for 15 min to inhibit endogenous peroxidase activity. After nonspecific reactions were blocked with 10% normal rabbit serum, the sections were incubated overnight at 4°C with rabbit polyclonal antibodies specific to Ki67 (GB13030-2, 1:200,

Servicebio). Then, the sections were washed, incubated at room temperature for 50 min with horseradish peroxidase-conjugated secondary antibody (GB23303, 1:200, Servicebio), and counterstained with hematoxylin.

TUNEL assay

The TUNEL assay was performed according to the kit protocol (11684817910, Roche). Briefly, tumor tissue sections were deparaffinized in xylene, rehydrated in PBS, and incubated with proteinase K working solution for 25 min at 37°C. After three washes in PBS, the sections were incubated in permeabilization working solution for 20 min. Then, TdT and dUTP were mixed at a 1:9 ratio; the tissue samples were incubated with the resulting mixture in a flat wet box at 37°C for 3-4 h. After three washes in PBS, the slides were immersed in 3% H_2O_2 at room temperature for 15 min in the dark. After three washes in PBS, the specimens were covered with converter-POD for 30 min and then washed three times in PBS. The slides were visualized with the DAB substrate and observed by microscopy (OLYMPUS, Japan). TUNEL-positive cells were counted with ImageJ, and the apoptotic index was calculated as the ratio of apoptotic cells to total cells in each field.

Immunofluorescence

After antigen retrieval, nonspecific binding was blocked with 1% bovine serum albumin for 30 min, and the tissue sections were incubated overnight at 4°C with a primary antibody against PD-L1 (GB11339, 1:200, Servicebio). Thereafter, the sections were incubated with Alexa Fluor®488-conjugated goat anti-mouse IgG (GB25301, 1:400, Servicebio) for 50 min at room temperature. After incubation with CY3 reagent for 10 min, the sections were heated in a microwave to remove antibodies bound to the tissue. After nonspecific binding was blocked, the samples were incubated overnight at 4°C with a primary antibody against PRMT1 (sc-166963, 1:1000, Santa Cruz). Thereafter, the sections were incubated with horseradish peroxidase-labeled goat anti-mouse IgG (GB23301, 1:500, Servicebio) secondary antibody for 50 min at room temperature. Nuclei were stained with DAPI for 5 min at room temperature. Immunopositive cells were analyzed using a fluorescence microscope (Eclipse ci, NIKON, Japan).

Statistical analysis

All data are shown as the mean ± SE. All data were assessed by *t*-tests or one-way ANOVA (GraphPad Prism 6.0). P values < 0.05 were considered to indicate statistical significance.

RESULTS

PD-L1 is expressed in PDAC in vivo but not in vitro

To determine PD-L1 expression in tumor-bearing mice, we transplanted Panc02 cells into C57BL/6 mice (Figure 1A). PD-L1 expression on tumor cells was quantified by the mean fluorescence intensity (MFI) (Figure 1B). Panc02 cells grown *in vitro* did not express PD-L1, but subcutaneous Panc02-derived tumor cells expressed PD-L1. We speculated that the increased PD-L1 expression *in vivo* is related to the tumor microenvironment.

PT1001B reverses anti-PD-L1 resistance in a PDAC mouse model

We then used PT1001B (formerly known as compound 28d, DCPR049_12), a novel selective inhibitor of type I PRMTs that effectively inhibits cancer cell proliferation[19]. We wondered whether PT1001B can enhance the efficacy of anti-PD-L1 therapy in Panc02-bearing C57BL/6 mice. The tumor-bearing mice were treated with PT1001B and anti-PD-L1 mAb, alone or in combination. As shown in Figure 2A, the tumors were resistant to anti-PD-L1 monotherapy. PT1001B or anti-PD-L1 mAb therapy alone did not decrease tumor growth compared to no treatment. Interestingly, when the anti-PD-L1 mAb was combined with PT1001B, the tumors showed a better response, as assessed by tumor volume (1054.00 ± 61.37 mm^3 *vs* 555.80 ± 74.42 mm^3) and weight (0.83 ± 0.06 g *vs* 0.38 ± 0.02 g) (Figure 2B). Importantly, treatment with PT1001B and PD-L1 blockade, alone or in combination, did not result in any overt signs of toxicity, as evidenced by weight gain in all the evaluated animal groups (Figure 2C). There was no difference in mouse body weight in different treatment groups. Therefore, these findings suggest the potential of combination therapy with PT1001B to reverse anti-

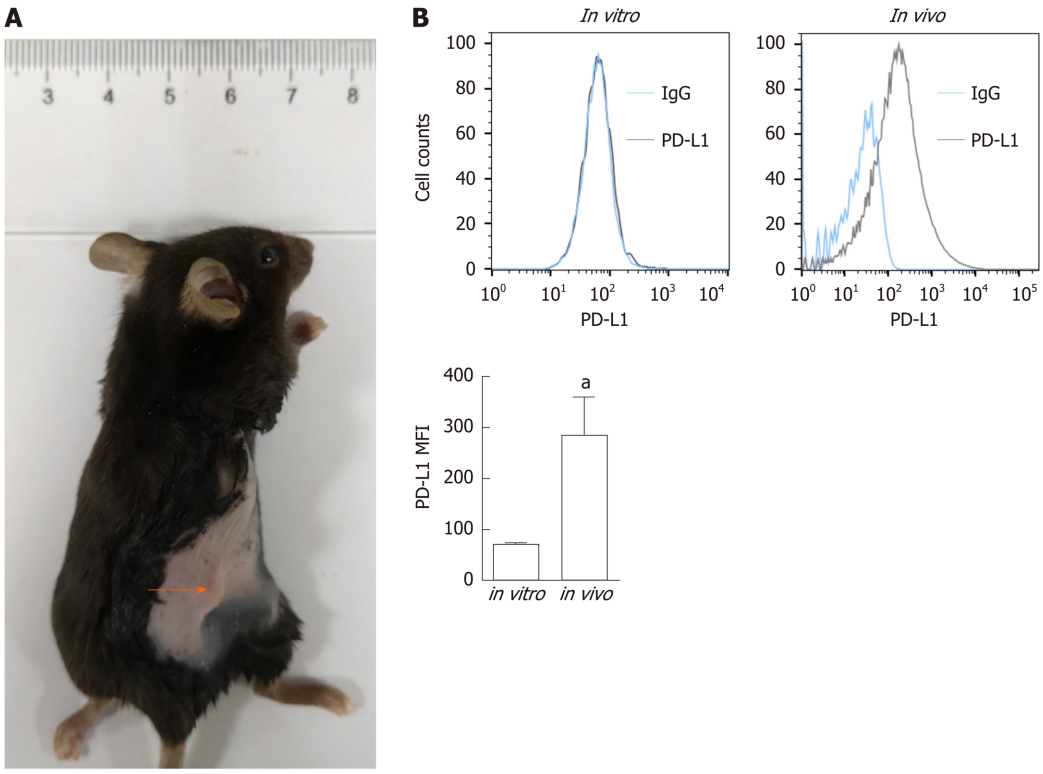

Figure 1 Programmed death-ligand-1 expression in pancreatic ductal adenocarcinoma *in vitro* and *in vivo*. A: Panc02 cells were subcutaneously transplanted into C57BL/6 mice to establish pancreatic tumors (orange arrow); B: Programmed death-ligand-1 expression levels in cultured pancreatic cancer cells (*in vitro*) and tumors (*in vivo*). The mean fluorescence intensity was used to quantify protein expression levels, and the values were statistically analyzed by a two-sided *t*-test; the results are presented at the bottom. Data represent the mean ± SE ($n = 3$). $^{a}P < 0.05$ *vs in vitro* condition. PD-L1: Programmed death-ligand-1; MFI: Mean fluorescence intensity.

PD-L1 resistance in PDAC.

PT1001B enhances antitumor immunity

To determine whether PT1001B can enhance antitumor immunity, single-cell suspensions of tumor and spleen extracts were stained for FCM analysis. As shown in Figure 3A, PT1001B decreased PD-L1 expression on cancer cells (32.74% ± 5.89% in the control group *vs* 17.95% ± 1.92% in the PT1001B group). PD-L1 expression was dramatically lower in the anti-PD-L1 + PT1001B group than in the control group (4.21% ± 0.82% *vs* 32.74% ± 5.89%). In tumors, PD-1+ leukocytes were downregulated in the three treated groups (19.93% ± 3.65% in the PT1001B group, 15.53% ± 1.71% in the anti-PD-L1 group, and 6.48% ± 1.08 % in the anti-PD-L1 + PT1001B group *vs* 35.77% ± 3.30% in the control group) (Figure 3B). In the spleen, PD-1+ leukocytes were downregulated to a greater extent in the anti-PD-L1 + PT1001B group than in the anti-PD-L1 group (5.98% ± 1.26% in the anti-PD-L1 + PT1001B group *vs* 10.35% ± 0.46% in the anti-PD-L1 group) (Figure 3C). Analysis of T cell populations from the tumors and spleens revealed that PT1001B further increased the anti-PD-L1 mAb-induced tumor infiltration of CD8+ cytotoxic T lymphocytes (CTLs) (tumor: 8.14% ± 0.82% in the anti-PD-L1 group *vs* 13.83% ± 0.97% in the anti-PD-L1+PT1001B group; spleen: 7.54% ± 1.09% in the anti-PD-L1 group *vs* 12.90% ± 0.15% in the anti-PD-L1 + PT1001B group) (Figure 3D and E). These observations suggest that PT1001B enhanced antitumor immunity by upregulating tumor infiltrating CD8+ T lymphocytes, decreasing PD-L1 expression by cancer cells, and downregulating PD-1+ leukocytes.

Effects of PT1001B and anti-PD-L1 mAb on PDAC cell proliferation and apoptosis

To estimate the effect of PT1001B on apoptosis, FCM analysis was performed after double staining with annexin V-FITC/PI. As shown in Figure 4A, the rates of early and late apoptosis were dramatically higher in the combination group than in the control group (49.00% ± 0.64% *vs* 24.36% ± 3.67%), while the rates showed no significant changes in the other treatment groups compared to the control. We performed immunohistochemistry analysis of tumor tissues to examine Ki67

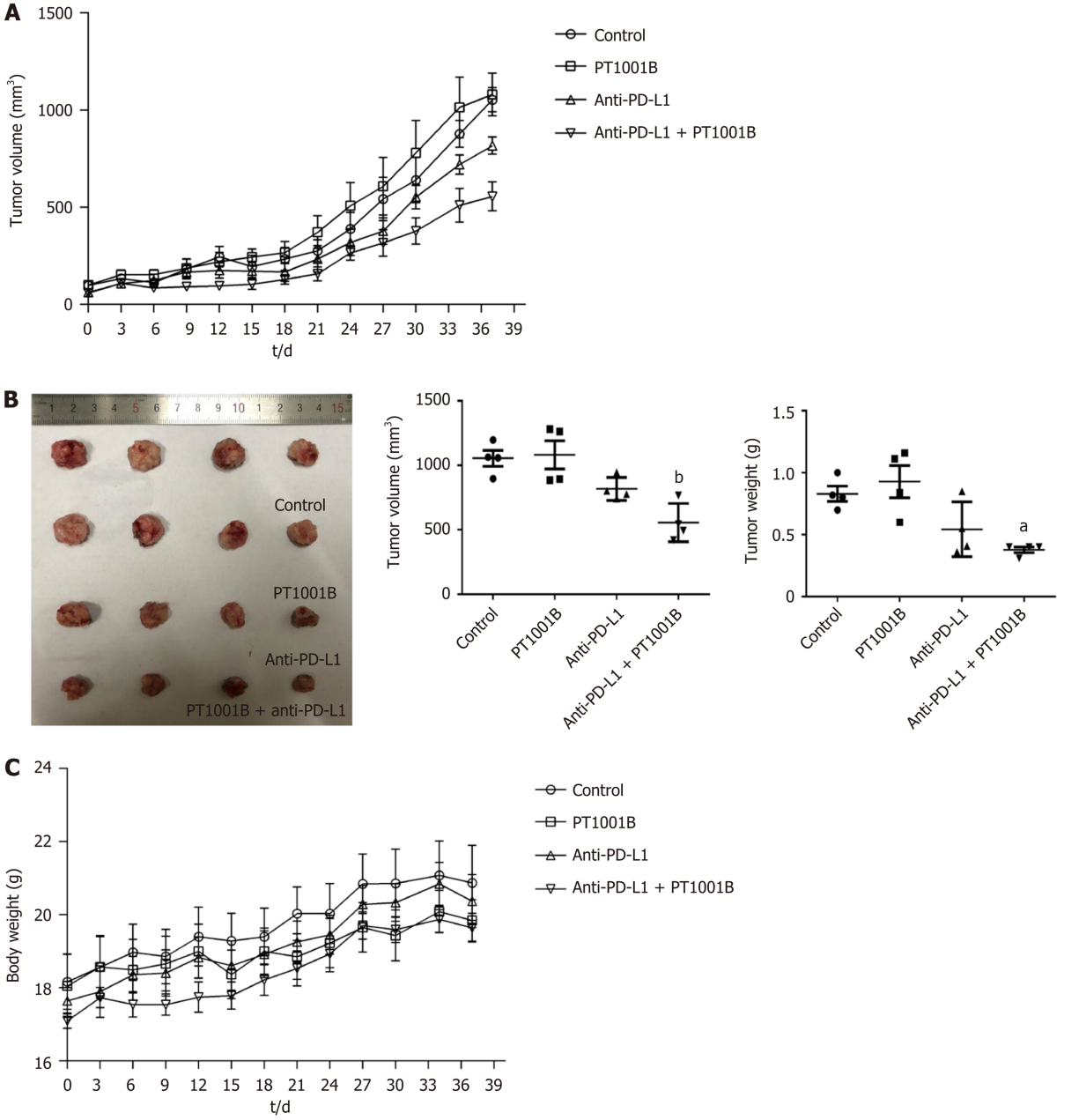

Figure 2 The combination of PT1001B and programmed death-ligand-1 blockade inhibits the development of pancreatic ductal adenocarcinoma in mice. Panc02 cells were surgically transplanted into C57BL/6 mice. One week later, tumors reached approximately 100 mm^3, and tumor-bearing mice were randomly divided into four groups that were treated with PT1001B (30 mg/kg body weight, once daily) or anti- programmed death-ligand-1 (PD-L1) mAb (200 μg/mouse, every 2 d for 5 intervals) alone or in combination *via* intraperitoneal injection for 37 d. A: The combination of PT1001B and anti-PD-L1 mAb significantly inhibited tumor growth; B: Tumors in different treated groups; C: Mouse body weight curve. The values were analyzed by one-way ANOVA. Data represent the mean ± SE (n = 4). $^aP < 0.05$, $^bP < 0.01$ *vs* control group. PD-L1: Programmed death-ligand-1.

expression and TUNEL positive cells, which are common markers of proliferation and apoptosis, respectively. Consistent with the greater degree of tumor growth inhibition, PT1001B significantly increased the efficacy of anti-PD-L1 therapy in suppressing tumor cell proliferation and inducing tumor cell apoptosis *in vivo* (Figure 4B and C).

PRMT1 expression correlates with PD-L1 expression

Immunofluorescence was performed to detect the levels of PRMT1 and PD-L1 in tumor tissues (Figure 5). PT1001B promoted the downregulation of PRMT1 and PD-L1, as indicated by the reduction in fluorescence. In particular, the anti-PD-L1 + PT1001B group showed the most drastic effect, with the lowest intensity of PD-L1-positive staining in tumor tissue.

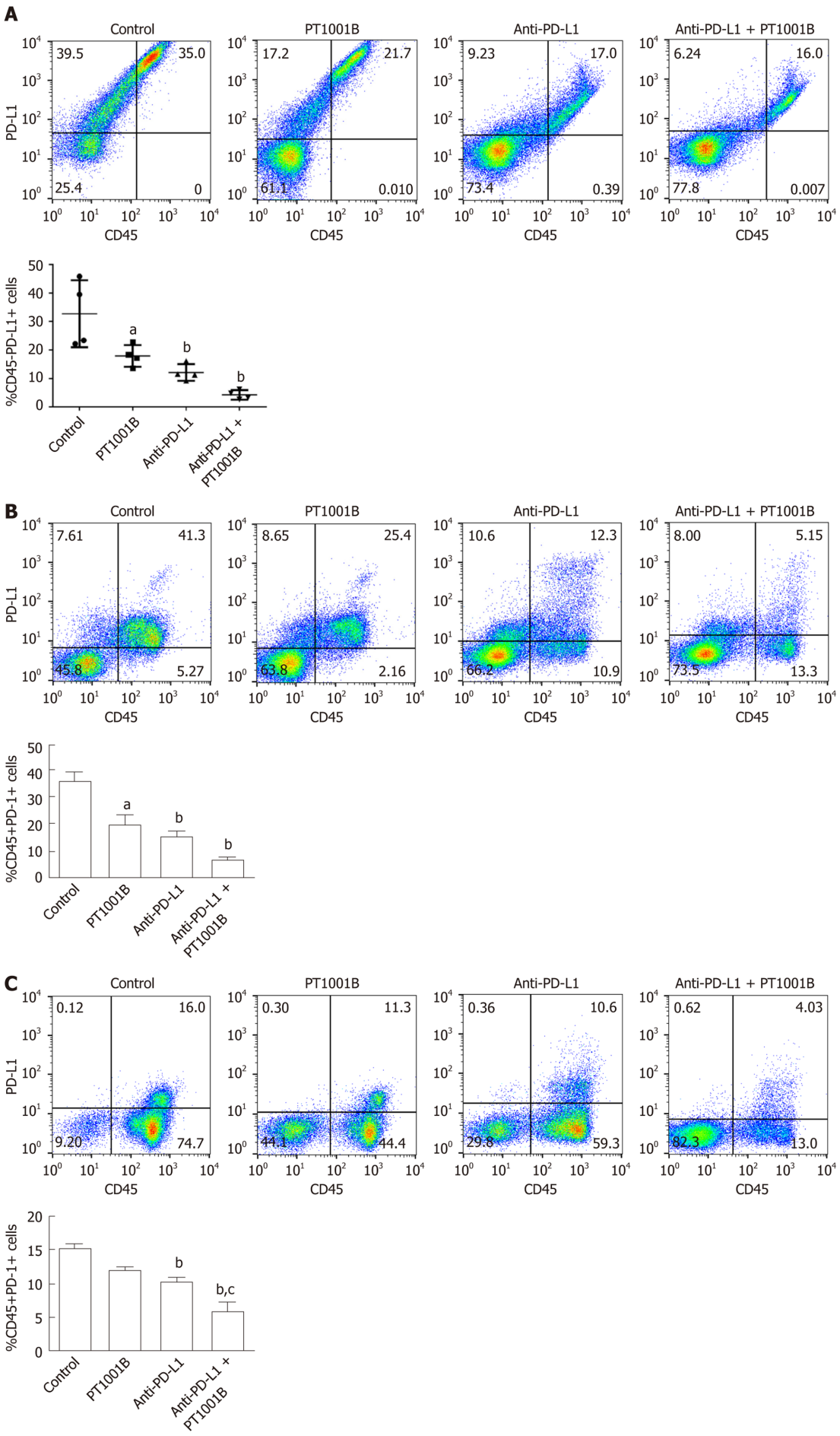
A
Control
PT1001B
Anti-PD-L1
Anti-PD-L1 + PT1001B
PD-L1
CD45
39.5
35.0
25.4
0
17.2
21.7
61.1
0.010
9.23
17.0
73.4
0.39
6.24
16.0
77.8
0.007
%CD45-PD-L1+ cells
a
b
b
Control
PT1001B
Anti-PD-L1
Anti-PD-L1 + PT1001B
B
7.61
41.3
45.8
5.27
8.65
25.4
63.8
2.16
10.6
12.3
66.2
10.9
8.00
5.15
73.5
13.3
%CD45+PD-1+ cells
a
b
b
C
0.12
16.0
9.20
74.7
0.30
11.3
44.1
44.4
0.36
10.6
29.8
59.3
0.62
4.03
82.3
13.0
b
b,c

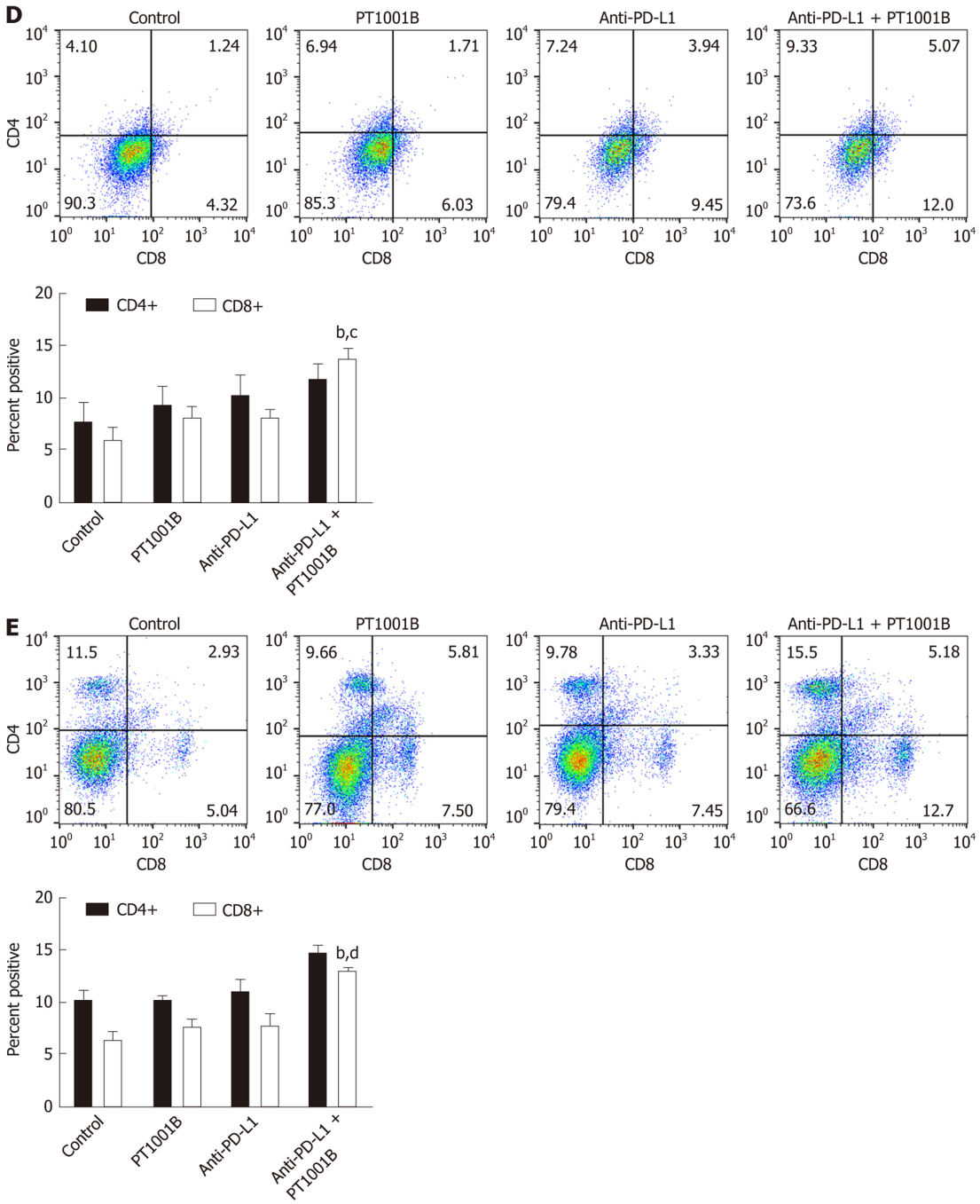

Figure 3 PT1001B enhances antitumor immunity. Cell suspensions were prepared from pancreatic tumor tissues and spleens from the four groups of tumor-bearing mice and stained with CD45-, CD4-, CD8-, PD-L1-, and PD-1-specific antibodies. Stained cells were analyzed by flow cytometry. The left panel presents representative images, and the right panel shows the statistical analysis. A: Analysis of CD45-/PD-L1+ cells in the tumors; B: Analysis of CD45+/PD-1+ cells in the tumors; C: Analysis of CD45+/PD-1+ cells in the spleens; D: Analysis of CD4+ T cells and CD8+ T cells in the tumors; E: Analysis of CD4+ T cells and CD8+ T cells in the spleens. Differences in the percentages of cells were analyzed by one-way ANOVA. Data represent the mean ± SE (n = 4). $^{a}P < 0.05$, $^{b}P < 0.01$ *vs* control group; $^{c}P < 0.05$, $^{d}P < 0.01$ *vs* anti-PD-L1 group. PD-L1: Programmed death-ligand-1; PD-1: Programmed death-1.

DISCUSSION

Immunotherapy failure in pancreatic cancer stems from the nonimmunogenic characteristic, especially the immunosuppressive microenvironment, poor T cell infiltration, and the low mutational burden, which contribute to creating an immunoprivileged environment[20]. Increased PD-L1 expression by cancer or stroma cells is a fundamental mechanism of escape from host immunity[21]. Tumor cells can inhibit the proliferation, survival, and effector function of T lymphocytes, especially CD8+ T lymphocytes, through the PD-L1/PD-1 pathway[22]. PD-L1 blockade can relieve immunosuppression, enhance antitumor immunity, and lead to the expansion of tumor-infiltrating lymphocytes[23]. Immune checkpoint blockade reverses

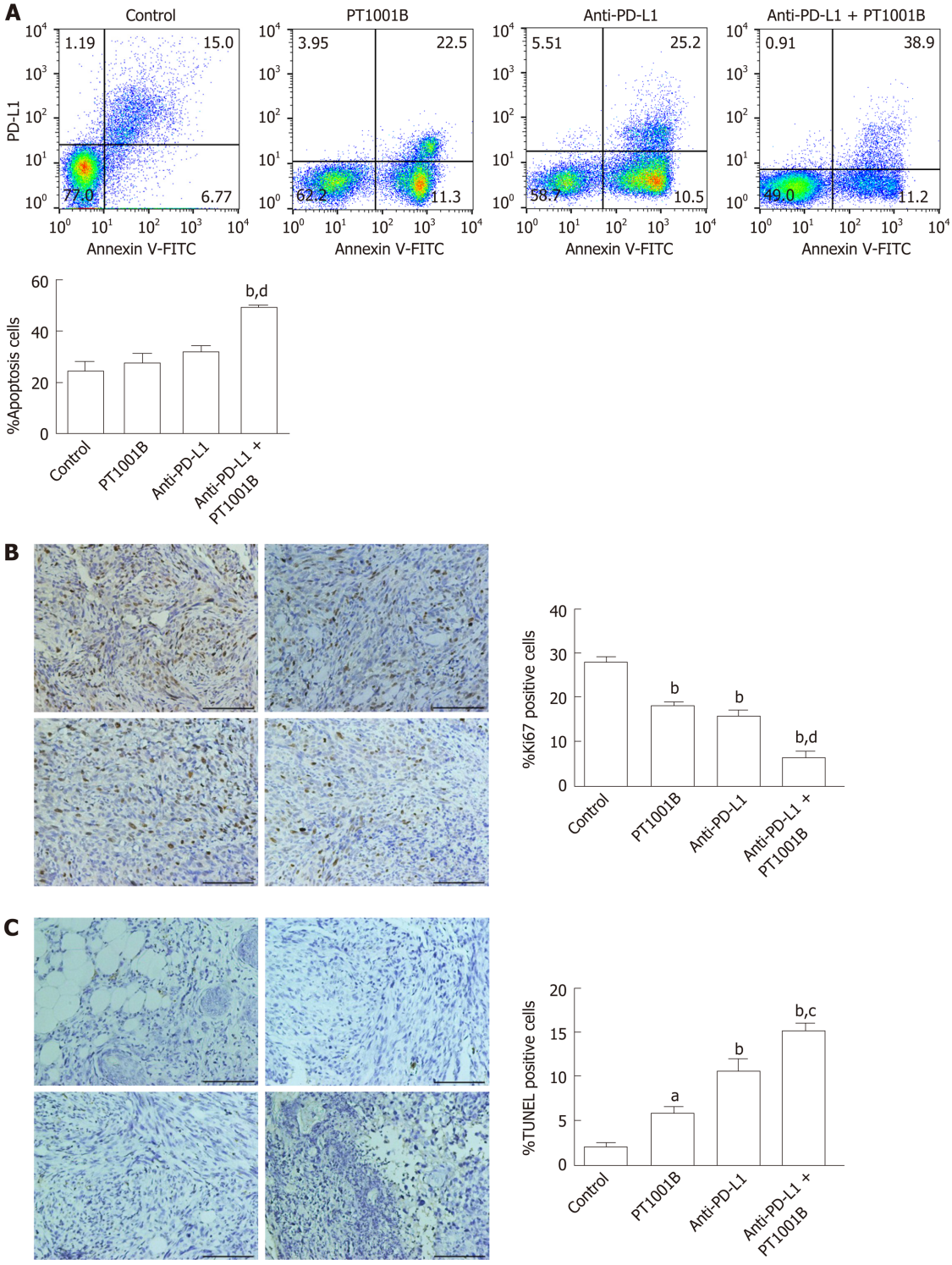

Figure 4 Effect of PT1001B and anti-programmed death-ligand-1 mAb on tumor cell proliferation and apoptosis. A: Cell suspensions prepared from pancreatic tumor tissues were stained with annexin V and propidium iodide to analyze the apoptosis rate by flow cytometry; B: The four groups of tumors were sectioned and stained for Ki67 (brown); C: The four groups of tumors were sectioned and subjected to TUNEL assay (brown). Representative images are shown. a: Control; b: PT1001B; c: Anti-programmed death-ligand-1 (PD-L1) mAb; d: Anti-PD-L1 mAb + PT1001B. Scale bars = 100 μm. The populations of apoptotic cells, Ki67-positive, or TUNEL-positive cells were analyzed by one-way ANOVA. Data represent the mean ± SE (n = 4). $^{a}P < 0.05$, $^{b}P < 0.01$ *vs* control group; $^{c}P < 0.05$, $^{d}P < 0.01$ *vs* anti-PD-L1 group. PI: Propidium iodide; FITC: Fluorescein Isothiocyanate; PD-L1: Programmed death-ligand-1; TUNEL: Terminal deoxynucleotidyl transferase mediated dUTP nick-end labeling.

immunosuppression to activate tumor-reactive CTLs that directly target tumor cells for apoptosis[24]. However, pancreatic cancer cannot be cured by PD-1/PD-L1 blockade alone because of the specific tumor microenvironment[25]. Therefore, the search for effective combination therapy will provide new clues that affect the efficacy of

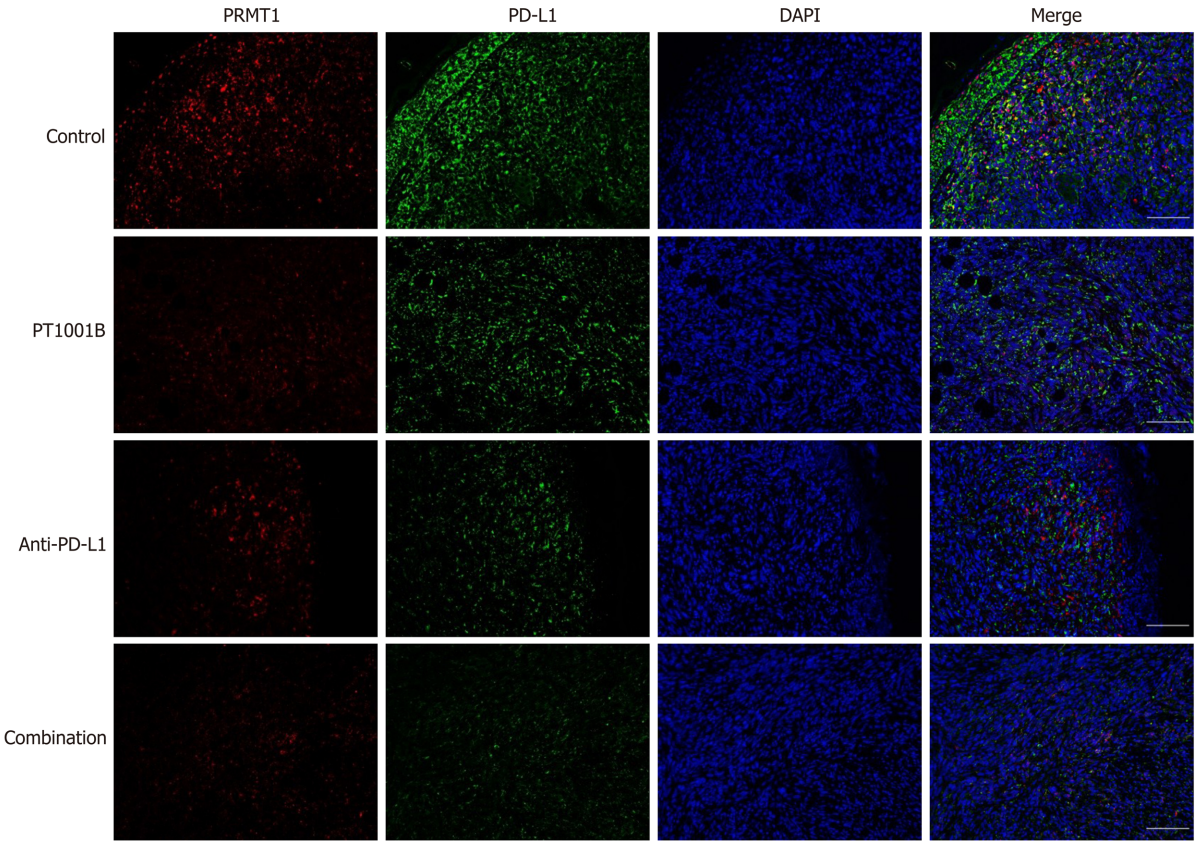

Figure 5 Immunofluorescence analysis of protein arginine methyltransferase and programmed death-ligand-1 in tumor tissue. Protein arginine methyltransferase 1 is shown in red, programmed death-ligand-1 is shown in green, and DAPI staining indicates the nucleus. Scale bars = 100 μm. PRMT: Protein arginine methyltransferase; PD-L1: Programmed death-ligand-1; DAPI: 2-(4-Amidinophenyl)-6-indolecarbamidine dihydrochloride.

immunotherapy. It was previously reported that MEK inhibitors, BET inhibitors, and mTOR inhibitors decreased PD-L1 expression *in vitro* and *in vivo*[26-28]. In our study, we identified a novel small-molecule inhibitor of type I PRMTs that also suppressed PD-L1 expression in pancreatic cancer cells.

In the present study, we demonstrated that the combination of PD-L1 blockade and PT1001B showed increased efficacy. A limited response to anti-PD-L1 monotherapy was observed in our PDAC model. Interestingly, the resistance to anti-PD-L1 therapy was reversed by the addition of PT1001B. When analyzing the expression of key immune checkpoint proteins and immune infiltration in the tumor microenvironment and spleen, we observed that the proportion of tumor-infiltrating effector cells was increased and the proportion of PD-1+ leukocytes was decreased in the combination group. This result is significant, as limited T cell infiltration is considered a barrier to the efficacy of immunotherapy in PDAC. CTLs primarily use perforin and Fas-mediated effector mechanisms to induce tumor cell apoptosis[29]. PD-1 is mainly expressed on activated CD4+ T cells, CD8+ T cells, and B cells in the periphery[30]. PD-1 inhibition can result in the loss of peripheral tolerance and an increase in autoimmunity[31]. In addition, PT1001B amplified the inhibitory effect of anti-PD-L1 on tumor cell proliferation and enhanced the induction of tumor cell apoptosis.

PRMT1 is the major methyltransferase in mammalian cells and is usually considered an epigenetic molecular marker. A previous study suggested that PRMT1 is overexpressed in pancreatic cancer cells and that elevated PRMT1 levels predict a poor clinical outcome. Moreover, PRMT1 knockdown was shown to inhibit tumor growth *in vivo*[13]. However, our results indicated that PT1001B alone did not decrease tumor growth. The discrepancy between our study and previous reports might be due to the use of different mouse models, cell lines, and inhibition methods. Our study results showed that PRMT1 downregulation was correlated with PD-L1 downregulation in PDAC tumors. Studies suggest that PRMT1 regulates *c-myc* gene expression and function[32,33]. Current data show that *c-myc*, an important signaling hub and driver gene, is commonly overexpressed and aberrantly activated in PDAC[34,35]. The activation of *c-myc* has been shown to stimulate PD-L1 expression in some cancer cells, causing immune evasion[36], and *c-myc* regulates PD-L1 expression in PDAC[37].

Therefore, we speculated that PT1001B might downregulate PD-L1 expression by inhibiting the master transcription amplifier *c-myc*. One limitation of this study is that PT1001B inhibits four PRMTs in addition to PRMT1 (PRMT3, PRMT4, PRMT6, and PRMT8), suggesting that it is a pan inhibitor of type I PRMTs[19]. Therefore, the specificity of PT1001B as an epigenetic agent in cancer therapy remains to be further studied.

In summary, our data demonstrate that the combination of the type I PRMT inhibitor and PD-L1 blockade may be an effective therapeutic approach for PDAC. PRMT1 expression is correlated with PD-L1 expression, and PRMT1 is a potential therapeutic target. Additional research aimed at elucidating the mechanisms by which PRMT1 regulates PD-L1 protein levels is warranted.

ARTICLE HIGHLIGHTS

Research background

The mechanism underlying pancreatic cancer resistance to anti-programmed death-1 (PD-1)/programmed death-ligand-1 (PD-L1) immunotherapy is poorly understood, but it has been suggested that PD-L1 expression in tumors is an important indicator of checkpoint immunotherapy efficacy. Considered an epigenetic molecular marker, protein arginine methyltransferases (PRMT)1 is the predominant type I methyltransferase responsible for the majority of cellular arginine methylation events. PRMT1 is deregulated in a wide variety of cancer types, whose biological role in tumor immunity is undefined.

Research motivation

We hope to search for new small-molecule inhibitors that influence PD-L1 expression and affect the efficacy of immunotherapy in pancreatic cancer.

Research objectives

To explore the combined antitumor effects of anti-PD-L1 and type I PRMT inhibitor on pancreatic cancer and the underlying mechanisms *in vivo*.

Research methods

The murine pancreatic ductal adenocarcinoma (PDAC) cells Panc02 were implanted subcutaneously in C57BL/6 mice, and the tumor-bearing mice were used to assess the drug efficacy, toxic and side effects, and tumor growth *in vivo*. We determined the expression of key immune checkpoint proteins, detected the apoptosis in tumor tissues, and analyzed the immune cells by flow cytometry (FCM). Immunohistochemistry staining for Ki67, TUNEL assay, and PRMT1/PD-L1 immunofluorescence were exploited to elucidate the underlying molecular mechanism.

Research results

Cultured Panc02 cells did not express PD-L1 *in vitro*, but tumor cells derived from Panc02 transplanted tumors expressed PD-L1. Drug treatment had no obvious toxic and side effects on mice. Neither PT1001B nor anti-PD-L1 mAb alone inhibited tumor growth compared to the control. However, the therapeutic efficacy of anti-PD-L1 mAb was significantly enhanced by the addition of PT1001B. PT1001B improved antitumor immunity by inhibiting PD-L1 expression on tumor cells, upregulating tumor-infiltrating CD8+ T lymphocytes, and decreasing PD-1+ leukocytes. In addition, PT1001B amplified the inhibitory effect of anti-PD-L1 mAb in inhibiting proliferation and promoting apoptosis of tumor cells. In tumor tissues, the downregulation of PRMT1 was related to the downregulation of PD-L1.

Research conclusions

PT1001B enhances anti-tumor immunity and combining it with anti-PD-L1 inhibits tumor growth effectively, reversing the resistance of PDAC to immunotherapy.

Research perspectives

Our data demonstrate that PT1001B is a promising inhibitor to change the tumor microenvironment in pancreatic cancer. PRMT1 is a potential therapeutic target, and additional research aimed at elucidating the mechanisms by which PRMT1 regulates PD-L1 is warranted.

ACKNOWLEDGEMENTS

The authors would like to acknowledge Cheng Luo and Yuanyuan Zhang (Chinese Academy of Sciences Shanghai Institute of Materia Medica, Shanghai, China) for providing PT1001B.

REFERENCES

1 **Ferlay J**, Soerjomataram I, Dikshit R, Eser S, Mathers C, Rebelo M, Parkin DM, Forman D, Bray F. Cancer incidence and mortality worldwide: sources, methods and major patterns in GLOBOCAN 2012. *Int J Cancer* 2015; **136**: E359-E386 [PMID: 25220842 DOI: 10.1002/ijc.29210]

2 **Siegel RL**, Miller KD, Jemal A. Cancer statistics, 2016. *CA Cancer J Clin* 2016; **66**: 7-30 [PMID: 26742998 DOI: 10.3322/caac.21332]

3 **Collisson EA**, Olive KP. Pancreatic Cancer: Progress and Challenges in a Rapidly Moving Field. *Cancer Res* 2017; **77**: 1060-1062 [PMID: 28209609 DOI: 10.1158/0008-5472.CAN-16-2452]

4 **Goldberg MV**, Maris CH, Hipkiss EL, Flies AS, Zhen L, Tuder RM, Grosso JF, Harris TJ, Getnet D, Whartenby KA, Brockstedt DG, Dubensky TW Jr, Chen L, Pardoll DM, Drake CG. Role of PD-1 and its ligand, B7-H1, in early fate decisions of CD8 T cells. *Blood* 2007; **110**: 186-192 [PMID: 17392506 DOI: 10.1182/blood-2006-12-062422]

5 **Wolchok JD**, Kluger H, Callahan MK, Postow MA, Rizvi NA, Lesokhin AM, Segal NH, Ariyan CE, Gordon RA, Reed K, Burke MM, Caldwell A, Kronenberg SA, Agunwamba BU, Zhang X, Lowy I, Inzunza HD, Feely W, Horak CE, Hong Q, Korman AJ, Wigginton JM, Gupta A, Sznol M. Nivolumab plus ipilimumab in advanced melanoma. *N Engl J Med* 2013; **369**: 122-133 [PMID: 23724867 DOI: 10.1056/NEJMoa1302369]

6 **Zheng L**. PD-L1 Expression in Pancreatic Cancer. *J Natl Cancer Inst* 2017; 109 [PMID: 28131993 DOI: 10.1093/jnci/djw304]

7 **Brahmer JR**, Tykodi SS, Chow LQ, Hwu WJ, Topalian SL, Hwu P, Drake CG, Camacho LH, Kauh J, Odunsi K, Pitot HC, Hamid O, Bhatia S, Martins R, Eaton K, Chen S, Salay TM, Alaparthy S, Grosso JF, Korman AJ, Parker SM, Agrawal S, Goldberg SM, Pardoll DM, Gupta A, Wigginton JM. Safety and activity of anti-PD-L1 antibody in patients with advanced cancer. *N Engl J Med* 2012; **366**: 2455-2465 [PMID: 22658128 DOI: 10.1056/NEJMoa1200694]

8 **Topalian SL**, Drake CG, Pardoll DM. Immune checkpoint blockade: a common denominator approach to cancer therapy. *Cancer Cell* 2015; **27**: 450-461 [PMID: 25858804 DOI: 10.1016/j.ccell.2015.03.001]

9 **Dong H**, Strome SE, Salomao DR, Tamura H, Hirano F, Flies DB, Roche PC, Lu J, Zhu G, Tamada K, Lennon VA, Celis E, Chen L. Tumor-associated B7-H1 promotes T-cell apoptosis: a potential mechanism of immune evasion. *Nat Med* 2002; **8**: 793-800 [PMID: 12091876 DOI: 10.1038/nm730]

10 **Bedford MT**, Richard S. Arginine methylation an emerging regulator of protein function. *Mol Cell* 2005; **18**: 263-272 [PMID: 15866169 DOI: 10.1016/j.molcel.2005.04.003]

11 **Smith E**, Zhou W, Shindiapina P, Sif S, Li C, Baiocchi RA. Recent advances in targeting protein arginine methyltransferase enzymes in cancer therapy. *Expert Opin Ther Targets* 2018; **22**: 527-545 [PMID: 29781349 DOI: 10.1080/14728222.2018.1474203]

12 **Wang Y**, Hsu JM, Kang Y, Wei Y, Lee PC, Chang SJ, Hsu YH, Hsu JL, Wang HL, Chang WC, Li CW, Liao HW, Chang SS, Xia W, Ko HW, Chou CK, Fleming JB, Wang H, Hwang RF, Chen Y, Qin J, Hung MC. Oncogenic Functions of Gli1 in Pancreatic Adenocarcinoma Are Supported by Its PRMT1-Mediated Methylation. *Cancer Res* 2016; **76**: 7049-7058 [PMID: 27758883 DOI: 10.1158/0008-5472.can-16-0715]

13 **Song C**, Chen T, He L, Ma N, Li JA, Rong YF, Fang Y, Liu M, Xie D, Lou W. PRMT1 promotes pancreatic cancer growth and predicts poor prognosis. *Cell Oncol (Dordr)* 2020; **43**: 51-62 [PMID: 31520395 DOI: 10.1007/s13402-019-00435-1]

14 **Altan B**, Yokobori T, Ide M, Mochiki E, Toyomasu Y, Kogure N, Kimura A, Hara K, Bai T, Bao P, Suzuki M, Ogata K, Asao T, Nishiyama M, Oyama T, Kuwano H. Nuclear PRMT1 expression is associated with poor prognosis and chemosensitivity in gastric cancer patients. *Gastric Cancer* 2016; **19**: 789-797 [PMID: 26472729 DOI: 10.1007/s10120-015-0551-7]

15 **Madreiter-Sokolowski CT**, Győrffy B, Klec C, Sokolowski AA, Rost R, Waldeck-Weiermair M, Malli R, Graier WF. UCP2 and PRMT1 are key prognostic markers for lung carcinoma patients. *Oncotarget* 2017; **8**: 80278-80285 [PMID: 29113301 DOI: 10.18632/oncotarget.20571]

16 **Zhang Y**, Wang D, Zhang M, Wei H, Lu Y, Sun Y, Zhou M, Gu S, Feng W, Wang H, Zeng J, Gong A, Xu M. Protein arginine methyltransferase 1 coordinates the epithelial-mesenchymal transition/proliferation dichotomy in gastric cancer cells. *Exp Cell Res* 2018; **362**: 43-50 [PMID: 29097184 DOI: 10.1016/j.yexcr.2017.10.035]

17 **Liao HW**, Hsu JM, Xia W, Wang HL, Wang YN, Chang WC, Arold ST, Chou CK, Tsou PH, Yamaguchi H, Fang YF, Lee HJ, Lee HH, Tai SK, Yang MH, Morelli MP, Sen M, Ladbury JE, Chen CH, Grandis JR, Kopetz S, Hung MC. PRMT1-mediated methylation of the EGF receptor regulates signaling and cetuximab response. *J Clin Invest* 2015; **125**: 4529-4543 [PMID: 26571401 DOI: 10.1172/JCI82826]

18 **Cha B**, Kim W, Kim YK, Hwang BN, Park SY, Yoon JW, Park WS, Cho JW, Bedford MT, Jho EH. Methylation by protein arginine methyltransferase 1 increases stability of Axin, a negative regulator of Wnt signaling. *Oncogene* 2011; **30**: 2379-2389 [PMID: 21242974 DOI: 10.1038/onc.2010.610]

19 **Wang C**, Jiang H, Jin J, Xie Y, Chen Z, Zhang H, Lian F, Liu YC, Zhang C, Ding H, Chen S, Zhang N, Zhang Y, Jiang H, Chen K, Ye F, Yao Z, Luo C. Development of Potent Type I Protein Arginine Methyltransferase (PRMT) Inhibitors of Leukemia Cell Proliferation. *J Med Chem* 2017; **60**: 8888-8905 [PMID: 29019697 DOI: 10.1021/acs.jmedchem.7b01134]

20 **Torphy RJ**, Zhu Y, Schulick RD. Immunotherapy for pancreatic cancer: Barriers and breakthroughs. *Ann*

Gastroenterol Surg 2018; **2**: 274-281 [PMID: 30003190 DOI: 10.1002/ags3.12176]

21 **Mace TA**, Shakya R, Pitarresi JR, Swanson B, McQuinn CW, Loftus S, Nordquist E, Cruz-Monserrate Z, Yu L, Young G, Zhong X, Zimmers TA, Ostrowski MC, Ludwig T, Bloomston M, Bekaii-Saab T, Lesinski GB. IL-6 and PD-L1 antibody blockade combination therapy reduces tumour progression in murine models of pancreatic cancer. *Gut* 2018; **67**: 320-332 [PMID: 27797936 DOI: 10.1136/gutjnl-2016-311585]

22 **Xu C**, Fillmore CM, Koyama S, Wu H, Zhao Y, Chen Z, Herter-Sprie GS, Akbay EA, Tchaicha JH, Altabef A, Reibel JB, Walton Z, Ji H, Watanabe H, Jänne PA, Castrillon DH, Rustgi AK, Bass AJ, Freeman GJ, Padera RF, Dranoff G, Hammerman PS, Kim CF, Wong KK. Loss of Lkb1 and Pten leads to lung squamous cell carcinoma with elevated PD-L1 expression. *Cancer Cell* 2014; **25**: 590-604 [PMID: 24794706 DOI: 10.1016/j.ccr.2014.03.033]

23 **Alvarez Arias DA**, Kim HJ, Zhou P, Holderried TA, Wang X, Dranoff G, Cantor H. Disruption of CD8+ Treg activity results in expansion of T follicular helper cells and enhanced antitumor immunity. *Cancer Immunol Res* 2014; **2**: 207-216 [PMID: 24778317 DOI: 10.1158/2326-6066.CIR-13-0121]

24 **Herbst RS**, Soria JC, Kowanetz M, Fine GD, Hamid O, Gordon MS, Sosman JA, McDermott DF, Powderly JD, Gettinger SN, Kohrt HE, Horn L, Lawrence DP, Rost S, Leabman M, Xiao Y, Mokatrin A, Koeppen H, Hegde PS, Mellman I, Chen DS, Hodi FS. Predictive correlates of response to the anti-PD-L1 antibody MPDL3280A in cancer patients. *Nature* 2014; **515**: 563-567 [PMID: 25428504 DOI: 10.1038/nature14011]

25 **Feng M**, Xiong G, Cao Z, Yang G, Zheng S, Song X, You L, Zheng L, Zhang T, Zhao Y. PD-1/PD-L1 and immunotherapy for pancreatic cancer. *Cancer Lett* 2017; **407**: 57-65 [PMID: 28826722 DOI: 10.1016/j.canlet.2017.08.006]

26 **Hogg SJ**, Vervoort SJ, Deswal S, Ott CJ, Li J, Cluse LA, Beavis PA, Darcy PK, Martin BP, Spencer A, Traunbauer AK, Sadovnik I, Bauer K, Valent P, Bradner JE, Zuber J, Shortt J, Johnstone RW. BET-Bromodomain Inhibitors Engage the Host Immune System and Regulate Expression of the Immune Checkpoint Ligand PD-L1. *Cell Rep* 2017; **18**: 2162-2174 [PMID: 28249162 DOI: 10.1016/j.celrep.2017.02.011]

27 **Qiu XY**, Hu DX, Chen WQ, Chen RQ, Qian SR, Li CY, Li YJ, Xiong XX, Liu D, Pan F, Yu SB, Chen XQ. PD-L1 confers glioblastoma multiforme malignancy via Ras binding and Ras/Erk/EMT activation. *Biochim Biophys Acta Mol Basis Dis* 2018; **1864**: 1754-1769 [PMID: 29510196 DOI: 10.1016/j.bbadis.2018.03.002]

28 **Lastwika KJ**, Wilson W 3rd, Li QK, Norris J, Xu H, Ghazarian SR, Kitagawa H, Kawabata S, Taube JM, Yao S, Liu LN, Gills JJ, Dennis PA. Control of PD-L1 Expression by Oncogenic Activation of the AKT-mTOR Pathway in Non-Small Cell Lung Cancer. *Cancer Res* 2016; **76**: 227-238 [PMID: 26637667 DOI: 10.1158/0008-5472.CAN-14-3362]

29 **Lu C**, Paschall AV, Shi H, Savage N, Waller JL, Sabbatini ME, Oberlies NH, Pearce C, Liu K. The MLL1-H3K4me3 Axis-Mediated PD-L1 Expression and Pancreatic Cancer Immune Evasion. *J Natl Cancer Inst* 2017; 109 [PMID: 28131992 DOI: 10.1093/jnci/djw283]

30 **Ishida Y**, Agata Y, Shibahara K, Honjo T. Induced expression of PD-1, a novel member of the immunoglobulin gene superfamily, upon programmed cell death. *EMBO J* 1992; **11**: 3887-3895 [PMID: 1396582 DOI: 10.1002/j.1460-2075.1992.tb05481.x]

31 **Nishimura H**, Okazaki T, Tanaka Y, Nakatani K, Hara M, Matsumori A, Sasayama S, Mizoguchi A, Hiai H, Minato N, Honjo T. Autoimmune dilated cardiomyopathy in PD-1 receptor-deficient mice. *Science* 2001; **291**: 319-322 [PMID: 11209085 DOI: 10.1126/science.291.5502.319]

32 **Tikhanovich I**, Zhao J, Bridges B, Kumer S, Roberts B, Weinman SA. Arginine methylation regulates c-Myc-dependent transcription by altering promoter recruitment of the acetyltransferase p300. *J Biol Chem* 2017; **292**: 13333-13344 [PMID: 28652407 DOI: 10.1074/jbc.M117.797928]

33 **Favia A**, Salvatori L, Nanni S, Iwamoto-Stohl LK, Valente S, Mai A, Scagnoli F, Fontanella RA, Totta P, Nasi S, Illi B. The Protein Arginine Methyltransferases 1 and 5 affect Myc properties in glioblastoma stem cells. *Sci Rep* 2019; **9**: 15925 [PMID: 31685892 DOI: 10.1038/s41598-019-52291-6]

34 **Wirth M**, Mahboobi S, Krämer OH, Schneider G. Concepts to Target MYC in Pancreatic Cancer. *Mol Cancer Ther* 2016; **15**: 1792-1798 [PMID: 27406986 DOI: 10.1158/1535-7163.MCT-16-0050]

35 **Hessmann E**, Schneider G, Ellenrieder V, Siveke JT. MYC in pancreatic cancer: novel mechanistic insights and their translation into therapeutic strategies. *Oncogene* 2016; **35**: 1609-1618 [PMID: 26119937 DOI: 10.1038/onc.2015.216]

36 **Casey SC**, Tong L, Li Y, Do R, Walz S, Fitzgerald KN, Gouw AM, Baylot V, Gütgemann I, Eilers M, Felsher DW. MYC regulates the antitumor immune response through CD47 and PD-L1. *Science* 2016; **352**: 227-231 [PMID: 26966191 DOI: 10.1126/science.aac9935]

37 **Pan Y**, Fei Q, Xiong P, Yang J, Zhang Z, Lin X, Pan M, Lu F, Huang H. Synergistic inhibition of pancreatic cancer with anti-PD-L1 and c-Myc inhibitor JQ1. *Oncoimmunology* 2019; **8**: e1581529 [PMID: 31069140 DOI: 10.1080/2162402X.2019.1581529]

World Journal of Gastroenterology

Submit a Manuscript: https://www.f6publishing.com

World J Gastroenterol 2020 July 14; 26(26): 3750-3766

DOI: 10.3748/wjg.v26.i26.3750

ISSN 1007-9327 (print) ISSN 2219-2840 (online)

ORIGINAL ARTICLE

Basic Study

Adipose-derived mesenchymal stem cells alleviate TNBS-induced colitis in rats by influencing intestinal epithelial cell regeneration, Wnt signaling, and T cell immunity

Jian-Guo Gao, Mo-Sang Yu, Meng-Meng Zhang, Xue-Wei Gu, Yue Ren, Xin-Xin Zhou, Dong Chen, Tian-Lian Yan, You-Ming Li, Xi Jin

ORCID number: Jian-Guo Gao 0000-0002-9414-5395; Mo-Sang Yu 0000-0002-5614-0227; Meng-Meng Zhang 0000-0002-5390-7947; Xue-Wei Gu 0000-0002-8391-6182; Yue Ren 0000-0001-9071-2738; Xin-Xin Zhou 0000-0003-0183-6400; Dong Chen 0000-0002-9581-8774; Tian-Lian Yan 0000-0003-2322-5029; You-Ming Li 0000-0001-9279-2903; Xi Jin 0000-0001-9985-3035.

Author contributions: Gao JG and Yu MS contributed equally to this work, and they designed the study and drafted the manuscript; Zhang MM, Gu XW, Ren Y, and Zhou XX performed the study; Chen D conducted the statistical analysis; Zhang MM and Yan TL provided guidance during revision; Jin X and Li YM supervised the study and provided consultation during the entire study.

Supported by National Natural Science Foundation of China, No. 81770574, No. 81600414, and No. 81600447.

Institutional animal care and use committee statement: This study was carried out in accordance with the recommendations in the Guide for the Care and Use of Laboratory Animals of the National Institutes

Jian-Guo Gao, Mo-Sang Yu, Meng-Meng Zhang, Xue-Wei Gu, Yue Ren, Xin-Xin Zhou, Tian-Lian Yan, You-Ming Li, Xi Jin, Department of Gastroenterology, The First Affiliated Hospital, School of Medicine, Zhejiang University, Hangzhou 310003, Zhejiang Province, China

Dong Chen, Department of Colorectal Surgery, The First Affiliated Hospital, School of Medicine, Zhejiang University, Hangzhou 310003, Zhejiang Province, China

Corresponding author: Xi Jin, PhD, Associate Chief Physician, Department of Gastroenterology, The First Affiliated Hospital, School of Medicine, Zhejiang University, No. 79, Qingchun Road, Hangzhou 310003, Zhejiang Province, China. jxfl007@zju.edu.cn

Abstract

BACKGROUND

Conventional Crohn's disease (CD) treatments are supportive rather than curative and have serious side effects. Adipose-derived mesenchymal stem cells (ADSCs) have been gradually applied to treat various diseases. The therapeutic effect and underlying mechanism of ADSCs on CD are still not clear.

AIM

To investigate the effect of ADSC administration on CD and explore the potential mechanisms.

METHODS

Wistar rats were administered with 2,4,6-trinitrobenzene sulfonic acid (TNBS) to establish a rat model of CD, followed by tail injections of green fluorescent protein (GFP)-modified ADSCs. Flow cytometry, qRT-PCR, and Western blot were used to detect changes in the Wnt signaling pathway, T cell subtypes, and their related cytokines.

RESULTS

The isolated cells showed the characteristics of ADSCs, including spindle-shaped morphology, high expression of CD29, CD44, and CD90, low expression of CD34 and CD45, and osteogenic/adipogenic ability. ADSC therapy markedly reduced disease activity index and ameliorated colitis severity in the TNBS-induced rat

model of CD. Furthermore, serum anti-sacchromyces cerevisiae antibody and p-anti-neutrophil cytoplasmic antibody levels were significantly reduced in ADSC-treated rats. Mechanistically, the GFP-ADSCs were colocalized with intestinal epithelial cells (IECs) in the CD rat model. GFP-ADSC delivery significantly antagonized TNBS-induced increased canonical Wnt pathway expression, decreased noncanonical Wnt signaling pathway expression, and increased apoptosis rates and protein level of cleaved caspase-3 in rats. In addition, ADSCs attenuated TNBS-induced abnormal inflammatory cytokine production, disturbed T cell subtypes, and their related markers in rats.

CONCLUSION

Successfully isolated ADSCs show therapeutic effects in CD by regulating IEC proliferation, the Wnt signaling pathway, and T cell immunity.

Key words: Crohn's disease; Adipose-derived mesenchymal stem cell; Intestinal epithelial cell; Wnt pathway; T cell; Inflammation

Core tip: The prevalence and mortality of Crohn's disease (CD) have been increasing globally, including in areas of Asia that previously had a low incidence. We aimed to investigate the effect and explore potential mechanisms of adipose-derived mesenchymal stem cells (ADSCs) in a 2,4,6-trinitrobenzene sulfonic acid-induced rat model of CD. Our study for the first time provided evidence that successfully isolated ADSCs show therapeutic effects in CD by regulating intestinal epithelial cell proliferation, the Wnt signaling pathway, and T cell immunity.

Citation: Gao JG, Yu MS, Zhang MM, Gu XW, Ren Y, Zhou XX, Chen D, Yan TL, Li YM, Jin X. Adipose-derived mesenchymal stem cells alleviate TNBS-induced colitis in rats by influencing intestinal epithelial cell regeneration, Wnt signaling, and T cell immunity. *World J Gastroenterol* 2020; 26(26): 3750-3766
URL: https://www.wjgnet.com/1007-9327/full/v26/i26/3750.htm
DOI: https://dx.doi.org/10.3748/wjg.v26.i26.3750

INTRODUCTION

Crohn's disease (CD), a major subtype of inflammatory bowel disease (IBD), is a chronic inflammatory disorder of the gastrointestinal tract. Patients with CD exhibit diverse symptoms and lesions ranging from abdominal pain, diarrhea, hematochezia, ulceration, and perforation of the gastrointestinal tract[1]. The prevalence and mortality of CD have been increasing globally, including in areas of Asia that previously had a low incidence[2]. Conventional CD treatments consist of aminosalicylates, corticosteroids, antitumor necrosis factor agents, and immunomodulators[3]. Although the majority of patients benefit from these treatments, the treatments are supportive rather than curative and have serious side effects.

Mesenchymal stem cells (MSCs) are progenitor cells with self-renewal abilities, multiple-lineage differentiation potential, rapid growth, and immunomodulatory capabilities[4]. MSCs can be isolated from many tissues, including bone marrow (BM-MSC) and adipose tissue (ADSC). MSCs have been gradually applied to treat various diseases, mainly by transplantation to repair pathological cells and reconstruct normal cells[5]. The application of MSCs in treating IBD has become a hot research topic, but the underlying mechanisms are still vague[6]. The Wnt signaling (canonical and noncanonical) pathway is a major pathway in stem cell proliferation and differentiation[7]. The canonical Wnt pathway is activated by the binding of Wnt3a to the frizzled receptor (Fz) and its coreceptor complex[8]. This leads to stabilization of β-catenin, which translocates to the nucleus and interacts with T cell factor/lymphoid enhancer factor[9], further stimulating intestinal crypt cell proliferation and maintaining a stem cell state[10]. Noncanonical signaling is activated by Wnt5a and is implicated in the establishment of cell polarity and migration, inflammation, and cancer development. Ror2 acts as a receptor or coreceptor for Wnt5a and regulates

of Health. The animal protocol was approved by the institutional review board of the First Affiliated Hospital of Zhejiang University and adhered to the standards articulated in Animal Research. The study was reviewed and approved by Animal Experimental Ethical Inspection of the First Affiliated Hospital, College of Medicine, Zhejiang University.

Conflict-of-interest statement: The authors have no conflicts of interest to disclose.

Data sharing statement: No additional data are available.

ARRIVE guidelines statement: Authors have read the ARRIVE guidelines and prepared and revised the manuscript according to the ARRIVE guidelines.

Manuscript source: Invited manuscript

Received: December 27, 2019
Peer-review started: December 27, 2019
First decision: February 14, 2020
Revised: May 14, 2020
Accepted: June 3, 2020
Article in press: June 3, 2020
Published online: July 14, 2020

P-Reviewer: Scaringi S
S-Editor: Liu M
L-Editor: Wang TQ
E-Editor: Ma YJ

Wnt5a-induced activation of planar cell polarity and Wnt-Ca^{2+} pathways, playing an important role in the maintenance of stemness[11]. A previous study showed the activation of Wnt3a in IBD rats, suggesting the potential involvement of the canonical Wnt pathway in CD[12]. However, the mechanisms of the noncanonical Wnt pathway in CD remain unclear and require further investigation.

Disturbances in the immune system also play an important role in the pathogenesis of CD. T cells play central roles in immune regulation and can be divided into T helper type 1 (Th1), Th2, Th17, and regulatory T (Treg) cells according to their different functions[13]. Previous studies showed that T cells are important mediators of the inflammatory response in CD[14], and the proportions of Th1 and Th17 cells was higher, while that of Treg cells was lower in CD patients compared to healthy controls. Moreover, patients with lower Treg/Th1 and Treg/Th17 ratios suffer a higher risk of CD recurrence, while Treg restoration prevented colitis in a mouse CD model[15]. These findings suggest that the imbalance in T cell subgroups is related to the activation and progression of CD. Since ADSCs have been shown to treat systemic lupus erythematosus by increasing the number of Treg cells and reducing Th17 cells[16], it is plausible that its therapeutic effect on CD may be through regulating T cell immunity. In addition to the Wnt pathway and T cell immunity, intestinal cell regeneration is also vital in CD progression, mainly by accelerating mucosal healing[17]. However, whether the therapeutic effect of ADSCs on CD occurs by influencing intestinal cell regeneration has not been reported.

The trinitrobenzene sulfonic acid (TNBS)-induced rat colitis model is one of the most commonly used experimental CD models[18]. Therefore, in this study, we explored the therapeutic effect of ADSCs by tail administration in a TNBS-induced rat CD model. We then traced the location of injected ADSCs to study its roles in repairing damaged intestinal epithelium, involving Wnt signaling pathways and T cell balance.

MATERIALS AND METHODS

Ethics

This study was carried out in accordance with the recommendations in the Guide for the Care and Use of Laboratory Animals of the National Institutes of Health. The animal protocol was approved by the institutional review board of the First Affiliated Hospital of Zhejiang University and adhered to the standards articulated in animal research.

Isolation, culture, identification, and evaluation of ADSCs from inguinal fat

Inguinal fat, one of the major sources of MSCs, was obtained aseptically from rats and digested with collagenase type I in Dulbecco's modified Eagle's medium at 37°C for 45 min. Cell suspensions were sequentially filtered, centrifuged, resuspended, and cultured in DMEM-F12 medium [supplemented with 10% fetal bovine serum (FBS), 20 ng/μL transforming growth factor, and 1% penicillin/streptomycin] at 37°C with 5% CO_2. When the adherent cells reached 80% to 90% confluence, the replication-defective recombinant lentiviral vector carrying green fluorescent protein (GFP) (LT88008, Vigene Biosciences) was added and cultured for 72 h, followed by phosphate buffered saline (PBS) washing and trypsinization. The final third-passage cells were used to evaluate the ADSC phenotype. The immunophenotyping of ADSCs was analyzed by flow cytometry. Thereafter, cell counting kit-8 was used to measure the number of live cells at days 0, 2, 4, 6, 8, and 10. ADSCs were separately cultured with osteogenic-inducing medium and adipogenic-inducing medium for 14 d. To assess the osteogenic capacity, alkaline phosphatase (ALP) activity was measured using an ELISA kit (C059-1, Nanjing Jiancheng, China) by detecting the absorbance at 520 nm. To assess the adipogenic capacity, routine red O staining was performed, and the dyed ADSCs were observed under a microscope.

CD model establishment in rats by TNBS administration and the effect of ADSC injection

Thirty male Wistar rats (150-200 g) aged 6 wk (Cavens Lab Animal, Suzhou, China) were randomly divided into three groups (n = 8 for each): Control, CD, and CD + GFP-ADSCs. All rats received food and water *ad libitum* and were maintained on a 12/12 h light/dark cycle. After 1 wk, rats in the CD and CD + GFP-ADSCs groups were administered with 1.0 mL of 20 mg TNBS in a 50% ethanol solution following a 24 h

fast. Enemas were performed by inserting an 8 cm soft tube into the rat's anus under inhalation anesthesia with 3% sodium phenobarbital. In the control group, the rats underwent with the same procedure and were administered with an equivalent amount of physiological saline. Subsequently, on day 8, the GFP-ADSCs were injected *via* the tail vein at a dose of 1×10^7 cells in 0.3 mL of PBS into the rats in the CD + GFP-ADSCs group. In the control and CD groups, the rats received 0.3 mL of PBS without ADSCs following the same protocol.

The body weight, stool consistency, and rectal bleeding of each rat were recorded on day 7 after model establishment and days 7, 14, 21, and 28 after ADSC treatment. A well-known formula to determine the serial disease activity index (DAI), ranging from 0 to 12, including aspects of weight loss, stool characteristics, and bloody stool, was used to assess the clinical severity of colitis. On day 28, all rats were sacrificed, and blood and tissue samples were collected. The colon was retrieved to observe morphological changes. A 0.5 cm length of colonic tissue from the area 6 cm above the anus was collected for hematoxylin and eosin (HE) staining, followed by Lgr5/CK-20 immunofluorescence detection by confocal microscopy, apoptosis analysis by the TUNEL method, and Western blot/qRT-PCR analysis for Wnt pathway/T cell immunity-related proteins and mRNA. Finally, the serum anti-sacchromyces cerevisiae antibody (ASCA) and p-antineutrophil cytoplasmic antibody (p-ANCA) levels were measured with ELISA kits (CK-EN34476, CK-EN35015, Yuanye Co. Ltd, Shanghai, China).

Tracing GFP-ADSC distribution and TUNEL assay

To test the effect of ADSCs on colonic epithelial cell regeneration, ADSCs were transfected with a lentiviral vector containing green fluorescent protein (LV-GFP). After 28 d of GFP-ADSC treatment, the rats were sacrificed, and the heart, liver, spleen, lung, kidney, and colon tissues were collected to detect the GFP-positive cell expression pattern throughout the body by fluorescence confocal microscopy. The colon section was additionally stained with antibodies against GFP, CD20, and Lgr5, followed by visualization using FITC-conjugated secondary antibodies under a confocal microscope. The number of positive cells was calculated and compared between different groups. For apoptosis analysis of the intestinal cells, colon tissue specimens were embedded in paraffin and sectioned at 5 μm for processing by the TUNEL method (Roche, Shanghai, China). The apoptotic cells were dyed and observed under an Olympus microscope. Ten visual fields were selected, 100 cells within each field were counted, and the following formula was applied: Apoptosis index = (apoptosis cell/total cell) × 100%[19].

Analysis of T cell subtypes in peripheral blood by flow cytometry

Blood samples were collected in sterile vacutainer tubes containing heparin (100 U/mL). Peripheral blood mononuclear cells (PBMCs) were isolated by sequential centrifugation and suspended in RPMI-1640 with 10% FBS, followed by incubation at 37°C in a 5% CO_2 incubator for 2-3 h. PBMCs with a viability greater than 95% as determined by the trypan blue dyeing method were chosen for further experiments. For Th1, Th2, and Th17 cell analysis, 200 mL of PBMC (1×10^7/mL) suspension was added with phorbol ester (50 ng/mL), ionomycin (1 μg/mL), and monensin (2 μmol/L) and incubated in a 5% CO_2 incubator for 6 h. After triple washing with PBS, the resuspended PBMC suspension was separately added with CD4 monoclonal antibody and IFN-γ/IL-4/IL-17 monoclonal antibody. The mixture was cultured at 4°C for 30 min and analyzed by flow cytometry. For Treg cell analysis, the same amount of PBMC suspension was stained at 4 °C for 30 min with CD4 and CD25 monoclonal antibodies. Thereafter, 10 μL of Foxp3 monoclonal antibody was added and cultured for an additional 20 min, followed by flow cytometry analysis.

Western blot and qRT-PCR

The transcription factor Foxp3 is a marker of Treg cells, GATA3 is a marker of T helper cells, RORγt is a transcription factor that is specific for Th17 lineage commitment, and T-bet is a biomarker for Th1 cells[13,20]. They were used as supplementary markers for different T cell types and routinely quantified by Western blot using an ECL chemiluminescence kit (Santa Cruz, United States). The levels of Wnt pathway/T cell immunity-related mRNA were detected by qRT-PCR. Total RNA was extracted from colon tissues with TRIzol reagent, and the concentration and quality were assessed. The RNA was then reverse-transcribed using a FastQuant RT kit according to the manufacturer's protocol. qRT-PCR was conducted using SYBR Green SuperReal PreMix Plus and a 7500 Real-time PCR system. Gene expression levels were

determined using the comparative threshold cycle (ΔΔCt) method. β-actin was used as an internal control for both Western blot and qRT-PCR. The detailed primer sequences for qRT-PCR are shown in Supplementary Table 1.

Statistics analysis

Statistical analyses were performed by using Statistical Package for the Social Sciences version 16.0. The data are presented as the mean ± standard deviation when they were normally distributed or as medians when the distribution was skewed. Unpaired *t*-test and Mann-Whitney *U* test for parametric and nonparametric analyses were used for comparisons between two groups. The Kruskal-Wallis test was used for comparisons among three groups. A P value < 0.05 was considered statistically significant.

RESULTS

Isolation and characterization of ADSCs

The isolated cells were evaluated based on morphology, molecular biomarkers, and stemness. As shown in Figure 1A, cells extracted from groin fat exhibited the characteristics of ADSCs, including spindle-shaped morphology and whirlpool/radial-arranged growth. The lentivirus-mediated construction of GFP-ADSCs was confirmed by green fluorescence detection. Flow cytometry showed that these cells had the typical marker pattern of ADSCs, including high expression of CD29, CD44, and CD90 but low levels of CD34 and CD45 (Figure 1B). The quality of the isolated cells was good, evidenced by a typical S-like proliferation curve (Figure 1C). The stemness of the isolated cells was evaluated by osteogenic and adipogenic induction. After osteogenic induction, ADSCs and GFP-ADSCs showed significantly higher ALP activity compared with that of controls (Figure 1D). After adipogenic induction, lipid droplets were observed in the cytoplasm of ADSCs and GFP-ADSCs, as shown by a brick-red color change after staining with Oil red O (Figure 1E). Taken together, these data suggested that these isolated cells presented a typical phenotype of ADSCs.

ADSCs alleviate TNBS-induced experimental colitis in rats

The therapeutic effect of ADSCs was evaluated in rats with TNBS-induced experimental colitis. To assess the severity of colitis, DAI and body weight changes were recorded every 7 d. The DAI was significantly increased, while the body weight was significantly decreased after TNBS administration, and ADSC therapy significantly reduced DAI in a time-dependent manner (Figure 2A). Although there was self-alleviation of DAI in the CD group after withdrawal of TNBS, a significantly lower DAI was observed in the CD + GFP-ADSCs group starting 7 d after TNBS delivery compared with that of the CD group. On day 28, the rat weight in the CD + GFP-ADSCs group became significantly higher than that in the CD group (Supplementary Table 2).

The colon length was significantly shorter in the CD group than in the control group, which partially recovered after ADSC therapy, although this difference was not statistically significant (Figure 2B). The intestinal ulceration and inflammation severity were further evaluated by HE staining. As illustrated in Figure 2C, the colon tissue structure of control rats was clear, the mucosa was complete, and the intestinal glands in the lamina propria were rich and closely arranged; in the CD group, the arrangement of intestinal glands was disordered, the mucosa was damaged, and there were a large number of infiltrated inflammatory cells; after ADSC treatment, the damaged mucosa and the disordered intestinal glands in the lamina propria were improved. Furthermore, we found a significant reduction in plasma ASCA and p-ANCA concentrations in GFP-ADSC-treated rats (Figure 2D).

ADSC therapy stimulates colonic epithelial proliferation in rats with TNBS-induced colitis

The distribution of ADSCs was detected by adding GFP to ADSCs and observed by using fluorescence confocal microscopy. GFP fluorescence was detected in the spleen, lung, and colon of the CD + GFP-ADSCs group, and the density was relatively higher in the colon. In contrast, GFP fluorescence was not observed in the heart, liver, and kidney (Figure 3A). CK-20 is a biomarker for intestinal epithelial cells (IECs) and is indicative of mucosal healing and proliferation. As shown in Figure 3B, more CK-20-positive cells were present in the bottom of the crypts in the ADSC-treated group than

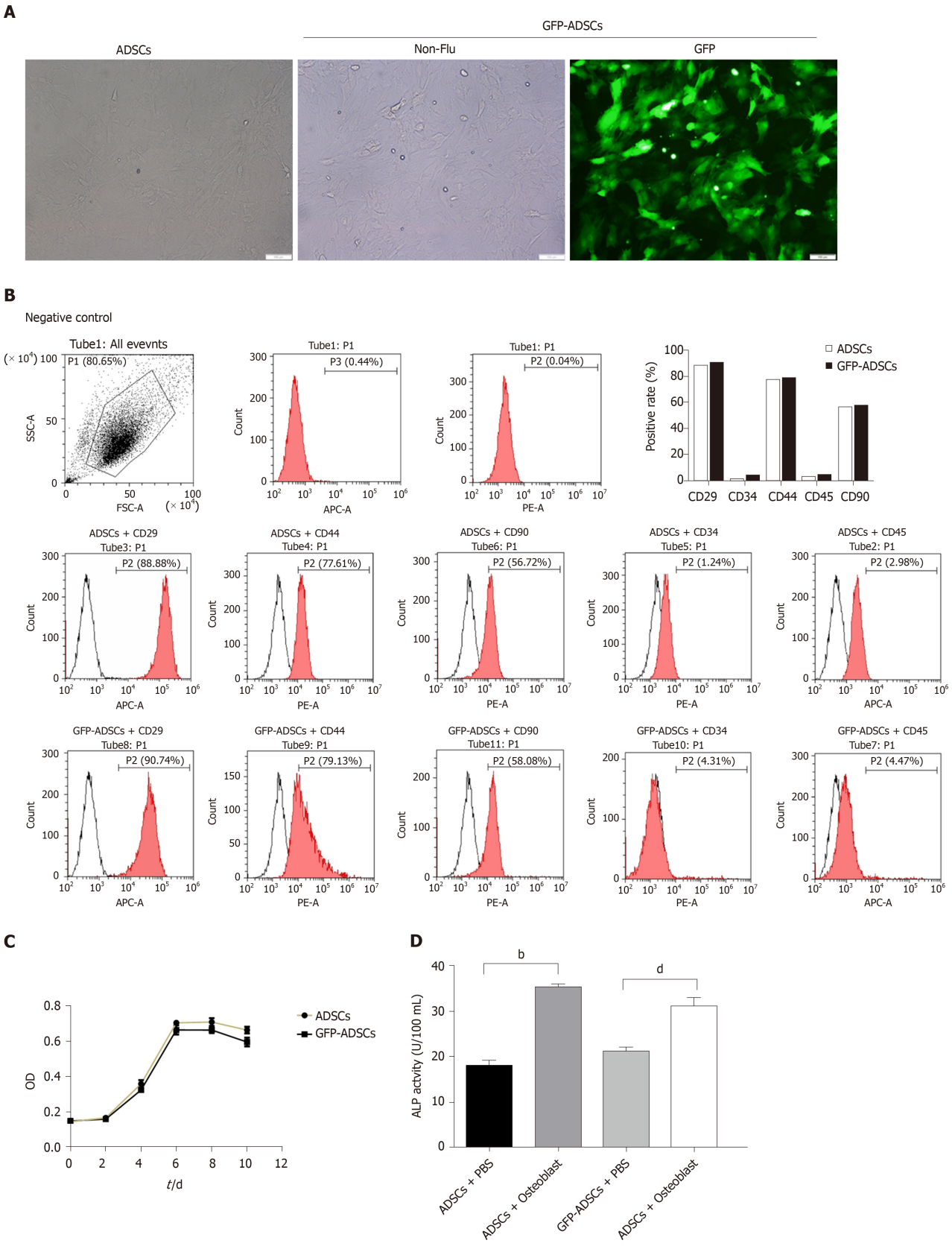
A
GFP-ADSCs
ADSCs
Non-Flu
GFP
B
Negative control
Tube1: All evevnts
P1 (80.65%)
SSC-A
FSC-A
Tube1: P1
P3 (0.44%)
Count
APC-A
Tube1: P1
P2 (0.04%)
PE-A
Positive rate (%)
ADSCs
GFP-ADSCs
CD29
CD34
CD44
CD45
CD90
ADSCs + CD29
Tube3: P1
P2 (88.88%)
ADSCs + CD44
Tube4: P1
P2 (77.61%)
ADSCs + CD90
Tube6: P1
P2 (56.72%)
ADSCs + CD34
Tube5: P1
P2 (1.24%)
ADSCs + CD45
Tube2: P1
P2 (2.98%)
GFP-ADSCs + CD29
Tube8: P1
P2 (90.74%)
GFP-ADSCs + CD44
Tube9: P1
P2 (79.13%)
GFP-ADSCs + CD90
Tube11: P1
P2 (58.08%)
GFP-ADSCs + CD34
Tube10: P1
P2 (4.31%)
GFP-ADSCs + CD45
Tube7: P1
P2 (4.47%)
C
OD
t/d
ADSCs
GFP-ADSCs
D
ALP activity (U/100 mL)
b
d
ADSCs + PBS
ADSCs + Osteoblast
GFP-ADSCs + PBS
ADSCs + Osteoblast

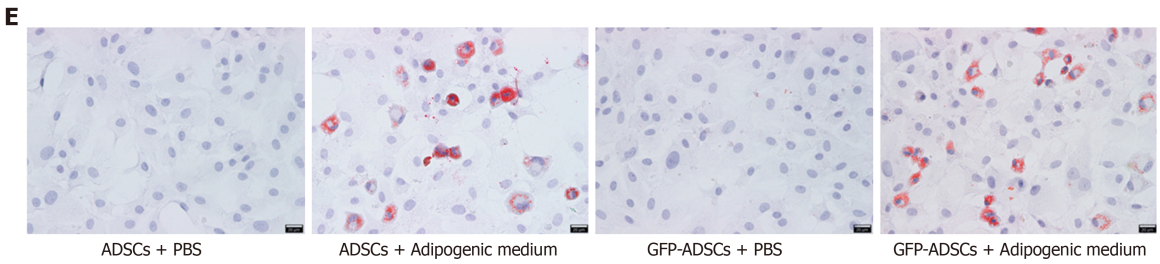

Figure 1 Isolation, culture, and identification of adipose-derived mesenchymal stem cells. A: Well-grown adipose-derived mesenchymal stem cells (ADSCs) were observed under a microscope (scale bar: 100 μm), and stable expression of green fluorescent protein (GFP) was identified in GFP-ADSCs under a fluorescence microscope (scale bar: 100 μm); B: ADSC surface antigen analysis was carried out by flow cytometry. The characteristic surface biomarkers for ADSCs were confirmed, including CD29, CD44, and CD90 positivity and CD34 and CD45 negativity; C: ADSCs presented a typical S-like proliferation curve; D: Differentiation into osteocytes was confirmed by increased ALP. $^{b}P < 0.01$ *vs* ADSCs + PBS, $^{d}P < 0.01$ *vs* GFP-ADSCs + PBS; E: Differentiation into adipocytes was confirmed by the presence of lipid vesicles stained with oil red O (scale bar: 20 μm). ADSCs: Adipose-derived mesenchymal stem cells; GFP: Green fluorescent protein.

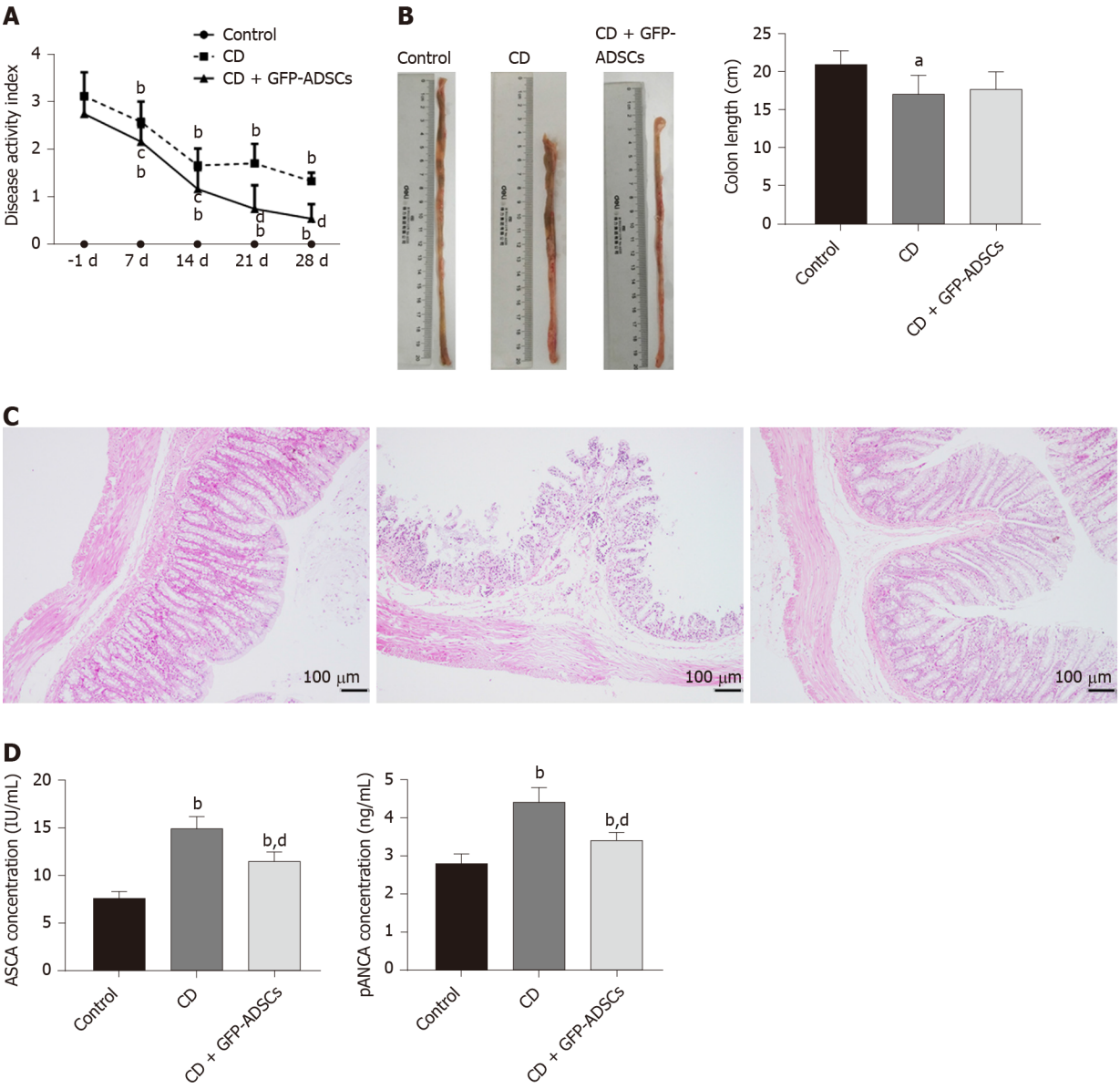

Figure 2 Tail injection of adipose-derived mesenchymal stem cells in rats protects against TNBS-induced colitis. A: Disease activity index of respective groups from baseline. -1 d indicates the day before adipose-derived mesenchymal stem cell (ADSC) injection, 7 d, 14 d, 21 d, and 28 d represent 7 d, 14 d, 21 d, and 28 d after ADSC therapy, respectively; B: Gross morphology of colon tissue and colon length among the groups; C: Representative hematoxylin and eosin staining of colon tissue in the three groups (scale bar: 100 μm); D: Serum concentrations of anti-sacchromyces cerevisiae antibody and p-antineutrophil cytoplasmic antibody detected by ELISA. Data are presented as the mean ± SD. $^{a}P < 0.05$, $^{b}P < 0.01$ *vs* control group; $^{c}P < 0.05$, $^{d}P < 0.01$ *vs* CD group. ADSCs: Adipose-derived mesenchymal stem cells; CD: Crohn's disease; GFP: Green fluorescent protein.

in the CD group, indicating an accelerated mucosal healing process. GFP green fluorescence merged images supported the specific proximity between epithelial cells and ADSCs, suggesting potential interplay. On the other hand, the typical biomarker of intestinal stem cells (ISCs), Lgr5, was weakly detected in the control and CD groups. The coexpression of GFP and Lgr5 was not observed in the CD + GFP-ADSCs group, indicating that ADSCs had no direct effect on ISCs (Figure 3C).

ADSC therapy activates the noncanonical Wnt signaling pathway and reduces cell apoptosis in rats with TNBS-induced colitis

Expression of the Wnt signaling pathway was evaluated by qRT-PCR. The expression levels of Wnt3a, Fzd3, and β-catenin were significantly increased in the CD group compared with the control group, while GFP-ADSC treatment significantly antagonized such changes (Figure 4A). The expression levels of Wnt5a, Fzd5, and Ror2 were significantly decreased in the CD group compared with the control group, and GFP-ADSC delivery also antagonized such changes (Figure 4B). The apoptosis rate in colon tissue was assessed by a TUNEL assay (Figure 4C). Semiquantitative analysis

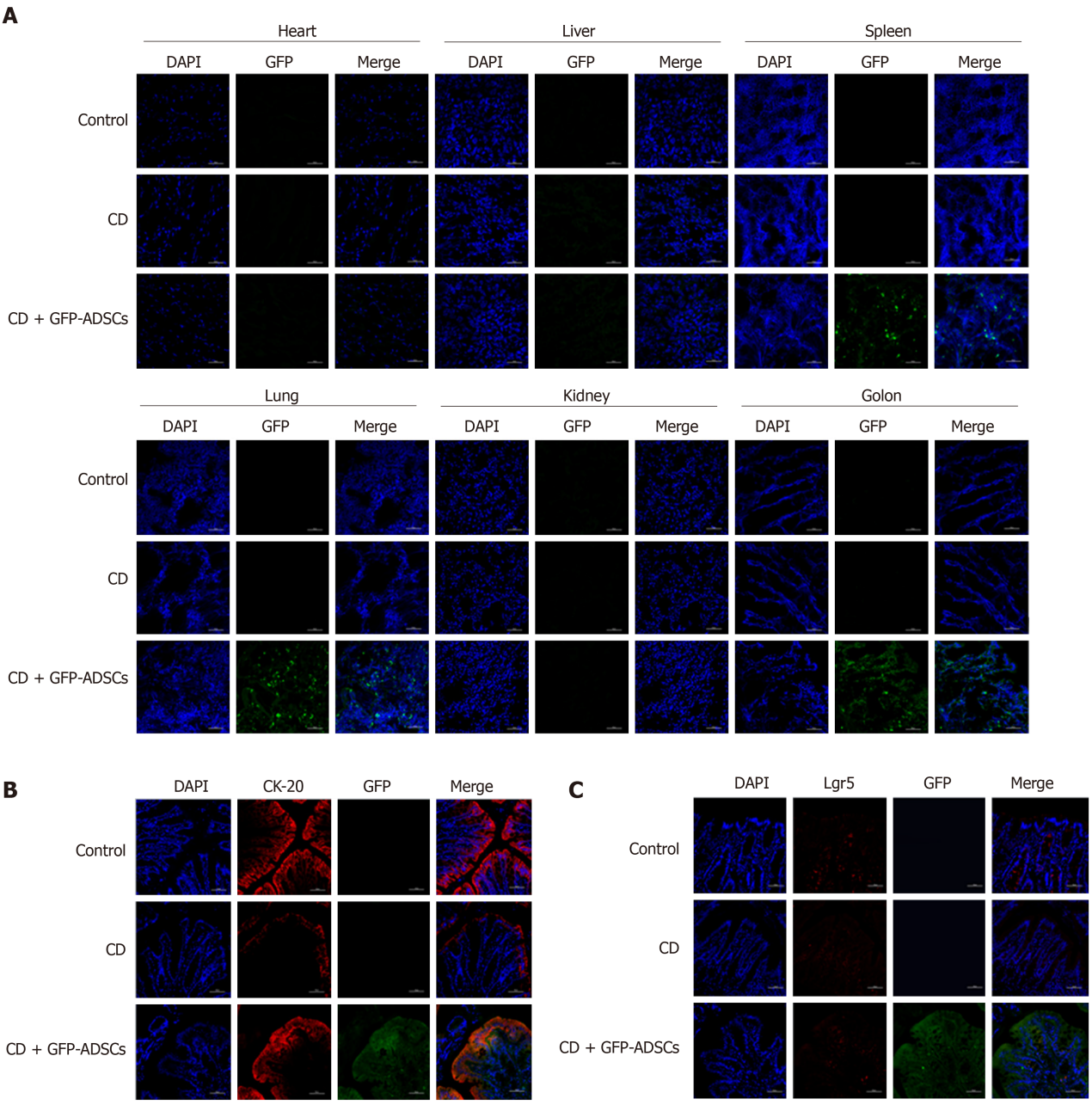

Figure 3 Distribution of adipose-derived mesenchymal stem cells and their colocalization with intestinal stem cells and intestinal epithelial cells. A: Distribution of green fluorescent protein (GFP)-positive adipose-derived mesenchymal stem cells (ADSCs) was detected mostly in the inflamed colon (scale bar: 50 μm); B: Immunofluorescence analysis for GFP and CK-20 showed the colocalization between ADSCs and intestinal epithelial cells (scale bar: 50 μm); C: Immunofluorescence analysis for GFP and Lgr5 showed that there was no colocalization between ADSCs and intestinal stem cells (scale bar: 50 μm). ADSCs: adipose-derived mesenchymal stem cells; CD: Crohn's disease; GFP: Green fluorescent protein.

showed that the number of TdT-positive cells was significantly increased in the rats administered with TNBS compared with the control group. GFP-ADSC administration significantly antagonized such change. Although the caspase-3 level was similar in the control, CD, and GFP-ADSC groups, Western blot analysis showed that the cleaved caspase-3 level was significantly increased in the CD group, and was significantly decreased in the GFP-ADSCs group compared with that in the CD group (Figure 4D).

ADSCs ameliorate abnormal inflammatory cytokine production and disturbed T cell subtypes in rats with TNBS-induced colitis

We investigated whether GFP-ADSC administration influences the production of inflammatory cytokines involved in intestinal inflammation. We observed an obvious increase in the expression of proinflammatory cytokine (IFN-γ, IL-2, IL-17, and IL-23) and a decrease in the expression of anti-inflammatory cytokine (IL-4, IL-13, IL-10, and TGF-β) in CD, which were further ameliorated after GFP-ADSC treatment (Figure 5A).

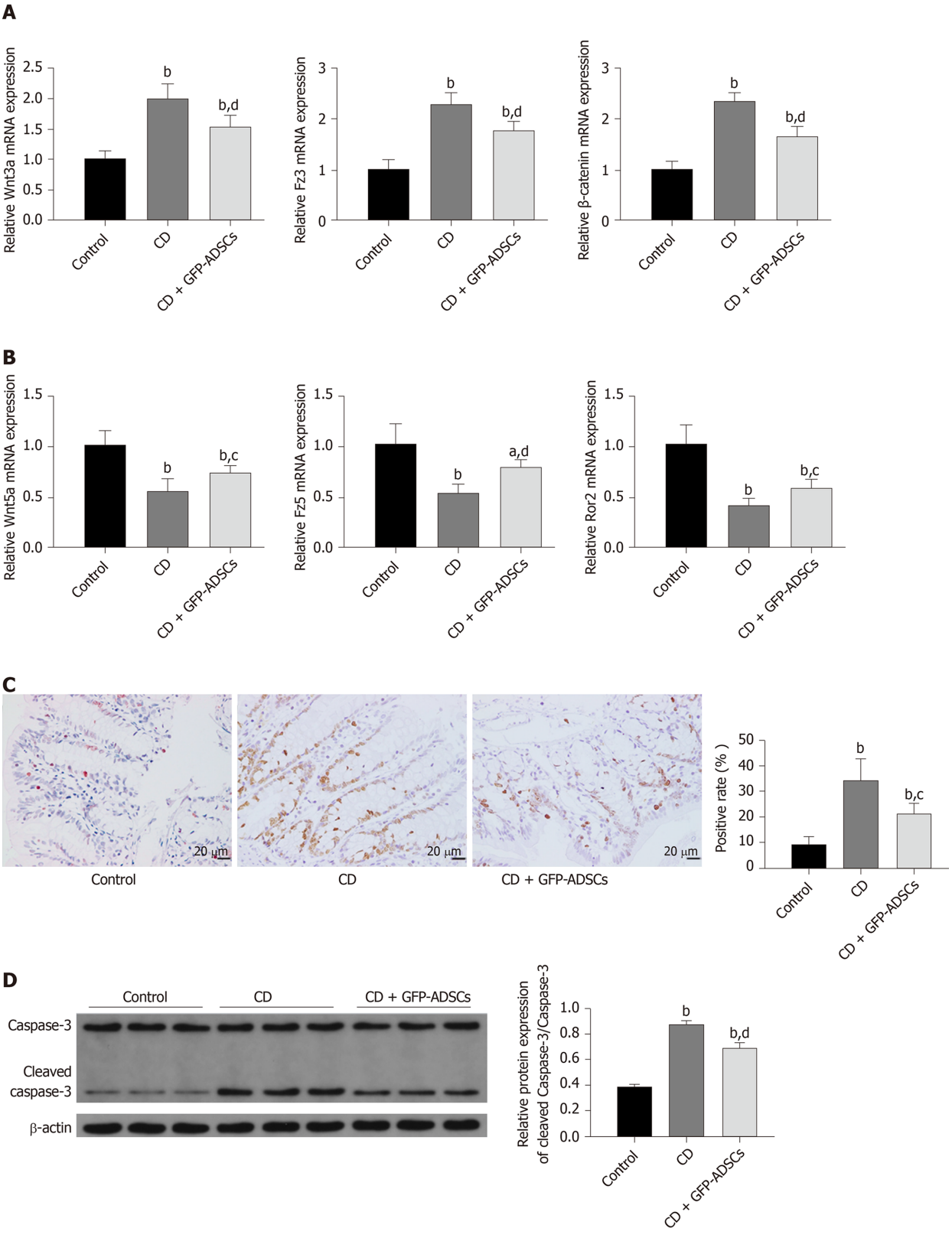

Figure 4 Effect and mechanism of adipose-derived mesenchymal stem cell administration in rats with TNBS-induced colitis. A: mRNA from colonic extracts was analyzed by qRT-PCR for the major molecules in the canonical Wnt signaling pathway: Wnt3a, Fz3, and β-catenin; B: mRNA from colonic extracts was analyzed by qRT-PCR for the major molecules in the noncanonical Wnt signaling pathway: Wnt5a, Fz5, and Ror2. Expression is presented as a ratio of cytokine/β-actin; C: Apoptosis of colonic cells was visualized by a TUNEL assay (scale bar: 20 μm), and semiquantitative analysis was performed; D: The expression of caspase-3 and cleaved-caspase 3 was evaluated by Western blot and compared among the control, CD, and GFP-ADSC therapy groups. Quantification is expressed as the fold induction. Data are presented as the mean ± SD. $^{a}P < 0.05$, $^{b}P < 0.01$ *vs* control group; $^{c}P < 0.05$, $^{d}P < 0.01$ *vs* CD group. ADSCs: Adipose-derived mesenchymal stem cells; CD: Crohn's disease; GFP: Green fluorescent protein.

Western blot analysis demonstrated that after TNBS delivery, the expression of Foxp3

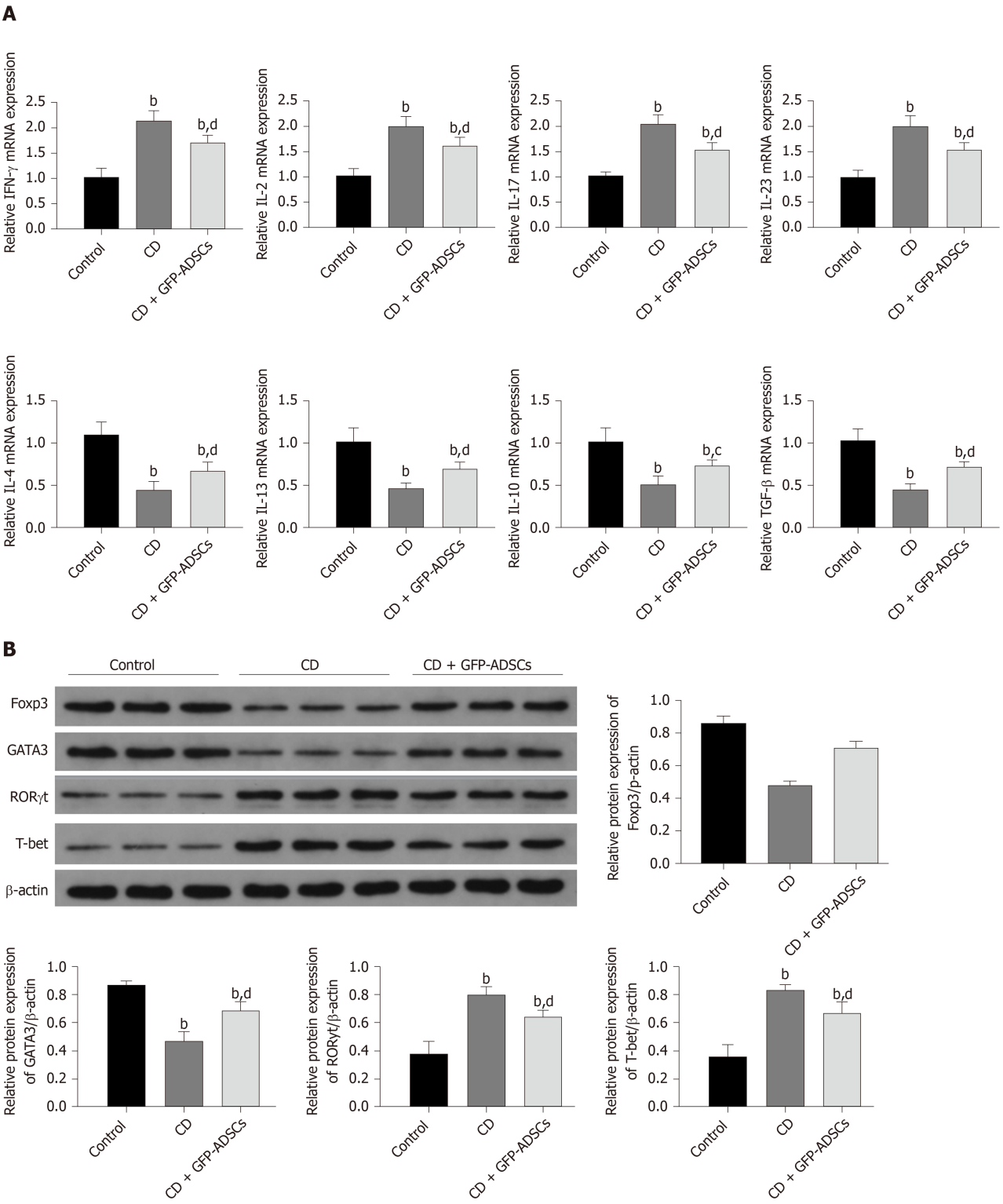

Figure 5 Changes in inflammatory markers and T cell-secreted molecules. A: Total mRNA from colonic extracts was analyzed by qRT-PCR for inflammatory cytokines involved in colitis: IFN-γ, IL-2, IL-17, IL-23, IL-4, IL-13, IL-10, and TGF-β; B: Western blot analysis of Foxp3, GATA3, RORγ, and T-bet. Data are presented as the mean ± SD. $^{b}P < 0.01$ *vs* control group; $^{c}P < 0.05$, $^{d}P < 0.01$ *vs* CD group. IFN-γ: Interferon-γ; IL-6: Interleukin-6; IL-17: Interleukin-17; IL-23: Interleukin-23; IL-4: Interleukin-4; IL-13: Interleukin-13; IL-10: Interleukin-10; TGF-β: Transforming growth factor. ADSCs: Adipose-derived mesenchymal stem cells; CD: Crohn's disease; GFP: Green fluorescent protein.

DISCUSSION

MSCs were first identified as a marrow-derived clonal source of cells in the 1960s[21]. Despite different sources, MSCs have common features and behavioral traits, which not only provide cells for tissue reconstitution but also regulate inflammation and "educate" other cells to facilitate tissue repair[22]. Accumulating evidence suggests a

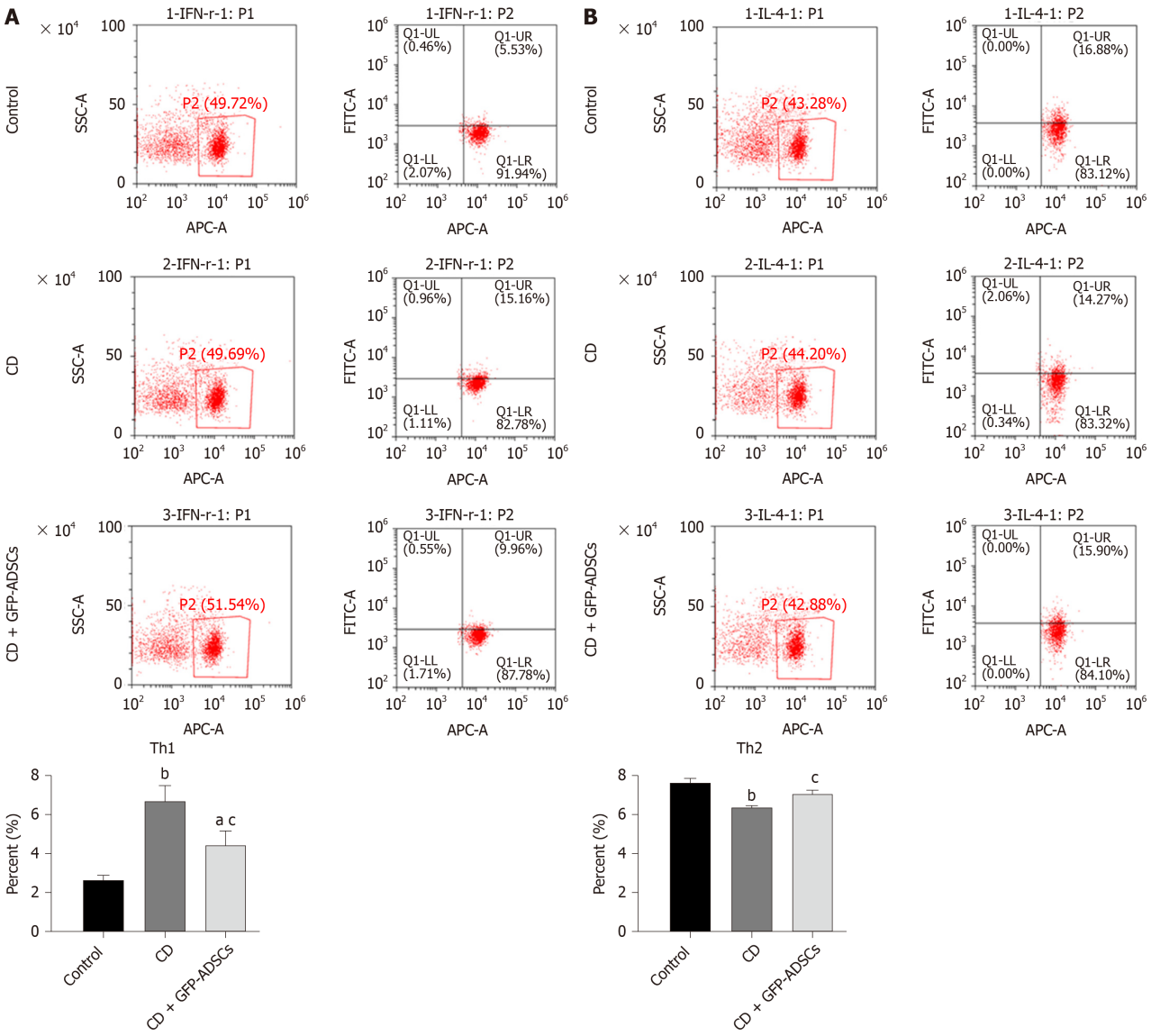
A
B
Control
CD
CD + GFP-ADSCs
1-IFN-r-1: P1
1-IFN-r-1: P2
2-IFN-r-1: P1
2-IFN-r-1: P2
3-IFN-r-1: P1
3-IFN-r-1: P2
1-IL-4-1: P1
1-IL-4-1: P2
2-IL-4-1: P1
2-IL-4-1: P2
3-IL-4-1: P1
3-IL-4-1: P2
P2 (49.72%)
P2 (49.69%)
P2 (51.54%)
P2 (43.28%)
P2 (44.20%)
P2 (42.88%)
Q1-UL (0.46%)
Q1-UR (5.53%)
Q1-LL (2.07%)
Q1-LR 91.94%)
Q1-UL (0.96%)
Q1-UR (15.16%)
Q1-LL (1.11%)
Q1-LR 82.78%)
Q1-UL (0.55%)
Q1-UR (9.96%)
Q1-LL (1.71%)
Q1-LR (87.78%)
Q1-UL (0.00%)
Q1-UR (16.88%)
Q1-LL (0.00%)
Q1-LR (83.12%)
Q1-UL (2.06%)
Q1-UR (14.27%)
Q1-LL (0.34%)
Q1-LR (83.32%)
Q1-UL (0.00%)
Q1-UR (15.90%)
Q1-LL (0.00%)
Q1-LR (84.10%)
SSC-A
FITC-A
APC-A
Th1
Th2
Percent (%)
a c
b
c
Control
CD
CD + GFP-ADSCs

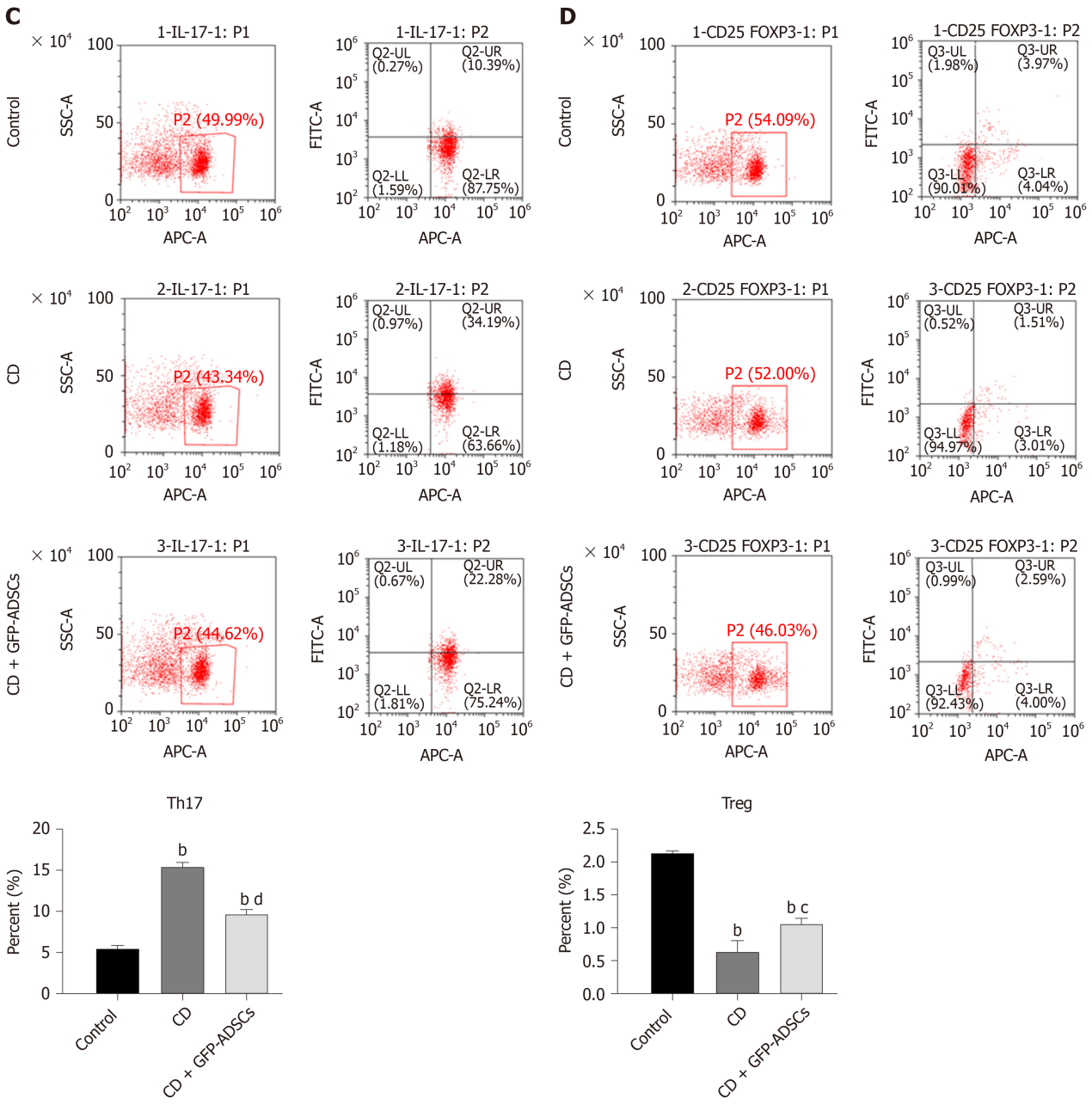

Figure 6 Tail injection of adipose-derived mesenchymal stem cells corrects the T cell imbalance in TNBS-induced colitis. The administration of ADSCs suppressed the overproduction of Th1 and Th17 cells induced by trinitrobenzene sulfonic acid and upregulated the decline of Th2 and Treg cells, as shown by flow cytometry. A: Th1 expression; B: Th2 expression; C: Th17 expression; D: Treg expression. Data are presented as the mean ± SD. $^{a}P < 0.05$, $^{b}P < 0.01$ *vs* control group; $^{c}P < 0.05$, $^{d}P < 0.01$ *vs* CD group. ADSCs: Adipose-derived mesenchymal stem cells; GFP: CD: Crohn's disease; Green fluorescent protein.

therapeutic effect of MSCs in IBD[23,24] and ADSCs have been widely used because of their easy acquisition. In 2005, the first phase I clinical trial showed that 75% of fistulas were healed by ADSC therapy without any side effects[25], which opened the window to ADSC therapy for CD. Further studies showed that ADSC injection modulated the abnormal immune response in CD patients, resulting in clinical improvement[26]. However, the underlying mechanisms of ADSCs in CD are still vague. In this study, we demonstrated that ADSC administration alleviates TNBS-induced colitis by accelerating IEC regeneration, partially restoring the dysregulated Wnt signaling pathway and rebalancing T cell repertoire, which reinforces the effectiveness of ADSC therapy in CD and provides novel clues for further mechanism exploration.

Mucosal healing is associated with a more favorable prognosis for CD. Previous studies showed the therapeutic effects of ISCs in improving mucosal healing and functional engraftment of the derived colon epithelial cells after successful transplantation[27,28]. However, a lack of immunoregulation capacity may hamper further application of ISCs, especially compared with that of MSCs. Moreover,

accumulating evidences suggest that systemically transplanted BM-MSCs may home to the injured gut and transdifferentiate into ISCs or interstitial lineage cells to repair the damaged tissue[29]. A recent study showed that intraperitoneally administered MSCs homing to inflamed tissues were a prerequisite to achieve their beneficial effect[30]. However, the effects of ADSC administration on CD and the mechanisms of mucosal healing have rarely been reported. Our results not only showed the therapeutic effect of ADSCs on the CD phenotype in TNBS-induced rats but also demonstrated that ADSCs engrafted into damaged colon and colocalized with IECs but not ISCs, partially clarifying the mechanisms of ADSCs in mucosal healing. This result enhances previous findings showing the therapeutic effect of local MSC administration in experimental colitis[31].

The Wnt signaling pathway was chosen as the candidate because of its capacity to regulate the self-renewal and differentiation of MSCs and to determine the fates of ISCs[32,33]. Therefore, this pathway acts as a bridge between MSCs and receptors. Previous studies showed activated canonical and suppressed noncanonical Wnt signaling in IBD[34]. In this study, when the intestinal epithelium was inflamed, canonical Wnt signaling was activated. After ADSC transplantation, the canonical Wnt signaling-related genes were downregulated. For the noncanonical Wnt pathway, the levels of relative genes were significantly decreased in the CD group but partially recovered after ADSC administration. Since the canonical Wnt pathway enhances MSC proliferation and the noncanonical Wnt pathway exerts the opposite effects, we speculated that the noncanonical Wnt pathway activated by ADSC transplantation may contribute to the transition of cell status from "proliferation" into "differentiation"[35].

Disturbed T cell immunity and changes in its associated cytokine network are actively involved in IBD[36]. It has been well accepted that the predominant inflammatory profile in CD involves activated Th1/Th17 but depressed Th2/Treg cell responses. In this study, we reconfirmed these findings in TNBS-induced rats with CD phenotype and further showed that the alleviation of colitis after ADSC administration was partially mediated by antagonizing those changes. Several molecular markers were selected, and the same trend was observed in the changes in T cell subtype. Our results were consistent with previous reports showing the contribution of T cells to the therapeutic effect of BM-MSCs on TNBS-induced colitis[37]. It is theoretically plausible that MSCs have the ability to suppress the proliferation and expansion of T helper cells while inducing the differentiation and activation of Treg cells, while the latter has the capacity to inhibit autoimmunity[38]. Additionally, a previous study showed that apoptosis was exacerbated in CD[39], which was also found in our study by the TUNEL method and the expression level of active caspase-3.

There are several limitations that should be acknowledged. First, it is well known that ISCs are located at the base of the intestinal crypts and renew the epithelium through differentiation to multiple epithelial lineages[40]. Although our results identified that ADSCs were colocalized with IECs but not ISCs, whether ADSCs could transdifferentiate into epithelial cells and the potential regulators are still unclear. Second, although we found a change in T cell immunity in CD and after ADSC treatment, the detailed mechanisms are still vague. Third, although we identified the change in the Wnt signaling pathway in CD and after ADSC therapy, further mechanism exploration has not been performed. Previous studies showed the effect of the Wnt signaling pathway on the balance between cell proliferation and its potential regulators[41]. Whether these factors are applicable in ADSC therapy requires further study. Fourth, studies are required to understand the potential risks of ADSC treatment, such as tumorigenicity and immune rejection[42]. Fifth, it may be not sufficient to use CK-20 as the marker of IECs and combination with Ki-67 should be considered in the future. Finally, the relationship between the Wnt signaling pathway and T cell distribution remains unclear. The mechanisms of ADSCs in modulating the interactions between them warrant further research.

In conclusion, our findings not only confirmed the biological characteristics of ADSCs, such as localization and multilineage differentiation potential, but also suggested the effect of ADSC therapy in treating CD phenotype in a TNBS-induced rat model. We further investigated the potential underlining mechanisms, involving IEC proliferation, the Wnt signaling pathway, and T cell immunity, which provided novel clues for the pathogenesis and treatment of CD (Figure 7).

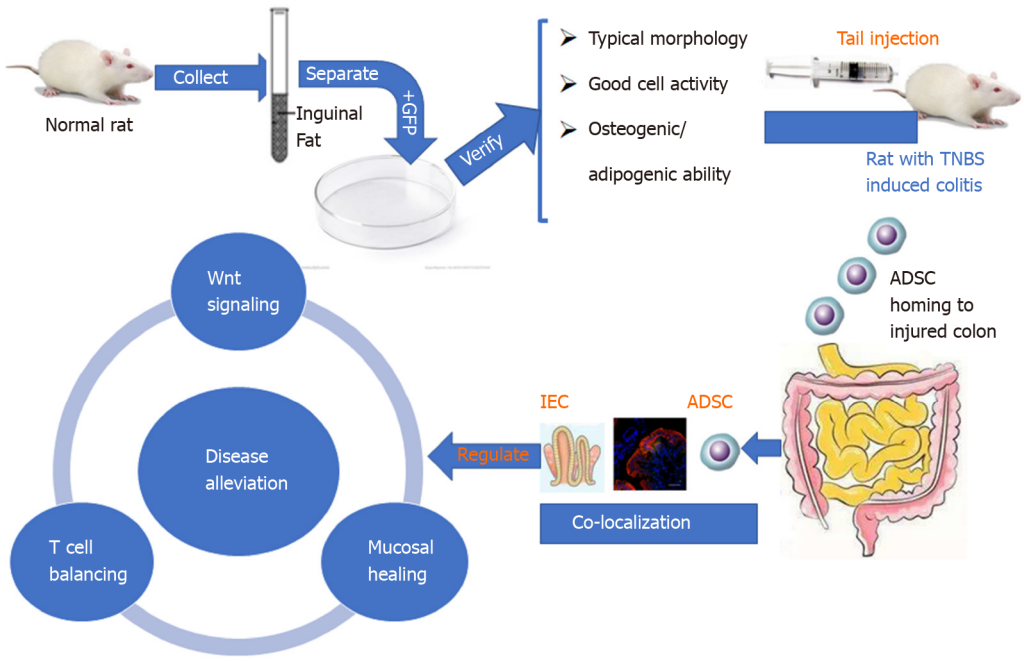

Figure 7 Schematic diagram of the sequential steps and potential mechanism of adipose-derived mesenchymal stem cells in treating the Crohn's disease phenotype. ADSC: Adipose-derived mesenchymal stem cell; GFP: Green fluorescent protein; TNBS: Trinitrobenzene sulfonic acid; IEC: intestinal epithelial cell.

ARTICLE HIGHLIGHTS

Research background

Crohn's disease (CD) is a chronic relapsing inflammatory disorder of the gastrointestinal tract, especially involving the distal small intestine and the colonic mucosa. Conventional treatments are supportive rather than curative and have serious side effects.

Research motivation

Adipose-derived mesenchymal stem cells (ADSCs) have been gradually applied to treat various diseases. The therapeutic effect and underlying mechanism of ADSCs on CD are still not clear.

Research objectives

This study aimed to investigate the effect of ADSC administration on CD and explore potential mechanisms on intestinal epithelial cell regeneration, Wnt signaling, and T cell immunity.

Research methods

Wistar rats were administered with 2,4,6-trinitrobenzene sulfonic acid (TNBS) to establish a rat model of CD, followed by tail injections of green fluorescent protein (GFP)-modified ADSCs. After tracing *in vivo* ADSC distribution, flow cytometry, qRT-PCR, and Western blot were used to detect changes in the Wnt signaling pathway, T cell subtypes, and their related cytokines.

Research results

The isolated cells showed the characteristics of ADSCs, including spindle-shaped morphology, high expression of CD29, CD44, and CD90, low expression of CD34 and CD45, and osteogenic/adipogenic ability. ADSC therapy markedly reduced disease activity index and ameliorated colitis severity in the TNBS-induced rat model of CD. Furthermore, serum anti-sacchromyces cerevisiae antibody and p-anti-neutrophil cytoplasmic antibody levels were significantly reduced in ADSC-treated rats. Mechanistically, the GFP-ADSCs were colocalized with intestinal epithelial cells in the CD rat model. GFP-ADSC delivery significantly antagonized TNBS-induced increased canonical Wnt pathway expression, decreased noncanonical Wnt signaling pathway expression, and increased apoptosis rates and protein level of cleaved caspase-3 in

rats. In addition, ADSCs attenuated TNBS-induced abnormal inflammatory cytokine production, disturbed T cell subtypes, and their related markers in rats.

Research conclusions

Successfully isolated ADSCs show co-location with IEC and therapeutic effects in CD by regulating IEC proliferation, the Wnt signaling pathway, and T cell immunity.

Research perspective

Systemic ADSC infusion may be a potential choice for CD therapy.

REFERENCES

1 **Abraham C**, Cho JH. Inflammatory bowel disease. *N Engl J Med* 2009; **361**: 2066-2078 [PMID: 19923578 DOI: 10.1056/NEJMra0804647]
2 **Engel MA**, Khalil M, Neurath MF. Highlights in inflammatory bowel disease--from bench to bedside. *Clin Chem Lab Med* 2012; **50**: 1229-1235 [PMID: 23024984 DOI: 10.1515/cclm-2011-0831]
3 **Shi HY**, Ng SC. The state of the art on treatment of Crohn's disease. *J Gastroenterol* 2018; **53**: 989-998 [PMID: 29980848 DOI: 10.1007/s00535-018-1479-6]
4 **Zaher W**, Harkness L, Jafari A, Kassem M. An update of human mesenchymal stem cell biology and their clinical uses. *Arch Toxicol* 2014; **88**: 1069-1082 [PMID: 24691703 DOI: 10.1007/s00204-014-1232-8]
5 **Casteilla L**, Planat-Benard V, Laharrague P, Cousin B. Adipose-derived stromal cells: Their identity and uses in clinical trials, an update. *World J Stem Cells* 2011; **3**: 25-33 [PMID: 21607134 DOI: 10.4252/wjsc.v3.i4.25]
6 **Dave M**, Mehta K, Luther J, Baruah A, Dietz AB, Faubion WA Jr. Mesenchymal Stem Cell Therapy for Inflammatory Bowel Disease: A Systematic Review and Meta-analysis. *Inflamm Bowel Dis* 2015; **21**: 2696-2707 [PMID: 26230863 DOI: 10.1097/MIB.0000000000000543]
7 **Nusse R**, Clevers H. Wnt/β-Catenin Signaling, Disease, and Emerging Therapeutic Modalities. *Cell* 2017; **169**: 985-999 [PMID: 28575679 DOI: 10.1016/j.cell.2017.05.016]
8 **Steinhart Z**, Angers S. Wnt signaling in development and tissue homeostasis. *Development* 2018; **145**: dev146589 [PMID: 29884654 DOI: 10.1242/dev.146589]
9 **Koch S**. Extrinsic control of Wnt signaling in the intestine. *Differentiation* 2017; **97**: 1-8 [PMID: 28802143 DOI: 10.1016/j.diff.2017.08.003]
10 **Shi J**, Chi S, Xue J, Yang J, Li F, Liu X. Emerging Role and Therapeutic Implication of Wnt Signaling Pathways in Autoimmune Diseases. *J Immunol Res* 2016; **2016**: 9392132 [PMID: 27110577 DOI: 10.1155/2016/9392132]
11 **Endo M**, Nishita M, Fujii M, Minami Y. Insight into the role of Wnt5a-induced signaling in normal and cancer cells. *Int Rev Cell Mol Biol* 2015; **314**: 117-148 [PMID: 25619716 DOI: 10.1016/bs.ircmb.2014.10.003]
12 **Cosín-Roger J**, Ortiz-Masiá D, Calatayud S, Hernández C, Esplugues JV, Barrachina MD. The activation of Wnt signaling by a STAT6-dependent macrophage phenotype promotes mucosal repair in murine IBD. *Mucosal Immunol* 2016; **9**: 986-998 [PMID: 26601901 DOI: 10.1038/mi.2015.123]
13 **Xiao J**, Zhu F, Liu X, Xiong J. Th1/Th2/Th17/Treg expression in cultured PBMCs with antiphospholipid antibodies. *Mol Med Rep* 2012; **6**: 1035-1039 [PMID: 22941119 DOI: 10.3892/mmr.2012.1055]
14 **Brand S**. Crohn's disease: Th1, Th17 or both? The change of a paradigm: new immunological and genetic insights implicate Th17 cells in the pathogenesis of Crohn's disease. *Gut* 2009; **58**: 1152-1167 [PMID: 19592695 DOI: 10.1136/gut.2008.163667]
15 **Chao K**, Zhang S, Yao J, He Y, Chen B, Zeng Z, Zhong B, Chen M. Imbalances of CD4(+) T-cell subgroups in Crohn's disease and their relationship with disease activity and prognosis. *J Gastroenterol Hepatol* 2014; **29**: 1808-1814 [PMID: 24720272 DOI: 10.1111/jgh.12592]
16 **Zhang W**, Feng YL, Pang CY, Lu FA, Wang YF. Transplantation of adipose tissue-derived stem cells ameliorates autoimmune pathogenesis in MRL/lpr mice : Modulation of the balance between Th17 and Treg. *Z Rheumatol* 2019; **78**: 82-88 [PMID: 29737401 DOI: 10.1007/s00393-018-0450-5]
17 **Carulli AJ**, Keeley TM, Demitrack ES, Chung J, Maillard I, Samuelson LC. Notch receptor regulation of intestinal stem cell homeostasis and crypt regeneration. *Dev Biol* 2015; **402**: 98-108 [PMID: 25835502 DOI: 10.1016/j.ydbio.2015.03.012]
18 **Antoniou E**, Margonis GA, Angelou A, Pikouli A, Argiri P, Karavokyros I, Papalois A, Pikoulis E. The TNBS-induced colitis animal model: An overview. *Ann Med Surg (Lond)* 2016; **11**: 9-15 [PMID: 27656280 DOI: 10.1016/j.amsu.2016.07.019]
19 **Jin X**, Chen D, Zheng RH, Zhang H, Chen YP, Xiang Z. miRNA-133a-UCP2 pathway regulates inflammatory bowel disease progress by influencing inflammation, oxidative stress and energy metabolism. *World J Gastroenterol* 2017; **23**: 76-86 [PMID: 28104982 DOI: 10.3748/wjg.v23.i1.76]
20 **Mirlekar B**, Ghorai S, Khetmalas M, Bopanna R, Chattopadhyay S. Nuclear matrix protein SMAR1 control regulatory T-cell fate during inflammatory bowel disease (IBD). *Mucosal Immunol* 2015; **8**: 1184-1200 [PMID: 25993445 DOI: 10.1038/mi.2015.42]
21 **BECKER AJ**, McCULLOCH EA, TILL JE. Cytological demonstration of the clonal nature of spleen colonies derived from transplanted mouse marrow cells. *Nature* 1963; **197**: 452-454 [PMID: 13970094 DOI: 10.1038/197452a0]
22 **Ke C**, Biao H, Qianqian L, Yunwei S, Xiaohua J. Mesenchymal stem cell therapy for inflammatory bowel diseases: promise and challenge. *Curr Stem Cell Res Ther* 2015; **10**: 499-508 [PMID: 26018234 DOI: 10.2174/1574888x10666150528143138]
23 **Fu ZW**, Zhang ZY, Ge HY. Mesenteric injection of adipose-derived mesenchymal stem cells relieves

experimentally-induced colitis in rats by regulating Th17/Treg cell balance. *Am J Transl Res* 2018; **10**: 54-66 [PMID: 29422993]

24 **Hoffman JM**, Sideri A, Ruiz JJ, Stavrakis D, Shih DQ, Turner JR, Pothoulakis C, Karagiannides I. Mesenteric Adipose-derived Stromal Cells From Crohn's Disease Patients Induce Protective Effects in Colonic Epithelial Cells and Mice With Colitis. *Cell Mol Gastroenterol Hepatol* 2018; **6**: 1-16 [PMID: 29928668 DOI: 10.1016/j.jcmgh.2018.02.001]

25 **García-Olmo D**, García-Arranz M, Herreros D, Pascual I, Peiro C, Rodríguez-Montes JA. A phase I clinical trial of the treatment of Crohn's fistula by adipose mesenchymal stem cell transplantation. *Dis Colon Rectum* 2005; **48**: 1416-1423 [PMID: 15933795 DOI: 10.1007/s10350-005-0052-6]

26 **González MA**, Gonzalez-Rey E, Rico L, Büscher D, Delgado M. Adipose-derived mesenchymal stem cells alleviate experimental colitis by inhibiting inflammatory and autoimmune responses. *Gastroenterology* 2009; **136**: 978-989 [PMID: 19135996 DOI: 10.1053/j.gastro.2008.11.041]

27 **Fukuda M**, Mizutani T, Mochizuki W, Matsumoto T, Nozaki K, Sakamaki Y, Ichinose S, Okada Y, Tanaka T, Watanabe M, Nakamura T. Small intestinal stem cell identity is maintained with functional Paneth cells in heterotopically grafted epithelium onto the colon. *Genes Dev* 2014; **28**: 1752-1757 [PMID: 25128495 DOI: 10.1101/gad.245233.114]

28 **Yui S**, Nakamura T, Sato T, Nemoto Y, Mizutani T, Zheng X, Ichinose S, Nagaishi T, Okamoto R, Tsuchiya K, Clevers H, Watanabe M. Functional engraftment of colon epithelium expanded in vitro from a single adult Lgr5^{+} stem cell. *Nat Med* 2012; **18**: 618-623 [PMID: 22406745 DOI: 10.1038/nm.2695]

29 **Qu B**, Xin GR, Zhao LX, Xing H, Lian LY, Jiang HY, Tong JZ, Wang BB, Jin SZ. Testing stem cell therapy in a rat model of inflammatory bowel disease: role of bone marrow stem cells and stem cell factor in mucosal regeneration. *PLoS One* 2014; **9**: e107891 [PMID: 25309991 DOI: 10.1371/journal.pone.0107891]

30 **Lopez-Santalla M**, Mancheño-Corvo P, Escolano A, Menta R, Delarosa O, Redondo JM, Bueren JA, Dalemans W, Lombardo E, Garin MI. Comparative Analysis between the In Vivo Biodistribution and Therapeutic Efficacy of Adipose-Derived Mesenchymal Stromal Cells Administered Intraperitoneally in Experimental Colitis. *Int J Mol Sci* 2018; **19**: 1853 [PMID: 29937494 DOI: 10.3390/ijms19071853]

31 **de la Portilla F**, Yuste Y, Pereira S, Olano C, Maestre MV, Padillo FJ. Local Mesenchymal Stem Cell Therapy in Experimentally Induced Colitis in the Rat. *Int J Stem Cells* 2018; **11**: 39-47 [PMID: 29699385 DOI: 10.15283/ijsc17074]

32 **Neth P**, Ciccarella M, Egea V, Hoelters J, Jochum M, Ries C. Wnt signaling regulates the invasion capacity of human mesenchymal stem cells. *Stem Cells* 2006; **24**: 1892-1903 [PMID: 16690780 DOI: 10.1634/stemcells.2005-0503]

33 **Scoville DH**, Sato T, He XC, Li L. Current view: intestinal stem cells and signaling. *Gastroenterology* 2008; **134**: 849-864 [PMID: 18325394 DOI: 10.1053/j.gastro.2008.01.079]

34 **Xing Y**, Chen X, Cao Y, Huang J, Xie X, Wei Y. Expression of Wnt and Notch signaling pathways in inflammatory bowel disease treated with mesenchymal stem cell transplantation: evaluation in a rat model. *Stem Cell Res Ther* 2015; **6**: 101 [PMID: 25998108 DOI: 10.1186/s13287-015-0092-3]

35 **Boland GM**, Perkins G, Hall DJ, Tuan RS. Wnt 3a promotes proliferation and suppresses osteogenic differentiation of adult human mesenchymal stem cells. *J Cell Biochem* 2004; **93**: 1210-1230 [PMID: 15486964 DOI: 10.1002/jcb.20284]

36 **Chen ML**, Sundrud MS. Cytokine Networks and T-Cell Subsets in Inflammatory Bowel Diseases. *Inflamm Bowel Dis* 2016; **22**: 1157-1167 [PMID: 26863267 DOI: 10.1097/MIB.0000000000000714]

37 **Zuo D**, Liu X, Shou Z, Fan H, Tang Q, Duan X, Cao D, Zou Z, Zhang L. Study on the interactions between transplanted bone marrow-derived mesenchymal stem cells and regulatory T cells for the treatment of experimental colitis. *Int J Mol Med* 2013; **32**: 1337-1344 [PMID: 24142133 DOI: 10.3892/ijmm.2013.1529]

38 **Corridoni D**, Arseneau KO, Cominelli F. Inflammatory bowel disease. *Immunol Lett* 2014; **161**: 231-235 [PMID: 24938525 DOI: 10.1016/j.imlet.2014.04.004]

39 **Sturm A**, de Souza HS, Fiocchi C. Mucosal T cell proliferation and apoptosis in inflammatory bowel disease. *Curr Drug Targets* 2008; **9**: 381-387 [PMID: 18473766 DOI: 10.2174/138945008784221198]

40 **Bjerknes M**, Cheng H. Intestinal epithelial stem cells and progenitors. *Methods Enzymol* 2006; **419**: 337-383 [PMID: 17141062 DOI: 10.1016/s0076-6879(06)19014-x]

41 **Vanuytsel T**, Senger S, Fasano A, Shea-Donohue T. Major signaling pathways in intestinal stem cells. *Biochim Biophys Acta* 2013; **1830**: 2410-2426 [PMID: 22922290 DOI: 10.1016/j.bbagen.2012.08.006]

42 **Liu Y**, Niu R, Yang F, Yan Y, Liang S, Sun Y, Shen P, Lin J. Biological characteristics of human menstrual blood-derived endometrial stem cells. *J Cell Mol Med* 2018; **22**: 1627-1639 [PMID: 29278305 DOI: 10.1111/jcmm.13437]

World Journal of Gastroenterology

Submit a Manuscript: https://www.f6publishing.com

World J Gastroenterol 2020 July 14; 26(26): 3767-3779

DOI: 10.3748/wjg.v26.i26.3767

ISSN 1007-9327 (print) ISSN 2219-2840 (online)

ORIGINAL ARTICLE

Clinical and Translational Research

SpyGlass application for duodenoscope working channel inspection: Impact on the microbiological surveillance

Tao-Chieh Liu, Chen-Ling Peng, Hsiu-Po Wang, Hsin-Hung Huang, Wei-Kuo Chang

ORCID number: Tao-Chieh Liu 0000-0003-4631-6185; Chen-Ling Peng 0000-0003-4689-4751; Hsiu-Po Wang 0000-0002-7741-9315; Hsin-Hung Huang 0000-0003-1105-4306; Wei-Kuo Chang 0000-0002-5738-2797.

Author contributions: Liu TC, Peng CL and Chang WK contributed to design of the study, making critical revisions related to important intellectual content of the manuscript, and final approval of the version of the article to be published; Wang HP and Huang HH contributed to analysis and interpretation of data.

Supported by the Ministry of Defense-Medical Affairs Bureau, Tri-Service General Hospital, No. TSGH-D-109182.

Institutional review board statement: This study was reviewed and approved by the Ethics Committee of the Tri-Service General Hospital, National Defense Medical Center, Taiwan.

Informed consent statement: Patients were not required to give informed consent to the study because the analysis used anonymous clinical data that were obtained after each patient agreed to treatment by written consent.

Conflict-of-interest statement: All

Tao-Chieh Liu, Wei-Kuo Chang, Division of Gastroenterology, Department of Internal Medicine, Tri-Service General Hospital, National Defense Medical Center, Taipei 114, Taiwan

Chen-Ling Peng, Department of Integrated Diagnostics & Therapeutics, National Taiwan University Hospital, National Taiwan University College of Medicine, Taipei 10002, Taiwan

Hsiu-Po Wang, Division of Gastroenterology and Hepatology, Department of Internal Medicine, National Taiwan University Hospital, National Taiwan University College of Medicine, Taipei 114, Taiwan

Hsin-Hung Huang, Division of Gastroenterology, Cheng Hsin General Hospital, National Defense Medical Center, Taipei 114, Taiwan

Corresponding author: Wei-Kuo Chang, MD, PhD, Associate Professor, Division of Gastroenterology, Department of Internal Medicine, Tri-Service General Hospital, National Defense Medical Center, No. 325, Chengong Road, Sec.2, Neihu, Taipei 114, Taiwan. weikuohome@hotmail.com

Abstract

BACKGROUND

Patient-ready duodenoscopes were designed with an assumed contamination rate of less than 0.4%; however, it has been reported that 5.4% of clinically used duodenoscopes remain contaminated with viable high-concern organisms despite following the manufacturer's instructions. Visual inspection of working channels has been proposed as a quality control measure for endoscope reprocessing. There are few studies related to this issue.

AIM

To investigate the types, severity rate, and locations of abnormal visual inspection findings inside patient-ready duodenoscopes and their microbiological significance.

METHODS

Visual inspections of channels were performed in 19 patient-ready duodenoscopes using the SpyGlass visualization system in two endoscopy units of tertiary care teaching hospitals (Tri-Service General Hospital and National Taiwan University Hospital) in Taiwan. Inspections were recorded and reviewed

authors declare that they have no conflicts of interest.

Data sharing statement: No additional data are available.

Manuscript source: Unsolicited manuscript

Received: February 16, 2020
Peer-review started: February 16, 2020
First decision: May 1, 2020
Revised: May 28, 2020
Accepted: June 23, 2020
Article in press: June 23, 2020
Published online: July 14, 2020

P-Reviewer: Kitamura K, Pavides M, Yildiz K
S-Editor: Gong ZM
L-Editor: MedE-Ma JY
E-Editor: Zhang YL

to evaluate the presence of channel scratches, buckling, stains, debris, and fluids. These findings were used to analyze the relevance of microbiological surveillance.

RESULTS

Seventy-two abnormal visual inspection findings in the 19 duodenoscopes were found, including scratches (n = 10, 52.6%), buckling (n = 15, 78.9%), stains (n = 14, 73.7%), debris (n = 14, 73.7%), and fluids (n = 6, 31.6%). Duodenoscopes > 12 mo old had a significantly higher number of abnormal visual inspection findings than those ≤ 12 mo old (46 findings *vs* 26 findings, $P < 0.001$). Multivariable regression analyses demonstrated that the bending section had a significantly higher risk of being scratched, buckled, and stained, and accumulating debris than the insertion tube. Debris and fluids showed a significant positive correlation with microbiological contamination ($P < 0.05$). There was no significant positive Spearman's correlation coefficient between negative bacterial cultures and debris, between that and fluids, and the concomitance of debris and fluids. This result demonstrated that the presence of fluid and debris was associated with positive cultures, but not negative cultures. Further multivariate analysis demonstrated that fluids, but not debris, is an independent factor for bacterial culture positivity.

CONCLUSION

In patient-ready duodenoscopes, scratches, buckling, stains, debris, and fluids inside the working channel are common, which increase the microbiological contamination susceptibility. The SpyGlass visualization system may be recommended to identify suboptimal reprocessing.

Key words: Duodenoscope; Working channel; Visual inspection; Microbiological surveillance; Reprocessing; Endoscope reprocessing

Core tip: This study demonstrated that the common abnormal visual inspection findings of patient-ready duodenoscopes were scratches (52.6%), buckling (78.9%), stains (73.7%), debris (73.7%), and fluids (31.6%). The risk of duodenoscopes of being scratched, buckled, and stained, and accumulating debris was significantly higher at the bending section than at the insertion tube. The presence of debris and fluids is susceptible to microbiological contamination. Multivariate analysis demonstrated that fluids, but not debris, was an independent factor for bacterial culture positivity. Working channel inspection may be added to the current recommendations to identify suboptimal reprocessing or duodenoscopes requiring evaluation, repair, or replacement.

Citation: Liu TC, Peng CL, Wang HP, Huang HH, Chang WK. SpyGlass application for duodenoscope working channel inspection: Impact on the microbiological surveillance. *World J Gastroenterol* 2020; 26(26): 3767-3779
URL: https://www.wjgnet.com/1007-9327/full/v26/i26/3767.htm
DOI: https://dx.doi.org/10.3748/wjg.v26.i26.3767

INTRODUCTION

Duodenoscopes undergo a multi-step cleaning and high-level disinfection (HLD) procedure, called reprocessing, so that they can be reused in patients. However, the complex design of duodenoscopes may impede effective cleaning[1-4]. Clinically, patient-ready duodenoscopes were designed with an assumed contamination rate of less than 0.4%[5]. The United States Food and Drug Administration (FDA) on April 12, 2019 reported that 5.4% of clinically used duodenoscopes remain contaminated with viable high-concern organisms despite following the manufacturer's reprocessing instructions[5]. Higher-than-expected contamination rates have occurred despite documented adherence to all steps, which suggests that the current guidelines of endoscope reprocessing may be inadequate[1,2,6,7].

Working channels are subjected to wear and tear; the damaged channels allow bacteria to adhere and hide, and the subsequent formation of biofilms are difficult to

remove[8,9]. Visual inspection of working channels of patient-ready endoscopes revealed various findings, including presence of scratches, adherent peel, stains, debris, and fluids[10-12]. Endoscopes with damaged working channels have been considered sources of microbiological contamination[8,13]. The FDA recommended to return the duodenoscopes to the manufacturer for inspection, servicing, and maintenance at least once a year[5]. Visual inspection may identify certain abnormalities and improve the quality and care of duodenoscope reprocessing.

However, many questions have been raised about the visual inspection findings on working channels in real-world situations[10,14]. Studies related to working channels in such situations are too limited to provide sufficient information. When should the visual inspections be performed? Which types of visual inspection findings hold clinical significance? Are the visual inspection findings correlated with microbiological contamination?

With the development of digital endoscopic technology, the SpyGlass visualization system has become increasingly available and easily accessible for clinical treatment in endoscopy units[15]. Video recordings of working channels can be used for communication, teaching, research, and education. An endoscopist may directly visualize the working channels with the SpyGlass visualization system to identify damaged duodenoscopes and return them to the manufacturer for evaluation, repair, or replacement.

This study aimed to investigate the type, severity, and location of the abnormal visual inspection findings inside working channels using the SpyGlass visualization system. We also aimed to assess the clinical significance of these visual inspection findings in microbiological surveillance of patient-ready duodenoscopes in endoscopy units.

MATERIALS AND METHODS

Study design

Visual inspections of patient-ready duodenoscopes (Olympus, Tokyo, Japan) were performed after HLD. The duodenoscope model, duodenoscope age, visual inspection abnormal findings, adenosine triphosphate (ATP) test results, and microbiological surveillance were collected for each duodenoscope. This study was conducted in two endoscopy units of tertiary care teaching hospitals (Tri-Service General Hospital and National Taiwan University Hospital) in Taiwan. A cross-sectional study of the findings of visual inspection of the duodenoscopes was carried out from January 2019 to December 2019. Duodenoscope culture reports were obtained for review and analysis *via* a longitudinal observational study. The present study was approved by the Institutional Review Board of Tri-Service General Hospital, Taipei, Taiwan.

Duodenoscope reprocessing

Patient-used duodenoscopes undergo standard pre-cleaning, manual cleaning, and HLD after each endoscopic retrograde cholangiopancreatography (ERCP) procedure[16]. HLD was undertaken using an automated endoscope reprocessor (AER) with ortho-phthalaldehyde (OPA) as the chemical disinfectant. The HLD cycle ends with alcohol flushes followed by an automated 1-min air purge within the AER. Patient-ready duodenoscopes were stored vertically in a storage cabinet equipped for humidity and temperature monitoring.

SpyGlass visualization system

Working channels were evaluated with the SpyGlass™ DS Direct Visualization System (Boston Scientific Corp, Natick, MA, United States), which consists of capital equipment and a SpyScope delivery catheter (SpyScope™ DS Catheter, SpyScope™ DS II Catheter). A SpyScope delivery catheter has a length of 214 cm, an outer diameter of 3.5 mm (10.5 Fr), a light source at its distal tip, an adjustable brightness, and a lens that enables high-resolution (24000 pixels) video recording during clinical treatment. A high-resolution monitor (1280 × 1024) is designed to be attached to the cart and to provide bright, clear images under various lighting conditions. The video was viewed on a Windows-based computer, which allows the capturing of both video and still images. The assigned SpyScope delivery catheter was reprocessed immediately before each visual inspection with alcohol wipes for a full 2 min of contact time, followed by air drying for 10 min[12]. After visual inspection, the delivery catheter was reprocessed with the OPA solution.

Location of visual inspection

Working channels were examined by manually advancing the SpyScope delivery catheter in an anterograde fashion from the biopsy channel opening of the endoscope handle. The SpyScope delivery catheter allows visualization of the entire length of the working channel (140 cm), including the insertion tube (130 cm) starting from the biopsy channel opening at the proximal part and the bending section (10 cm) proximal to the elevator mechanism (Figure 1).

Type and severity of visual inspection findings

Visual inspection of the working channels of the patient-ready endoscopes revealed various abnormal findings (Figure 2), including scratches, scratches with adherent peel, stains, debris (dark-colored debris, light-colored debris, and other debris), and fluids (clear and opaque fluids)[10-12]. The severity of the visual inspection findings was evaluated using a modified form of Barakat *et al*[12] 's classification system that utilized a 3-point scale with the following scores: 0 (none), 1 (mild), 2 (moderate), and 3 (severe). Visual inspection findings were recorded and reviewed by two endoscopists and two endoscopy nurses. In case of a discrepancy in the image of a given visual inspection, discussion would be held by four investigators. Repeated visual inspections were performed to validate consistency and confirm subtle findings of the duodenoscopes.

ATP test and microbiological surveillance

The ATP test was performed after duodenoscope manual cleaning as a routine quality control program[17]. ATP samples obtained were flushed with sterile water, and then the channel rinsate was harvested for the ATP test (Clean-Trace ATP Water, 3M, St Paul, MN, United States). ATP levels were expressed in relative light units (RLUs).

Microbiological surveillance of clinically used duodenoscopes followed the recommendation of the Digestive Endoscopy Society of Taiwan[16,18]. Ten milliliters of normal saline were injected into the working channel. The elution from the distal end was collected and mixed with 40-mL trypticase soy broth in the flask and then incubated at 37°C for 48 h. The turbid sample was chosen, and a subculture with Columbia CNA agar plate for gram-positive bacteria and MacConkey agar plate for gram-negative bacteria was performed overnight. The pure colony was picked up and underwent matrix-assisted laser desorption/ionization time-of-flight mass spectrometry to further identify the specific bacteria.

Statistical analysis

All data were entered into an Excel software (Microsoft Corp, Redmond, WA, United States) spreadsheet. Statistical analyses were carried out using SPSS 22.0 (IBM, Armonk, NY, United States). The McNemar test was used to compare the number of the visual inspection findings among different duodenoscope ages. Multivariable logistic regression analyses were performed to calculate the adjusted odds ratios with 95% confidence intervals (CIs) of the association between the bending section and visual inspection findings. Spearman's correlation coefficients were calculated between the visual inspection findings and microbiological contamination. Statistical significance was defined as a P value < 0.05.

RESULTS

Duodenoscope characteristics

A total of 19 patient-ready duodenoscopes (JF-260V, n = 5; TJF-260V, n = 14; Olympus Medical Systems, Tokyo, Japan) were examined in the endoscopy units (Table 1). The mean age of the duodenoscopes was 35 ± 38 mo, and mean usage count was 356 ± 400. The visual inspection findings of 19 duodenoscopes included scratches (n = 10, 52.6%), buckling (n = 15, 78.9%), stains (n = 14, 73.7%), debris (n = 14, 73.7%), and fluids (n = 6, 31.6%). The mean ATP levels were 70 ± 120 RLUs. There was a total of 134 samples for microbiological surveillance; of these, 6 (4.5%) samples showed positive results.

Duodenoscope service life vs visual inspection findings

The total number of abnormal visual inspection findings (42 findings *vs* 26 findings, P < 0.001) and scratches (11 findings *vs* 3 findings, P < 0.001) were significantly higher in > 12-mo-old duodenoscopes than in ≤ 12-mo-old duodenoscopes (Figure 3). The total number of abnormal visual inspection findings (21.3 ± 11.6 findings *vs* 11.1 ± 6.4

Table 1 Duodenoscope characteristics, inspection findings, ATP test, and microbiological surveillance

Number	Duodenoscope (model)	Age (mo)	Usages(*n*)	Inspection abnormal findings (Severity degree/location)									ATP test (RLU)	Microbiological surveillance		
				Scratches	Peel	Buckling	Stains	Debris			Fluid			Culture(*n*)	Positive(*n*)	Microorganism
								Dark color	Light color	Other	Clear	Opaque				
1	JF-260V	87	1284	3/B	2/B	2/B	2/B	1/B	3/B	-	3/I	-	135	34	2	*P. aeruginosa*
2	JF-260V	2	18	-	-	1/B	2/I	-	-	-	-	-	185	2	1	*P. aeruginosa*
3	JF-260V	79	1267	-	-	-	2/B	2/I	-	-	-	-	117	27	0	-
4	JF-260V	64	825	3/B	1/B	2/B	2/B	1/I	-	-	3/I	3/I	45	24	0	-
5	JF-260V	1	15	-	-	-	-	2/I	1/ I&B	1/B	3/I	-	19	2	1	*P. aeruginosa*
6	TJF-260V	126	649	3/I&B	-	2/I&B	2/I&B	2/I	-	1/B	3/I&B	3/I&B	48	29	2	*P. aeruginosa*
7	TJF-260V	3	34	-	-	2/B	-	-	-	-	-	-	12	2	0	-
8	TJF-260V	12	135	-	-	2/B	2/I	2/I	-	-	3/I	1/I	108	2	0	-
9	TJF-260V	18	48	-	-	2/I&B	2/I	-	-	-	-	-	63	2	0	-
10	TJF-260V	93	164	1/B	2/B	2/B	2/I&B	2/I&B	-	-	-	-	39	1	0	-
11	TJF-260V	51	425	3/B	-	2/B	2/I	--	-	-	-	-	21	1	0	-
12	TJF-260V	38	251	1/B	-	2/B	2/B	3/I&B	-	-	-	-	114	2	0	-
13	TJF-260V	37	612	3/B	2/B	2/B	2/B	3/I&B	1/I&B	1/I&B	-	-	153	2	0	-
14	TJF-260V	12	217	1/B	-	2/I&B	1/B	1/I	-	-	-	-	40	2	0	-
15	TJF-260V	16	251	-	-	-	1B	1/I	-	-	-	-	48	0	0	-
16	TJF-260V	16	341	2/B	-	1/B	1/B	1/I	-	-	-	-	127	1	0	-
17	TJF-260V	2	50	-	-	1/B	-	2/ I&B	-	-	-	-	29	0	0	-
18	TJF-260V	4	80	1/B	-	1/B	-	2/I&B	-	-	-	-	191	1	0	-
19	TJF-260V	4	67	-	-	-	-	-	-	-	3/I&B	-	97	0	0	-
Summary		35 ± 38	356 ± 400	10	4	15	14	14	3	3	6	3	84 ± 57	134	6	-

Severity degree: None (0), mild (1), moderate (2), severe (3); location site: insertion tube (I) and bending section (B). Data in summary row are expressed as sum or mean ± SD. ATP: Adenosine tri-phosphate; RLU: Relative light units; *P. aeruginosa*: *Pseudomonas aeruginosa*.

findings, $P = 0.043$) were significantly higher in duodenoscopes that had > 200 uses

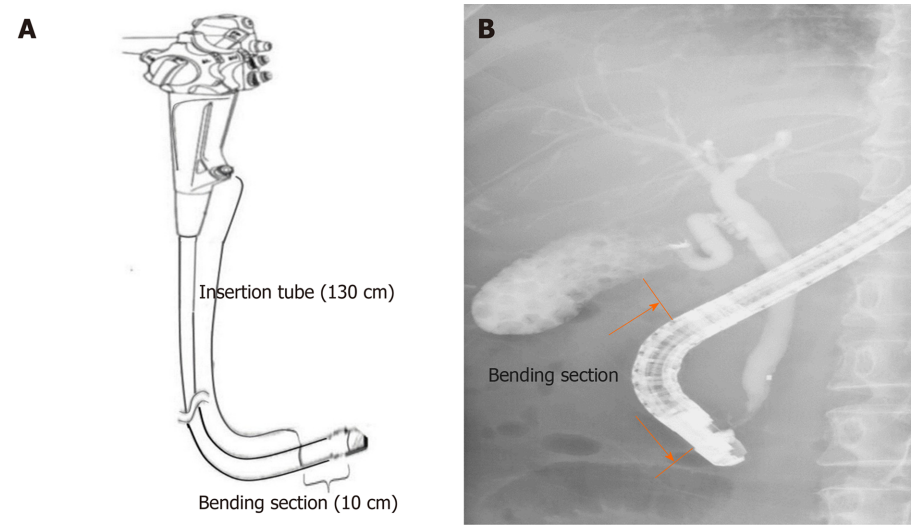

Figure 1 A scheme depicting the working channel of a duodenoscope. Insertion tube (130 cm) starting from the biopsy channel opening at the proximal part (A) and bending section (10 cm) proximal to the elevator mechanism (B).

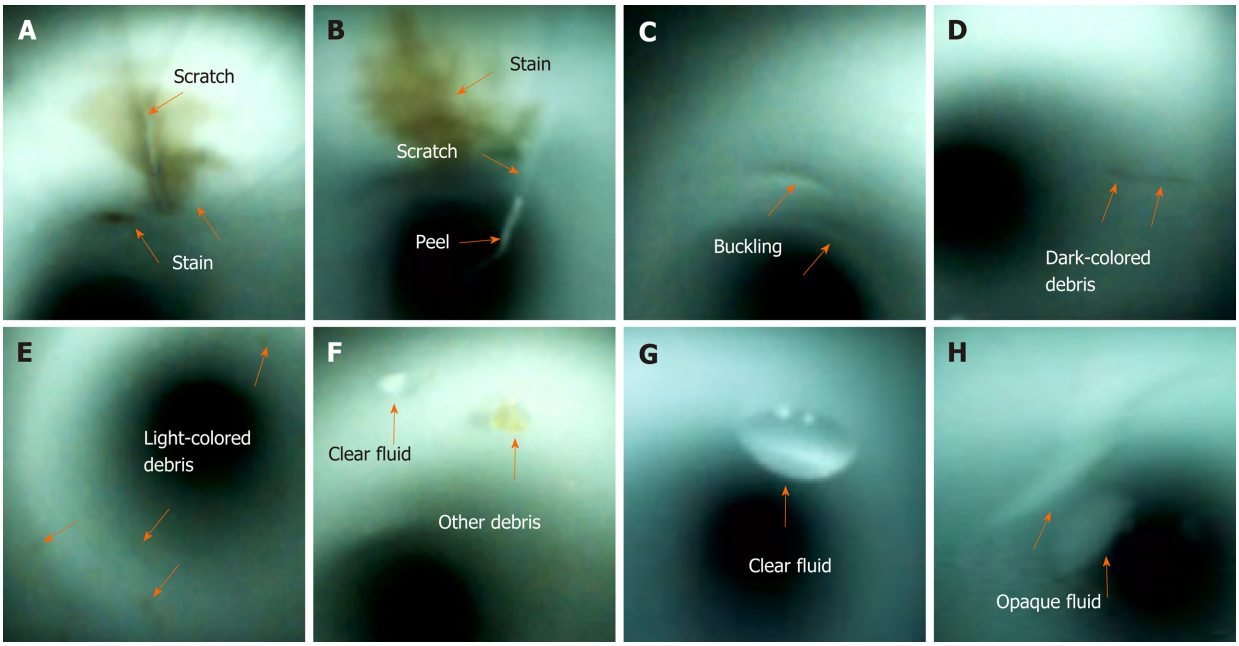

Figure 2 Abnormal visual inspection findings (orange arrow) inside the working channels, including scratches (A and B), scratch with an adherent peel (B), buckling (C), stains (A and B), dark-colored debris (D), light-colored debris (E), other debris (F), clear fluid (F and G), and opaque fluid (H).

than in those with < 200 uses.

Scratches, buckling, and stains were found at the same location during the follow-up inspections (Figure 4). They may worsen and progressively increase in length and width over time. However, debris and fluids may disappear after one or more cycles of reprocessing.

Bending section vs insertion tube

The number of abnormal visual inspection findings located at the bending section was higher than that located at the insertion tube (54 findings *vs* 39 findings), but it did not reach statistical significance (Figure 5). The number of buckling findings at the bending section was significantly higher than that at the insertion tube (15 findings *vs* 3 findings, $P < 0.001$). However, the number of fluid findings at the bending section was significantly lower than that at the insertion tube (3 findings *vs* 9 findings, $P < 0.001$).

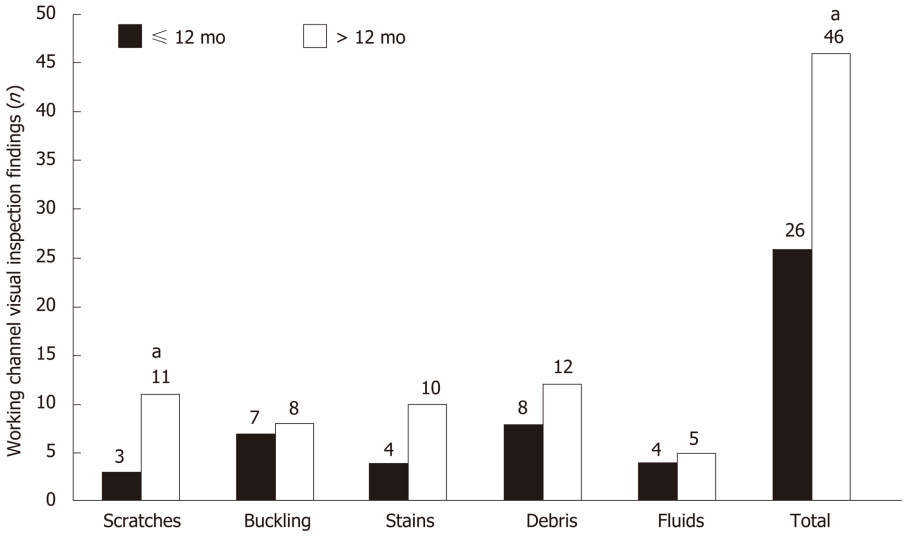

Figure 3 Comparison of visual inspection findings between > 12-mo-old and ≤ 12mo-old duodenoscopes. [a]Indicates statistically significant difference.

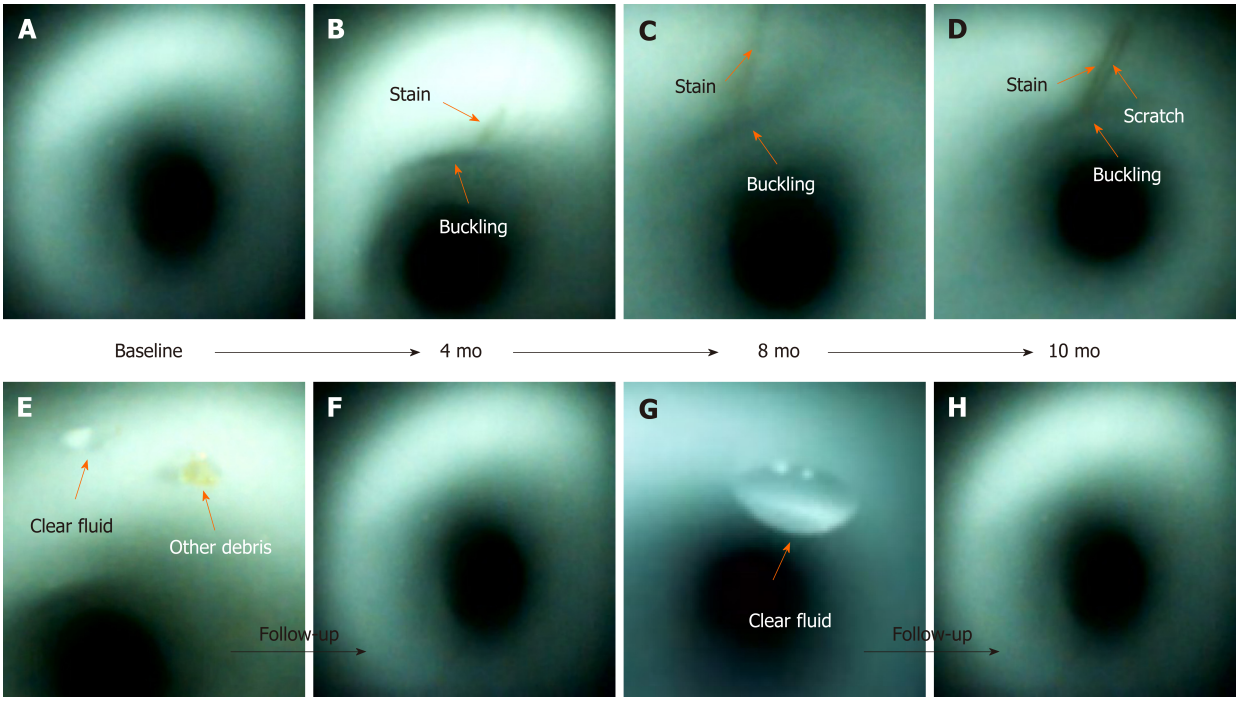

Figure 4 Scratches, buckling, and stains (orange arrow) appeared at the same location inside the working channel during the follow-up inspections (B-D). Buckling and stains progressively increased in length and width (A-D). A scratch (D) was found. Debris (E and F) and clear fluid (E-H) disappeared after one or more cycles of reprocessing.

Bending section is vulnerable to damage

Multivariable logistic regression analyses (Table 2) demonstrated that the risk of abnormal visual inspection findings, including scratches (adjusted odds ratio = 2.60, 95%CI: 2.09-3.12, $P < 0.001$), buckling (adjusted odds ratio = 2.00, 95%CI: 1.68-2.39, $P < 0.001$), stains (adjusted odds ratio = 1.72, 95%CI: 1.16-2.56, $P = 0.008$), and debris (adjusted odds ratio = 1.88, 95%CI: 1.50-2.36, $P < 0.001$) , was significantly higher at the bending section, but this location had a significantly lower risk of fluid accumulation (adjusted odds ratio = 0.30, 95%CI: 0.21-0.42, $P < 0.001$) as compared to the insertion tube.

Table 2 Multivariate regression analysis of abnormal visual inspection findings of the bending section and insertion tube

Variable	Adjusted odds ratio	95%CI	*P* value
Scratches	2.60	2.09-3.12	< 0.001
Buckling	2.00	1.68-2.39	< 0.001
Stains	1.72	1.16-2.56	0.008
Debris	1.88	1.50-2.36	< 0.001
Fluids	0.30	0.21-0.42	< 0.001

Reference: Insertion tube; CI: Confidence interval.

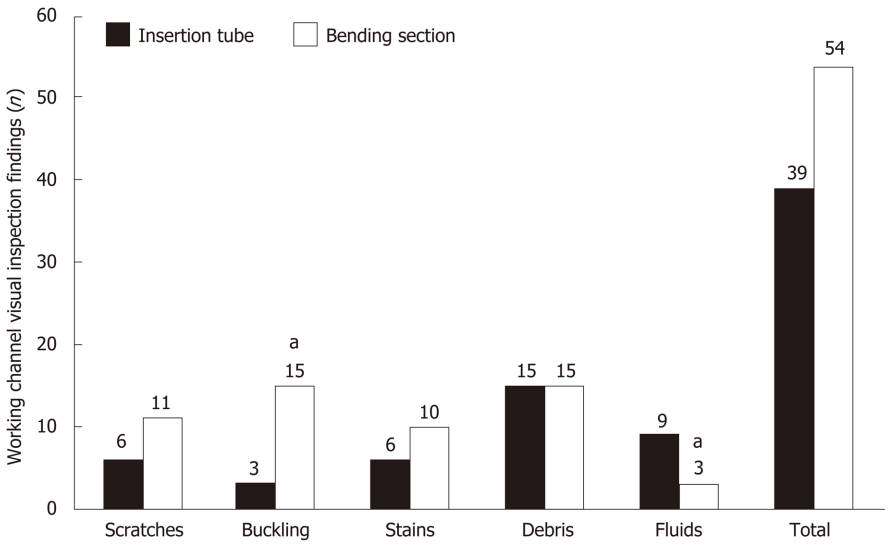

Figure 5 Comparison of visual inspection findings between the bending section and insertion tube. [a]Indicates statistically significant difference.

ATP test and microbiological surveillance

The number of abnormal visual inspection findings was not significantly associated with ATP values after HLD (data not shown). Spearman's correlation coefficients were calculated between abnormal visual inspection findings and microbiological surveillance (Table 3). There was a significant positive Spearman's correlation coefficient between microbiological surveillance and debris (correlation coefficient = 0.423, P = 0.029), between that and fluids, (correlation coefficient = 0.476, P = 0.037), and between that and concomitant debris and fluids (correlation coefficient = 0.702, P = 0.018).

There was no significant Spearman's correlation coefficient between negative bacterial cultures and debris (correlation coefficient = 0.512, P = 0.086), between that and fluids (correlation coefficient = 0.114, P = 0.289), and between that and concomitant debris and fluids (correlation coefficient = 0.617, P = 0.174). This result demonstrated that the presence of fluid and debris is associated with positive cultures, but not negative cultures.

Fluids is an independent factor for culture positivity

To clarify whether the debris or fluids determine bacterial culture positivity, we further performed multivariate analyses to measure the relationship between two variables whilst controlling for the effect of the other variable (Table 4). There was a significant positive partial correlation coefficient between bacterial culture positivity and fluids (correlation coefficient = 0.462, P = 0.046), but not between that and debris (partial correlation coefficient = 0.316, P = 0.187). This result demonstrated that fluids, but not debris, is an independent factor for bacterial culture positivity.

Table 3 Correlation between abnormal visual inspection findings and microbiological surveillance

Variable	Microbiological surveillance	
	Spearman's correlation coefficient	*P* value
Scratches	0.088	0.694
Buckling	-0.080	0.746
Stains	0.133	0.587
Debris	0.423	0.029
Fluids	0.476	0.037
Debris + fluids	0.702	0.018

Table 4 Multivariate analysis of abnormal visual inspection findings and microbiological surveillance

Variable	Microbiological surveillance	
	Partial correlation coefficient	*P* value
Debris	0.316	0.187
Fluids	0.462	0.046

Controlling for number of samples taken.

DISCUSSION

This study demonstrated that (1) the common abnormal visual inspection findings of patient-ready duodenoscopes were scratches (52.6%), buckling (78.9%), stains (73.7%), debris (73.7%), and fluids (31.6%); (2) the abnormal visual inspection findings, especially for scratches inside the working channels, were significantly increased in >12-mo-old duodenoscopes; (3) the risk of duodenoscopes of being scratched, buckled, and stained, and accumulating debris was significantly higher at the bending section than at the insertion tube; (4) the presence of debris and fluids makes the duodenoscope susceptible to microbiological contamination; and (5) the presence of fluids is an independent factor for bacterial culture positivity.

The results of this study are consistent with those of previous studies[11,19,20] reporting that the inside of working channels of patient-ready duodenoscopes commonly have scratches, buckling, stains, debris, and fluids (Table 5). A previous guideline only recommended to identify the wear and tear of the external surface, but it did not require the inspection of the internal surface of the working channel[7]. The recently published guidelines from several societies have recommended the performance of visual inspections of working channels during endoscope care and reprocessing[6,21,22]. This study demonstrated that abnormal visual inspection findings may accumulate during long-term endoscope use; these abnormal findings may progressively increase in length and width over time. Visual inspection may identify certain abnormalities and improve the quality of duodenoscope reprocessing in endoscopy units.

The Spyglass visualization system is designed to interface with computer software and to record both still and video images[10,15]. This system has been widely applied to treat biliopancreatic diseases[23]. Currently, the available borescopes have short lengths of 95-110 cm[10]; therefore, borescopes do not allow for a one-step complete inspection of the 140-cm working channel of a duodenoscope. Conversely, a SpyScope delivery catheter is 214 cm in length; therefore, a one-step visual inspection of the working channel can be done with a SpyScope. Endoscopists should routinely or intermittently visualize the working channel during working hours. Early detection of these abnormal visual inspection findings may allow early reporting to the manufacturers and may promote prompt performance of quality assurance interventions before the channel lumen becomes comprised, which could impair manual cleaning. Our study is the first one to use the SpyScope delivery catheter as a tool for visual inspection, besides its original clinical role in treating biliopancreatic diseases.

Endoscopic accessories, such as biopsy forceps, biliary stent, polypectomy snare, and catheter guidewire, are frequently inserted into the working channel[24]. Forcing instrumentation through the channel can cause damages or scratches to the channel[25].

Table 5 Summary of studies on abnormal visual inspection findings in clinically used endoscopes

Study	Endoscopes (duodenoscopes), *n* (*n*)	Scratches (%)	Buckling (%)	Stains (%)	Debris (%)	Fluids (%)
Thaker *et al*[11], 2018	59 (14)	86	NR	59	22	8
Ofstead *et al*[19], 2018[19]	45 (5)	NR	NR	NR	NR	47
Barakat *et al*[20], 2018	68 (7)	99	3	NR	96	43
This study	19 (19)	52.6	78.9	73.7	73.7	31.6

NR: Not reported.

This frequently occurs at the bending section when the endoscope is extremely angulated[26]. It seems inevitable that the endoscopes undergo repeated mechanical damage at the bending section during endoscopy procedures. Multivariable logistic regression analyses (Table 3) demonstrated that the risk of developing scratches, buckling, stains, and debris is significantly higher at the bending section than at the insertion tube.

The bacteria may form biofilms in the endoscope channel, especially when the working channels are damaged, and can contribute to the failure of the decontamination process[8,27]. Colonizing microorganisms proceed with an initial attachment to the preconditioned surface. At this point, the preconditioning film and microorganisms or visible debris are loosely attached and can be easily removed by manual cleaning[28]. Bacterial biofilms or visible stains can develop inside endoscope channels if established reprocessing protocols are not met, and these biofilms can be difficult to remove[28]. *Pseudomonas aeruginosa* prefers a moist environment and forms biofilms that are extremely difficult to remove from endoscope channels[27].

For duodenoscopes contaminated with *Pseudomonas aeruginosa*, double cycles of HLD, peracetic acid high-level disinfection, and ethylene oxide sterilization[29] may not be effective; thus, endoscopists should return them to the manufacturer for replacement. With continuous use of the damaged endoscope and its accessories, organic debris may enter into different areas of the device, thereby interfering with reprocessing; this might increase the likelihood of biofilm development. Based on the results of this study, our endoscopy units developed a protocol to ensure the quality of reprocessing procedures. Duodenoscopes will be sent to the manufacturer for checking or repairing immediately under the following conditions: (1) Presence of an endoscope leak; (2) Structural or functional damage of the endoscope; (3) Repeated positive bacterial cultures despite reprocessing by well-trained personnel; and (4) Isolation of *Pseudomonas aeruginosa* by bacterial culture, associated with significant abnormal visual inspection findings. Duodenoscopes used for more than a year are sent to the manufacturer for annual checks.

LIMITATIONS

This study has several limitations. The number of samples taken for culture ranged from 0 to 34 (Table 1). A total of 134 samples were available for microbiological surveillance. We excluded three cases from the analysis (cases 15, 17, and 19, as shown in Table 1) where no samples were taken for culture. We analyzed the number of samples taken for culture by the service age of the duodenoscopes (> 12 mo *vs* ≤ 12 mo). The number of samples taken for culture surveillance was higher in duodenoscopes used for > 12 mo (11.2 ± 13.9 number of cultures, n = 11) than those used for ≤ 12 mo (1.4 ± 0.9 number of cultures, n = 8). This study showed that in real-world situations, there will be variations between the samples taken from the instruments. The duodenoscopes were observed for only a short period of time, which may have caused inconsistencies. Furthermore, this was a two-site study with a small sample size, so the findings may not be generalizable. Due to the limited number of duodenoscopes, it was difficult to conduct a subgroup analysis, which may have affected the results.

CONCLUSION

Patient-ready duodenoscopes commonly have scratches, buckling, stains, debris, and fluids inside the working channel. The presence of debris and fluids makes these devices vulnerable to microbiological contamination. We found that the presence of fluids was an independent factor for bacterial culture positivity. Routine visualization of the working channels may provide the opportunity for early quality assurance measures to be taken before the channel lumens become damaged, which may impair manual cleaning. The visual channel inspection approach in our study may be added to existing visual inspection recommendations to identify suboptimal reprocessing or endoscopes requiring repair or replacement.

ARTICLE HIGHLIGHTS

Research background

The working channels of endoscopes are subjected to wear and tear. Damaged channels allow bacteria to adhere and hide, and the biofilms that form are subsequently difficult to remove. Visual channel inspection has been proposed as a quality control measure for endoscope reprocessing.

Research motivation

Endoscopes with damaged working channels have been considered as sources of microbiological contamination. The FDA recommended returning duodenoscopes to the manufacturer for inspection, servicing, and maintenance at least once a year. Visual inspection may identify certain abnormalities and improve endoscopic quality and care of duodenoscope reprocessing. However, many questions have been raised regarding the visual inspection findings on working channels in real-world situations. Studies related to such situations are too limited to provide sufficient information.

Research objectives

We aimed to investigate the type, severity, location, and clinical significance of visual inspections inside patient-ready duodenoscopes.

Research methods

Visual inspection of channels was performed in 19 duodenoscopes. Inspections were recorded and reviewed to evaluate for channel damage (scratches, buckling, and stains), debris (dark-colored debris, light-colored debris, and other debris), and fluids (clear fluid and opaque fluid). Visual inspection findings were used to analyze the relevance of microbiological surveillance.

Research results

We found 72 abnormal visual inspection findings in the 19 duodenoscopes viewed in our study, including scratches (n = 10, 52.6%), buckling (n = 15, 78.9%), stains (n = 14, 73.7%), debris (n = 14, 73.7%), and fluids (n = 6, 31.6%). Duodenoscopes > 12 mo old had a significantly higher number of abnormal visual inspection findings than those ≤ 12 mo old (46 findings *vs* 26 findings, $P < 0.001$). Multivariable regression analyses demonstrated that the bending section had a significantly higher risk of being scratched, buckled, and stained, and accumulating debris than the insertion tube. Debris and fluids showed a significant positive correlation with microbiological contamination ($P < 0.05$).

Research conclusions

In patient-ready duodenoscopes, scratches, buckling, stains, debris, and fluids inside the working channel are common. Presence of debris and fluids increases the susceptibility to microbiological contamination. The presence of fluids was found to be an independent factor for bacterial culture positivity. Visual channel inspection using the SpyGlass visualization system may be added to the existing visual inspection recommendations to identify suboptimal reprocessing or endoscopes requiring repair or replacement.

Research perspectives

Endoscopists should routinely or intermittently visualize the working channel during

working hours. Early detection of these abnormal visual inspection findings may allow timely reporting to the manufacturers and promote prompt performance of quality assurance interventions before the channel lumen becomes comprised, which could impair manual cleaning.

ACKNOWLEDGEMENTS

We thank Wu-Chien Chien and Chi-Hsiang Chung (Associate Professor and Assistant Professor, respectively, in the School of Public Health, National Defense Medical Center, Taiwan) for their help with the statistical analysis. We are also grateful to Ming-Chin Chan and Sun-Kang Chiu (Infection Control Office, Tri-Service General Hospital, Taiwan) for the assistance with microbiological surveillance consultation. Finally, we thank I-Hsuan Hunag (Division of Gastroenterology, Department of Internal Medicine, Tri-Service General Hospital, National Defense Medical Center, Taipei, Taiwan) for the assistance in medical illustration.

REFERENCES

1 **Reprocessing Guideline Task Force**; Petersen BT, Cohen J, Hambrick RD 3rd, Buttar N, Greenwald DA, Buscaglia JM, Collins J, Eisen G. Multisociety guideline on reprocessing flexible GI endoscopes: 2016 update. *Gastrointest Endosc* 2017; **85**: 282-294.e1 [PMID: 28069113 DOI: 10.1016/j.gie.2016.10.002]

2 **Petersen BT**, Chennat J, Cohen J, Cotton PB, Greenwald DA, Kowalski TE, Krinsky ML, Park WG, Pike IM, Romagnuolo J; ASGE Quality Assurance in Endoscopy Committee, Rutala WA; Society for Healthcare Epidemiology of America. Multisociety guideline on reprocessing flexible GI endoscopes: 2011. *Infect Control Hosp Epidemiol* 2011; **32**: 527-537 [PMID: 21558764 DOI: 10.1086/660676]

3 **Ross AS**, Baliga C, Verma P, Duchin J, Gluck M. A quarantine process for the resolution of duodenoscope-associated transmission of multidrug-resistant Escherichia coli. *Gastrointest Endosc* 2015; **82**: 477-483 [PMID: 26092616 DOI: 10.1016/j.gie.2015.04.036]

4 **Muscarella LF**. Risk of transmission of carbapenem-resistant Enterobacteriaceae and related "superbugs" during gastrointestinal endoscopy. *World J Gastrointest Endosc* 2014; **6**: 457-474 [PMID: 25324917 DOI: 10.4253/wjge.v6.i10.457]

5 **U.S. Food and Drug Administration**. The FDA Continues to Remind Facilities of the Importance of Following Duodenoscope Reprocessing Instructions: FDA Safety Communication. 2019. Available from: https://wwwfdagov/medical-devices/safety-communications/fda-continues-remind-facilities-importance-following-duodenoscope-reprocessing-instructions-fda

6 **World Gastroenterology Organisation**. Endoscope disinfection update: a guide to resource-sensitive reprocessing. Available from: https://wwwworldgastroenterologyorg/guidelines/global-guidelines/endoscope-disinfection/endoscope-disinfection-english

7 **Beilenhoff U**, Biering H, Blum R, Brljak J, Cimbro M, Dumonceau JM, Hassan C, Jung M, Neumann C, Pietsch M, Pineau L, Ponchon T, Rejchrt S, Rey JF, Schmidt V, Tillett J, van Hooft J. Prevention of multidrug-resistant infections from contaminated duodenoscopes: Position Statement of the European Society of Gastrointestinal Endoscopy (ESGE) and European Society of Gastroenterology Nurses and Associates (ESGENA). *Endoscopy* 2017; **49**: 1098-1106 [PMID: 29036747 DOI: 10.1055/s-0043-120523]

8 **Buss AJ**, Been MH, Borgers RP, Stokroos I, Melchers WJ, Peters FT, Limburg AJ, Degener JE. Endoscope disinfection and its pitfalls--requirement for retrograde surveillance cultures. *Endoscopy* 2008; **40**: 327-332 [PMID: 18264888 DOI: 10.1055/s-2007-995477]

9 **Bang JY**, Sutton B, Hawes R, Varadarajulu S. Concept of disposable duodenoscope: at what cost? *Gut* 2019; **68**: 1915-1917 [PMID: 30772837 DOI: 10.1136/gutjnl-2019-318227]

10 **Visrodia K**, Petersen BT. Borescope examination: Is there value in visual assessment of endoscope channels? *Gastrointest Endosc* 2018; **88**: 620-623 [PMID: 30217239 DOI: 10.1016/j.gie.2018.07.005]

11 **Thaker AM**, Kim S, Sedarat A, Watson RR, Muthusamy VR. Inspection of endoscope instrument channels after reprocessing using a prototype borescope. *Gastrointest Endosc* 2018; **88**: 612-619 [PMID: 29753038 DOI: 10.1016/j.gie.2018.04.2366]

12 **Barakat MT**, Huang RJ, Banerjee S. Comparison of automated and manual drying in the elimination of residual endoscope working channel fluid after reprocessing (with video). *Gastrointest Endosc* 2019; **89**: 124-132.e2 [PMID: 30148992 DOI: 10.1016/j.gie.2018.08.033]

13 **Rauwers AW**, Troelstra A, Fluit AC, Wissink C, Loeve AJ, Vleggaar FP, Bruno MJ, Vos MC, Bode LG, Monkelbaan JF. Independent root-cause analysis of contributing factors, including dismantling of 2 duodenoscopes, to investigate an outbreak of multidrug-resistant Klebsiella pneumoniae. *Gastrointest Endosc* 2019; **90**: 793-804 [PMID: 31102643 DOI: 10.1016/j.gie.2019.05.016]

14 **The Lancet Gastroenterology Hepatology**. Scoping the problem: endoscopy-associated infections. *Lancet Gastroenterol Hepatol* 2018; **3**: 445 [PMID: 29893228 DOI: 10.1016/S2468-1253(18)30168-7]

15 **Dimas ID**, Vardas E, Papastergiou V, Fragaki M, Velegraki M, Mpitouli A, Voudoukis E, Theodoropoulou A, Giannikaki E, Chlouverakis G, Paspatis GA. Comparison of digital versus fiberoptic cholangioscopy in patients requiring evaluation of bile duct disease or treatment of biliary stones. *Ann Gastroenterol* 2019; **32**: 199-204 [PMID: 30837794 DOI: 10.20524/aog.2019.0358]

16 Digestive Endoscopy Society of Taiwan (DEST) guideline on duodenoscope reprocessing: cleaning, disinfection and sterilization. 2018. Avalable from: https://wwwdestorgtw/DB/News/file/386-2pdf. 2018.

Accessed December 9, 2019

17 **Chang WK**, Liu TC, Liu TL, Peng CL, Wang HP. Enhanced manual cleaning efficacy of duodenoscope in endoscopy units: Results of a multicenter comprehensive quality control program. *Am J Infect Control* 2019; **47**: 1233-1239 [PMID: 31126624 DOI: 10.1016/j.ajic.2019.03.029]

18 **Centers for Disease Control and Prevention**. Duodenoscope Surveillance Sampling and Culturing Protocols. Available from: https://wwwfdagov/media/111081/download

19 **Ofstead CL**, Heymann OL, Quick MR, Eiland JE, Wetzler HP. Residual moisture and waterborne pathogens inside flexible endoscopes: Evidence from a multisite study of endoscope drying effectiveness. *Am J Infect Control* 2018; **46**: 689-696 [PMID: 29609854 DOI: 10.1016/j.ajic.2018.03.002]

20 **Barakat MT**, Girotra M, Huang RJ, Banerjee S. Scoping the scope: endoscopic evaluation of endoscope working channels with a new high-resolution inspection endoscope (with video). *Gastrointest Endosc* 2018; **88**: 601-611.e1 [PMID: 29425885 DOI: 10.1016/j.gie.2018.01.018]

21 **Sharon A**, Van Wicklin RC, Cynthia Spry; Association of periOperative Registered Nurses. Guideline for processing flexible endoscopes. 2018: 799-882. Available from: https://wwwaornorg/websitedata/cearticle/pdf_file/CEA16516-0001pdf

22 **Kaneoka A**, Krisciunas GP, Walsh K, Raade AS, Langmore SE. A comparison of 2 methods of endoscopic laryngeal sensory testing: a preliminary study. *Ann Otol Rhinol Laryngol* 2015; **124**: 187-193 [PMID: 25225213 DOI: 10.1177/0003489414550241]

23 **Karagyozov P**, Boeva I, Tishkov I. Role of digital single-operator cholangioscopy in the diagnosis and treatment of biliary disorders. *World J Gastrointest Endosc* 2019; **11**: 31-40 [PMID: 30705730 DOI: 10.4253/wjge.v11.i1.31]

24 **Mammen A**, Haber G. Difficult Biliary Access: Advanced Cannulation and Sphincterotomy Technique. *Gastrointest Endosc Clin N Am* 2015; **25**: 619-630 [PMID: 26431594 DOI: 10.1016/j.giec.2015.06.007]

25 **Tytgat GN**, Ignacio JG. Technicalities of endoscopic biopsy. *Endoscopy* 1995; **27**: 683-688 [PMID: 8903983 DOI: 10.1055/s-2007-1005788]

26 **Rozeboom ED**, Reilink R, Schwartz MP, Fockens P, Broeders IA. Evaluation of the tip-bending response in clinically used endoscopes. *Endosc Int Open* 2016; **4**: E466-E471 [PMID: 27092330 DOI: 10.1055/s-0042-104115]

27 **Kovaleva J**, Peters FT, van der Mei HC, Degener JE. Transmission of infection by flexible gastrointestinal endoscopy and bronchoscopy. *Clin Microbiol Rev* 2013; **26**: 231-254 [PMID: 23554415 DOI: 10.1128/CMR.00085-12]

28 **Roberts CG**. The role of biofilms in reprocessing medical devices. *Am J Infect Control* 2013; **41**: S77-S80 [PMID: 23622755 DOI: 10.1016/j.ajic.2012.12.008]

29 **Rutala WA**, Weber DJ. Reprocessing semicritical items: Outbreaks and current issues. *Am J Infect Control* 2019; **47S**: A79-A89 [PMID: 31146856 DOI: 10.1016/j.ajic.2019.01.015]

World Journal of Gastroenterology

Submit a Manuscript: https://www.f6publishing.com

World J Gastroenterol 2020 July 14; 26(26): 3780-3791

DOI: 10.3748/wjg.v26.i26.3780

ISSN 1007-9327 (print) ISSN 2219-2840 (online)

ORIGINAL ARTICLE

Retrospective Cohort Study

Non-invasive prediction of persistent villous atrophy in celiac disease

Barbora Packova, Petra Kovalcikova, Zdenek Pavlovsky, Daniel Bartusek, Jitka Prokesova, Jiri Dolina, Radek Kroupa

ORCID number: Barbora Packova 0000-0002-9369-3971; Petra Kovalcikova 0000-0001-9515-7075; Zdenek Pavlovsky 0000-0002-3154-7557; Daniel Bartusek 0000-0003-2761-2712; Jitka Prokesova 0000-0002-9308-4893; Jiri Dolina 0000-0002-9061-5273; Radek Kroupa 0000-0003-2315-8305.

Author contributions: Packova B was involved in the conceptualization, data collection, investigation, project administration, writing original draft; Kovalcikova P took part in methodology and was responsible for statistical analysis; Pavlovsky Z was involved in the data collection, investigation; writing review and editing; Bartusek D was involved in the data collection, investigation; writing review and editing; Prokesova J was involved in the data collection, writing review and editing ; Dolina J took part in the supervision and editing; Kroupa R performed the conceptualization, methodology, project administration, supervision, validation, visualization, writing review and editing. All authors have read and approve the final manuscript.

Supported by Ministry of Health, Czech Republic – conceptual

Barbora Packova, Jitka Prokesova, Jiri Dolina, Radek Kroupa, Department of Gastroenterology and Internal Medicine, University Hospital Brno, Faculty of Medicine, Masaryk University, Brno 62500, Czech Republic

Petra Kovalcikova, Institute of Biostatistics and Analyses, Faculty of Medicine, Masaryk University, Brno 62500, Czech Republic

Zdenek Pavlovsky, Department of Pathology, University Hospital Brno, Faculty of Medicine, Masaryk University, Brno 62500, Czech Republic

Daniel Bartusek, Department of Radiology and Nuclear Medicine, University Hospital Brno, Faculty of Medicine, Masaryk University, Brno 62500, Czech Republic

Corresponding author: Radek Kroupa, MD, PhD, Doctor, Research Assistant Professor, Department of Gastroenterology and Internal Medicine, University Hospital Brno, Faculty of Medicine, Masaryk University, Jihlavska 20, Brno 62500, Czech Republic. kroupa.radek@fnbrno.cz

Abstract

BACKGROUND

Celiac disease (CD) is an immune-mediated enteropathy that is primarily treated with a gluten-free diet (GFD). Mucosal healing is the main target of the therapy. Currently, duodenal biopsy is the only way to evaluate mucosal healing, and non-invasive markers are challenging. Persistent elevation of anti-tissue transglutaminase antibodies (aTTG) is not an ideal predictor of persistent villous atrophy (VA). Data regarding prediction of atrophy using anti-deamidated gliadin peptide antibodies (aDGP) and abdominal ultrasonography are lacking.

AIM

To evaluate the ability of aTTG, aDGP, small bowel ultrasonography, and clinical and laboratory parameters in predicting persistent VA determined using histology.

METHODS

Patients with CD at least 1 year on a GFD and available follow-up duodenal biopsy, levels of aTTG and aDGP, and underwent small bowel ultrasonography

development of research organization, No. FNBr, 65269705.

Institutional review board statement: The study protocol was approved by Institutional review board University hospital Brno.

Informed consent statement: All the patients signed informed consent.

Conflict-of-interest statement: The authors do not have any conflict of interest.

Data sharing statement: No additional data are available.

STROBE statement: The authors have read the STROBE Statement-checklist of items, and the manuscript was prepared and revised according to the STROBE Statement-checklist of items.

Manuscript source: Invited manuscript

Received: January 16, 2020
Peer-review started: January 16, 2020
First decision: April 8, 2020
Revised: May 13, 2020
Accepted: July 1, 2020
Article in press: July 1, 2020
Published online: July 14, 2020

P-Reviewer: Gassler N, Ierardi E, Neri M, Ribaldone DG, Vorobjova T
S-Editor: Dou Y
L-Editor: A
E-Editor: Zhang YL

were included in this retrospective cohort study. We evaluated the sensitivity, specificity, and positive and negative predictive values of aTTG, aDGP, small bowel ultrasonography, laboratory and clinical parameters to predict persistent VA. A receiver operating characteristic (ROC) curve analysis of antibody levels was used to calculate cut off values with the highest accuracy for atrophy prediction.

RESULTS

Complete data were available for 82 patients who were followed up over a period of four years (2014-2018). Among patients included in the analysis, women (67, 81.7%) were predominant and the mean age at diagnosis was 33.8 years. Follow-up biopsy revealed persistent VA in 19 patients (23.2%). The sensitivity and specificity of aTTG using the manufacturer's diagnostic cutoff value to predict atrophy was 50% and 85.7%, respectively, while the sensitivity and specificity of aDGP (using the diagnostic cutoff value) was 77.8% and 75%, respectively. Calculation of an optimal cutoff value using ROC analysis (13.4 U/mL for aTTG IgA and 22.6 U/mL for aDGP IgA) increased the accuracy and reached 72.2% [95% confidence interval (CI): 46.5-90.3] sensitivity and 90% (95%CI: 79.5-96.2) specificity for aDGP IgA and 66.7% (95%CI: 41.0-86.7) sensitivity and 93.7% (95%CI: 84.5-98.2) specificity for aTTG IgA. The sensitivity and specificity of small bowel ultrasonography was 64.7% and 73.5%, respectively. A combination of serology with ultrasound imaging to predict persistent atrophy increased the positive predictive value and specificity to 88.9% and 98% for aTTG IgA and to 90.0% and 97.8% for aDGP IgA. Laboratory and clinical parameters had poor predictive values.

CONCLUSION

The sensitivity, specificity, and negative predictive value of aTTG and aDGP for predicting persistent VA improved by calculating the best cutoff values. The combination of serology and experienced bowel ultrasound examination may achieve better accuracy for the detection of atrophy.

Key words: Celiac disease; Villous atrophy; Anti-tissue transglutaminase antibodies; Anti-deamidated gliadin peptide antibodies; Abdominal ultrasound; Gluten-free diet

Core tip: We attempted to determine whether indicators such as anti-tissue transglutaminase antibodies (aTTG), anti-deamidated gliadin peptide antibodies (aDGP), and abdominal ultrasonography could predict villous atrophy (VA). We studied patients who were diagnosed with celiac disease and were on a gluten-free diet for at least one year; they were followed up for a maximum of four years. We determined that aTTG and aDGP were not optimal markers of persistent VA. However, we found that a combination of serology and bowel ultrasound examination enabled detection of VA with better accuracy.

Citation: Packova B, Kovalcikova P, Pavlovsky Z, Bartusek D, Prokesova J, Dolina J, Kroupa R. Non-invasive prediction of persistent villous atrophy in celiac disease. *World J Gastroenterol* 2020; 26(26): 3780-3791
URL: https://www.wjgnet.com/1007-9327/full/v26/i26/3780.htm
DOI: https://dx.doi.org/10.3748/wjg.v26.i26.3780

INTRODUCTION

Celiac disease (CD) is an immune-mediated enteropathy triggered by gluten in genetically susceptible individuals. The only therapy for CD is a gluten-free diet (GFD). Mucosal healing (Marsh 0 or 1 on follow-up biopsy) is the main endpoint of this therapy; however, this goal has been achieved in approximately 60% of patients after one year of GFD, especially in cases of CD diagnosed in adulthood[1,2]. In contrast,

some recent studies state that up to 81% of patients achieved mucosal healing, as seen on long-term follow-ups[3].

Currently, duodenal biopsy is the only way to evaluate mucosal healing. There is no reliable widely available non-invasive marker of persistent villous atrophy (VA), which is one of the core pathological signs of CD. Many authors regard anti-tissue transglutaminase antibodies (aTTG) as a poor predictor of persistent VA[2,4], with a low sensitivity 0.50 [95% confidence interval (CI): 0.41-0.60] and a relatively high level of specificity 0.83 (95%CI: 0.79-0.87) for TTG IgA assay[5]. However, there is not much data on anti-deamidated gliadin peptide antibodies (aDGP). There is one study evaluating aDGP as a reliable marker of persistent VA[6], while another study found only 48% sensitivity and 91% specificity of aDGP IgA for predicting persistent VA[7]. Currently, to the best of our knowledge, there are no studies indicating the absolute necessity of routine follow-up biopsy[8,9]; however, many centers recommend its implementation[9,10] and itis considered as an important tool in the follow-up of symptomatic patients with CD, based on the recommendations by the American Gastroenterology Association[11]. A personalized approach with respect to risk factors is essential. Together with factors such as the advanced age at diagnosis, the male sex, and untreated CD, even asymptomatic persistent VA is considered to be a risk factor for lymphoproliferative malignancy[12] and possibly higher mortality rates[13]. Other parameters potentially related to VA may be available in the standard clinical care process[14]. Besides counseling with a qualified dietitian, only few objective methods to assess persistent gluten intake are available. There might be a clinical advantage in using non-invasive methods for the detection of patients with high risks of VA, independent of improvement in symptoms after at least 1 year on GFD. Abdominal ultrasound is a widely available method, and several studies have reported specific abnormalities on small bowel imaging that could be related to CD[15,16]. Persistence of these findings might indicate the absence of mucosal healing. Awareness of the risk factors is essential for the selection of patients indicated for thorough follow-up.

Our aim was to evaluate the ability of non-invasive markers (aTTG, aDGP, small bowel ultrasonography, and clinical and laboratory parameters) to predict persistent VA determined using histology in patients with CD who had been on a GFD for at least one year.

MATERIALS AND METHODS

Patient selection

The records of 190 patients with CD from 2014 to 2018 were available in the hospital database at the Department of Gastroenterology and Internal Medicine, University Hospital Brno.The initial diagnosis of CD was based on the presence of VA on an intestinal biopsy, positivity of aTTG and/or aDGP, or the clinical effect of a GFD in cases of seronegative CD. Adherence to a GFD was evaluated by an experienced dietitian. Follow-up duodenal biopsy and ultrasound examination at least after 1 year of GFD was proposed to all patients, independent of symptoms. Patients who had agreed to undergo follow-up biopsy were selected for further evaluation. In our retrospective cohort study, we included patients who had been on complete GFD for at least one year and for whom data on follow-up duodenal biopsy and quantitative evaluation of aTTG and/or aDGP using the enzyme-linked immunosorbent assay (ELISA) method were available as well. Abdominal ultrasonography focused on bowel imaging within 30 d from when duodenal biopsy was performed.

The patients included in the study were divided in two subgroups: (1) The study group with patients with persistent VA on follow-up duodenal biopsy; and (2) Control group with patients classified as Marsh 0 or Marsh 1 on follow-up duodenal biopsy. All patients signed an informed consent regarding anonymous data collection, and the study protocol was approved by the multicentric ethical committee of the University Hospital Brno (No. 03-180919/EK).

Duodenal sampling and assessment of histological findings

All the selected patients underwent esophagogastroscopy with biopsies from the second part of the duodenum and one from duodenal bulb; at least four biopsy specimens were fixed in 40 g/L formaldehyde. Paraffin-embedding blocks were created for basic hematoxylin-eosin staining and special staining. The Marsh classification modified by Oberhuber was used for microscopic evaluation[17]. Mucosal architecture (villus height, crypt depth), intraepithelial lymphocytes, inflammatory cell infiltrate, and level of epithelial differentiation were evaluated. The pathologist was

blinded to the clinical and antibody results.

Methods of serologic testing

Serum samples were collected within 30 d after duodenal biopsy. Sera were assayed for aTTG IgA and IgG and aDGP IgA and IgG using ELISA. Cutoff values over 18 U/mL and 20 U/mL for aTTG and aDGP, respectively, were regarded as positive by the kit manufacturer. Lab kits for analyses were provided by TestLine Clinical Diagnostics Ltd., Brno, Czech Republic.

Ultrasonography evaluation

Ultrasonography examinations of the intestine within 30 d from duodenal biopsy were available for 66 patients. The remainder of the patients underwent ultrasonography at longer periods from duodenal biopsy; therefore, these results were excluded from the analysis. Using a high-frequency linear probe, it was possible to evaluate the intestinal wall, intestinal folds, surrounding mesentery, mesenteric lymph nodes, and other characteristics. The main ultrasound findings in patients with active CD were decreased numbers of jejunal folds, increased numbers of ileal folds and thickening of bowel folds, dysmotility, jejunal dilatation, and intermittent intussusception[15,16]. Mostly non-enlarged mesenteric lymph nodes were detected. As a positive result, persistent ultrasound abnormalities usually related to CD were assessed by an experienced physician who was blinded to serology and biopsy results.

Clinical and laboratory parameters

Clinical symptoms typical of active CD, such as diarrhea, abdominal pain, and weight loss, were reviewed. Laboratory signs of nutritional deficiency, such as anemia (hemoglobin level less than 135 g/L in men and less than 120 g/L in women), sideropenia (ferritin level less than 30 μg/Lin men and less than 13 μg/L in women), and vitamin D deficiency (less than 50 nmol/L), were evaluated.

Statistical analysis

The mean, standard deviation, median, minimum, and maximum were used to analyze quantitative parameters. Absolute and relative frequency were used to analyze qualitative parameters. Sensitivity, specificity, and positive and negative predictive value were calculated from frequency of VA and positivity ofaTTG and aDGP and were reported with their 95%CI. To quantify antibody titers (aTTG IgA, aTTG IgG, aDGP IgA, aDGP IgG) receiver operating characteristic analysis was used to evaluate the best cutoff values with highest total sensitivity and specificity. Sensitivity, specificity, and positive and negative predictive value were calculated for these new cutoff values. The Mann–Whitney test or Fisher's exact test were used for comparison of aTTG and aDGP positive and negative patients as well as for comparison of patients according to the persistence of VA. A P value < 0.05 was considered statistically significant. SPSS software version 23.0 for Windows (SPSS Inc., Chicago, IL, United States) was used for the statistical analyses.

RESULTS

Eighty-two patients fulfilled the inclusion criteria and were further analyzed. In this group, 67 (81.7%) patients were women and the mean age at diagnosis was 33.8 ± 17.4 years. Mean length of the disease at the time of follow-up biopsy was 9.1 years, and mean age at follow-up biopsy was 42.1 ± 13.4 years. Seventy patients (85.4%) were on a GFD longer than 2 years. All patients had CD that was initially properly diagnosed, with positive duodenal biopsy graded according tothe Marsh classification modified by Oberhuber (2× Marsh 2, 17× Marsh 3a, 30× Marsh 3b, 33× Marsh 3c) and either positivity of aTTG and/or aDGP (74×) or clinical effect of GFD in case of seronegative CD (8×). No seronegative patient was in the persistent VA group, as other diagnoses needed to be considered in such cases.

The most frequent clinical symptoms and laboratory signs of malnutrition at the time of follow-up biopsy were diarrhea (23.2%), abdominal pain (20.7%), weight loss (9.8%), sideropenia (26.8%), vitamin D deficiency (20.7%), and anemia (11.0%). Autoantibodies for aTTG were positive (cutoff value 18 U/mL recommended by manufacturer) in 18 cases (22.2%); those of aDGP were positive (cutoff value 20 U/mL determined by laboratory) in 29 cases (37.2%) at the time of follow-up biopsy. Ultrasonography was available in 66 patients with signs correlating with active CD found in 24 (29.3%) cases (details in Table 1).

Table 1 Summary of patient characteristics at the time of biopsy on gluten-free diet

Characteristic	Category	All patients with celiac disease (*n* = 82)	
		n	%
Gender	Female	67	81.7
	Male	15	18.3
Villous atrophy	No	63	76.8
	Yes	19	23.2
Marsh in follow-up biopsy	Marsh 0	44	53.7
	Marsh 1	19	23.2
	Marsh 3a	10	12.2
	Marsh 3b	4	4.9
	Marsh 3c	5	6.1
Autoantibodies aTTG	Negative	63	77.8
	Positive	18	22.2
	Unknown	1	1.2
Autoantibodies aDGP	Negative	49	62.8
	Positive	29	37.2
	Unknown	4	4.9
Diarrhea	No	62	75.6
	Yes	19	23.2
	Unknown	1	1.2
Weight loss	No	73	89.0
	Yes	8	9.8
	Unknown	1	1.2
Abdominal pain	No	64	78.0
	Yes	17	20.7
	Unknown	1	1.2
Anemia	No	71	86.6
	Yes	9	11.0
	Unknown	2	2.4
Sideropenia	No	58	70.7
	Yes	22	26.8
	Unknown	2	2.4
Vitamin D deficiency	No	63	76.8
	Yes	17	20.7
	Unknown	2	2.4
Ultrasonography	Negative	42	51.2
	Positive	24	29.3
	Unknown	16	19.5

aTTG: Anti-tissue transglutaminase antibodies; aDGP: Anti-deamidated gliadin peptide antibodies.

Data of 19 patients (23.2%) with persistent VA (10× Marsh 3a, 4× Marsh 3b, 5× Marsh 3c) were compared with data of 63 patients (76.8%) with either Marsh 0 (44×) or Marsh 1 (19×) classification on the follow-up duodenal biopsy. These two groups did

not differ with respect to age at diagnosis, sex, or length of GFD at follow-up biopsy (details in Table 2).

In patients with persistent VA aTTG IgA was positive in nine cases; IgG was positive in one case (nine cases in any aTTG); aDGP IgA was positive in 13 cases; and aDGP IgG was positive in 11 cases (14 cases in any aDGP). In this study group, abdominal ultrasonography was available in 17 cases, and signs of active CD were found in 11 of these. Eight patients had diarrhea, four had weight loss, three had abdominal pain, on had anemia, four had sideropenia, and eight had vitamin D deficiency (Table 3). Only diarrhea and vitamin D deficiency were significantly more common in patients with persistent VA than in patients with mucosal recovery.

The sensitivity, specificity, and positive and negative predictive value of aTTG IgA positivity for prediction of VA were 50%, 96.8%, 81.8%, and 87.1%, respectively. The sensitivity, specificity, and positive and negative predictive value of aDGP IgA positivity for prediction of VA were 72.2%, 81.7%, 54.2%, and 90.7%, respectively (Table 4). In analysis of antibody titers, we calculated the cutoff values with highest total sensitivity and specificity. The calculated cutoff values were 13.4 U/mL and 6.7 U/mL for aTTG IgA and IgG, respectively, and 22.6 U/mL and 28.8 U/mL for aDGP IgA and IgG, respectively. For these cutoff values, we reached sensitivity and specificity of 66.7% (95%CI: 41.0-86.7) and 93.7% (95%CI: 84.5-98.2) for aTTG IgA and 72.2% (95%CI: 46.5-90.3) and 90.0% (95%CI: 79.5-96.2) for aDGP IgA, respectively (details in Table 5). Recalculation of the optimal cutoff values showed the best negative predictive value for aDGP IgA 91.5% (95%CI: 83.6-95.8).

The sensitivity, specificity, and the positive and negative predictive value of ultrasonography for prediction of persistent VA were 64.7%, 73.5%, 45.8%, and 85.7%, respectively. The positive predictive value of diarrhea, abdominal pain, sideropenia, or anemia for VA was low (Table 6). The combination of recalculated cutoff values for aTTG IgA and aDGP IgA with small bowel ultrasonography increased the specificity and positive predictive value for VA prediction. Ultrasonography combined with aTTG IgA reached 98% (95%CI: 89.2-99.9) specificity and 88.9% (95%CI: 51.9-98.3) positive predictive value, with aDGP IgA 97.8% (95%CI: 88.5-99.9) specificity and 90.0% (95%CI: 55.2-98.5) positive predictive value. Negative predictive value was slightly decreased, 84.2% (95%CI: 77.3-89.3) and 84.9% (95%CI: 77.2-90.3) for small bowel ultrasonography combined with aTTG IgA and aDGP IgA respectively (Table 5).

DISCUSSION

In our study, we searched for non-invasive markers of persistent VA in patients with CD who claimed to adhere to GFD. Persistent VA is one of the risk factors for lymphoproliferative malignancy[12] and possibly higher mortality rates[13], irrespective of the cause of VA. Identification of patients at higher risk of persistent VA could lead to more personalized approaches and closer follow-ups, including repeated evaluation of adherence to GFD, and thorough searches for nutritional deficiencies and complications of CD. Potential benefits of a repeated biopsy are broadly discussed[2]. Any non-invasive method that can facilitate creating indications for repeated biopsy or facilitate discharge of patients that tested negative from specific gastroenterological care would be helpful. Serology and ultrasonography are considered non-sensitive markers of persistent VA. In our study, we demonstrated 50% sensitivity and 85.7% specificity for aTTG and 77.8% sensitivity and 75% specificity for aDGP. There are conflicting results regarding this topic in the literature. A recent metanalysis demonstrated a sensitivity of 50% for aTTG IgA and a sensitivity of only 45% (95%CI: 34-57) for anti-endomysium antibodies[5]. Nevertheless, it is essential to stress that these tests be designed for detection of new cases of CD, for which purpose their cutoff values were determined. Even after determining the new cutoff values, the sensitivity of autoantibodies for prediction of VA improved slightly to 66.7% for aTTG IgA and 72.2% for aDGP IgA; however, we were able to reach high specificity and negative predictive values of 93.7% and 90.8%, respectively, for aTTG IgA, and 90% and 91.5%, respectively, for aDGP IgA. The recalculated cutoff value for TTG IgA in our study is about one-third lower than the standard diagnostic cutoff value. Not only the negative result of test but also the numeric value of antibodies might be important for test accuracy and clinical consequences. Patients with lower levels do not need to undergo follow-up duodenal biopsy to evaluate persistent VA. A similar study was performed for aTTG IgA in a larger group by Fang *et al*[18], who found significant differences in mucosal healing between undetectable and detectable aTTG IgA; however, owing to

Table 2 Comparison of characteristics according to persistence of villous atrophy

Characteristics	Category	No villous atrophy (*n* = 63)	Villous atrophy (*n* = 19)	
		n (%)	*n* (%)	*P* value
Gender	Female	52 (82.5)	15 (78.9)	0.741
	Male	11 (17.5)	4 (21.1)	
Follow-up biopsy	Less than 2 years	10 (15.9)	1 (5.3)	0.147
	Two years and more	53 (84.1)	17 (89.5)	
	Unknown	0 (0.0)	1 (5.3)	
		Mean (SD)	Mean (SD)	*P* value
Length of disease at follow-up biopsy (yr)		7.9 (8.2)	13.1 (13.4)	0.092
Age at follow-up biopsy (yr)		32.3 (14.6)	38.7 (24.4)	0.231

SD: Standard deviation.

limitations of the serology kit,they were unable to determine an ideal cutoff limit. Intermittent gluten exposure may explain the false negative serology tests even in the presence of incomplete mucosal recovery and non-optimal sensitivity of aTTG IgA.

The use of aDGP appears to be a better method than the use of aTTG IgA for detection of persistent VA, particularly in the use of both IgA and IgG antibodies. A combination of aDGP tests led to a sensitivity of 77.8% and a negative predictive value of 91.8%. One study found 87% sensitivity and 89% specificity of aDGP IgG for prediction of nonresponsive CD[6], while another study found only 48% sensitivity but 91% specificity of aDGP IgA for prediction of persistent VA[7]. The wide use of aDGP in future studies may contribute to a more precise role of it in detection of VA despite GFD. Although one study referred to a poor outcome of aDGP IgA in detection of absence of mucosal healing in children[19], other studies obtained different, more positive results[20,21]. A commercially available point-of-care test for both DGP antibodies was referred to as an alternative to classical serology testing with better sensitivity for CD follow-up in one prospective study[22].

The strengths of our study include a complex analysis of many non-invasive parameters for detection of persistent VA in patients with CD on a long-term GFD combining serology tests, clinical parameters, and bowel ultrasound. Many radiologic studies regarding CD are limited to some specific findings on cross-sectional imaging[23]. The role of bowel ultrasound is firmly established in the diagnosis and management of Crohn's disease[24]. Experience with bowel ultrasound in CD is rather limited; however, its use is expanding and signs corresponding with malabsorption and active CD are well defined[15,16,25]. This examination is routinely used during follow-up of CD patients in our hospital. With easier access to ultrasound examination and increasing experience in many institutions in recent years, it may be challenging to use it for the follow-up of patients with CD in the future. Particularly in patients with positive aTTG IgA or aDGP IgA, ultrasound abnormalities should indicate the need for endoscopic biopsy of duodenal mucosa despite the absence of clinical symptoms.

The limitations of our study are its retrospective design and a relatively small number of patients in the study group. Because the study group was small, we could not subdivide the patients with simple VA and patients with refractory CD. This could have an impact on the results because most patients have negative CD-specific antibodies at the time of refractory CD diagnosis. However positive CD-specific serology can be present in 19%-30% of patients with refractory CD and does not exclude the diagnosis[26]. Another limitation is an inability to evaluate adherence to a GFD using any objective method. It is well known that negative serology is not a reliable marker of adherence to a GFD[27]. Consultation with a skilled dietitian is regarded as the gold standard for monitoring adherence to a GFD[28]. The positivity of gliadin-33-mer or gluten immunogenic peptides in stool are good markers of ongoing gluten consumption[29,30]; however, it is not widely available and is able to evaluate only consumption of gluten in the last few days prior to the examination. Any objective method for long-term GFD evaluation could theoretically improve the result of all studies on this topic and patient management[31].

Relatively higher prevalence of any symptom despite adherence to GFD may be caused by some overlap of CD and functional disorders in patients consenting with

Table 3 Comparison of autoantibodies´ positivity, ultrasonography, laboratory and clinical markers in patients with and without villous atrophy, in groups with available parameters

Characteristics	Categories	Villous atrophy		
		Yes (%)	No (%)	*P* value
Autoantibodies aTTG (*n* = 81)	Positive	9 (50)	9 (14.3)	0.003[b]
	Negative	9 (50)	54 (85.7)	
	Total	18 (100)	63 (100)	
Autoantibodies aDGP (*n* = 78)	Positive	14 (77.8)	15 (25)	< 0.001[b]
	Negative	4 (22.2)	45 (75)	
	Total	18 (100)	60 (100)	
Autoantibodies aTTG IgA (*n* = 81)	Positive	9 (50)	2 (3.2)	< 0.001[b]
	Negative	9 (50)	61 (96.8)	
	Total	18 (100)	63 (100)	
Autoantibodies aTTG IgG (*n* = 81)	Positive	1 (5.6)	7 (11.1)	0.677
	Negative	17 (94.4)	56 (88.9)	
	Total	18 (100)	63 (100)	
Autoantibodies aDGP IgA (*n* = 78)	Positive	13 (72.2)	11 (18.3)	< 0.001[b]
	Negative	5 (27.8)	49 (81.7)	
	Total	18 (100)	60 (100)	
Autoantibodies aDGP IgG (*n* = 78)	Positive	11 (61.1)	9 (15)	< 0.001[b]
	Negative	7 (38.9)	51 (85)	
	Total	18 (100)	60 (100)	
Ultrasonography (*n* = 66)	Positive	11 (64.7)	13 (26.5)	0.008[b]
	Negative	6 (35.3)	36 (73.5)	
	Total	17 (100)	49 (100)	
Diarrhea (*n* = 81)	Yes	8 (44.4)	11 (17.5)	0.027[a]
	No	10 (55.6)	52 (82.5)	
	Total	18 (100)	63 (100)	
	Yes	4 (22.2)	4 (6.4)	0.068
Weight loss (*n* = 81)	No	14 (77.8)	59 (93.6)	
	Total	18 (100)	63 (100)	
Abdominal pain (*n* = 81)	Yes	3 (16.7)	14 (22.2)	0.751
	No	15 (83.3)	49 (77.8)	
	Total	18 (100)	63 (100)	
Anemia (*n* = 80)	Positive	1 (5.6)	8 (12.9)	0.676
	Negative	17 (94.4)	54 (87.1)	
	Total	18 (100)	62 (100)	
Sideropenia (*n* = 80)	Positive	4 (22.2)	18 (29)	0.766
	Negative	14 (77.8)	44 (71)	
	Total	18 (100)	62 (100)	
Vitamin D deficiency (*n* = 80)	Positive	8 (44.4)	9 (14.5)	0.018[a]
	Negative	10 (55.6)	53 (85.5)	
	Total	18 (100)	62 (100)	

[a]$P < 0.05$.

[b]$P < 0.01$. aTTG: Anti-tissue transglutaminase antibodies; aDGP: Anti-deamidated gliadin peptide antibodies.

Table 4 Sensitivity, specificity, positive and negative predictive value of anti-tissue transglutaminase antibodies and anti-deamidated gliadin peptide antibodies autoantibodies (with standard cutoff values according to laboratory references 18 U/mL for anti-tissue transglutaminase antibodies and 20 U/mL for anti-deamidated gliadin peptide antibodies) for prediction of villous atrophy in patients with celiac disease

Characteristics	Sensitivity (%) (95%CI)	Specificity (%) (95%CI)	Accuracy (%) (95%CI)	Positive predictive value (%) (95%CI)	Negative predictive value (%) (95%CI)
Autoantibodies aTTG	50.0 (26.0-74.0)	85.7 (74.6-93.3)	77.8 (67.2-86.3)	50.0 (31.8-68.2)	85.7 (78.9-90.6)
Autoantibodies aDGP	77.8 (52.4-93.6)	75.0 (62.1-85.3)	75.6 (64.6-84.7)	48.3 (36.1-60.7)	91.8 (82.4-96.4)
Autoantibodies aTTG IgA	50.0 (26.0-74.0)	96.8 (89.0-99.6)	86.4 (77.0-93.0)	81.8 (51.6-95.0)	87.1 (81.0-91.5)
Autoantibodies aTTG IgG	5.6 (0.1-27.3)	88.9 (78.4-95.4)	70.4 (59.2-80.0)	12.5 (1.8-52.1)	76.7 (74.1-79.2)
Autoantibodies aDGP IgA	72.2 (46.5-90.3)	81.7 (69.6-90.5)	79.5 (68.8-87.8)	54.2 (39.2-68.4)	90.7 (82.2-95.4)
Autoantibodies aDGP IgG	61.1 (35.8-82.7)	85.0 (73.4-92.9)	79.5 (68.8-87.8)	55.0 (37.6-71.2)	87.9 (80.2-92.9)

aTTG: Anti-tissue transglutaminase antibodies; aDGP: Anti-deamidated gliadin peptide antibodies; CI: Confidence interval.

Table 5 Sensitivity, specificity, positive and negative predictive value of recalculated cutoff values of anti-tissue transglutaminase antibodies and anti-deamidated gliadin peptide antibodies autoantibodies titers and their combination with small bowel ultrasonography for prediction of villous atrophy in patients with celiac disease

Characteristics	Sensitivity (%) (95%CI)	Specificity (%) (95%CI)	Accuracy (%) (95%CI)	Positive predictive value (%) (95%CI)	Negative predictive value (%) (95%CI)
Autoantibodies aTTG IgA (cutoff: 13.4)	66.7 (41.0-86.7)	93.7 (84.5-98.2)	87.7 (78.5-93.9)	75.0 (52.4-89.1)	90.8 (83.6-95.0)
Autoantibodies aTTG IgG (cutoff: 6.7)	33.3 (13.3-59.0)	87.3 (76.5-94.4)	75.3 (64.5-84.2)	42.9 (23.0-65.3)	82.1 (76.5-86.6)
Autoantibodies aDGP IgA (cutoff: 22.6)	72.2 (46.5-90.3)	90.0 (79.5-96.2)	85.9 (76.2-92.7)	68.4 (49.1-83.0)	91.5 (83.6-95.8)
Autoantibodies aDGP IgG (cutoff: 28.8)	61.1 (35.8-82.7)	90.0 (79.5-96.2)	83.3 (73.2-90.8)	64.7 (44.1-81.0)	88.5 (81.1-93.3)
Autoantibodies aTTG IgA (cutoff 13.4) AND ultrasonography	47.1 (23.0-72.2)	98.0 (89.2-99.9)	84.9 (73.9-92.5)	88.9 (51.9-98.3)	84.2 (77.3-89.3)
Autoantibodies aDGP IgA (cutoff 22.6) AND ultrasonography	52.9 (27.8-77.0)	97.8 (88.5-99.9)	85.7 (74.6-93.3)	90.0 (55.2-98.5)	84.9 (77.2-90.3)

aTTG: Anti-tissue transglutaminase antibodies; aDGP: Anti-deamidated gliadin peptide antibodies; CI: Confidence interval.

invasive examination. Nevertheless, either symptom related to CD may stimulate the patient to undergo uncomfortable endoscopy. We cannot assess asymptomatic patients' refusals of follow-up endoscopy owing to their well-being. This situation in a retrospective study represents real-life medicine.

Most patients in our study were known to have avoided gluten consumption for more than 2 years; therefore, inter-individual differential mucosal recovery likely plays no role in our results. In patients with VA, some symptoms and signs of malabsorption are more common; nevertheless, the predictive role of diarrhea and vitamin D deficiency for the diagnosis of atrophy was poor. In symptomatic patients on GFD, a re-biopsy should be considered[11].

In our study, we did not show that serologic tests of aTTG and aDGP with standard diagnostic cutoff values were optimal markers of persistent VA. Nevertheless, calculation of the best cutoff values of aTTG and aDGP IgA for prediction of VA improved the sensitivity, specificity, and negative predictive value. The combination

Table 6 Sensitivity, specificity, positive and negative predictive value of bowel ultrasonography, clinical and laboratory markers for prediction of villous atrophy in patients with celiac disease

Characteristics	Sensitivity (%) (95%CI)	Specificity (%) (95%CI)	Accuracy (%) (95%CI)	Positive predictive value (%) (95%CI)	Negative predictive value (%) (95%CI)
Ultrasonography	64.7 (38.3-85.8)	73.5 (58.9-85.1)	71.2 (58.8-81.7)	45.8 (32.1-60.3)	85.7 (75.5-92.1)
Diarrhea	44.4 (21.5-69.2)	82.5 (70.9-91.0)	74.1 (63.1-83.2)	42.1 (25.7-60.5)	83.9 (77.2-88.9)
Weight loss	22.2 (6.4-47.6)	93.7 (84.5-98.2)	77.8 (67.2-86.3)	50.0 (21.7-78.3)	80.8 (76.6-84.5)
Abdominal pain	16.7 (3.6-41.4)	77.8 (65.5-87.3)	64.2 (52.8-74.6)	17.7 (6.5-39.9)	76.6 (71.9-80.7)
Anemia	5.6 (0.1-27.3)	87.1 (76.2-94.3)	68.8 (57.4-78.7)	11.1 (1.6-48.3)	76.1 (73.3-78.6)
Sideropenia	22.2 (6.4-47.6)	71.0 (58.1-81.8)	60.0 (48.4-70.8)	18.2 (7.9-36.4)	75.9 (70.1-80.8)
Vitamin D deficiency	44.4 (21.5-69.2)	85.5 (74.2-93.1)	76.3 (65.4-85.1)	47.1 (28.7-66.3)	84.1 (77.6-89.0)

CI: Confidence interval.

of serology and expert bowel ultrasound examination may achieve better accuracy for the detection of atrophy. Signs of persistent VA should be considered after 1-2 years of GFD. Asymptomatic patients with lower levels of both aDGP IgA and IgG do not need to undergo follow-up duodenal biopsy to determine the presence of persistent VA.

ARTICLE HIGHLIGHTS

Research background

Currently, duodenal biopsy is the only way to evaluate mucosal healing in celiac disease (CD). There is no reliable widely available non-invasive marker of persistent villous atrophy (VA), which is one of the core pathological signs of active CD.

Research motivation

There is ongoing attempt to search for non-invasive markers for mucosal healing in CD, as persistent VA is one of the risk factors for malignant complications and possibly higher mortality rates in CD.

Research objectives

Closer analysis of currently available non-invasive CD relevant markers, such as the exact value of anti-tissue transglutaminase antibodies (aTTG), anti-deamidated gliadin peptide antibodies (aDGP), or combination with ultrasonographic signs of active CD could help in prediction of persistent VA.

Research methods

We analyzed data from the database of patients with CD followed-up at the Department of Gastroenterology and Internal Medicine, University Hospital Brno from 2014 to 2018. The symptoms, laboratory signs, exact values of aTTG, aDGP, ultrasonographic signs of active CD were correlated to persistent VA.

Research results

Calculation of new cut-off values of aTTG and aDGP IgA improved the sensitivity, specificity, and negative predictive value for VA. The combination with expert bowel ultrasound examination achieved even better accuracy.

Research conclusions

We found out that a combination of currently available non-invasive CD relevant markers could help in prediction of persistent VA.

Research perspectives

This could lead to more personalized approaches and closer follow-ups of CD patients, including repeated evaluation of adherence to GFD, thorough searches for nutritional deficiencies and possibly also follow-up duodenal biopsy and search for complications

of CD.

REFERENCES

1 **Lebwohl B**, Granath F, Ekbom A, Montgomery SM, Murray JA, Rubio-Tapia A, Green PH, Ludvigsson JF. Mucosal healing and mortality in coeliac disease. *Aliment Pharmacol Ther* 2013; **37**: 332-339 [PMID: 23190299 DOI: 10.1111/apt.12164]

2 **Sharkey LM**, Corbett G, Currie E, Lee J, Sweeney N, Woodward JM. Optimising delivery of care in coeliac disease - comparison of the benefits of repeat biopsy and serological follow-up. *Aliment Pharmacol Ther* 2013; **38**: 1278-1291 [PMID: 24117503 DOI: 10.1111/apt.12510]

3 **Hære P**, Høie O, Schulz T, Schönhardt I, Raki M, Lundin KE. Long-term mucosal recovery and healing in celiac disease is the rule - not the exception. *Scand J Gastroenterol* 2016; **51**: 1439-1446 [PMID: 27534885 DOI: 10.1080/00365521.2016.1218540]

4 **Leonard MM**, Weir DC, DeGroote M, Mitchell PD, Singh P, Silvester JA, Leichtner AM, Fasano A. Value of IgA tTG in Predicting Mucosal Recovery in Children With Celiac Disease on a Gluten-Free Diet. *J Pediatr Gastroenterol Nutr* 2017; **64**: 286-291 [PMID: 28112686 DOI: 10.1097/MPG.0000000000001460]

5 **Silvester JA**, Kurada S, Szwajcer A, Kelly CP, Leffler DA, Duerksen DR. Tests for Serum Transglutaminase and Endomysial Antibodies Do Not Detect Most Patients With Celiac Disease and Persistent Villous Atrophy on Gluten-free Diets: a Meta-analysis. *Gastroenterology* 2017; **153**: 689-701.e1 [PMID: 28545781 DOI: 10.1053/j.gastro.2017.05.015]

6 **Spatola BN**, Kaukinen K, Collin P, Mäki M, Kagnoff MF, Daugherty PS. Persistence of elevated deamidated gliadin peptide antibodies on a gluten-free diet indicates nonresponsive coeliac disease. *Aliment Pharmacol Ther* 2014; **39**: 407-417 [PMID: 24392888 DOI: 10.1111/apt.12603]

7 **Choung RS**, Khaleghi Rostamkolaei S, Ju JM, Marietta EV, Van Dyke CT, Rajasekaran JJ, Jayaraman V, Wang T, Bei K, Rajasekaran KE, Krishna K, Krishnamurthy HK, Murray JA. Synthetic Neoepitopes of the Transglutaminase-Deamidated Gliadin Complex as Biomarkers for Diagnosing and Monitoring Celiac Disease. *Gastroenterology* 2019; **156**: 582-591.e1 [PMID: 30342033 DOI: 10.1053/j.gastro.2018.10.025]

8 **Al-Toma A**, Volta U, Auricchio R, Castillejo G, Sanders DS, Cellier C, Mulder CJ, Lundin KEA. European Society for the Study of Coeliac Disease (ESsCD) guideline for coeliac disease and other gluten-related disorders. *United European Gastroenterol J* 2019; **7**: 583-613 [PMID: 31210940 DOI: 10.1177/2050640619844125]

9 **Lebwohl B**, Sanders DS, Green PHR. Coeliac disease. *Lancet* 2018; **391**: 70-81 [PMID: 28760445 DOI: 10.1016/S0140-6736(17)31796-8]

10 **Leonard MM**, Sapone A, Catassi C, Fasano A. Celiac Disease and Nonceliac Gluten Sensitivity: A Review. *JAMA* 2017; **318**: 647-656 [PMID: 28810029 DOI: 10.1001/jama.2017.9730]

11 **Husby S**, Murray JA, Katzka DA. AGA Clinical Practice Update on Diagnosis and Monitoring of Celiac Disease-Changing Utility of Serology and Histologic Measures: Expert Review. *Gastroenterology* 2019; **156**: 885-889 [PMID: 30578783 DOI: 10.1053/j.gastro.2018.12.010]

12 **Lebwohl B**, Granath F, Ekbom A, Smedby KE, Murray JA, Neugut AI, Green PH, Ludvigsson JF. Mucosal healing and risk for lymphoproliferative malignancy in celiac disease: a population-based cohort study. *Ann Intern Med* 2013; **159**: 169-175 [PMID: 23922062 DOI: 10.7326/0003-4819-159-3-201308060-00006]

13 **Rubio-Tapia A**, Rahim MW, See JA, Lahr BD, Wu TT, Murray JA. Mucosal recovery and mortality in adults with celiac disease after treatment with a gluten-free diet. *Am J Gastroenterol* 2010; **105**: 1412-1420 [PMID: 20145607 DOI: 10.1038/ajg.2010.10]

14 **Freeman HJ**. Iron deficiency anemia in celiac disease. *World J Gastroenterol* 2015; **21**: 9233-9238 [PMID: 26309349 DOI: 10.3748/wjg.v21.i31.9233]

15 **Bartusek D**, Valek V, Husty J, Uteseny J. Small bowel ultrasound in patients with celiac disease. Retrospective study. *Eur J Radiol* 2007; **63**: 302-306 [PMID: 17336477 DOI: 10.1016/j.ejrad.2007.01.028]

16 **Dietrich CF**, Hollerweger A, Dirks K, Higginson A, Serra C, Calabrese E, Dong Y, Hausken T, Maconi G, Mihmanli I, Nürnberg D, Nylund K, Pallotta N, Ripollés T, Romanini L, Săftoiu A, Sporea I, Wüstner M, Maaser C, Gilja OH. EFSUMB Gastrointestinal Ultrasound (GIUS) Task Force Group: Celiac sprue and other rare gastrointestinal diseases ultrasound features. *Med Ultrason* 2019; **21**: 299-315 [PMID: 31476211 DOI: 10.11152/mu-2162]

17 **Oberhuber G**, Granditsch G, Vogelsang H. The histopathology of coeliac disease: time for a standardized report scheme for pathologists. *Eur J Gastroenterol Hepatol* 1999; **11**: 1185-1194 [PMID: 10524652 DOI: 10.1097/00042737-199910000-00019]

18 **Fang H**, King KS, Larson JJ, Snyder MR, Wu TT, Gandhi MJ, Murray JA. Undetectable negative tissue transglutaminase IgA antibodies predict mucosal healing in treated coeliac disease patients. *Aliment Pharmacol Ther* 2017; **46**: 681-687 [PMID: 28782118 DOI: 10.1111/apt.14250]

19 **Vécsei E**, Steinwendner S, Kogler H, Innerhofer A, Hammer K, Haas OA, Amann G, Chott A, Vogelsang H, Schoenlechner R, Huf W, Vécsei A. Follow-up of pediatric celiac disease: value of antibodies in predicting mucosal healing, a prospective cohort study. *BMC Gastroenterol* 2014; **14**: 28 [PMID: 24524430 DOI: 10.1186/1471-230X-14-28]

20 **Bannister EG**, Cameron DJ, Ng J, Chow CW, Oliver MR, Alex G, Catto-Smith AG, Heine RG, Webb A, McGrath K, Simpson D, Hardikar W. Can celiac serology alone be used as a marker of duodenal mucosal recovery in children with celiac disease on a gluten-free diet? *Am J Gastroenterol* 2014; **109**: 1478-1483 [PMID: 25070050 DOI: 10.1038/ajg.2014.200]

21 **Monzani A**, Rapa A, Fonio P, Tognato E, Panigati L, Oderda G. Use of deamidated gliadin peptide antibodies to monitor diet compliance in childhood celiac disease. *J Pediatr Gastroenterol Nutr* 2011; **53**: 55-60 [PMID: 21694536 DOI: 10.1097/MPG.0b013e3182145511]

22 **Lau MS**, Mooney PD, White WL, Rees MA, Wong SH, Kurien M, Trott N, Leffler DA, Hadjivassiliou M, Sanders DS. The Role of an IgA/IgG-Deamidated Gliadin Peptide Point-of-Care Test in Predicting

Persistent Villous Atrophy in Patients With Celiac Disease on a Gluten-Free Diet. *Am J Gastroenterol* 2017; **112**: 1859-1867 [PMID: 29016564 DOI: 10.1038/ajg.2017.357]

23 **Sheedy SP**, Barlow JM, Fletcher JG, Smyrk TC, Scholz FJ, Codipilly DC, Al Bawardy BF, Fidler JL. Beyond moulage sign and TTG levels: the role of cross-sectional imaging in celiac sprue. *Abdom Radiol (NY)* 2017; **42**: 361-388 [PMID: 28154909 DOI: 10.1007/s00261-016-1006-2]

24 **Maaser C**, Sturm A, Vavricka SR, Kucharzik T, Fiorino G, Annese V, Calabrese E, Baumgart DC, Bettenworth D, Borralho Nunes P, Burisch J, Castiglione F, Eliakim R, Ellul P, Gonzalez-Lama Y, Gordon H, Halligan S, Katsanos K, Kopylov U, Kotze PG, Krustins E, Laghi A, Limdi JK, Rieder F, Rimola J, Taylor SA, Tolan D, van Rheenen P, Verstockt B, Stoker J; European Crohn´s and Colitis Organisation [ECCO] and the European Society of Gastrointestinal and Abdominal Radiology [ESGAR]. ECCO-ESGAR Guideline for Diagnostic Assessment in IBD Part 1: Initial diagnosis, monitoring of known IBD, detection of complications. *J Crohns Colitis* 2019; **13**: 144-164 [PMID: 30137275 DOI: 10.1093/ecco-jcc/jjy113]

25 **Fraquelli M**, Sciola V, Villa C, Conte D. The role of ultrasonography in patients with celiac disease. *World J Gastroenterol* 2006; **12**: 1001-1004 [PMID: 16534837 DOI: 10.3748/wjg.v12.i7.1001]

26 **Rubio-Tapia A**, Murray JA. Classification and management of refractory coeliac disease. *Gut* 2010; **59**: 547-557 [PMID: 20332526 DOI: 10.1136/gut.2009.195131]

27 **Vahedi K**, Mascart F, Mary JY, Laberenne JE, Bouhnik Y, Morin MC, Ocmant A, Velly C, Colombel JF, Matuchansky C. Reliability of antitransglutaminase antibodies as predictors of gluten-free diet compliance in adult celiac disease. *Am J Gastroenterol* 2003; **98**: 1079-1087 [PMID: 12809831 DOI: 10.1111/j.1572-0241.2003.07284.x]

28 **Simpson S**, Thompson T. Nutrition assessment in celiac disease. *Gastrointest Endosc Clin N Am* 2012; **22**: 797-809 [PMID: 23083994 DOI: 10.1016/j.giec.2012.07.010]

29 **Comino I**, Segura V, Ortigosa L, Espín B, Castillejo G, Garrote JA, Sierra C, Millán A, Ribes-Koninckx C, Román E, Rodríguez-Herrera A, Díaz J, Silvester JA, Cebolla Á, Sousa C. Prospective longitudinal study: use of faecal gluten immunogenic peptides to monitor children diagnosed with coeliac disease during transition to a gluten-free diet. *Aliment Pharmacol Ther* 2019; **49**: 1484-1492 [PMID: 31074004 DOI: 10.1111/apt.15277]

30 **Comino I**, Real A, Vivas S, Síglez MÁ, Caminero A, Nistal E, Casqueiro J, Rodríguez-Herrera A, Cebolla A, Sousa C. Monitoring of gluten-free diet compliance in celiac patients by assessment of gliadin 33-mer equivalent epitopes in feces. *Am J Clin Nutr* 2012; **95**: 670-677 [PMID: 22258271 DOI: 10.3945/ajcn.111.026708]

31 **Comino I**, Fernández-Bañares F, Esteve M, Ortigosa L, Castillejo G, Fambuena B, Ribes-Koninckx C, Sierra C, Rodríguez-Herrera A, Salazar JC, Caunedo Á, Marugán-Miguelsanz JM, Garrote JA, Vivas S, Lo Iacono O, Nuñez A, Vaquero L, Vegas AM, Crespo L, Fernández-Salazar L, Arranz E, Jiménez-García VA, Antonio Montes-Cano M, Espín B, Galera A, Valverde J, Girón FJ, Bolonio M, Millán A, Cerezo FM, Guajardo C, Alberto JR, Rosinach M, Segura V, León F, Marinich J, Muñoz-Suano A, Romero-Gómez M, Cebolla Á, Sousa C. Fecal Gluten Peptides Reveal Limitations of Serological Tests and Food Questionnaires for Monitoring Gluten-Free Diet in Celiac Disease Patients. *Am J Gastroenterol* 2016; **111**: 1456-1465 [PMID: 27644734 DOI: 10.1038/ajg.2016.439]

World Journal of Gastroenterology

Submit a Manuscript: https://www.f6publishing.com

World J Gastroenterol 2020 July 14; 26(26): 3792-3799

DOI: 10.3748/wjg.v26.i26.3792

ISSN 1007-9327 (print) ISSN 2219-2840 (online)

ORIGINAL ARTICLE

Retrospective Cohort Study

Two-day enema antibiotic therapy for parasite eradication and resolution of symptoms

Niloufar Roshan, Annabel Clancy, Anoja W Gunaratne, Antoinette LeBusque, Denise Pilarinos, Thomas J Borody

ORCID number: Niloufar Roshan 0000-0002-2087-6398; Annabel Clancy 0000-0001-7589-1766; Anoja W Gunaratne 0000-0002-6767-614X; Antoinette LeBusque 0000-0001-7969-7362; Denise Pilarinos 0000-0002-7448-4111; Thomas J Borody 0000-0002-0519-4698.

Author contributions: Roshan N was involved in data collection, analysis and writing the original draft; Clancy A was involved in supervision, writing, review and editing; Gunaratne AW contributed to the data collection and writing review; LeBusque A performed the data collection and writing review; Pilarinos D was involved in data collection and writing review; Borody TJ contributed to the supervision, writing review and editing; All authors have read and approve the final manuscript.

Institutional review board statement: This study was approved by the institutional ethics committee (CDD19/C02).

Informed consent statement: A waiver of consent was granted for this study. Patients were not required to give informed consent for this study because the analysis used de-identified data that was

Niloufar Roshan, Annabel Clancy, Anoja W Gunaratne, Antoinette LeBusque, Denise Pilarinos, Thomas J Borody, Centre for Digestive Diseases, New South Wales 2046, Australia

Corresponding author: Niloufar Roshan, PhD, Research Fellow, Research, Centre for Digestive Diseases, Level 1, 229 Great North Road, New South Wales 2046, Australia. niloufar.roshanhesari@cdd.com.au

Abstract

BACKGROUND

Blastocystis hominis (*B. hominis*) and *Dientamoeba fragilis* (*D. fragilis*) are two protozoan parasites of human bowel that are found throughout the world. There is still debate about the pathogenicity of these protozoans, despite them being commonly associated with gastrointestinal symptoms and can cause health issue in both children and adults. These parasites are usually transmitted through faecal-oral contact particularly under poor hygiene conditions or food/water contamination. Once a person is infected, the parasites live in the large intestine and are passed in the faeces.

AIM

To investigate the effect of triple antibiotic therapy using enema infusion in the treatment of *B. hominis* and *D. fragilis* infections.

METHODS

This retrospective longitudinal study was conducted in a single medical centre, which included fifty-four patients (≥ 18 years) who were positive for *D. fragilis*, *B. hominis* or both between 2017 and 2018. The treatment consisted of triple antibiotics that were infused over two consecutive days through rectal enema. Faecal samples were collected from participants pre- and post-treatment and were tested for parasites using microscopy and polymerase chain reaction. Patients' symptoms were recorded prior and after the treatment as well as patient demographic data.

RESULTS

Patients (n = 54), were either positive for *B. hominis* (37%), *D. fragilis* (35%) or both (28%). All patients completed the two-day treatment and no serious adverse effect was reported. The most common side effect experienced by the patients during

the treatment was urine discolouration which was cleared by six weeks of follow-up. Common symptoms reported prior to treatment were diarrhoea, abdominal pain, constipation and fatigue. Other symptoms included abdominal discomfort, dizziness and blood in the stool. Eighty-nine percent of patients completed a final stool test post-treatment. At six weeks post-treatment, 79% of patients cleared the parasites from their faeces. Symptoms such as abdominal discomfort, dizziness and blood in the stool decreased significantly at both seven days and six weeks post-treatment ($P < 0.040$). The enema retention time, bowel preparation, previous antibiotic treatment or previous gastrointestinal problems had no significant effect on parasite eradication.

CONCLUSION

Overall, eradication of parasites and improvement of clinical outcomes were observed in treated patients, showing the efficacy of this combination to eradicate the parasites and provide positive clinical outcome.

Key words: *Blastocystis hominis*; Dientamoeba fragilis; Parasitic infection; Antibiotics; Triple therapy; Rectal enema route

Core tip: Intestinal parasitic infections caused by *Blastocystis hominis* (*B. hominis*) and *Dientamoeba fragilis* (*D. fragilis*) have the ability to cause illness. This study investigated the effect of a triple antibiotic therapy using 2-d enema infusion for treatment of patients who were positive to *B. hominis*, *D. fragilis* or both. A significant reduction in major symptoms as well as parasite eradication were observed post-treatment. Larger clinical trials should further investigate improvements of such therapy using larger volume enemas and alternative delivery routes.

Citation: Roshan N, Clancy A, Gunaratne AW, LeBusque A, Pilarinos D, Borody TJ. Two-day enema antibiotic therapy for parasite eradication and resolution of symptoms. *World J Gastroenterol* 2020; 26(26): 3792-3799
URL: https://www.wjgnet.com/1007-9327/full/v26/i26/3792.htm
DOI: https://dx.doi.org/10.3748/wjg.v26.i26.3792

INTRODUCTION

The two anaerobic protozoa, *Blastocystis hominis* (*B. hominis*) and *Dientamoeba fragilis* (*D. fragilis*) are described as "neglected parasites", which are found in the intestinal tract of humans[1]. Intestinal protozoan infections are a global problem in both developed and developing countries and can cause considerable morbidity especially in children[1]. In many low-income countries, poverty and poor sanitation are the main causal factors for transmission. Both parasites are generally transmitted through faecal-oral contact or water/food contamination and are often detected in the stool of patients with gastrointestinal problems[2,3]. These symptoms are comparable with those experienced with irritable bowel syndrome (IBS) and inflammatory bowel disease (IBD). As such, a possible link between these infections, IBD and IBS has been suggested[3]. Thus, the eradication of these parasitic infections may be necessary when they are the only infectious agents detected in symptomatic patients.

Blastocystis species (spp) are unicellular enteric parasites present in most species of animals and have extensive genetic diversity. *B. hominis* is the only member of Stramenopiles that infects humans and exists in four different forms; cyst, ameboid, granular and vacuolar[4]. *Blastocystis* spp have a global distribution. Its prevalence in humans, in developing countries is estimated to be around 76%-100% compared to 5% in developed countries[5]. Symptoms associated with *Blastocystis* infection include abdominal pain, diarrhoea, nausea, bloating and fatigue[5].

The other protozoan, *D. fragilis*, was described for the first time by Jepps and Dobell in England in 1918[6]. It was initially misclassified as an amoeba, and was later re-classified as a unicellular flagellate despite lacking a flagellum[7]. The global distribution of *D. fragilis* is reported to range between 0.4% to 71%, with developed

obtained after each patient agreed to treatment.

Conflict-of-interest statement:: Professor Thomas J Borody has a pecuniary interest in the Centre for Digestive Diseases and has filed patents for antibiotic therapies for parasitic infections. Dr Niloufar Roshan, Dr Annabel Clancy, Dr Anoja Gunaratne, Ms Antoinette LeBusque and Ms Denise Pilarinos have no disclosures.

Data sharing statement: All data requests should be submitted to the corresponding author for consideration.

STROBE statement: The authors have read the STROBE statement-checklist of items, the manuscript was prepared according to the STROBE statement-checklist of items.

Manuscript source: Unsolicited manuscript

Received: November 19, 2020
Peer-review started: November 19, 2020
First decision: April 2, 2020
Revised: May 9, 2020
Accepted: June 20, 2020
Article in press: June 20, 2020
Published online: July 14, 2020

P-Reviewer: García-Elorriaga G, Manenti A
S-Editor: Liu M
L-Editor: A
E-Editor: Ma YJ

countries showing a higher prevalence. *D. fragilis* has been associated with symptoms such as abdominal pain, diarrhoea and loose stools[5,8].

Although, these parasites have a well-documented pathogenic potential, there is still debate on whether these infections should be treated and there are few studies that have investigated the treatment options for these infections. In addition, these parasites are relatively difficult to eradicate and there are often side effects associated with oral antibiotic therapy.

Metronidazole as an oral antiprotozoal antibiotic was first developed in 1962 and was originally used for management of trichomoniasis[9]. Some studies have reported the success of metronidazole in the treatment of *D. fragilis* and *B. hominis* infections[10], while others showed treatment failure[11]. In a study investigating the treatment of *D. fragilis* with metronidazole or tetracycline, a microbiological response was observed in 60% of patients and relief of symptoms was shown in only 30% of patients treated with metronidazole, while tetracycline had no effect[9]. These findings suggested that a substantial number of patients were insufficiently treated with metronidazole and more efficient drugs were needed for treating this infection. Some studies combined several anti-parasite medications to achieve higher efficacy[12,13].

Other studies have combined anti-parasitic antibiotics to be used intra-luminally for treating resistant parasitic infections. Triple antibiotic therapy using nitazoxanide, secnidazole and furazolidone through colonic infusion may be an effective method for eradicating *D. fragilis* and *B. hominis* infections for those who fail oral antibiotic therapy[14]. Nitazoxanide was first described as a human cestocidal drug in 1984[9]. Clinical trials have demonstrated relief of metronidazole-resistant parasite diarrhoea following treatment with nitazoxanide. Adverse effects associated with nitazoxanide are uncommon and the incidence is reported to be lower than metronidazole[9,15]. The other antibiotic that has been considered for the treatment of these parasites is secnidazole, which has a longer half-life compared to metronidazole. It has been used for treatment of trichomoniasis, giardiasis and amoebiasis, with a cure rate of 80%-100%. Mild nausea is one of the side effects reported in a few patients. Another antibiotic with a broader antibacterial and antiprotozoal activity is furazolidone, which is a synthetic nitrofuran derivative[9]. It has shown activity particularly against *Entamoeba histolytica* and *Giardia lamblia* and is suggested as an alternative drug in the case of treatment failure with first line agents. There has not been any studies assessing the efficacy of furazolidone specifically in the treatment of *D. fragilis* or *B. hominis* infections[9]. Our study aimed to investigate the effect of combined antibiotics administered *via* enema infusion to eradicate *D. fragilis* and *B. hominis* and improve symptoms.

MATERIALS AND METHODS

This retrospective, single centre longitudinal study was conducted between January 2017 and December 2018. Patients 18 years or older, who were positive for *D. fragilis*, *B. hominis* or both were invited to participate in this study. The treatment consisted of triple antibiotics (furazolidone 0.9 g, nitazoxanide 3 g and secnidazole 3.6 g) infused over two consecutive days through rectal enema. The antibiotic enema was administered *via* enema bag (gravity fed) containing the medication diluted in 300 ml of normal saline and delivered *via* rectum into the bowel. In the case of allergy, the culprit drug was replaced by paromomycin 4.5 g or diloxanide furoate 4.5 g. Faecal specimens were collected from study participants at baseline and six weeks after completion of treatment. Stool microscopy and polymerase chain reaction were used for parasite detection. Symptoms were recorded by the patients on a standard questionnaire prior to treatment and subsequently at three days, seven days and six weeks after the treatment. Patient demographic data (age, gender, previous treatment, concomitant medications and relevant medical history) were also collected to identify any confounding variables within the study population.

Statistical analysis was conducted using GraphPad Prism v.8 (La Jolla, CA, United States) software. Statistical differences between three or more sets of data were analysed using one-way analysis of variance and nonparametric technique, followed by Tukey's multiple comparison post-test if the P value was significant. Wilcoxon matched-pairs signed rank test was used to compare the differences between two sets of data. The association between categorical variables were determined using Chi-square and Fisher's exact test. P values of < 0.05 were considered significant. The study was approved by the institutions Ethics Committee (CDD19/C02).

RESULTS

Fifty-four (16 males) patients with an age range of 21-81 years (median age 49 years) participated in the study and all the patients completed the treatment. Twenty-three patients had received prior antibiotic therapy (including diloxanide furoate, metronidazole, trimethoprim/sulfamethoxazole (bactrim), secnidazole, tinidazole, furazolidone, doxycycline, paromomycin and nitazoxanide) and 18 patients had history of gastrointestinal symptoms (Table 1). Of the 54 patients, 37% were positive to *B. hominis*, 35% to *D. fragilis* and 28% to both. Only one patient was asymptomatic prior to the treatment; 83% of the patients had five or more of the symptoms listed in Table 1. The most common symptoms were diarrhoea, constipation, abdominal pain and fatigue. All patients completed the two days of antibiotic enema infusions administered in a volume of 300 mL. The median retention time for the enema among the patients was 3 h (ranging from 0.5 h to 12 h) and 39% of the patients had bowel preparation prior to the treatment. No serious adverse event was reported. The most common side effect experienced by the patients undergoing the treatment was urine discolouration, which cleared by six weeks of follow-up. Out of 54 patients, 48 completed a final stool test for investigation of parasite eradication at six weeks post-treatment. Overall 79% of patients cleared the parasites from their faeces at six weeks (Table 2).

There was a significant reduction in abdominal discomfort, dizziness and blood in the stool at both seven days and six weeks post-treatment ($P < 0.040$) (Figure 1). Symptoms such as diarrhoea, constipation, bloating, flatulence, nausea, vomiting, anal itching, muscular weakness, itchy skin and skin rash showed significant improvement at six weeks post-treatment ($P < 0.040$). A significant improvement in patients' mood was shown at all time-points, three days, seven days and six weeks post-treatment ($P < 0.001$). There was no significant association between the enema retention time, bowel preparation, previous antibiotic treatment or previous gastrointestinal problems and eradication of parasites.

In this study, successful eradication of *B. hominis* and *D. fragilis* infections occurred in 79% of patients at six weeks post-treatment with 2-d enema infusion using triple antibiotic therapy. An improvement in major clinical symptoms, diarrhoea and abdominal pain was also observed six weeks after the treatment. To our knowledge, this is the first study to investigate the efficacy of three novel antibiotics through a different route of delivery - enema infusion - in patients seeking treatment for *B. hominis* and *D. fragilis* infections.

B. hominis and *D. fragilis* have a worldwide distribution and are more commonly found than both *G. lamblia* and *Cryptosporidium* spp[5]. Exploring combinations of antibiotics and alternative methods of delivery is important to improve the clearance rate of *B. hominis* and *D. fragilis* infections and to eradicate the resistant strains. Therefore, this study examined the effect of a new combination of drugs infused *via* enema in a small group of patients seeking treatment for parasite infection. This showed a successful eradication of parasites and improvement of clinical outcomes. Although, treatment did not work for approximately 20% of patients, it still showed a higher achievement compared to monotherapy with conventional drugs such as metronidazole. The success and tolerability of this therapy may be due to the delivery of a high concentration of drugs to the colon where *B. hominis* and *D. fragilis* usually reside, with insignificant systemic absorption. Using an enema as the mode of delivery may be beneficial by bypassing the systemic absorption seen in oral dosing and hence, minimising the side effects.

Previously, a small number of studies have reported the effect of different antibiotic treatments in treating these parasitic infections. In a placebo-controlled trial, the efficacy of metronidazole in inducing remission and eradicating the parasites was investigated[16]. The study showed a higher eradication rate, one month following the treatment. However, the six months follow-up showed a high rate of recrudescence in patients treated with metronidazole. Therefore, it was concluded that metronidazole may be ineffective in achieving complete eradication of *B. hominis*, mainly due to drug resistance[5]. Another longitudinal, prospective case study on 11 symptomatic patients positive for *Blastocystis* showed that metronidazole failed to cure any of the patients[17]. Resistance to metronidazole was first reported in 1991, which brought doubt about its value as a first line treatment[18]. Metronidazole might be an effective treatment for certain patients, but does not necessarily provide complete eradication in patients with severe infection[17]. The variation in treatment response can be due to existence of resistance subtypes of parasite[9], which question the use of metronidazole as the single and first line of therapy.

In another longitudinal, prospective case study, 10 patients with diarrhoea-

Table 1 Baseline demographic data of participants

Gender (*n*)	Female (38), male (16)
Age mean (range), yr	49 (21-81)
Bowel preparation (*n*)	Yes (21), no (33)
Parasite present (*n*)	BH only (20), DF only (19), both (15)
Prior antibiotic treatment for parasite eradication (*n*)	23
History of gastrointestinal problems (*n*)	18
Symptoms *n*)	
Diarrhoea (36)	Fatigue (38)
Constipation (27)	Lethargy (12)
Bloating (39)	Malaise (15)
Flatulence (37)	Blood in the stool (10)
Trapped wind/gurgling (14)	Low mood (22)
Loss of appetite (18)	Anxiety (13)
Dizziness/light headed (26)	Reflux/heartburn (15)
Headaches (22)	Muscular weakness (22)
Nausea (21)	Itchy skin (15)
Vomiting (7)	Skin rash (7)
Anal itching (21)	Discoloured urine (11)
Metallic taste (14)	Abdominal discomfort/pain (38)
Photo-sensitivity (9)	

BH: *Blastocystis hominis*; DF: *Dientamoeba fragilis*.

Table 2 Parasite eradication, *n* (%)

	Parasite			
	BH only	DFonly	Both	Total
Number of patients	20	19	15	54
Number tested at 6 wk	19	16	13	48
Number cleared at 6 wk	14 (29)	13 (27)	11 (23)	38 (79)

BH: *Blastocystis hominis;* DF: *Dientamoeba fragilis*.

predominant IBS who were positive to *B. hominis* were treated with oral triple antibiotic therapy including diloxanide furoate, trimethoprim/sulfamethoxazole and secnidazole[14]. The parasite was eradicated in 60% of patients with IBS, which showed an improvement over conventional monotherapy such has metronidazole[14]. Similarly, in a retrospective cohort study from the Netherlands, 93 symptomatic patients were treated with paromomycin, along with other antibiotics such as, clioquinol and metronidazole[19]. Paromomycin showed a higher eradication rate of 98% compared to clioquinol (83%) and metronidazole (57%)[19]. While a number of antibiotics have shown to be effective in treating either *B. hominis* or *D. fragilis* infection and are recommended as therapeutic options, these recommendations are mainly based on a small number of non-randomised studies[9]. Moreover, there is little *in vitro* susceptibility data for these parasites. Further, prospective randomised studies are required to better understand the effectiveness of antibiotic combinations and modes of administration in *B. hominis* or *D. fragilis* infection eradication.

B. hominis and *D. fragilis* establish in the anaerobic environment of the human colon and thrive in presence of bacteria and in some circumstances can invade the intestinal

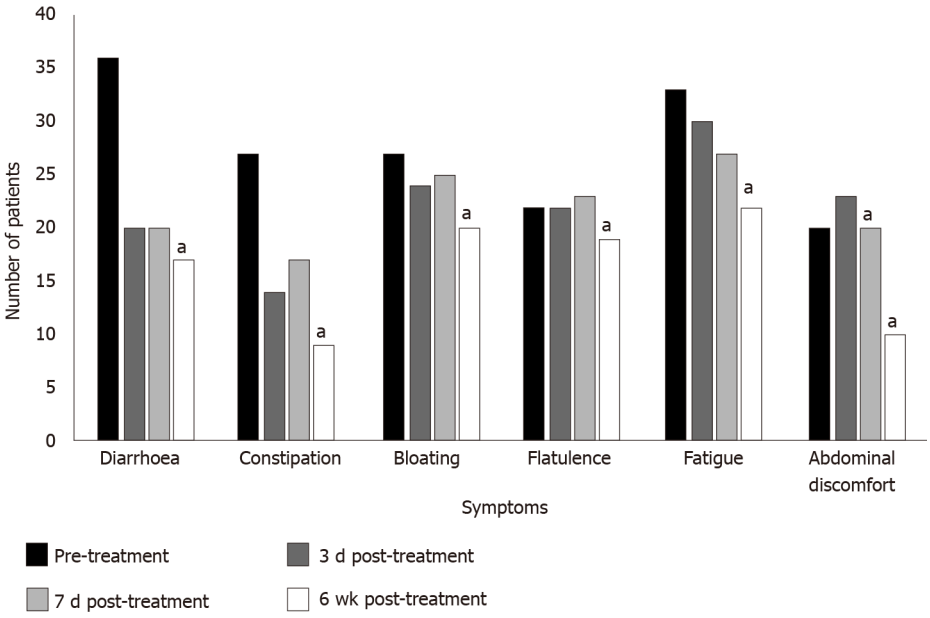

Figure 1 Common clinical symptoms pre- and post-treatment. Statistical significance: $^{a}P < 0.05$.

mucosa[20]. Although, these two parasites are considered harmless, they are associated with a range of symptoms such as diarrhoea and abdominal pain[21], and have been associated with IBD and IBS[18]. It is suggested that they may contribute to symptoms *via* the disruption of gut microbiota, resulting in a decrease in beneficial bacteria such as *Bifidobacterium* and *Lactobacillus* spp. In this study, patients reported post-treatment symptoms at three different time points. Some of the symptoms such as abdominal discomfort and blood in the stools were resolved as early as seven days post-treatment. A few other studies have followed-up the possible adverse effects and symptoms post-treatment; however, those treatments were based on a mono-therapy[8,16]. In a study by Nigro *et al*[16], the six months follow-up on patients treated with metronidazole for *B. hominis* infection showed parasite recrudescence with return of symptoms.

This study reported both parasite eradication and pre- and post-treatment symptom comparisons. Other variables such as enema retention time were measured to investigate the possible factors contributing to efficacy. There are a number of limitations of this study, such as the relatively small sample size and lack of control group. Also, patients were followed-up for duration of six weeks while a longer follow-up period may give us information of late symptom return. Moreover, further studies with larger sample size and a control group could provide broader understanding of the treatment efficacy.

Overall, this study showed a significant achievement in both parasitic eradication and improvement of clinical outcomes which points to the use of combination therapies with an alternative delivery as first line of therapy. Larger scale randomised controlled trials could help improve efficacy and so symptom resolution.

ARTICLE HIGHLIGHTS

Research background

Blastocystis hominis (*B. hominis*) and *Dientamoeba fragilis* (*D. fragilis*) are the two anaerobic protozoa which can be found in the intestinal tract of humans and can be transmitted *via* faecal-oral contact. Patients infected with these parasites can experience symptoms similar to those with irritable bowel syndrome such as abdominal pain, constipation, bloating or diarrhoea. The infections caused by the intestinal protozoa are global problems in both developed and developing countries and can cause considerable morbidity in the younger population.

Research motivation

A high failure rate has been observed with use of single drugs such as metronidazole

in the treatment of *B. hominis* and *D. fragilis* parasitic infections, thus this has led to the development of novel combination therapies.

Research objectives

This study aimed to investigate the effect of combined antibiotics administered via enema infusion to eradicate *D. fragilis* and *B. hominis* and to determine their effect on resolution of symptoms.

Research methods

A retrospective, single centre longitudinal study was conducted between 2017-2018 on patients 18 years or older, who were positive for *D. fragilis*, *B. hominis* or both. Triple antibiotics were infused over two days through rectal enema. Faecal specimens were screened for parasites from patients at baseline and six weeks after completion of treatment. Symptoms were recorded at three days, seven days and six weeks after the treatment. Patient demographic data were also collected to identify any confounding variables within the study population.

Research results

The results showed that the majority of patients (79%) showed complete clearance of parasites post-antibiotic enema infusion treatment. Improvement was observed in major clinical symptoms such as abdominal pain post-treatment. The most common side effects experienced were urine discolouration, which improved following the treatment.

Research conclusions

A significant achievement in both parasitic eradication and improvement of clinical outcomes were observed, with minimal side effects. These points to the use of combination therapies via enema as a potential first line of therapy for parasite eradication.

Research perspectives

In order to better understand the effect of antibiotic combinations and mode of administration in eradication of *B. hominis* or *D. fragilis* infections, further prospective randomised studies are required.

REFERENCES

1 **Ibrahim AN**, Al-Ashkar AM, Nazeer JT. Additional Glance on the Role of *Dientamoeba fragilis* & *Blastocystis hominis* in Patients with Irritable Bowel Syndrome. *Iran J Parasitol* 2018; **13**: 100-107 [PMID: 29963091]

2 **Coyle CM**, Varughese J, Weiss LM, Tanowitz HB. Blastocystis: to treat or not to treat. *Clin Infect Dis* 2012; **54**: 105-110 [PMID: 22075794 DOI: 10.1093/cid/cir810]

3 **Stark D**, van Hal S, Marriott D, Ellis J, Harkness J. Irritable bowel syndrome: a review on the role of intestinal protozoa and the importance of their detection and diagnosis. *Int J Parasitol* 2007; **37**: 11-20 [PMID: 17070814 DOI: 10.1016/j.ijpara.2006.09.009]

4 **Stensvold CR**, Smith HV, Nagel R, Olsen KE, Traub RJ. Eradication of Blastocystis carriage with antimicrobials: reality or delusion? *J Clin Gastroenterol* 2010; **44**: 85-90 [PMID: 19834337 DOI: 10.1097/MCG.0b013e3181bb86ba]

5 **Rostami A**, Riahi SM, Haghighi A, Saber V, Armon B, Seyyedtabaei SJ. The role of Blastocystis sp. and Dientamoeba fragilis in irritable bowel syndrome: a systematic review and meta-analysis. *Parasitol Res* 2017; **116**: 2361-2371 [PMID: 28668983 DOI: 10.1007/s00436-017-5535-6]

6 **Windsor JJ**, Macfarlane L, Hughes-Thapa G, Jones SK, Whiteside TM. Detection of Dientamoeba fragilis by culture. *Br J Biomed Sci* 2003; **60**: 79-83 [PMID: 12866914 DOI: 10.1080/09674845.2003.11783678]

7 **Garcia LS**. Dientamoeba fragilis, One of the Neglected Intestinal Protozoa. *J Clin Microbiol* 2016; **54**: 2243-2250 [PMID: 27053676 DOI: 10.1128/JCM.00400-16]

8 **Girginkardeşler N**, Coşkun S, Cüneyt Balcioğlu I, Ertan P, Ok UZ. Dientamoeba fragilis, a neglected cause of diarrhea, successfully treated with secnidazole. *Clin Microbiol Infect* 2003; **9**: 110-113 [PMID: 12588330 DOI: 10.1046/j.1469-0691.2003.00504.x]

9 **Nagata N**, Marriott D, Harkness J, Ellis JT, Stark D. Current treatment options for Dientamoeba fragilis infections. *Int J Parasitol Drugs Drug Resist* 2012; **2**: 204-215 [PMID: 24533282 DOI: 10.1016/j.ijpddr.2012.08.002]

10 **Stark D**, Barratt J, Roberts T, Marriott D, Harkness J, Ellis J. A review of the clinical presentation of dientamoebiasis. *Am J Trop Med Hyg* 2010; **82**: 614-619 [PMID: 20348509 DOI: 10.4269/ajtmh.2010.09-0478]

11 **Roberts T**, Stark D, Harkness J, Ellis J. Update on the pathogenic potential and treatment options for Blastocystis sp. *Gut Pathog* 2014; **6**: 17 [PMID: 24883113 DOI: 10.1186/1757-4749-6-17]

12 **Hui W**, Li T, Liu W, Zhou C, Gao F. Fecal microbiota transplantation for treatment of recurrent C. difficile

infection: An updated randomized controlled trial meta-analysis. *PLoS One* 2019; **14**: e0210016 [PMID: 30673716 DOI: 10.1371/journal.pone.0210016]

13 **Borody TJ**, Grippi D, Le Busque A, Gadalla S, Dawson V, Jaworski A. Improved eradication protocol for Blastocystis hominis. *Am J Gatroenterol* 2015; **110**: S590 [DOI: 10.14309/00000434-201510001-01363]

14 **Nagel R**, Bielefeldt-Ohmann H, Traub R. Clinical pilot study: efficacy of triple antibiotic therapy in Blastocystis positive irritable bowel syndrome patients. *Gut Pathog* 2014; **6**: 34 [PMID: 25349629 DOI: 10.1186/s13099-014-0034-0]

15 **Fox LM**, Saravolatz LD. Nitazoxanide: a new thiazolide antiparasitic agent. *Clin Infect Dis* 2005; **40**: 1173-1180 [PMID: 15791519 DOI: 10.1086/428839]

16 **Nigro L**, Larocca L, Massarelli L, Patamia I, Minniti S, Palermo F, Cacopardo B. A placebo-controlled treatment trial of Blastocystis hominis infection with metronidazole. *J Travel Med* 2003; **10**: 128-130 [PMID: 12650658 DOI: 10.2310/7060.2003.31714]

17 **Nagel R**, Cuttell L, Stensvold CR, Mills PC, Bielefeldt-Ohmann H, Traub RJ. Blastocystis subtypes in symptomatic and asymptomatic family members and pets and response to therapy. *Intern Med J* 2012; **42**: 1187-1195 [PMID: 22032439 DOI: 10.1111/j.1445-5994.2011.02626.x]

18 **Sekar U**, Shanthi M. Blastocystis: Consensus of treatment and controversies. *Trop Parasitol* 2013; **3**: 35-39 [PMID: 23961439 DOI: 10.4103/2229-5070.113901]

19 **van Hellemond JJ**, Molhoek N, Koelewijn R, Wismans PJ, van Genderen PJ. Is paromomycin the drug of choice for eradication of Dientamoeba fragilis in adults? *Int J Parasitol Drugs Drug Resist* 2012; **2**: 162-165 [PMID: 24533277 DOI: 10.1016/j.ijpddr.2012.03.002]

20 **Yason JA**, Liang YR, Png CW, Zhang Y, Tan KSW. Interactions between a pathogenic Blastocystis subtype and gut microbiota: in vitro and in vivo studies. *Microbiome* 2019; **7**: 30 [PMID: 30853028 DOI: 10.1186/s40168-019-0644-3]

21 **Kurt Ö**, Doğruman Al F, Tanyüksel M. Eradication of Blastocystis in humans: Really necessary for all? *Parasitol Int* 2016; **65**: 797-801 [PMID: 26780545 DOI: 10.1016/j.parint.2016.01.010]

World Journal of Gastroenterology

Submit a Manuscript: https://www.f6publishing.com

World J Gastroenterol 2020 July 14; 26(26): 3800-3813

DOI: 10.3748/wjg.v26.i26.3800

ISSN 1007-9327 (print) ISSN 2219-2840 (online)

ORIGINAL ARTICLE

Retrospective Cohort Study

Nomogram for predicting transmural bowel infarction in patients with acute superior mesenteric venous thrombosis

Meng Jiang, Chang-Li Li, Chun-Qiu Pan, Wen-Zhi Lv, Yu-Fei Ren, Xin-Wu Cui, Christoph F Dietrich

ORCID number: Meng Jiang 0000-0002-6669-547X; Chang-Li Li 0000-0001-8756-1473; Chun-Qiu Pan 0000-0003-3464-6363; Wen-Zhi Lv 0000-0002-4083-1779; Yu-Fei Ren 0000-0003-3749-8036; Xin-Wu Cui 0000-0003-3890-6660; Christoph F Dietrich 0000-0001-6382-6377.

Author contributions: Jiang M, Cui XW and Li CL designed the study; Ren YF and Cui XW supervised the study; Jiang M, Pan CQ and Lv WZ collected and analyzed the data; Ren YF performed the R Script; Jiang M prepared the figures and tables, and drafted the manuscript; Dietrich CF revised the manuscript for important intellectual content; Ren YF and Cui XW contributed equally as co-corresponding authors.

Supported by Wuhan Tongji Hospital, No. 2017A002; and Wuhan Science and Technology Bureau, No. 2017060201010181.

Institutional review board statement: This study was reviewed and approved by the Ethics Committee of the Tongji Medical college, Huazhong University of Science and Technology.

Informed consent statement: Patients were not required to give informed consent to the study

Meng Jiang, Xin-Wu Cui, Sino-German Tongji-Caritas Research Center of Ultrasound in Medicine, Department of Medical Ultrasound, Tongji Hospital, Tongji Medical College, Huazhong University of Science and Technology, Wuhan 430030, Hubei Province, China

Chang-Li Li, Department of Geratology, Hubei Provincial Hospital of Integrated Chinese and Western Medicine, Wuhan 430015, Hubei Province, China

Chun-Qiu Pan, Department of Emergency Medicine, Nanfang Hospital, Southern Medical University, Guangzhou 510515, Guangdong Province, China

Wen-Zhi Lv, Department of Artificial Intelligence, Julei Technology Company, Wuhan 430030, Hubei Province, China

Yu-Fei Ren, Department of Computer Center, Tongji Hospital, Tongji Medical College, Huazhong University of Science and Technology, Wuhan 430030, Hubei Province, China

Christoph F Dietrich, Department of Internal Medicine, Hirslanden Clinic, Berne 27804, Switzerland

Corresponding author: Xin-Wu Cui, MD, PhD, Professor, Deputy Director, Sino-German Tongji-Caritas Research Center of Ultrasound in Medicine, Department of Medical Ultrasound, Tongji Hospital, Tongji Medical College, Huazhong University of Science and Technology, No. 1095, Jiefang Avenue, Wuhan 430030, Hubei Province, China. cuixinwu@live.cn

Abstract

BACKGROUND

The prognosis of acute mesenteric ischemia (AMI) caused by superior mesenteric venous thrombosis (SMVT) remains undetermined and early detection of transmural bowel infarction (TBI) is crucial. The predisposition to develop TBI is of clinical concern, which can lead to fatal sepsis with hemodynamic instability and multi-organ failure. Early resection of necrotic bowel could improve the prognosis of AMI, however, accurate prediction of TBI remains a challenge for clinicians. When determining the eligibility for explorative laparotomy, the underlying risk factors for bowel infarction should be fully evaluated.

AIM

To develop and externally validate a nomogram for prediction of TBI in patients

with acute SMVT.

METHODS

Consecutive data from 207 acute SMVT patients at the Wuhan Tongji Hospital and 89 patients at the Guangzhou Nanfang Hospital between July 2005 and December 2018 were included in this study. They were grouped as training and external validation cohort. The 207 cases (training cohort) from Tongji Hospital were divided into TBI and reversible intestinal ischemia groups based on the final therapeutic outcomes. Univariate and multivariate logistic regression analyses were conducted to identify independent risk factors for TBI using the training data, and a nomogram was subsequently developed. The performance of the nomogram was evaluated with respect to discrimination, calibration, and clinical usefulness in the training and external validation cohort.

RESULTS

Univariate and multivariate logistic regression analyses identified the following independent prognostic factors associated with TBI in the training cohort: The decreased bowel wall enhancement (OR = 6.37, $P < 0.001$), rebound tenderness (OR = 7.14, $P < 0.001$), serum lactate levels > 2 mmol/L (OR = 3.14, $P = 0.009$) and previous history of deep venous thrombosis (OR = 6.37, $P < 0.001$). Incorporating these four factors, the nomogram achieved good calibration in the training set [area under the receiver operator characteristic curve (AUC) 0.860; 95%CI: 0.771-0.925] and the external validation set (AUC 0.851; 95%CI: 0.796-0.897). The positive and negative predictive values (95%CIs) of the nomogram were calculated, resulting in positive predictive values of 54.55% (40.07%-68.29%) and 53.85% (43.66%-63.72%) and negative predictive values of 93.33% (82.14%-97.71%) and 92.24% (85.91%-95.86%) for the training and validation cohorts, respectively. Based on the nomogram, patients who had a Nomo-score of more than 90 were considered to have high risk for TBI. Decision curve analysis indicated that the nomogram was clinically useful.

CONCLUSION

The nomogram achieved an optimal prediction of TBI in patients with AMI. Using the model, the risk for an individual patient inclined to TBI can be assessed, thus providing a rational therapeutic choice.

Key words: Superior mesenteric venous thrombosis; Acute mesenteric ischemia; Transmural bowel infarction; Reversible intestinal ischemia; Predictors; Nomogram

Core tip: The high mortality rate of acute superior mesenteric venous thrombosis is closely associated with the occurrence of transmural bowel infarction (TBI). Early detection and subsequent resection of irreversible necrotic intestine before sepsis and multi-organ failure could improve the functional outcome of the small bowel and patient prognosis. We found that the decreased bowel wall enhancement, rebound tenderness, serum lactate levels > 2 mmol/L and previous history of deep venous thrombosis independently predicted TBI. A nomogram that incorporated these four risk factors achieved an area under the receiver operator characteristic curve of 0.860 and 0.851 in the training and validation cohort, respectively, with good calibration. The nomogram can be conveniently used to facilitate the individualized prediction of TBI in patients with acute mesenteric ischemia.

Citation: Jiang M, Li CL, Pan CQ, Lv WZ, Ren YF, Cui XW, Dietrich CF. Nomogram for predicting transmural bowel infarction in patients with acute superior mesenteric venous thrombosis. *World J Gastroenterol* 2020; 26(26): 3800-3813
URL: https://www.wjgnet.com/1007-9327/full/v26/i26/3800.htm
DOI: https://dx.doi.org/10.3748/wjg.v26.i26.3800

because the analysis used anonymous clinical data that were obtained after each patient agreed to treatment by written consent.

Conflict-of-interest statement: We have no financial relationships to disclose.

Data sharing statement: No additional data are available.

STROBE statement: The authors have read the STROBE Statement-checklist of items, and the manuscript was prepared and revised according to the STROBE Statement-checklist of items.

Manuscript source: Invited manuscript

Received: February 25, 2020
Peer-review started: February 25, 2020
First decision: May 22, 2020
Revised: May 23, 2020
Accepted: June 5, 2020
Article in press: June 5, 2020
Published online: July 14, 2020

P-Reviewer: Isaji S, Kimura Y, Leal RF, Richardson WS, Soresi M
S-Editor: Dou Y
L-Editor: MedE-Ma JY
E-Editor: Zhang YL

INTRODUCTION

As a rare insidious condition, acute mesenteric venous thrombosis (MVT) has an incidence of 1 in 1000 emergency laparotomies for acute abdomen[1]. The prevalence of MVT has increased over the last two decades, likely as a result of the wide use of abdominal contrast-enhanced computed tomography (CT). Superior MVT (SMVT) is the most common type of MVT that accounts for approximately 5% - 10% of all mesenteric ischemia[2]. Despite advances in managing thromboembolic diseases over the past 40 years, the average 30-d mortality of acute SMVT is still as high as 32.1% in severe cases[3]. The predisposition to develop transmural bowel infarction (TBI) is of clinical concern, which can lead to fatal sepsis with hemodynamic instability and multi-organ failure[4].

Advances in imaging modalities, especially CT angiography, have greatly enabled early detection of SMVT in the setting of acute abdominal pain. Unfortunately, TBI is not rare, and intestinal resection is still mandatory for some patients. TBI often leads to a complex clinical situation and increases the patients' physiological burden, which poses a major challenge for clinicians. Thus, accurate and reliable prediction of bowel infarction is critical for decision-making in an emergency setting. Preventing the progression from reversible intestinal ischemia to TBI should be a primary goal in the management of SMVT.

Nomograms can provide individualized and highly accurate risk estimation, which are easy to use and can facilitate clinical decision-making. We undertook the present study to develop and externally validate a nomogram to predict TBI in patients with acute SMVT.

MATERIALS AND METHODS

Patients

Consecutive patients with SMVT from Tongji Hospital of Huazhong University of Science and Technology, Wuhan, China (as training cohort) and from Nanfang Hospital of Southern Medical University, Guangzhou, China (as validation cohort) were included. This retrospective study (clinical trial number: ChiCTR1900026320) was approved by the institutional review board of the two hospitals. Since the study was retrospectively designed and did not cause any harm to the patients, the informed consent was waived by the board.

We retrospectively reviewed the electronic medical record system using the key word "mesenteric venous thrombosis" to identify SMVT patients with acute mesenteric ischemia (AMI) who underwent contrast-enhanced CT at the two institutions. SMVT-related AMI was defined as the association of acute abdominal symptoms, CT features of bowel injury, as well as vascular insufficiency of the superior mesenteric vein. Two senior radiologists reviewed all CT images and confirmed the presence of thrombosis and bowel injury based on consensus. K statistics was used to evaluate the concordance between the two radiologists, and any disagreements were resolved by discussion. Diagnosis was confirmed pathologically in cases that intestinal resection was performed. To explore the effect of SMVT on bowel infarction without confounding risk factors, we excluded patients who had coexisting mesenteric artery thrombosis. In addition, cases in that acute SMVT was secondary to mechanical small bowel obstruction were also excluded.

Treatment protocol

At the two tertiary referral centers in China, we have employed a standard protocol for the treatment of acute SMVT. The treatment protocol included bowel rest, nasogastric tube decompression for patients with abdominal distention, intravenous fluids, prophylactic antibiotics, prompt anticoagulation or surgical exploration if necessary. For all patients, once acute SMVT was diagnosed, intravenous administration of unfractionated heparin (3000-5000 IU/d) or subcutaneous administration of low-molecular-weight heparin (LMWH or enoxaparin, 1 mg/kg per day) was applied at first. Thereafter, for patients with anticipated surgery, intravenous unfractionated heparin was administered according to the active partial thrombin time. Patients who received conservative treatment were injected with LMWH (1 mg/kg; BID) subcutaneously and monitored closely. Transmural bowel necrosis from resected specimens was confirmed histologically.

Outcomes

To determine the indicators of TBI, patients were divided into two groups according to the final therapeutic outcome. The TBI group was defined as: (1) Pathology assessment as extensive, transmural intestinal necrosis; (2) Definite imaging of bowel perforation on CT; or (3) Unresected patients with extensive bowel necrosis assessed during open-close laparotomy procedures. All resected specimens were retrospectively reviewed by a senior pathologist. The patients who did not progress to transmural bowel necrosis but recovered from AMI or superficial ischemic lesions after systemic anticoagulation or thrombectomy were categorized as reversible intestinal ischemia group. This was confirmed by explorative laparotomy, repeated CT scan or clinical follow-up.

Statistical analysis

Continuous variables were presented as median (interquartile range), and were compared between the training and validation cohort using Mann-Whitney U test or *t* test as appropriate. Categorical variables were reported as whole numbers and proportions and were compared by the χ^2 test or Fisher's exact test where appropriate. Statistical analyses were conducted using R software (version 3.6.1) and SPSS 20.0 software (SPSS Inc., Chicago, IL, United States). All the statistical significance levels were two-sided, with *P* value less than 0.05. The detailed description of the decision curve analysis (DCA) algorithm is provided in the Supplementary text.

Data collection

Demographic and clinical data were extracted from case records, including age, gender, coexisting medical conditions (*e.g.*, tobacco use, malignant disease, or previous history of deep venous thrombosis), clinical manifestations, physical findings and laboratory test results. All serum biochemical parameters were collected at the onset of symptoms. Radiologic features including extent of thrombus and associated conditions (*e.g.*, decreased bowel wall enhancement, bowel wall thickening and pneumatosis intestinalis) were also recorded. We also extracted the suspected risk factors for acute SMVT, such as recent surgery, intraperitoneal inflammation, and liver cirrhosis.

Construction of the nomogram

Continuous variables were transformed into dichotomous variables using the upper value of normal as the cutoff level (*e.g.*, white blood cell count > 10×10^9/L, percentage of neutrophil granulocyte > 75%, creatinine > 106 μmol/L, or venous lactate levels > 2 mmol/L), and C-reactive protein (50 mg/L as cutoff value in line with previous study[5].

Univariate logistic regression analysis was conducted to assess each variable in the training cohort for investigating the independent risk factors associated with TBI. Then, a multivariate logistic regression analysis incorporating all the significant risk variables was performed, using backward step-down selection procedure with a liberal $P < 0.05$ as the retention criteria to select the final indicators of TBI. A nomogram was developed based on the results of multivariate logistic regression analysis.

Performance of the nomogram

Calibration of the nomogram was evaluated using calibration curve and Hosmer-Lemeshow test (non-significance of the Hosmer-Lemeshow test indicates good agreement)[6]. The discrimination performance of the nomogram was assessed using the area under the receiver operator characteristic curve (AUC). The nomogram was subjected to bootstrapping validation (1000 bootstrap resamples) to calculate a relatively corrected AUC. Then the performance of the nomogram was tested in the external validation cohort by calibration curve and AUC.

Clinical use assessment

DCA was performed to estimate the clinical usefulness of the prediction model by quantifying the net benefits at different threshold probabilities[7,8]. For clinical use, the total scores (defined as Nomo-score in this study) of each case were calculated according to the nomogram algorithm. Then the optimal cutoff value of the Nomo-score was determined by maximizing the Youden index. Performance of the optimal cutoff value of the Nomo-score was assessed by the sensitivity, specificity, as well as positive and negative predictive values.

RESULTS

Patient selection

After excluding 12 patients with chronic SMVT, chart review yielded 230 consecutive patients who had acute SMVT in the training cohort between July 2005 and June 2018 (Wuhan cohort). Of the 230 patients, 13 cases were excluded from the analysis as the acute SMVT was secondary to mechanical small bowel obstruction. Acute SMVT concomitant with mesenteric artery thrombosis was found in 10 patients, who were also excluded, leaving a final sample of 207 patients. Explorative laparotomy was performed in 78 (38%) patients , and bowel resection was performed in 65 (83%) of these patients based on assessment of bowel viability with respect to color, dilatation and peristaltic motion of the bowel, pulsations of the mesenteric arcade arteries, as well as bleeding from cut surfaces. Thrombectomy was performed in 11 (14%) patients, and 2 (3%) received open-close procedure due to extensive bowel necrosis, who refused further treatment and died at last. The algorithm of patient screening in the training cohort is shown in Figure 1A. Pathological analysis of the surgical specimens confirmed TBI in 56 (86%) of the 65 patients, while superficial ischemic lesions were seen in 9 (14%) patients. The mean time between admission and surgical exploration for patients with and without TBI was 41.6 ± 30.5 (8-192) h and 32.4 ± 23.7 (5-96) h, respectively.

In this study, patients with superficial ischemic lesions confirmed by pathological examination and clinically recovered through thrombectomy were classified as reversible intestinal ischemia group, while patients who underwent open-close procedure due to extensive bowel necrosis were deemed as TBI. One hundred twenty-nine patients (62%) who did not progress to surgery and recovered after conservative therapy were considered as having reversible intestinal ischemia. Eventually, reversible intestinal ischemia and TBI were the final diagnosis in 149 (72%) and 58 (28%) patients, respectively.

In the external validation cohort (Guangzhou cohort), 89 eligible cases were retrieved from August 2007 to December 2018 using the same criteria (Figure 1B). TBI was confirmed in 27 (30%) of these patients.

Characteristics of the study population

The patients' clinical characteristics in the training and validation cohorts are summarized in Table 1. There were no differences in the clinicopathological characteristics between the two cohorts in most of the comparisons. In the training cohort, 82 patients had a clinical history of liver cirrhosis, and 20.7% (17/82) cases developed TBI. In the validation cohort, 18.9% (7/37) of the patients with liver cirrhosis progressed to TBI finally.

Development and validation of a TBI-predicting nomogram

The results of univariate logistic analysis are presented in Table 2. Stepwise multivariate logistic regression indicated that the decreased bowel wall enhancement (OR = 6.37, $P < 0.001$), rebound tenderness (OR = 7.14, $P < 0.001$), serum lactate levels > 2 mmol/L (OR = 3.14, $P = 0.009$) and previous history of deep venous thrombosis (DVT) (OR = 6.37, $P < 0.001$) all independently predicted TBI (Table 3). These independently associated risk factors were used to construct a TBI risk estimation nomogram (Figure 2A). The scoring system is shown in Supplementary Table 1, which can be used for a more accurate calculation of predictions than drawing lines on the nomogram. Figure 2B shows the calibration curve of the nomogram. The calibration curve and Hosmer-Lemeshow test statistics ($P = 0.316$) showed good calibration in the training cohort. An AUC of 0.860 (95%CI: 0.771-0.925) also showed good discrimination by the nomogram (Figure 2D). The favorable calibration of the nomogram was also confirmed in the external validation set (Figure 2C). The Hosmer-Lemeshow test yielded a P value of 0.203, and the AUC of the validation cohort was 0.851 (95%CI: 0.796-0.897) (Figure 2E). Thus, our nomogram performed well in both the training and external validation sets.

Decision curve analysis DCA was used to facilitate the assessment of the nomogram. Figure 3A shows the basic plot of model performance for the nomogram. The DCA graphically demonstrated the clinical value of the model based on a continuum of threshold for TBI risk (X axis) and the net benefit of using the model to stratify the risk of the patients (Y axis) relative to the hypothesis that no patient will have a TBI. The decision curve indicated that when the threshold probability for a patient or a doctor is within a range from 0 to 1.0, the nomogram adds more net benefit than the "treat-all"

Table 1 Participant characteristics

Variable	Cohort, *n* (%)		
	Training (*n* = 207)	Validation (*n* = 89)	*P* value
Age, yrs	48.5 ± 13.2	51.3 ± 8.2	0.07
Gender			0.52
Male	145 (70.0)	59 (66.3)	
Female	62 (30.0)	30 (33.7)	
Tobacco use	40 (19.3)	25 (28.1)	0.09
Coexisting medical conditions			
Hypertension	19 (9.2)	13 (14.6)	0.17
Diabetes	20 (9.7)	13 (14.6)	0.22
Ischemic heart disease	8 (3.9)	9 (10.1)	0.05
Previous history of DVT	39 (18.8)	17 (19.1)	0.81
Malignant disease	24 (2.4)	5 (5.6)	0.11
Clinical manifestations			
Diarrhea	22 (10.6)	14 (15.7)	0.22
Hematochezia or melena	62 (30.0)	19 (21.3)	0.13
Fever	26 (12.6)	13 (14.6)	0.63
Physical findings			
Abdominal distention	109 (52.7)	37 (41.6)	0.16
Abdominal tenderness	39 (18.8)	24 (27.0)	0.12
Rebound tenderness	38 (18.4)	21 (23.6)	0.3
Laboratory findings			
White blood cells, 10^9/L	7.0 (4.7-11.4)	11.0 (7.5-14.4)	0.05
Hemoglobin, g/L	109 (82-122)	113 (92-130)	0.11
Platelets, 10^9/L	191 (100-288)	168 (133-214)	0.06
C-reactive protein, mg/L	51.3 (7.7-67.5)	53.9 (18.2-75.1)	0.23
Serum lactate levels, mmol/L	4.3 (2.7-6.5)	3.9 (1.3-5.7)	0.31
Creatinine, μmol/L	72 (60-91)	76 (65-108)	0.07
D-dimer, mg/L	16.9 (3.0-179.6)	14.1 (6.9-60.2)	0.61
Procalcitonin, μg/L	0.5 (0.4-0.6)	0.4 (0.1-1.8)	0.17
Radiologic features			
Distal thrombosis	63 (30.4)	25 (28.1%)	0.69
Portal vein or/and splenic vein extension	143 (69.1)	54 (60.7)	0.16
Decreased bowel wall enhancement	70 (33.8)	36 (40.4)	0.28
Bowel wall thickening	42 (21.3)	19 (21.3)	0.84
Bowel loop dilation	41 (19.8)	16 (18.0)	0.71
Pneumatosis intestinalis	52 (25.1)	27 (30.3)	0.13
Ascites	91 (44.0)	31 (34.8)	0.14
Other risk factors			
Recent surgery	46 (22.2)	15 (16.9)	0.3
Intraperitoneal inflammation	73 (35.3)	31 (34.8)	0.94
Liver cirrhosis	82 (39.6)	37 (41.6)	0.75

Data are median (IQR) or *n* (%). *P* values were calculated by Mann-Whitney *U* test, *t* test, χ^2 test, or Fisher's exact test, as appropriate. DVT: Deep venous thrombosis.

Table 2 Univariate analysis of risk factors associated with transmural bowel infarction in the training cohort

Variable	OR (95%CI)	*P* value
Age, yr	0.97 (0.95-0.99)	0.01
Gender, male *vs* female	2.22 (1.06-4.65)	0.03
Tobacco use	1.03 (0.48-2.23)	0.94
Hypertension	1.10 (0.38-3.20)	0.86
Diabetes	3.85 (0.86-17.14)	0.08
Ischemic heart disease	2.81 (0.34-23.36)	0.34
Previous history of DVT	3.14 (1.53-6.47)	0.002
Malignant disease	0.41 (0.21-1.78)	0.99
Diarrhea	1.04 (0.39-2.81)	0.93
Hematochezia	2.53 (1.33-4.79)	0.004
Fever	1.16 (0.47-2.83)	0.75
Abdominal distention	3.56 (1.82-6.97)	< 0.001
Abdominal tenderness	7.25 (3.40-15.46)	< 0.001
Rebound tenderness	9.14 (4.17-20.04)	< 0.001
White blood cells, > 10×10^9/L *vs* ≤ 10×10^9/L	1.12 (1.06-1.17)	< 0.001
Hemoglobin, > 120 g/L *vs* ≤ 120 g/L	1.01 (1.00-1.02)	0.35
Platelets, > 100×10^9/L *vs* ≤ 100×10^9/L	1.00 (0.99-1.01)	0.96
C-reactive protein, > 50 mg/L *vs* ≤ 50 mg/L	1.02 (1.01-1.02)	0.05
Serum lactate levels, > 2 mmol/L *vs* ≤ 2 mmol/L	6.53 (3.27-13.04)	< 0.001
Creatinine, > 106 μmol/L *vs* ≤ 106 μmol/L	2.05 (0.96-4.41)	0.07
D-dimer, > 0.5 mg/L *vs* ≤ 0.5 mg/L	1.00 (1.00-1.01)	0.50
Procalcitonin, > 0.5 μg/L *vs* ≤ 0.5 μg/L	1.02 (0.92-1.12)	0.72
Distal thrombosis	2.13 (1.07-4.36)	0.02
Portal vein or/and splenic vein extension	1.01 (0.52-1.94)	0.98
Decreased bowel wall enhancement	9.00 (4.24-19.12)	< 0.001
Bowel wall thickening	1.99 (0.98-2.01)	0.24
Bowel loop dilation	2.21 (1.67-3.54)	0.03
Pneumatosis intestinalis	1.36 (1.23-3.15)	0.04
Ascites	1.40 (0.76-2.58)	0.28
Recent surgery	1.13 (0.54-2.38)	0.74
Intraperitoneal inflammation	1.63 (0.84-3.16)	0.15
Liver cirrhosis	2.44 (1.28-4.68)	0.007

OR: Odd ratio; CI: Confidence interval; DVT: Deep venous thrombosis.

or "treat-none" schemes. Figure 3B shows the estimated number of patients who would be at high risk for each potential risk threshold and visually demonstrates the proportion of the patients who are truly positive cases. For instance, if a 40% risk threshold was used, of 1000 patients screened, about 200 patients would be deemed at

Table 3 Multivariate logistic regression analysis of risk factors associated with transmural bowel infarction in the training cohort

Variable	β	OR	95%CI	*P* value
Decreased bowel wall enhancement	1.85	6.37	2.55-15.90	< 0.001
Rebound tenderness	1.97	7.14	2.73-18.65	< 0.001
Serum lactate levels > 2 mmol/L	1.44	3.14	1.33-7.41	0.009
DVT history	1.81	6.37	2.55-15.90	< 0.001

OR: Odd ratio; CI: Confidence interval; DVT: Deep venous thrombosis.

high risk, with about 180 of these patients being true TBI cases.

Predicting TBI based on the Nomo-score

The optimal cutoff value of the Nomo-score was determined to be 90. The sensitivity, specificity, positive predictive value, and negative predictive value when used in predicting TBI were 88.89%, 67.74%, 54.55%, and 93.33% in the training cohort, and 84.84%, 71.81%, 53.85%, and 92.24% in the external validation cohort, respectively (Table 4).

DISCUSSION

Acute SMVT is a rare but serious condition due to its intestinal ischemic complications. The widespread use of contrast-enhanced CT has made early diagnosis possible by a noninvasive approach, which can provide incremental information as evidence of ischemia warranting a change in treatment strategy. However, acute SMVT still carries a high risk of extensive intestinal infarction and surgical exploration with bowel resection is still mandatory for some patients. Recently, Kim *et al*[9] conducted a study involving 66 patients with acute SMVT, of whom 15 (23%) patients underwent bowel resection due to progressive intestinal ischemia and bowel infarction, and 3 (5%) patients died at last, despite adequate intravenous or subcutaneous anticoagulation were applied immediately at diagnosis. Another research reported the application of multidisciplinary stepwise management strategy for acute SMVT, and 18 of the 43 (42%) subjects underwent bowel resection due to TBI[10]. The reported rates of bowel infarction in existing literatures ranged from 6% to 42%, consistent with our rate of 29%[2,10-16]. Therefore, preventing the progression from reversible to irreversible ischemic bowel injury should be a primary goal in the management of acute SMVT[5]. However, the early detection of TBI remains a challenge and further investigation is required to identify the most important prognostic factors.

In this retrospective study, we developed and externally validated a nomogram to predict TBI in patients with acute SMVT. The decreased bowel wall enhancement, rebound tenderness, serum lactate levels > 2 mmol/L and previous history of DVT independently predicted this event. Incorporating these clinical, biological, and radiological factors into an easy-to-use prediction model can facilitate the individualized prediction of TBI. The nomogram also consistently predicted TBI with a high accuracy and provided good clinical usefulness throughout the range of bowel infarction risk as assessed by DCA.

Based on our findings, the previous history of DVT could increase the chances of bowel infarction in the setting of acute SMVT. Venous thrombosis often results from a combination of endothelial injury, hypercoagulability or stasis. The patients with a previous history of DVT may have had several episodes of undetected (possibly asymptomatic) MVT prior to the index event and thus have acute-on-chronic thrombosis with greater compromise of venous flow.

The decreased bowel wall enhancement on CT angiography is a strong established risk indictor for bowel infarction[9,17]. In our study, CT scan detected this feature in 70 patients, and among them, 34 patients had confirmed TBI finally. Previous studies demonstrated that the decreased bowel wall enhancement in patients with acute SMVT was significantly associated with surgical exploration and bowel resection[9,10].

Several other reports on AMI implied that the extent of venous thrombus was

Table 4 Performance of the nomogram for estimating the risk of transmural bowel infarction

Variable	Value (95%CI)	
	Training cohort (207)	Validation cohort (89)
Cutoff value	90	90
AUC	0.860 (0.771-0.925)	0.851 (0.796-0.897)
Sensitivity, %	88.89 (71.94-96.15)	84.48 (73.07-91.62)
Specificity, %	67.74 (55.37-78.05)	71.81 (64.11-78.42)
Positive predictive value, %	54.55 (40.07-68.29)	53.85 (43.66-63.72)
Negative predictive value, %	93.33 (82.14-97.71)	92.24 (85.91-95.86)
Positive likelihood ratio	2.76 (2.43-3.07)	3.00 (2.84-3.16)
Negative likelihood ratio	0.16 (0.08-0.32)	0.22 (0.17-0.27)
Diagnostic accuracy, %	74.16 (64.20-82.12)	75.36 (69.07-80.73)

AUC: Area under the receiver operator characteristic curve; CI: Confidence interval.

related to TBI[9,18]. However, Grisham *et al*[19] found no association between the presence of multiple vein thromboses and increased mortality rates. Additionally, Kumar *et al*[20] showed that patients with isolated SMVT were even at a greater risk of development of bowel infarction, and more likely to require surgery. In view of that the extent of venous thrombus did not show enough predictive strength on the basis of univariate association with bowel infarction, we excluded this variable for model construction.

Peritoneal signs, including involuntary guarding, rebound tenderness, and abdominal wall rigidity often present in the case of TBI. According to our results, the rebound tenderness could be a strong predictor for TBI. In parallel with our outcomes, Kim *et al*[9] found that rebound tenderness was observed more frequently in patients who underwent bowel resection than those who did not (33% *vs* 4%).

Lactate is an important parameter that closely related to necrosis, inflammation and hypoxia. Our results demonstrated that serum lactate levels > 2 mmol/L was significantly associated with the occurrence of TBI. In line with our findings, Higashizono and Nuzzo revealed that serum lactate levels tend to increase significantly after bowel infarction[5,21]. Additionally, Leone *et al*[22] indicated that serum lactate levels decreased significantly after resection of the necrotic bowel, further validating its predictive value for TBI.

Accurate identification of patients that will need surgery due to bowel infarction is crucial, because of the high morbidity and mortality associated with unidentified and unresected necrotic intestine[3,23,24]. Earlier resection of necrotic bowel before the development of multi-organ failure could improve the functional outcome of the small bowel and patient prognosis. However, this issue remains a challenge. In a study the authors presented 767 surgeons with a clinical vignette of AMI, and showed that the surgeons' decision on whether a surgery is required or not varies markedly[25].

In a previous study, Nuzzo *et al*[5] developed a risk score incorporating organ failure, serum lactate levels > 2 mmol/L and bowel loop dilation on CT scan to predict irreversible transmural bowel necrosis for AMI. The risk factors associated with bowel necrosis identified in this study was partly different from ours, probably because their cohort comprised venous and arterial occlusion, but we just included acute SMVT patients. In addition, we suggested that organ failure might be of late onset during the disease course. Furthermore, we think that the risk score based on the number of predictive factors could not reflect the weight of each parameter.

Although several studies have investigated the risk factors of TBI for AMI, to our knowledge, none have presented the data in the form of a validated nomogram[5,9,26,27]. Nomograms have advantages as they provide quantified individual risk assessment in a dynamic manner. For clinical use of our nomogram, we proposed the sensitivity, specificity, negative and positive predictive value in assessing the risk of TBI using 90 as the cut-off value (Table 4). We show that patients with a Nomo-score less than 90 are the subgroup of low-risk inclined to TBI (negative predictive value, 93.33% for training and 92.24% for validation). The AUC of our model was 0.860 and 0.851 in the training and external validation cohort, respectively. The calibration curves presented a good agreement between the actual probability and predicted probability of TBI.

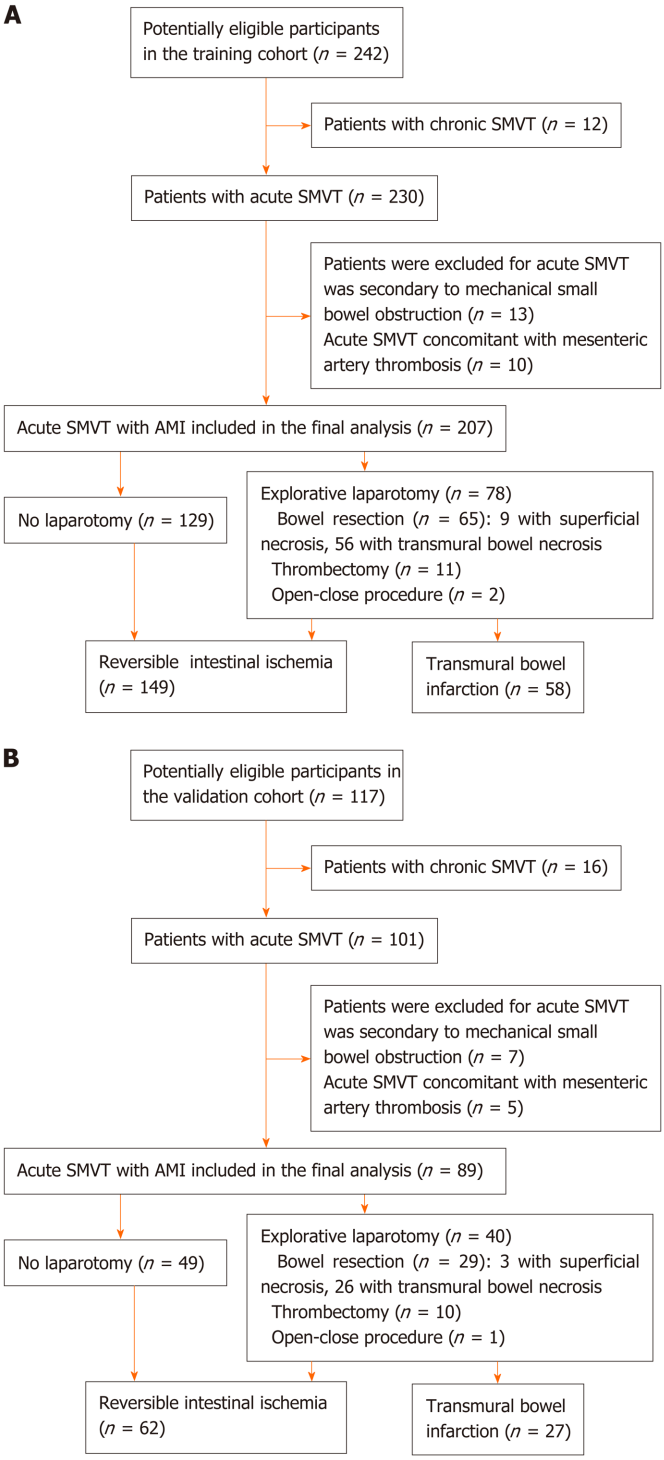

Figure 1 Flow diagram of study populations. A: Training cohort; B: Validation cohort. SMVT: Superior mesenteric venous thrombosis; AMI: Acute mesenteric ischemia.

Thus, we believe that our nomogram could be a reliable and objective tool that will provide clinicians favorable evidence for decision making.

Cautions should be exercised when interpreting the findings due to several limitations. First, some bias may inevitably exist and affect our analysis because it was a retrospective study. And thus, treatment strategy might not be entirely consistent among clinicians. Second, although we have validated the nomogram in an external cohort, the number of variables evaluated in respect to the number of primary outcome events may have led to an overfitting of the accuracy of the model, thus prospective multicenter validation using a larger group of patients is still necessary to acquire high-level evidence for further clinical application. Third, pathological

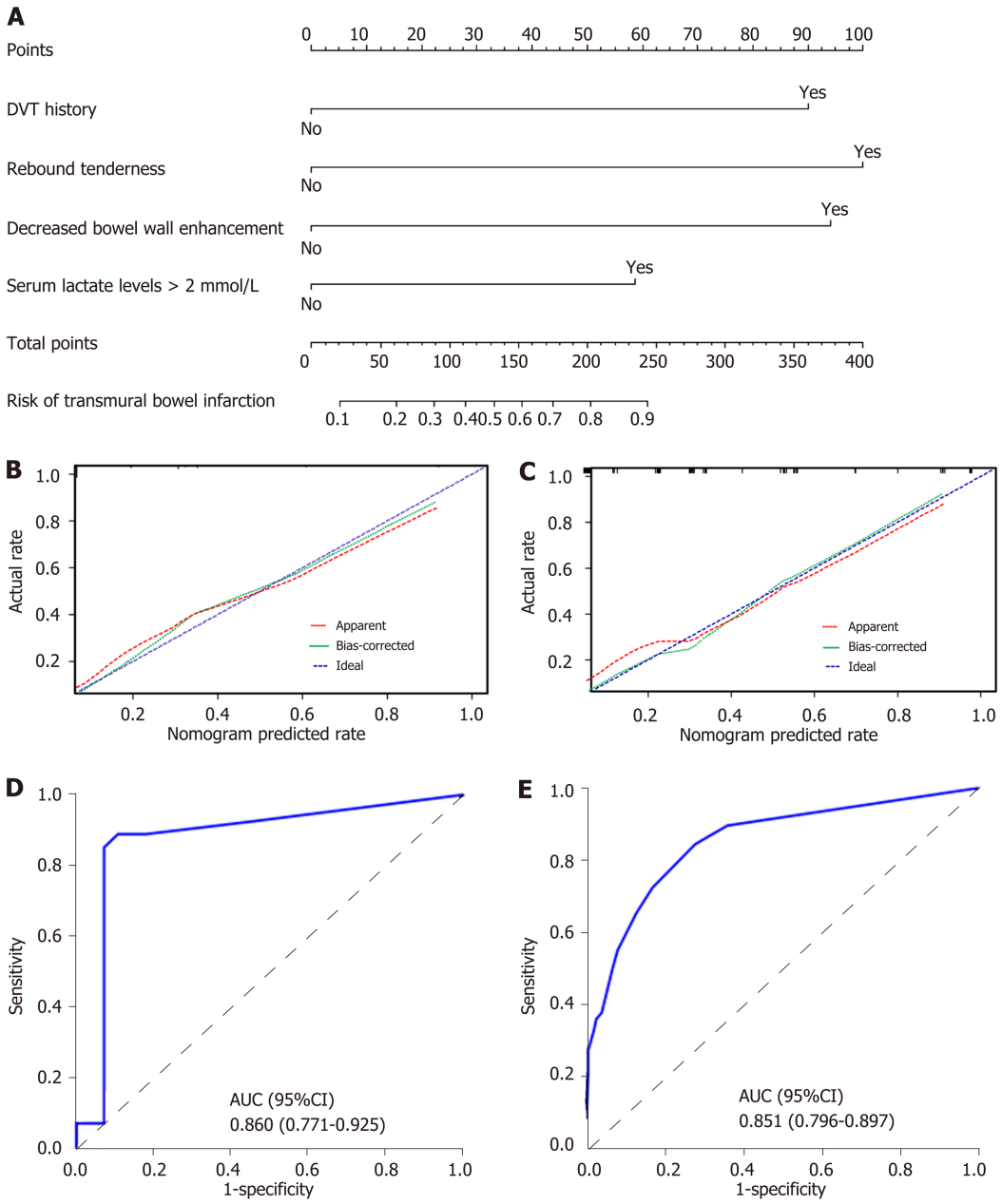

Figure 2 Nomogram for evaluation of transmural bowel infarction risk and its predictive performance. A: Nomogram for estimating the risk of transmural bowel infarction (TBI) in patients with acute mesenteric ischemia (AMI). The nomogram is used to find the position of each variable on the corresponding axis, draw a line to the points axis for the number of points, add the points from all of the variables, and draw a line from the total points axis to determine the risk of TBI at the lower line of the nomogram. For example, a 30-year-old male patient (have transmural bowel infarction finally) with a previous history of deep venous thrombosis and serum lactate levels > 2 mmol/L, no rebound tenderness and no decreased bowel wall enhancement, has a risk of 59% of TBI calculated by the nomogram; B and C: Calibration curves of the nomogram in the training and validation sets, respectively. Calibration curves depict the calibration of the model in terms of the agreement between the predicted probabilities of TBI and observed outcomes of TBI. The dotted blue line represents an ideal prediction, and the dotted red line represents the predictive ability of the nomogram. The closer the dotted red line fit is to the dotted blue line, the better the predictive accuracy of the nomogram is; D and E: The ROC curves of the nomogram in the training and validation sets, respectively. TBI: Transmural bowel infarction; AMI: Acute mesenteric ischemia; DVT: Deep venous thrombosis; AUC: Area under the receiver operator characteristic curve; ROC: Receiver operator characteristic curve.

evidence could not be obtained for patients that did not progress to surgery but confirmed by recovery from the specific vascular therapy. Fourth, evaluation of decreased bowel wall enhancement in the nomogram was related to the reading of CT images, and interpretation may vary among radiologists. In addition, since it is hard to assess the length of decreased bowel wall enhancement quantitatively on CT imaging, we did not examine the association between this factor and TBI. Further high-level evidence is needed to clarify this issue. Finally, data on the long-term outcomes of patients were unavailable, however, this will not affect our ability to identify risk factors of TBI associated with AMI.

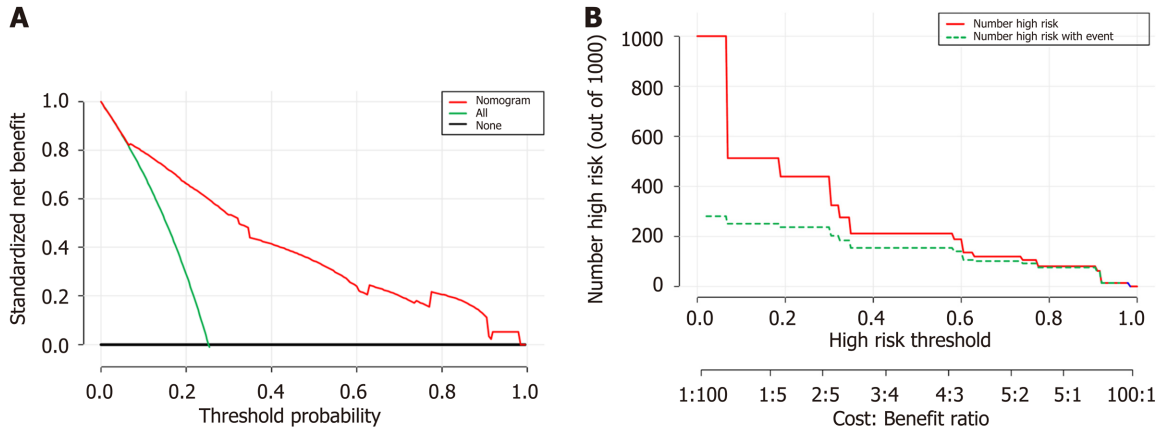

Figure 3 Decision curve analysis for the nomogram. A: The Y-axis shows the net benefit. The X-axis shows the corresponding risk threshold. The green line represents the assumption that all patients have transmural bowel infarction (TBI). The thin black line represents the assumption that no patients have TBI. The red line represents the nomogram. The decision curve in the validation cohort indicated that if the threshold probability is between 0 and 1.0, then using the nomogram to predict TBI adds more benefit than the treat-all-patients scheme or treat-none scheme; B: Clinical impact curve for the risk model. Of 1000 patients, the red solid line shows the total number who would be deemed at high risk for each risk threshold. The green dashed line shows how many of those would be true positives cases. DCA: Decision curve analysis; TBI: Transmural bowel infarction.

In conclusion, our nomogram is an individual predictive tool that incorporates four risk factors, shows favorable predictive accuracy for assessing TBI risk in patients with AMI. The model might facilitate timely recognition and effective management of high-risk patients.

ARTICLE HIGHLIGHTS

Research background

The prognosis of acute mesenteric ischemia (AMI) caused by superior mesenteric venous thrombosis (SMVT) remains obscure and early detection of transmural bowel infarction (TBI) is crucial. The predisposition to develop TBI is of clinical concern, which can lead to fatal sepsis with hemodynamic instability and multiorgan failure. Early resection of necrotic bowel could improve the prognosis of AMI, however, accurate prediction of TBI remains a challenge for clinicians. When determining eligibility for explorative laparotomy, the underlying risk factors for bowel infarction should be fully evaluated.

Research motivation

Nomograms can provide individualized and highly accurate risk estimation, which are easy to use and can facilitate clinical decision-making. We undertook the present study to develop and externally validate a nomogram to predict TBI in patients with acute SMVT.

Research methods

Consecutive data from 207 acute SMVT patients at the Wuhan Tongji Hospital and 89 patients at the Guangzhou Nanfang Hospital between July 2005 and December 2018 were included in this study. They were grouped as training and external validation cohort. The 207 cases (training cohort) from Tongji hospital were divided into TBI and reversible intestinal ischemia groups based on the final therapeutic outcomes. Then univariate and multivariate logistic regression analyses were conducted to identify independent risk factors for TBI using the training data, and a nomogram was subsequently developed. The performance of the nomogram was evaluated with respect to discrimination, calibration, and clinical usefulness in the training and external validation cohort.

Research results

Univariate and multivariate logistic regression analyses identified the following independent prognostic factors associated with TBI in the training cohort: The decreased bowel wall enhancement (OR = 6.37, $P < 0.001$), rebound tenderness (OR =

7.14, $P < 0.001$), serum lactate levels > 2 mmol/L (OR = 3.14, $P = 0.009$) and previous history of deep venous thrombosis (OR = 6.37, $P < 0.001$). Incorporating these four factors, the nomogram achieved good calibration in the training set (AUC 0.860; 95%CI: 0.771-0.925) and the external validation set (AUC 0.851; 95%CI: 0.796-0.897). The positive and negative predictive values (95%CIs) of the nomogram were calculated, resulting in positive predictive values of 54.55% (40.07%-68.29%) and 53.85% (43.66%-63.72%) and negative predictive values of 93.33% (82.14%-97.71%) and 92.24% (85.91%-95.86%) for the training and validation cohorts, respectively. Based on the nomogram, patients who had a Nomo-score of more than 90 were considered to have high risk for TBI. Decision curve analysis indicated that the nomogram was clinically useful.

Research conclusions

The nomogram achieved an optimal prediction of TBI in patients with AMI. Using the model, the risk for an individual patient inclined to TBI can be assessed, thus providing a rational therapeutic choice.

Research perspectives

Although we have validated the nomogram in an external cohort, the number of variables evaluated in respect to the number of primary outcome events may have led to an overfitting of the accuracy of the model, thus prospective multicenter validation using a larger group of patients is still necessary to acquire high-level evidence for further clinical application.

REFERENCES

1 **Blumberg SN**, Maldonado TS. Mesenteric venous thrombosis. *J Vasc Surg Venous Lymphat Disord* 2016; **4**: 501-507 [PMID: 27639007 DOI: 10.1016/j.jvsv.2016.04.002]

2 **Brunaud L**, Antunes L, Collinet-Adler S, Marchal F, Ayav A, Bresler L, Boissel P. Acute mesenteric venous thrombosis: case for nonoperative management. *J Vasc Surg* 2001; **34**: 673-679 [PMID: 11668323 DOI: 10.1067/mva.2001.117331]

3 **Schoots IG**, Koffeman GI, Legemate DA, Levi M, van Gulik TM. Systematic review of survival after acute mesenteric ischaemia according to disease aetiology. *Br J Surg* 2004; **91**: 17-27 [PMID: 14716789 DOI: 10.1002/bjs.4459]

4 **Klar E**, Rahmanian PB, Bücker A, Hauenstein K, Jauch KW, Luther B. Acute mesenteric ischemia: a vascular emergency. *Dtsch Arztebl Int* 2012; **109**: 249-256 [PMID: 22536301 DOI: 10.3238/arztebl.2012.0249]

5 **Nuzzo A**, Maggiori L, Ronot M, Becq A, Plessier A, Gault N, Joly F, Castier Y, Vilgrain V, Paugam C, Panis Y, Bouhnik Y, Cazals-Hatem D, Corcos O. Predictive Factors of Intestinal Necrosis in Acute Mesenteric Ischemia: Prospective Study from an Intestinal Stroke Center. *Am J Gastroenterol* 2017; **112**: 597-605 [PMID: 28266590 DOI: 10.1038/ajg.2017.38]

6 **Kramer AA**, Zimmerman JE. Assessing the calibration of mortality benchmarks in critical care: The Hosmer-Lemeshow test revisited. *Crit Care Med* 2007; **35**: 2052-2056 [PMID: 17568333 DOI: 10.1097/01.CCM.0000275267.64078.B0]

7 **Vickers AJ**, Elkin EB. Decision curve analysis: a novel method for evaluating prediction models. *Med Decis Making* 2006; **26**: 565-574 [PMID: 17099194 DOI: 10.1177/0272989X06295361]

8 **Kerr KF**, Brown MD, Zhu K, Janes H. Assessing the Clinical Impact of Risk Prediction Models With Decision Curves: Guidance for Correct Interpretation and Appropriate Use. *J Clin Oncol* 2016; **34**: 2534-2540 [PMID: 27247223 DOI: 10.1200/JCO.2015.65.5654]

9 **Kim HK**, Hwang D, Park S, Lee JM, Huh S. Treatment outcomes and risk factors for bowel infarction in patients with acute superior mesenteric venous thrombosis. *J Vasc Surg Venous Lymphat Disord* 2017; **5**: 638-646 [PMID: 28818214 DOI: 10.1016/j.jvsv.2017.04.011]

10 **Yang S**, Fan X, Ding W, Liu B, Meng J, Xu D, He C, Yu W, Wu X, Li J. Multidisciplinary stepwise management strategy for acute superior mesenteric venous thrombosis: an intestinal stroke center experience. *Thromb Res* 2015; **135**: 36-45 [PMID: 25466834 DOI: 10.1016/j.thromres.2014.10.018]

11 **Zhang J**, Duan ZQ, Song QB, Luo YW, Xin SJ, Zhang Q. Acute mesenteric venous thrombosis: a better outcome achieved through improved imaging techniques and a changed policy of clinical management. *Eur J Vasc Endovasc Surg* 2004; **28**: 329-334 [PMID: 15288639 DOI: 10.1016/j.ejvs.2004.06.001]

12 **Amitrano L**, Guardascione MA, Scaglione M, Pezzullo L, Sangiuliano N, Armellino MF, Manguso F, Margaglione M, Ames PR, Iannaccone L, Grandone E, Romano L, Balzano A. Prognostic factors in noncirrhotic patients with splanchnic vein thromboses. *Am J Gastroenterol* 2007; **102**: 2464-2470 [PMID: 17958760 DOI: 10.1111/j.1572-0241.2007.01477.x]

13 **Hedayati N**, Riha GM, Kougias P, Huynh TT, Cheng C, Bechara C, Bismuth J, Dardik A, Lin PH. Prognostic factors and treatment outcome in mesenteric vein thrombosis. *Vasc Endovascular Surg* 2008; **42**: 217-224 [PMID: 18332399 DOI: 10.1177/1538574407312653]

14 **Acosta S**, Alhadad A, Svensson P, Ekberg O. Epidemiology, risk and prognostic factors in mesenteric venous thrombosis. *Br J Surg* 2008; **95**: 1245-1251 [PMID: 18720461 DOI: 10.1002/bjs.6319]

15 **Zeng Q**, Fu QN, Li FH, Wang XH, Liu H, Zhao Y. Early initiation of argatroban therapy in the management of acute superior mesenteric venous thrombosis. *Exp Ther Med* 2017;

13: 1526-1534 [PMID: 28413504 DOI: 10.3892/etm.2017.4103]
16 **Yang S**, Zhang L, Liu K, Fan X, Ding W, He C, Wu X, Li J. Postoperative Catheter-Directed Thrombolysis Versus Systemic Anticoagulation for Acute Superior Mesenteric Venous Thrombosis. *Ann Vasc Surg* 2016; **35**: 88-97 [PMID: 27263813 DOI: 10.1016/j.avsg.2016.02.019]
17 **Russell CE**, Wadhera RK, Piazza G. Mesenteric venous thrombosis. *Circulation* 2015; **131**: 1599-1603 [PMID: 25940967 DOI: 10.1161/CIRCULATIONAHA.114.012871]
18 **Gertsch P**, Matthews J, Lerut J, Luder P, Blumgart LH. Acute thrombosis of the splanchnic veins. *Arch Surg* 1993; **128**: 341-345 [PMID: 8442693 DOI: 10.1001/archsurg.1993.01420150101018]
19 **Grisham A**, Lohr J, Guenther JM, Engel AM. Deciphering mesenteric venous thrombosis: imaging and treatment. *Vasc Endovascular Surg* 2005; **39**: 473-479 [PMID: 16382268 DOI: 10.1177/153857440503900603]
20 **Kumar S**, Kamath PS. Acute superior mesenteric venous thrombosis: one disease or two? *Am J Gastroenterol* 2003; **98**: 1299-1304 [PMID: 12818273 DOI: 10.1111/j.1572-0241.2003.07338.x]
21 **Higashizono K**, Yano H, Miyake O, Yamasawa K, Hashimoto M. Postoperative pneumatosis intestinalis (PI) and portal venous gas (PVG) may indicate bowel necrosis: a 52-case study. *BMC Surg* 2016; **16**: 42 [PMID: 27391125 DOI: 10.1186/s12893-016-0158-x]
22 **Leone M**, Bechis C, Baumstarck K, Ouattara A, Collange O, Augustin P, Annane D, Arbelot C, Asehnoune K, Baldési O, Bourcier S, Delapierre L, Demory D, Hengy B, Ichai C, Kipnis E, Brasdefer E, Lasocki S, Legrand M, Mimoz O, Rimmelé T, Aliane J, Bertrand PM, Bruder N, Klasen F, Friou E, Lévy B, Martinez O, Peytel E, Piton A, Richter E, Toufik K, Vogler MC, Wallet F, Boufi M, Allaouchiche B, Constantin JM, Martin C, Jaber S, Lefrant JY. Outcome of acute mesenteric ischemia in the intensive care unit: a retrospective, multicenter study of 780 cases. *Intensive Care Med* 2015; **41**: 667-676 [PMID: 25731634 DOI: 10.1007/s00134-015-3690-8]
23 **Turner JR**. Intestinal mucosal barrier function in health and disease. *Nat Rev Immunol* 2009; **9**: 799-809 [PMID: 19855405 DOI: 10.1038/nri2653]
24 **Piton G**, Belon F, Cypriani B, Regnard J, Puyraveau M, Manzon C, Navellou JC, Capellier G. Enterocyte damage in critically ill patients is associated with shock condition and 28-day mortality. *Crit Care Med* 2013; **41**: 2169-2176 [PMID: 23782971 DOI: 10.1097/CCM.0b013e31828c26b5]
25 **Sacks GD**, Dawes AJ, Ettner SL, Brook RH, Fox CR, Maggard-Gibbons M, Ko CY, Russell MM. Surgeon Perception of Risk and Benefit in the Decision to Operate. *Ann Surg* 2016; **264**: 896-903 [PMID: 27192348 DOI: 10.1097/SLA.0000000000001784]
26 **Wang Y**, Zhao R, Xia L, Cui YP, Zhou Y, Wu XT. Predictive Risk Factors of Intestinal Necrosis in Patients with Mesenteric Venous Thrombosis: Retrospective Study from a Single Center. *Can J Gastroenterol Hepatol* 2019; **2019**: 8906803 [PMID: 31205904 DOI: 10.1155/2019/8906803]
27 **Elkrief L**, Corcos O, Bruno O, Larroque B, Rautou PE, Zekrini K, Bretagnol F, Joly F, Francoz C, Bondjemah V, Cazals-Hatem D, Boudaoud L, De Raucourt E, Panis Y, Goria O, Hillaire S, Valla D, Plessier A. Type 2 diabetes mellitus as a risk factor for intestinal resection in patients with superior mesenteric vein thrombosis. *Liver Int* 2014; **34**: 1314-1321 [PMID: 24237969 DOI: 10.1111/liv.12386]

World Journal of Gastroenterology

Submit a Manuscript: https://www.f6publishing.com

World J Gastroenterol 2020 July 14; 26(26): 3814-3833

DOI: 10.3748/wjg.v26.i26.3814

ISSN 1007-9327 (print) ISSN 2219-2840 (online)

ORIGINAL ARTICLE

Retrospective Study

Expression of Notch pathway components (Numb, Itch, and Siah-1) in colorectal tumors: A clinicopathological study

Sinem Cil Gonulcu, Betul Unal, Ibrahim Cumhur Bassorgun, Mualla Ozcan, Hasan Senol Coskun, Gulsum Ozlem Elpek

ORCID number: Sinem Cil Gonulcu 0000-0001-7904-4556; Betul Unal 0000-0001-7860-1808; Ibrahim Cumhur Bassorgun 0000-0003-2440-511X; Mualla Ozcan 0000-0002-7153-9586; Hasan Senol Coskun 0000-0003-2969-7561; Gulsum Ozlem Elpek 0000-0002-1237-5454.

Author contributions: Gonulcu SC was involved in the conceptualization, data curation, funding acquisition, investigation, writing-original draft; Unal B took part in the resources, investigation, and writing review and editing; Bassorgun IC contributed to the investigation, visualization, and writing review and editing; Ozcan M was involved in the data curation, investigation and resources; Coskun HS provided clinical data and resources; Elpek GO performed the conceptualization, data curation, funding acquisition, investigation, methodology, project administration, supervision, visualization, writing review, and editing; all authors have read and approved the final manuscript.

Supported by Akdeniz University Scientific Research Foundation, Turkey, No. 2017040103020.

Institutional review board

Sinem Cil Gonulcu, Betul Unal, Ibrahim Cumhur Bassorgun, Mualla Ozcan, Gulsum Ozlem Elpek, Department of Pathology, Akdeniz University, School of Medicine, Antalya 07070, Turkey

Hasan Senol Coskun, Department of Oncology, Akdeniz University, School of Medicine, Antalya 07070, Turkey

Corresponding author: Gulsum Ozlem Elpek, MD, Professor, Department of Pathology, Akdeniz University, School of Medicine, Dumlupınar Bulvarı, Antalya 07070, Turkey. elpek@akdeniz.edu.tr

Abstract

BACKGROUND

The role of the Notch pathway in carcinogenesis and tumor progression has been demonstrated in many organs, including the colon. Accordingly, studies aimed at developing therapies targeting this pathway in various cancers require the identification of several factors that may play a role in regulating Notch-1 expression. Although Numb, Itch, and seven in absentia homolog-1 (Siah-1) have been shown to contribute to the regulation of Notch signaling, their role in colorectal carcinogenesis and tumor progression has not been fully elucidated to date.

AIM

To evaluate Numb, Itch, and Siah-1 expression in colorectal tumors to clarify their relationship with Notch-1 expression and their role in carcinogenesis and tumor behavior.

METHODS

Expression of Notch-1, Numb, Itch, and Siah-1 was investigated in 50 colorectal carcinomas, 30 adenomas, and 20 healthy colonic tissues by immunohistochemistry and quantitative real-time polymerase chain reaction (PCR) analyses.

RESULTS

In contrast to Notch-1, which is expressed at higher levels in tumor tissues and adenomas, expression of Numb, Itch, and Siah-1 was stronger and more frequent in normal mucosa ($P < 0.01$). There was a positive correlation between Notch-1

statement: The study was reviewed and approved for publication by our Institutional Reviewer.

Informed consent statement: Patients were not required to give informed consent to the study because the analysis used anonymous data that were obtained after each patient agreed to treatment by written consent.

Conflict-of-interest statement: All the authors have no conflict of interest related to the manuscript.

Data sharing statement: No additional data are available.

Manuscript source: Invited manuscript

Received: February 26, 2020
Peer-review started: February 26, 2020
First decision: March 18, 2020
Revised: May 18, 2020
Accepted: June 25, 2020
Article in press: June 25, 2020
Published online: July 14, 2020

P-Reviewer: Gassler N, Li XB
S-Editor: Gong ZM
L-Editor: A
E-Editor: Zhang YL

expression and high histological grade, the presence of lymph node metastasis, and advanced-stage tumors, whereas expression of Numb, Itch, and Siah-1 was absent or reduced in tumors with these clinicopathological parameters ($P < 0.05$). In survival analysis, expression of Notch was related to poor prognosis but that of Numb, Itch, and Siah-1 correlated with improved survival ($P < 0.05$). Multivariate analysis revealed Notch-1 expression and loss of Numb expression to be independent prognostic parameters together with lymph node metastasis ($P < 0.05$).

CONCLUSION

Our findings support the role of Notch-1 in colorectal carcinoma and indicate that loss of Numb, Itch, and Siah-1 expression is associated with carcinogenesis. Our data also suggest that these three proteins might be involved in the Notch-1 pathway during colorectal carcinoma (CRC) progression and might play an essential role in approaches targeting Notch as novel molecular therapies for CRC.

Key words: Colorectal adenomas; Colorectal cancer; Notch-1; Numb; Itch; Siah-1

Core tip: This report describes a preliminary study to investigate Numb, Itch, and Siah-1 expression in colorectal tumors and to evaluate their relationship with Notch-1 expression and their roles in oncogenesis and prognosis. Our findings confirm the role of Notch-1 in colorectal carcinoma (CRC) and emphasize that loss of Numb, Itch, and Siah-1 expression is associated with carcinogenesis. Our data also indicate that Numb, Itch, and Siah-1 might be involved in the Notch-1 signaling pathway during CRC progression. Accordingly, these three proteins might be key in possible therapies targeting Notch-1 to treat colorectal carcinoma.

Citation: Gonulcu SC, Unal B, Bassorgun IC, Ozcan M, Coskun HS, Elpek GO. Expression of Notch pathway components (Numb, Itch, and Siah-1) in colorectal tumors: A clinicopathological study. *World J Gastroenterol* 2020; 26(26): 3814-3833
URL: https://www.wjgnet.com/1007-9327/full/v26/i26/3814.htm
DOI: https://dx.doi.org/10.3748/wjg.v26.i26.3814

INTRODUCTION

Colorectal carcinoma (CRC) is one of the most common cancers worldwide and, despite significant advances in treatment, ranks third in cancer-related mortality and morbidity[1,2]. Although curative surgery is possible in some cases, the fact that one-fifth of patients have metastatic disease at the time of diagnosis and sixty percent of patients undergoing surgical resection experience recurrence and metastasis emphasizes the need to identify new strategies for the determination of CRC tumor behavior and treatment[3,4]. In this context, numerous studies have been conducted to elucidate signaling pathways that contribute to colorectal tumor development and progression and to use them as potential therapeutic targets, mainly to prevent aggressive tumor behavior and treatment resistance[5-7].

Although Notch signaling has traditionally been known for its role in determining cell fate, its identification as one of the most active pathways in cancer cells renders it a potential therapeutic target in CRC[8]. In recent years, the role of the Notch signaling pathway in gastrointestinal development and normal gut homeostasis has been thoroughly demonstrated[9]. However, differences in the findings of studies on its use in CRC as a therapeutic target exist, which necessitates an understanding of the roles of other components in the Notch pathway[10-12].

Numb is a conserved evolutionary protein that antagonizes Notch signaling activities in regulating the balance between proliferation and differentiation in development and homeostasis[13]. Ubiquitination of the membrane-bound Notch receptor Notch-1 and subsequent attenuation of its activity are the basis of this molecular mechanism, which involves the binding of Numb to the E3 ubiquitin-ligase

Itch. Numb and Itch function in concert to promote ubiquitination of the Notch receptor before activation[14]. Furthermore, the networking of Numb into E3 ubiquitin ligase-based circuitries in the regulation of Notch signaling involves other E3 ubiquitin ligases, including seven in Siah-1. Siah-1 has an inhibitory effect on Numb but a stimulatory effect on Notch-1[15]. In addition, data obtained in recent years indicate that Siah-1 may also play a role in the degradation of β-catenin[16]. Numb is expressed in many adult tissues, such as the breast, lung, testis, and salivary gland; it is detected in the villus crypt axis in the mouse intestine and participates in goblet cell transformation by inhibiting the Notch pathway in intestinal epithelial cells[17]. Numb also increases mucin secretion in intestinal cells and helps to maintain the integrity of the epithelial barrier. In recent years, there has been evidence that aggressive tumor behavior in various solid tumors is associated with loss of Numb expression[18].

Some experimental studies have suggested that loss of Numb expression is associated with tumor behavior in CRC[19,20]. Regardless, the relationship between expression of Numb and clinicopathological parameters, survival, and Notch-1 expression in patients with colorectal carcinoma remains to be investigated. Similarly, the roles of Itch and Siah-1 expression in colorectal carcinogenesis and their relationship to tumor behavior, survival, Notch-1 expression, and Numb expression in CRC have not been evaluated.

Therefore, this preliminary study was undertaken to investigate expression of Numb, Itch, and Siah-1 in colorectal tumors to clarify their relationship with Notch-1 expression and their role in carcinogenesis and tumor behavior.

MATERIALS AND METHODS

Study design

Expression of Notch-1, Numb, Itch, and Siah-1 was evaluated in 50 samples of CRC diagnosed as adenocarcinoma, not otherwise specified (NOS), in 30 adenomas (10 tubular, 10 tubulovillous and 10 villous), and in 20 healthy colonic tissues diagnosed at the Department of Pathology. The ethics committee of Akdeniz University Medical School approved the study.

Immunohistochemistry

Tissue sections from surgical specimens fixed in 40 g/L formaldehyde and embedded in paraffin were reviewed, and representative tissue blocks were selected. Slides were immunostained with anti-Notch-1 (Dilution 1/25), anti-Numb (Dilution 1/25), anti-Itch (Dilution 1/100), and anti-Siah-1 (Dilution 1/100) monoclonal antibodies (Thermo Fisher Scientific, United States) using the avidin-biotin immunoperoxidase technique.

Each sample was scored on a scale of 0-4, as follows: 0, negative; 1, positive staining in 1%-25% of tumor cells; 2, positive staining in 26%-50% of tumor cells; 3, positive staining in 51%-75% of tumor cells; and 4, positive staining in 76%-100% of tumor cells. The intensity of immunostaining was determined as follows: 0, negative staining; 1, weakly positive staining; 2, moderately positive staining; and 3, strongly positive staining. The distribution of staining was also evaluated.

Quantitative real-time PCR analysis

PCR analysis was performed using Solaris qPCR Gene Expression Assay for Human Gene Notch-1, Numb, Itch, Siah-1, and GAPDH Kits (Thermo Fisher Scientific). In particular, reverse transcription of total RNA was performed using Maxima First Strand complementary DNA (cDNA) Synthesis Kit for qPCR (Thermo Fisher Scientific). Data were analyzed by the C_T method.

RNA isolation

RNA extraction was performed according to the RNeasy formalin-fixed, paraffin-embedded (FFPE) Kit protocol (Qiagen GmbH, Hilden, Germany). Briefly, 10 μm thick sections were cut from formalin-fixed, paraffin-embedded blocks, and tumor areas were collected from the sections and transferred to a microcentrifuge tube. Deparaffinization was performed by adding 1 mL xylene and incubating for 10 min at room temperature. This step was repeated twice, after which 1 mL absolute ethanol was added. The deparaffinized tissue sections were incubated in lysis buffer containing proteinase K at 56 °C for 15 min and then 80 °C for 15 min. This step was followed by DNase treatment to eliminate all genomic DNA, including very small DNA fragments that are often present in FFPE samples. Next, ethanol was added to

provide binding conditions for RNA; lysate was applied to an RNeasy MinElute spin column, with the membrane binding total RNA. The RNA was eluted in a minimum *V* of 14 μL of RNase-free water. The *c* of the isolated RNA and the ratio of absorbance at 260 nm to 280 nm (A260/A280 ratio) were measured with a NanoDrop ND-1000 spectrophotometer (NanoDrop Technologies, Montchanin, DE, United States).

First-strand cDNA synthesis

Maxima First Strand cDNA Synthesis Kit (Thermo Fisher Scientific, Cat # K1641) was used according to the manufacturer's instructions. Five micrograms of RNA was transcribed with random primers. Briefly, 5X reaction mix, maximum enzyme mix, nuclease-free water, and template RNA were mixed and incubated for 10 min at 25°C followed by 15 min at 50°C; the reaction was terminated by heating at 85°C for 5 min. The product of the first-strand cDNA synthesis was stored at -20°C until qPCR.

qPCR

Gene expression analysis was performed using Solaris qPCR Gene Expression Assay (Thermo Fisher Scientific) for Human Gene Notch-1 (Cat # AX-007771-00-0100), Numb (Cat # AX-015902-00-100), Itch (Cat # AX-007196-00-0100), Siah-1 (Cat # AX-012598-00-0100), and GAPDH (Cat # AX-004253-00-0100). The probes were labeled with FAM-MGM dyes. Briefly, the reaction mixture consisted of 12.5 μL of the 2X Solaris qPCR Master Mix, 1.25 μL of the 20X Solaris Primer/Probe set, and PCR grade water. Five microliters of cDNA was used as a template for PCR in a final *V* of 25 μL. The master mix contains all components for real-time PCR: (1) Thermo-Start DNA polymerase, a hot-start version of Thermoprime DNA polymerase; (2) dNTPs, with dTTP replacing dUTP to maximize amplification efficiency; (3) Proprietary reaction buffer, optimized to work with Solaris primer/probe assays; and (4) ROX. The cycle conditions were set as follows: preincubation step for 15 min at 95°C for activation of the Thermo-Start DNA polymerase (1 cycle) followed by 40 cycles each of 15 s at 95°C for template denaturation and 60 s at 60°C for annealing/extension. A Rotor-Gene Q instrument was used. Expression data were normalized to GAPDH using the ΔΔCq method.

Statistical analysis

Data were analyzed by SPSS 20.0. The χ^2 test was employed to examine categorical data. Relative gene expression levels between the groups and their relationship with clinicopathological parameters were investigated by *t* test. Univariate analysis, including survival analysis, was estimated with the Kaplan-Meier method. The log-rank test was employed for comparison of survival rates. A Cox proportional hazards regression model was applied for multivariate analysis. A P value < 0.05 was considered to be significant. Spearman's correlation test was used to determine relationships between Notch-1, Numb, Itch, and Siah-1 expression.

RESULTS

As shown in Figure 1, both granular cytoplasmic and nuclear staining for Notch-1, Numb, Itch, and Siah-1 was observed; in some cases, Itch also displayed focal cytoplasmic staining. The intensity and distribution of staining did not differ between the groups. However, when considering the presence or absence of staining, Notch-1 staining occurred at a more frequent rate in CRC than in adenomas and controls, whereas the frequency of Numb, Itch, and Siah-1 staining was higher in controls and adenomas (P < 0.05) (Table 1). In terms of Notch-1, Numb, Itch, and Siah-1 expression, there was no significant difference between adenomas, healthy colon (controls), or tissues adjacent to carcinoma and adenomas (P > 0.05) (Table 1). Similarly, the distribution of Notch-1, Numb, Itch, and Siah-1 expression among adenoma subtypes did not differ (P > 0.05) (Table 1). Table 2 summarizes the correlations between immunohistochemical expression of Notch-1, Numb, Itch, and Siah-1 and clinicopathological parameters. Expression of Notch-1 was more frequently observed in tumors with poor histological grade, lymph node metastasis, and an advanced stage (P < 0.05). In contrast, Numb, Itch, and Siah-1 expression was more frequent in tumors with well-differentiated morphology, without lymph node metastasis, and at an earlier stage (P < 0.05). The survival of patients with Notch-1 expression was shorter than that among those without Notch-1 expression. Conversely, Numb, Itch, and Siah-1 expression was related to better survival (P < 0.05) (Table 2 and Figure 2).

Although the expression levels of Notch-1 were higher in colorectal carcinomas, those of Numb, Itch, and Siah-1 were higher in adenomas and healthy colonic mucosa,

Table 1 Distribution of immunohistochemical expression of Notch, Numb, Itch, and Siah-1 among the three groups, tissues adjacent to carcinoma, tissues adjacent to adenoma, and subtypes of adenomas

	Controls	Adenomas	Carcinomas	*P* value	Tissues adjacent to carcinoma[a]	Tissues adjacent to adenoma[a]	Subtypes of adenomas[a]		
							Tubular	Tubulovillous	Villous
Notch expression									
Negative (%)	15 (75)	12 (40)	18 (36)	0.02	25 (50)	16 (53)	4 (40)	5 (50)	3 (30)
Positive (%)	5 (25)	18 (60)	32 (64)		25 (50)	14 (47)	6 (60)	5 (50)	7 (70)
Numb expression									
Negative (%)	6 (30)	21 (70)	30 (60)	0.008	26 (52)	14 (47)	6 (60)	7 (70)	8 (80)
Positive (%)	14 (70)	9 (30)	20 (40)		24 (48)	16 (54)	4 (40)	3 (30)	2 (20)
Itch expression									
Negative (%)	8 (40)	24 (80)	30 (60)	0.01	27(54)	19 (63)	9 (90)	7 (70)	8 (80)
Positive (%)	12 (60)	6 (20)	20 (40)		23 (46)	11 (37)	1 (10)	3 (30)	2 (20)
Siah-1 expression									
Negative (%)	5 (25)	19 (63.3)	29 (58)	0.024	31(62)	21 (70)	7 (70)	5 (50)	7 (70)
Positive (%)	15 (75)	11 (36.7)	21 (42)		19 (38)	9 (30)	3 (30)	5 (50)	3 (30)

[a]$P < 0.05$.

consistent with the immunohistochemical findings ($P < 0.05$) (Table 3, Figure 3 and 4). The relationships between the gene expression levels of Notch-1, Numb, Itch, and Siah-1 and clinicopathological parameters are presented in Table 4, and the significant findings are illustrated in Figure 5. The level of Notch-1 gene expression was significantly higher in poorly differentiated and moderately differentiated tumors than in well-differentiated tumors ($P < 0.05$). This level was also 7-fold higher in tumors with lymph node metastases and 3-fold higher in advanced-stage tumors than in tumors without lymph node metastasis and in tumors with earlier stages, respectively ($P < 0.05$). Moreover, the mean level of Notch-1 gene expression was 8-fold higher in patients with shorter survival times than in patients who survived for more than 5 years ($P < 0.05$). Overall, the expression levels of Numb, Itch, and Siah-1 were higher in well-differentiated tumors (6-fold increase), with lymph node metastasis (8-fold increase) and at advanced stages (5-fold increase) ($P < 0.05$). The survival of patients with higher Numb, Itch, and Siah-1 expression levels was better than that of patients with a low expression level of these genes ($P < 0.05$).

Similarly, when cases were grouped according to upregulation and downregulation of gene expression, upregulation of Notch-1 was more frequently observed in poorly differentiated tumors, in tumors with lymph node metastasis and in advanced stages. However, Numb, Itch, and Siah-1 upregulation correlated with better differentiation, absence of lymph node metastasis, and earlier stages ($P < 0.05$) (Table 5). Downregulation of Notch-1 and upregulation of both Numb and Itch were associated with better prognosis ($P < 0.05$) (Table 5 and Figure 6). Spearman's test revealed that the Notch-1 expression correlated inversely with the levels of Numb (r: -0. 4, $P < 0.05$), Itch (r: -0.3, $P < 0.05$) and Siah-1 (r: -0.8, $P < 0.01$) expression.

In log-rank univariate analysis, the status of Notch-1, Numb, Itch, and Siah-1 expression and their expression levels, as well as lymph node metastasis and stage, were found to be significantly associated with survival among CRC patients (Figure 2 and Figure 6). According to Cox regression analysis, lymph node metastasis, upregulation of Notch, and downregulation of Numb were independent prognostic

Table 2 Correlations between immunohistochemical expression of Notch, Numb, Itch, and Siah-1 and clinicopathological parameters

Parameters	*n*	Notch		Numb		Itch		Siah-1	
		Negative (%)	Positive (%)	Negative (%)	Positive (%)	Negative (%)	Positive (%)	Negative (%)	Positive (%)
Age		18	32	30	20	30	20	29	21
64 ± 12.35 ≥	24	8 (44.3)	16 (66.7)	13 (54.1)	11 (45.9)	14 (58.3)	10 (41.7)	16 (66.7)	8 (33.3)
64 ± 12.35 <	26	10 (38.5)	16 (61.5)	17 (65.3)	9 (34.7)	16 (61.5)	10 (38.5)	13 (50)	13 (50)
Gender									
Female	17	6 (35.3)	11 (66.7)	10 (58.8)	7 (41.2)	10 (58.8)	7 (42.2)	7 (41.2)	10 (58.8)
Male	33	12 (36.4)	21 (63.6)	20 (60.6)	13 (39.4)	20 (60.6)	13 (39.4)	22 (66.7)	11 (33.3)
Localization									
Caecum	8	3 (37.59)	5 (62.5)	6 (75)	2 (25)	5 (62.5)	3 (37.5)	4 (50)	4 (50)
Colon	16	5 (31.3)	11 (68.7)	9 (56.3)	7 (43.7)	8 (50)	8 (50)	10 (62.5)	6 (37.5)
Sigmoid	10	4 (40)	6 (60)	7 (70)	3 (30)	7 (70)	3 (30)	5 (50)	5 (50)
Rectum	16	6 (37.5)	10 (62.5)	8 (50)	8 (50)	10 (62.5)	6 (37.5)	10(50)	6 (50)
Differentiation[a]									
WD	18	16 (88.8)	2 (11.2)	3 (16.6)	15 (83.4)	5 (27.8)	13 (72.8)	8 (44.5)	10 (55.5)
MD	15	1 (6.6)	14 (93.4)	12 (80)	3 (20)	10 (66.7)	5 (33.3)	10 (66.6)	5 (33.4)
PD	17	1 (5.8)	16 (94.2)	15 (88.2)	2 (11.8)	15 (88.2)	2 (11.8)	11 (64.8)	6 (35.2)
Invasion									
T1	7	6 (85.7)	1 (14.3)	4 (57.1)	3 (42.9)	2 (28.5)	5 (71.5)	3 (48.3)	4 (51.7)
T2	10	6 (60)	4 (40)	7 (70)	3 (30)	7 (70)	3 (30)	6 (60)	4 (40)
T3	23	4 (17.4)	19 (82.6)	12 (52.1)	11 (47.9)	15 (65.2)	8 (34.8)	14 (60.9)	9 (39.1)
T4	10	2 (20)	8 (80)	7 (70)	3 (30)	6 (60)	4 (40)	6 (60)	4 (40)
LNM[a]									
Absent	17	1 (5.3)	17 (94.7)	5 (29.4)	12 (70.6)	7 (41.1)	10 (58.9)	4 (23.6)	13 (76.4)
Present	33	17 (61.39)	21(38.7)	25 (75.8)	8 (24.2)	23 (69.6)	10 (30.4)	25 (75.8)	8 (24.2)
Lymphatic invasion									
Absent	37	17 (45.9)	20 (54.1)	22 (59.4)	15 (40.6)	23 (62.1)	14(37.9)	25 (67.6)	12 (32.4)
Present	13	1 (7.6)	12 (92.4)	8 (61.5)	5 (38.5)	7 (53.8)	6 (45.2)	4 (30.8)	9 (69.2)
Vascular invasion									
Absent	42	16 (38.1)	26 (61.9)	25 (61.9)	17(38.1)	27 (64.3)	15 (35.7)	26 (61.9)	16 (38.1)
Present	8	2 (25)	6 (75)	5 (62.5)	3 (37.5)	3 (62.5)	5 (37.5)	3 (37.5)	5 (62.5)
Perineural invasion									
Absent	31	11 (35,4)	20 (64.6)	21 (67.7)	10 (32.3)	20 (64.5)	11 (35.5)	18 (58.1)	13 (41.9)
Present	19	7 (36.8)	12 (63.2)	9 (47.4)	10 (52.6)	10 (52.6)	9 (47.4)	11 (57.9)	8 (42.1)
Stage[a]									
1 + 2	24	13 (54.1)	11 (45.9)	8 (33.4)	16 (66.6)	10 (41.6)	14 (58.4)	10 (41.7)	14 (58.3)
3 + 4	26	5 (19.2)	21 (80.8)	22 (84.6)	4 (15.4)	20 (76.9)	6 (23.1)	19 (73.1)	7 (26.9)
Distant metastasis									
Absent	26	8 (30.7)	18 (69.3)	15 (57.6)	11 (42.4)	13 (50)	13 (50)	15 (57.7)	11(42.3)
Present	24	10 (41.6)	14 (58.4)	15 (62.5)	9 (37.5)	17 (70.8)	7 (29.2)	14 (58.4)	10 (41.6)
Survival (mo)[a]									
60.62 ± 26.68 ≥	26	2 (7.6)	24 (92.4)	20 (76.9)	6 (23.1)	22 (84.6)	4 (15.4)	19 (73.1)	7 (26.9)

60.62 ± 26.68 <	24	16 (66.6)	8 (33.4)	10 (41.7)	14 (58.3)	8 (33.4)	16 (66.6)	10 (41.7)	14 (58.3)

[a]*P* < 0.05. WD: Well-differentiated; MD: Moderately differentiated; PD: Poorly differentiated; LNM: Lymph node metastasis.

Table 3 Distribution of Notch-1, Numb, Itch, and Siah-1 expression levels assessed by qPCR analysis in adenoma and carcinoma groups

Gene expression levels	Adenomas	Carcinomas	*P* value
Notch			
mean ± SD	3.1016 ± 1.0452	10.2628 ± 5.8043	0.03
Median	2.6992	1.5305	
Normal (%)	0	12 (24)	0.0001
(↑) (%)	15 (50)	22 (44)	
(↓) (%)	15 (50)	16 (32)	
Numb			
mean ± SD[1]	8.1362 ± 1.6299	2.3153 ± 2.2267	0.03
Median	4.0287	-2.2616	
Normal (%)	4 (13.3)	0	0.0001
(↑) (%)	18 (60)	24 (58)	
(↓) (%)	8 (26.7)	26 (52)	
Itch			
mean ± SD	9.2899 ± 2.7369	2.1982 ± 1.0461	0.006
Median	2.0422	1.5933	
Normal (%)	11 (36.7)	12 (32)	0.0001
(↑) (%)	15 (50)	18 (38)	
(↓) (%)	4 (13,3)	20 (30)	
Siah-1			
mean ± SD	5.9024 ± 1.18671	0.8358 ± 1.3831	0.03
median	1.4031	-2.0322	
Normal (%)	6 (20)	10 (20)	0.001
(↑) (%)	11 (36.7)	13 (26)	
(↓) (%)	13 (43.3)	27 (54)	

[1]Fold increase $2^{-\Delta\Delta Ct}$. (↑): Upregulation; (↓): Downregulation.

factors (Table 6).

DISCUSSION

In this study, Notch-1 gene and protein expression levels were higher in carcinoma and adenomas than in control tissues, and the expression differences among these three groups were significant. Our observation is not surprising, given the previous clinical and experimental data demonstrating the relationship of the Notch pathway with carcinogenesis in the colon[21,22]. In CRC, expression of Notch-1, its ligand Jagged-1 and its target genes Hes-1 and Hey-1 is significantly higher than in normal mucosa[23,24], and expression of Notch-1 and its ligands is also higher in precancerous conditions, such as inflammatory bowel diseases, than in the healthy colon[25]. In adenomas of adenomatous polyposis coli gene (APC)-mutant mice, γ-secretase inhibitors that suppress the Notch pathway promote goblet cell differentiation while

Table 4 Mean and median values of relative gene expression levels of Notch-1, Numb, Itch and Siah-1 in tumors with different clinicopathological parameters (qPCR analysis)

Parameters	*n*	Notch-1		Numb		Itch		Siah-1	
		mean ± SD[1]	Median	mean ± SD	Median	mean ± SD	Median	mean ± SD	Median
Age									
64 ± 12.35 ≥	24	11.23 ± 5.23	-1.18	1.08 ± 1.03	-1.03	1.73 ± 2.34	-1.22	0.81 ± 0.32	-1.22
64 ± 12.35 <	26	9.20 ± 4.34	1.67	3.28 ± 4.32	-2.26	3.35 ± 1.64	1.99	0.85 ± 0.42	-2.99
Gender									
Female	17	10.21 ± 6.02	1.38	1.74 ± 1.34	-2.43	1.93 ± 1.34	1.35	0.23 ± 0.03	-3.19
Male	33	10.58 ± 5.03	1.67	3.42 ± 3.42	4.67	2.70 ± 2.10	-1.21	2.00 ± 0.93	-1.22
Localization									
Caecum	8	13.10 ± 5.23	12.39	1.17 ± 1.45	1.31	1.85 ± 1.62	2.43	2.40 ± 1.11	0.41
Colon	16	7.99 ± 7.32	-1.50	2.60 ± 2.34	1.20	3.33 ± 2.03	2.30	0.26 ± 0.23	-2.56
Sigmoid	10	15.03 ± 6.23	20.79	3.69 ± 2.45	3.03	-1.03 ± 0.3	-1.75	-0.77 ± 0.22	-1.49
Rectum	16	8.37 ± 3.41	1.16	1.72 ± 1.65	-2.96	2.63 ± 1.22	1.67	1.62 ± 0.51	-3.48
Differentiation[a]									
WD	18	3.92 ± 2.45	-3.08	6.64 ± 3.46	9.92	5.26 ± 2.42	7.05	3.67 ± 1.53	-1.22
MD	15	9.85 ± 4.46	21.67	1.26 ± 1.04	-2.26	-1.20 ± 0.84	-2.41	-1.66 ± 0.66	-3.24
PD	17	17.28 ± 9.03	22.54	-3.62 ± 1.81	-4.45	-0.03 ± 0.01	-1.86	-1.91 ± 0.65	-4.21
Invasion									
T1	7	5.39 ± 5.93	-7.70	9.40 ± 4.72	14.62	10.04 ± 5.80	12.06	2.75 ± 1.36	-3.89
T2	10	10.01 ± 6.82	4.45	3.63 ± 2.45	-3.06	1.41 ± 0.56	-2.26	1.43 ± 0.92	-3.86
T3	23	11.38 ± 7.02	1.67	1.63 ± 1.85	-2.26	1.39 ± 0.8	-1.91	1.87 ± 0.23	-1.16
T4	10	11.75 ± 6.88	9.59	-2.40 ± 2.03	-3.39	-1.65 ± 0.3	-1.51	-3.51 ± 1.48	-2.94
LNM[a]									
Absent	17	2.45 ± 2.67	-4.54	8.66 ± 4.82	13.40	5.91 ± 2.20	7.84	5.77 ± 2.81	-1.16
Present	33	15.17 ± 6.89	19.90	-1.57 ± 1.24	-2.35	-1.07 ± 0.51	-1.65	-2.19 ± 1.08	-3.54
Lymphatic invasion									
Absent	37	10.84 ± 6.36	1.67	1.54 ± 3.42	-2.26	1.68 ± 0.83	1.35	0.45 ± 0.23	-3.19
Present	13	8.92 ± 5.32	1.38	4.51 ± 3.83	3.79	3.67 ± 1.43	1.38	1.90 ± 0.92	-1.35
Vascular invasion									
Absent	42	11.77 ± 8.43	1.67	1.92 ± 1.65	-2.26	1.44 ± 0.96	1.07	-0.48 ± 0.28	-3.22
Present	8	12.96 ± 7.32	-2.98	9.63 ± 5.32	13.13	6.17 ± 3.02	5.66	7.77 ± 3.82	5.50
Perineural invasion									
Absent	31	8.92 ± 5.32	-1.01	2.58 ± 2.48	-2.26	2.86 ± 1.32	2.00	1.22 ± 0.32	-3.22
Present	19	12.65 ± 6.02	17.79	1.87 ± 1.82	2.27	1.17 ± 0.61	-1.21	0.20 ± 0.80	5.50
Stage[a]									
1 + 2	24	4.45 ± 4.02	-9.81	12.85 ± 5.63	7.53	5.24 ± 2.31	6.89	1.24 ± 0.51	-1.64
3 + 4	26	15.78 ± 7.94	-8.25	9.72 ± 4.63	-2.29	-1.61 ± 0.22	-1.88	0.21 ± 0.03	-2.42
Distant metastasis									
Absent	26	9.83 ± 7.34	-1.18	3.42 ± 1.86	1.99	3.17 ± 1.24	1.77	0.99 ± 0.23	-2.45
Present	24	10.89 ± 6.53	1.67	1.11 ± 1.02	-2.86	1.14 ± 0.82	-1.15	0.66 ± 0.23	-2.02
Survival (mo)[a]									

60.62 ± 26.68 ≥	26	17.16 ± 6.04	21.22	-5.47 ± 2.24	-4.90	-2.03 ± 1.06	-2.47	-4.63 ± 2.07	-4.05
60.62 ± 26.68 <	24	2.95 ± 2.02	-5.33	10.75 ± 5.21	13.13	6.78 ± 2.83	8.51	6.76 ±	3.15

[a]$P < 0.05$.

[1]Fold increase ($2^{-\Delta\Delta Ct}$). WD: Well-differentiated; MD: Moderately differentiated; PD: Poorly differentiated; LNM: Lymph node metastasis.

reducing cell proliferation[26]. In addition, in both familial adenomatous polyposis and adenomas, upregulation of genes that function in the Notch pathway, including Notch-1, as well as the relationship between Notch-1 to Wnt-β-catenin are notable findings demonstrating the role of Notch-1 in tumor development[27,28]. Our findings, together with all these data, support the role of Notch signaling in CRC carcinogenesis.

To date, the relationship between tumor behavior and the Notch pathway in CRC has been investigated in many studies. Although Notch-1 has been shown to be associated with aggressive tumor characteristics, there are some inconsistencies among the results of these studies. In some studies, Notch-1 expression has been found to be associated with grade[29], lymph node metastasis[30], and advanced stage[31], similar to our findings; other studies have reported that Notch-1 expression is related to the presence of distant metastasis[32,33] and lymphatic and vascular invasion[34]. These different results may be explained by differences in the number of cases and in the techniques and antibodies used to detect Notch-1. In our study group, Notch-1 expression was associated with a poor prognosis: 25% of the patients with high Notch expression (32 cases) survived 5 years, but this rate was 88.8% in the group without Notch expression (18 cases). Moreover, multivariate analysis revealed Notch-1 to be an independent prognostic factor. Overall, the number of studies demonstrating that Notch-1 expression is associated with poor prognosis (although not identified as an independent prognostic factor in all of these studies) is considerably higher than those showing that it is not[35-39]. Despite the relatively small number of cases in the present study, our results support that Notch-1 expression plays a role in determining aggressive tumor behavior in CRC and a poor prognosis.

In contrast to Notch-1-related findings, Numb expression levels gradually decreased from normal tissue to carcinoma in our samples, and the difference between the groups was significant. Accumulated evidence indicates that Numb, which plays an essential role in stem cell compartment maintenance and cell fate determination, has the potential to function in the oncogenesis of many tumors[40-42]. However, Numb may have promoter function in some cancers and a suppressor function in others. For example, Numb overexpression inhibits tumor growth and the epithelial-mesenchymal transition in prostate carcinoma, esophageal squamous cell carcinoma, adenocarcinoma of the lung, and breast cancer[43,44], but it promotes cell proliferation in hepatocellular carcinoma and squamous cell carcinoma of the lung[45]. Therefore, the influence of Numb in oncogenesis might be related to the type of malignancy or the histological subtype. Although Numb has been studied during carcinogenesis in various organs due to its effect on Notch signaling, few studies have investigated variations in Numb expression during human colorectal carcinogenesis, and a vast majority of the studies investigating changes in Numb expression in colorectal tissues are experimental studies, particularly those involving carcinoma cell cultures[46,47]. In intestinal epithelial cells, Numb induces the goblet cell phenotype by inhibiting Notch[31]. In cell culture, inhibition of Numb by several microRNAs (miR-142-3p, miR-34-a, Musashi-1, and 2) induces stemness and proliferation of cancer cells. Parallel to our study, Zhao *et al*[48] reported that expression of Numb in CRC tissues was significantly lower than that in the adjacent normal intestinal mucosa, suggesting that Numb may exert a suppressor function in the development of CRC. Interestingly, these researchers also observed that splice variants of Numb might have different effects on colorectal carcinogenesis. In a study by Meng *et al*[23], Notch-1 expression was detected in patients with colon cancer, but Numb levels were decreased. To the best of our knowledge, no study has evaluated Numb expression in adenoma tissues. In our study, expression levels of Numb decreased significantly from adenomas to CRC. When all these data are evaluated together, our findings support that loss of Numb expression contributes to colorectal carcinogenesis.

The present study revealed that Numb expression is higher in well-differentiated tumors, at earlier stages, and in patients without lymph node metastases, in contrast to the findings for Notch-1. Numerous experimental studies have shown that Numb protein expression is associated with cell differentiation in both normal tissues and tumors, concluding that it is a determinant of cell fate[41-44]. Similar findings have been

Table 5 Correlations between expression levels of Notch, Numb, Itch, and Siah-1 and clinicopathological parameters in colorectal carcinoma

Levels		Notch			Numb		Itch			Siah-1		
Parameters	*n*	(-)	(↓)	(↑)	(↓)	(↑)	(-)	(↓)	(↑)	(-)	(↓)	(↑)
		12	16	22	26	24	16	19	15	10	27	13
Age												
64 ± 12.353 ≥	22	7 (31.8)	4 (18.2)	11 (50)	12 (54.5)	10 (45.5)	7 (31.8)	6 (27.3)	9 (40.9)	4 (18.2)	13 (59.1)	5 (22.7)
64 ± 12.353 <	28	5 (17.9)	12 (42 .9)	11 (39.3)	14 (50)	14 (50)	5 (17.9)	12 (42.9)	11(39.3)	6 (21.4)	14 (50)	8 (28.6)
Gender												
Female	17	3 (17.6)	5 (29.5)	9 (52.9)	17 (51.5)	16 (48.5)	6 (35.3)	7 (41.2)	4 (23.4)	3 (17.6)	10 (58.8)	4 (23.5)
Male	33	9 (27.3)	11 (33.3)	13 (39.4)	9 (52.9)	8 (47.1)	6 (18.2)	11 (33.3)	16 (48.5)	7 (21.2)	17 (51.5	9 (27.3)
Localisation												
Caecum	8	1 (12.5)	3 (37.5)	4 (50)	4 (50)	4(50)	0	3 (37.5)	5 (62.5)	2 (25)	4 (50)	2 (25)
Colon	16	3 (18.8)	3 (18.8)	10 (62.5)	9 (56.2)	7 (43.8)	5 (31.2)	5 (31.2)	6 (37.5)	3 (18.8)	9 (56.2)	4 (25)
Sigmoid	16	7 (43.8)	7 (43.8)	2 (12.5)	6 (60)	4 (40)	3 (30)	3 (30)	4 (40)	2 (12.5)	10 (62.5)	4 (25)
Rectum	10	1 (10)	3 (30)	6 (60)	7 (43.8)	9 (56.2)	4 (25)	7 (43.8)	5 (31.2)	3 (30)	4 (40)	3 (30)
Differentiation[a]												
WD MD	24 13	6 (25) 4 (30.7)	13 (54.1) 2 (15.3)	5 (20.9) 7 (54)	8 (33.3) 8 (61.5)	16 (66.7) 5 (38.5)	5 (20.8) 3 (23.1)	5 (20.8) 5 (38.5)	14 (58.3) 5 (38.5)	7 (29.2) 2 (15.49	7 (29.2) 10 (76.9)	10 (41.7) 1 (7.7)
PD	13	2 (15.4)	1 (7.7)	10 (76.9)	10 (76.9)	3 (23.1)	4 (30.8)	8 (61.5)	1 (7.7)	1 (7.7)	10 (76.9)	2 (15.4)
Invasion												
T1	7	1 (14.3)	1 (14.3)	5 (71.4)	1 (14.3)	6 (85.7)	2 (20)	0	5 (71.4)	2 (28.6)	3 (42.9)	2 (28.6)
T2	10	3 (30)	3 (30)	4 (40)	6 (60)	4 (40)	2 (20)	(30)	5 (50)	1 (10)	5 (50)	4 (40)
T3	23	6 (26.1)	7 (30.4)	10 (43.5)	15 (65.2)	8 (34.8)	5 (21.7)	11 (47.8)	7 (30.4)	5 (21.7)	5 (50)	4 (17.4)
T4	10	2 (20)	5 (50)	3 (30)	4 (40)	6 (60)	24 (30)	18 (36)	20 (40)	2 (20)	5 (50)	3 (30)
LNM[a]												
Absent	19	3 (15.8)	13 (68.4)	3 (15.8)	6 (31.6)	13 (68.4)	5 (26.3)	2 (10.5)	12 (63.2)	6 (31.6)	5 (26.3)	8 (42.1)
Present	31	9 (29)	3 (9.7)	19 (61.3)	20 (64.5)	11 (35.5)	7 (22.6)	16 (88.9)	8 (25.8)	4 (12.9)	22 (71)	5 (16.1)
Lymphatic invasion												
Absent	37	11(29.7)	13 (35.1)	13 (35.1)	20 (54.1)	17 (45.9)	7(18.9)	13 (35.1)	17 (45.9)	7 (18.9)	24 (64.9)	6 (16.2)

Present	13	1 (7.7)	3 (23.1)	9 (69.2)	6 (46.2)	7 (53.8)	5 (38.5)	5 (38.5)	3 (23.1)	3 (23.1)	3 (23.1)	7 (53.8)
Vascular invasion												
Absent	42	12(28.6)	14(33.3)	16 (38.1)	23 (54.8)	19 (45.2)	8 (19)	16 (38.1)	18 (42.9)	8 (19)	25 (59.5)	9 (21.4)
Present	8	0	2 (25)	6 (75)	3 (37.5)	5 (62.5)	4 (50)	2 (25)	2 (25)	2 (25)	2 (25)	4 (50)
Perineural invasion												
Absent present	31	6 (19.4)	12 (38.7)	13 (41.9)	15 (48.4)	16 (51.6)	8 (25.8)	10 (32.3)	13 (41.9)	5 (16.1)	17 (54.8)	9 (29)
	19	6 (31.6)	4 (21.1)	9 (47.4)	11 (57.9)	8 (42.1)	4 (21.1)	8 (42.1)	7 (36.8)	5 (26.3)	10 (52.6)	4 (21.1)
Stage[a]												
1 + 2	24	8 (33.3)	15 (62.5)	9(4.2)	7 (29.2)	17 (70.8)	5 (20.8)	4 (16.7)	15 (62.5)	7 (29.2)	9 (37.5)	8 (33.3)
3 + 4	26	4 (15.4)	1(11.6)	19(73)	19 (73.1)	7 (26.9)	7 (26.9)	14 (53.8)	5 (19.1)	3 (11.5)	18 (69.2)	5 (19.2)
Distant metastasis												
Absent	26	7 (26.9)	8 (30.8)	11 (42.3)	11 (42.3)	15 (57.7)	7 (26.9)	7 (26.9)	12 (46.2)	4 (15.4)	16 (61.5)	6 (23.1)
Present	24	12(20.8)	8 (33.3)	11 (45.8)	15 (62.5)	9 (37.5)	5 (20.8)	11 (45.8)	8 (33.3)	6 (25)	11 (45.8)	7 (39.2)
Survival (mo)[a]												
60.62 ± 26.68 ≥	26	11 (42.3)	0	15 (57.7)	22 (84.6)	4 (15.4)	7 (26.9)	15 (57.6)	4 (42.4)	4 (15.5)	21 (80.7)	1 (3.8)
60.62 ± 26.68 <	24	1 (4.2)	16 (66.6)	7 (29.2)	4 (16.7)	20 (83.3)	5 (20.8)	3 (12.5)	16 (87.5)	6 (25)	6 (25)	12 (50)

[a]$P < 0.05$. Downregulation of Notch and upregulation of Numb, Itch, and Siah-1 are associated with better prognosis. (↑): Upregulation, (↓): Downregulation; WD: Well-differentiated; MD: Moderately differentiated; PD: Poorly differentiated; LNM: Lymph node metastasis.

obtained in experimental studies involving CRC cell culture. Indeed, many microRNAs that induce stemness and aggressive behavior in CRC stem cells stabilize β-catenin through Numb repression[46,47]. A recent study demonstrated that low Numb serum levels are associated with cetuximab resistance and worse prognosis in patients with CRC, suggesting that Numb is a contributor to the prevention of tumor aggression[49]. In another, Numb expression was investigated in patients with CRC[48], and similar to our data, Numb expression was found to be reduced in patients with lymph node metastasis, deeper invasive tumors, and at a more advanced stage, though the difference was not significant.

Nonetheless, our study revealed a significant inverse correlation between these parameters and Numb expression. Although our results need to be supported by further studies in larger patient series, the results show that Numb plays a role in preventing aggressive tumor behavior in CRC. To the best of our knowledge, the relationship between Numb expression and survival in CRC has not been investigated

Table 6 Independent prognostic factors according to Cox regression analysis

Parameter	Regression coefficient	*P* value	Relative risk
LN metastasis	2.406	0.001	11.088
Notch expression levels	1.579	0.03	3.677
Numb expression levels	-1.166	0.01	0.561

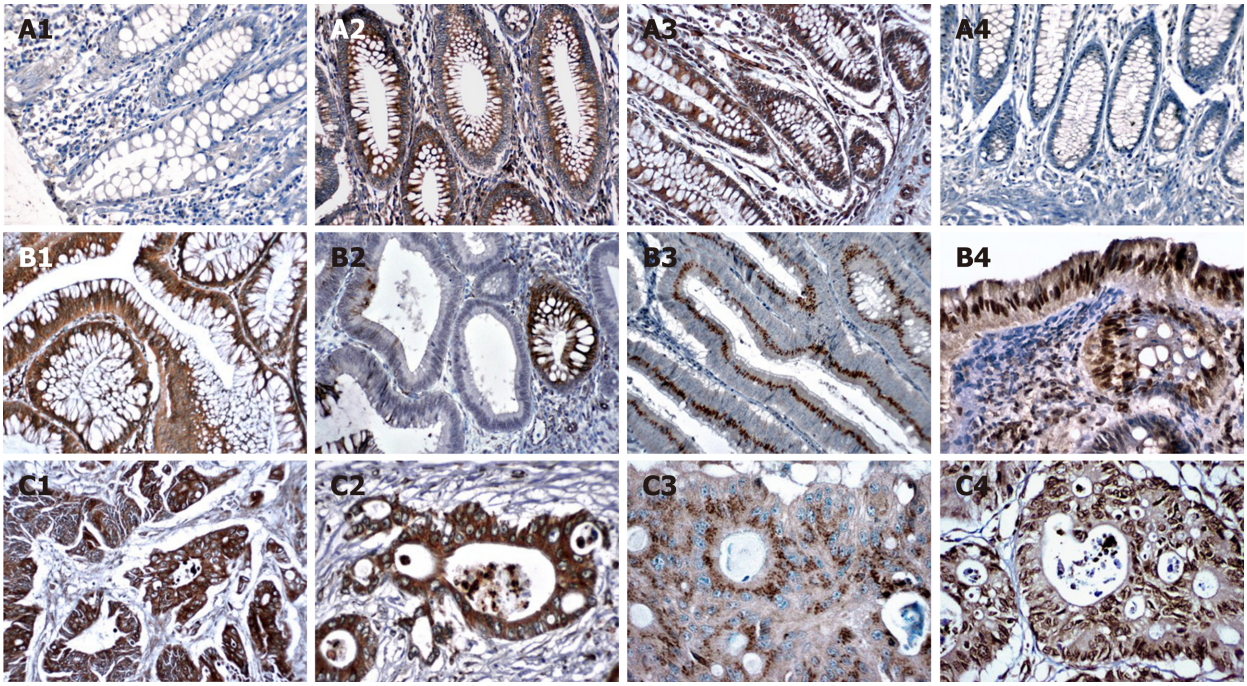

Figure 1 Notch (A1, B1 and C1), Numb (A2, B2 and C2), Itch (A3, B3 and C3), and Siah-1(A4, B4 and C4) immunohistochemical expression in the three groups. Expression of Notch is higher in CRCs (C1-4), and that of Numb Itch and Siah-1 is higher in adenomas (B1-4) and controls (A1-4).

to date. Our results indicate that loss of Numb expression is an independent prognostic factor and predictor of poor prognosis in CRC.

In our study, Itch gene expression was normal in all healthy colon mucosa samples. In adenomas, Itch levels were decreased, paralleling *Numb* gene expression, and we observed an inverse correlation between Itch and Notch-1 gene expression. The frequency of cases with low Itch gene expression was higher in the adenocarcinoma group, and our immunohistochemical evaluation revealed similar correlations. This finding is in line with the results of several studies in which Itch was shown to induce activity of the Numb protein, thereby acting as a suppressor of Notch-1 expression and leading to a reduction in its level[50]. Although there are few studies investigating Itch expression in the colon, in an elegant study by Kathania *et al*[51], Itch-depleted animals showed increased inflammation in the colon, increased proinflammatory cytokines, and a tendency to develop cancer associated with colitis. Interestingly, in the same study, it was noted that the effect of Itch on homeostasis in the small intestine differed, suggesting organ-specific effects in the gastrointestinal tract. In another study, Huang *et al*[52] found less frequent expression of Itch in colorectal carcinoma than in normal tissue in 45 cases, and it was concluded that Itch can suppress carcinogenesis by suppressing the Wnt-β catenin pathway. These findings, together with our findings, suggest that loss of Itch expression participates in colorectal carcinogenesis *via* the Notch-1-Numb axis.

The study presented herein revealed that similar to Numb, increases in Itch expression and upregulation are associated with better characteristics of tumor behavior and better survival in CRC. Recent studies investigating the role of Itch in tumors of different organs have reported different results[53-55]. For instance, some investigators have observed that Itch has a role in treatment resistance and poor prognosis, and the use of Itch inhibitors due to its interaction with p63 and p73,

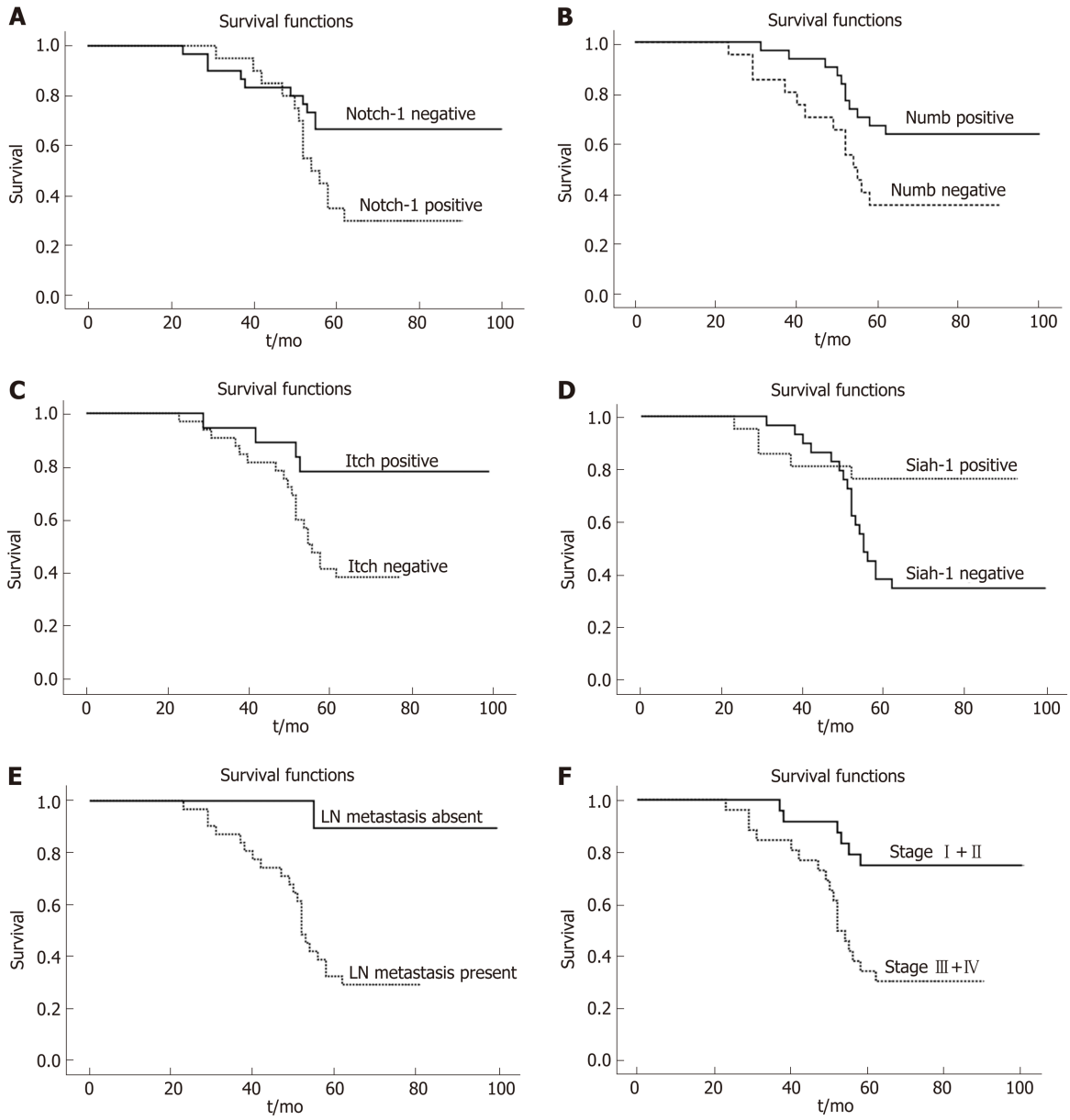

Figure 2 Survival of patients according to Notch (A), Numb (B), Itch (C), and Siah-1 (D) immunohistochemical expression, lymph node metastasis (E), and stage (F). Survival of patients with Notch expression is shorter than that of those without Notch expression. In contrast, expression of Numb, Itch, and Siah-1 is related to better survival.

especially in tumors without functional p53, has been proposed[56,57]. Because Itch is associated with many pathways, including Notch-1 signaling, researchers have suggested that not only its inhibition but also its stimulation can be used in some cancers. Peng *et al*[58] demonstrated that lithium exerts its antitumor effect *via* Itch stimulation in pancreatic cancer. In general, neither the role of Itch as a potential treatment target nor its role in tumor behavior has been completely clarified. The effect of Itch in the colon has been investigated owing to its association with IL-17, which plays a role in colorectal inflammation and carcinogenesis[51]. Unfortunately, we could not find any studies in the literature examining the relationship between Itch expression and CRC tumor behavior and survival for a comparison with our results. Only one recent study was found, demonstrating that a decrease in circ-Itch, a circulating antitumor-acting RNA that affects the function of Itch, is associated with a poor prognosis in patients with CRC[52]. The current data suggest that loss of Itch expression is associated with a poor prognosis and aggressive tumor behavior in CRC, warranting further large-scale studies.

In our study group, Siah-1 was expressed more frequently in healthy mucosa, and similar to Numb and Itch, its gene expression was normal. However, Siah-1 expression, as detected by immunohistochemistry, and its gene expression level, as

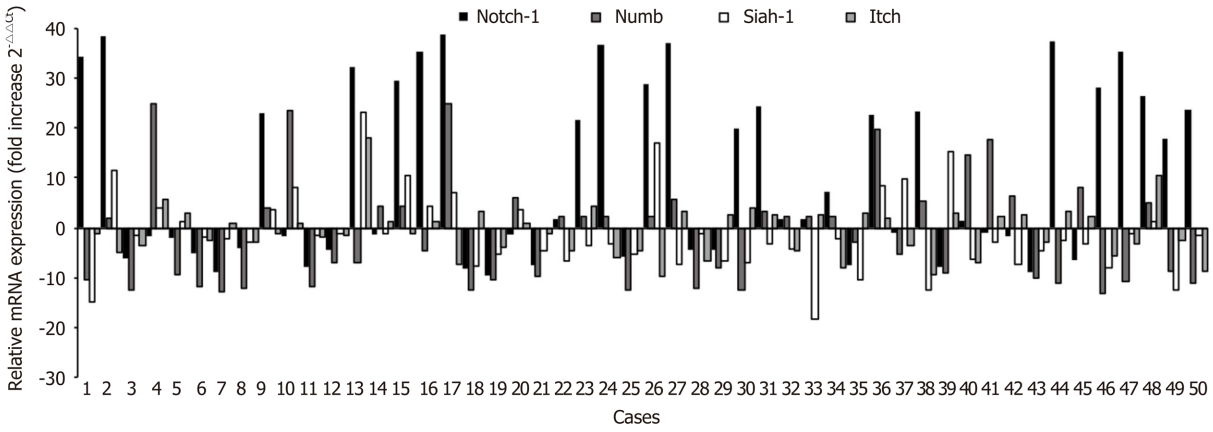

Figure 3 Relative gene expression levels of Notch, Numb, Itch, and Siah-1 in 50 patients diagnosed with colorectal carcinoma (qPCR analysis).

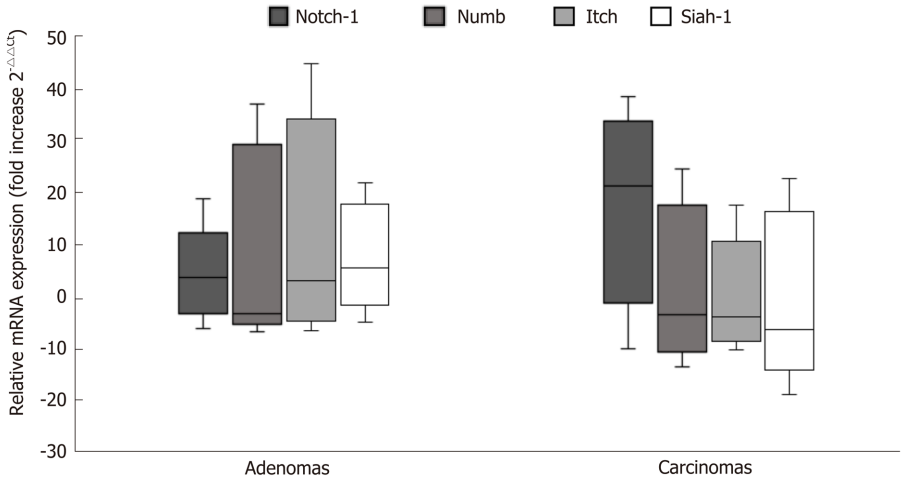

Figure 4 Levels of Notch, Numb, Itch, and Siah-1 expression in adenomas and carcinomas. Expression levels of Notch are higher in colorectal carcinoma; in contrast, expression levels of Numb, Itch, and Siah-1 are higher in adenomas (qPCR analysis).

determined by molecular methods, were decreased in adenomas compared to the control group, and this decrease was more pronounced in the adenocarcinoma group. Unfortunately, the relationship between Siah-1 and colorectal carcinogenesis and tumor behavior has not been addressed in any study to date. In a few early studies, data suggesting that Siah-1 may act as a stimulator of Notch-1 due to its ability to target Numb for degradation[19]. However, the results of subsequent studies have shown that the effect of Siah-1 is not limited to Numb and Notch and that it also plays a role in Ras and hypoxia pathways. More notably, Siah-1 plays an active role in the degradation of β-catenin, which is constitutively activated in the development of most CRC (90%)[59]. Siah-1 interacts with the carboxyl terminus of APC, recruiting the ubiquitination complex and promoting the degradation of β-catenin in the E3 ubiquitin ligase complex. Although further studies should be carried out to test this hypothesis, in light of all these data, our results suggest that Siah-1 is involved in Notch-1 suppression, rather than its stimulation, in colorectal carcinogenesis.

Among our cases, loss of and downregulation of Siah-1 expression were associated with aggressive tumor behavior and poor prognosis, similar to Numb and Itch and in contrast to Notch-1 expression. At present, data on the potential use of Siah-1 as a prognostic marker and as a therapeutic target vary depending on the organ and even according to different histological types of tumors of the same organ[60,61]. However, in addition to its relationship with Notch-1, numerous studies have shown that Siah-1 is involved in β-catenin degradation, which supports evidence that Siah-1 has a tumor-suppressor role. Indeed, an experimental study in CRC demonstrated that Siah-1 interacts with the APC gene and degrades β-catenin[62]. Regardless, to the best of our

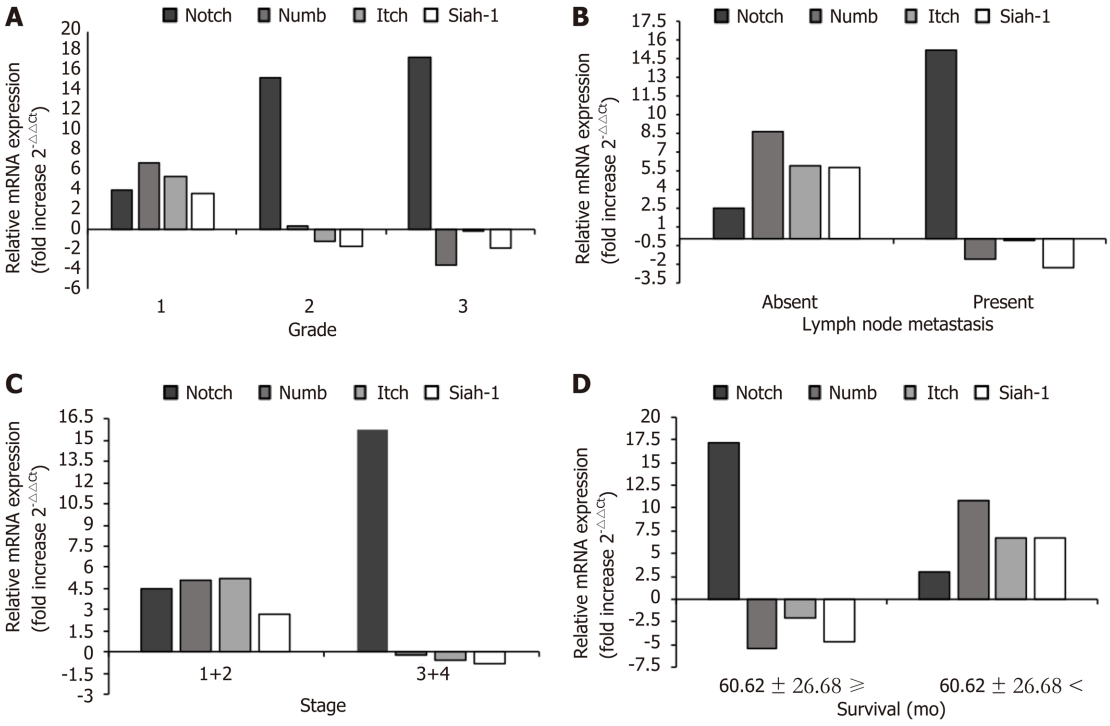

Figure 5 Distribution of relative gene expression levels of Notch, Numb, Itch, and Siah-1 according to grade (A), lymph node metastasis (B), stage (C) and survival (D) in colorectal carcinoma (qPCR analysis).

knowledge, no study has investigated the relationship between Siah-1 expression and the clinicopathological parameters of and survival in CRC patients. Our results suggest that Siah-1 expression plays an important role in the negative regulation of CRC progression, and our data are not consistent with the findings that Siah-1 induces Notch-1 by inhibiting Numb. In contrast to the negative correlation of Siah-1 with Notch-1, its positive association with Numb and Itch indicates that in CRC, its effect is not limited to Notch-1 induction and also involves other pathways.

In conclusion, this preliminary study indicates that overexpression of Notch-1, as well as loss of Numb, Itch, and Siah-1 expression, contributes to colorectal carcinogenesis. In patients with CRC, Notch-1 expression is associated with aggressive tumor behavior and is an independent adverse prognostic marker. In our study group, decreased Numb expression supports the findings that loss of Numb expression in CRC is a determinant of aggressive tumor behavior, indicating that it is an independent prognostic parameter. Similar to Numb, reductions in Itch and Siah-1 expression are associated with aggressive tumor behavior and prognosis in CRC. Positive relationships between Numb, Itch, and Siah-1 and their inverse correlation with Notch-1 expression indicate that these proteins are involved in the Notch pathway during CRC progression. Finally, Numb, Itch, and Siah-1 may be useful in determining the progression of CRC and are also potential new therapeutic targets. However, our results should be supported by further studies involving large numbers of cases. Another essential factor to be considered is that this study was conducted only using samples from patients diagnosed with adenocarcinoma, NOS. Therefore, the relationship between Notch-1, Numb, Itch, and Siah-1 expression and their impacts on carcinogenesis and tumor behavior should be investigated in other histological subtypes of CRC as well as their precursors, particularly in subtypes with a more aggressive course, such as serrated carcinoma.

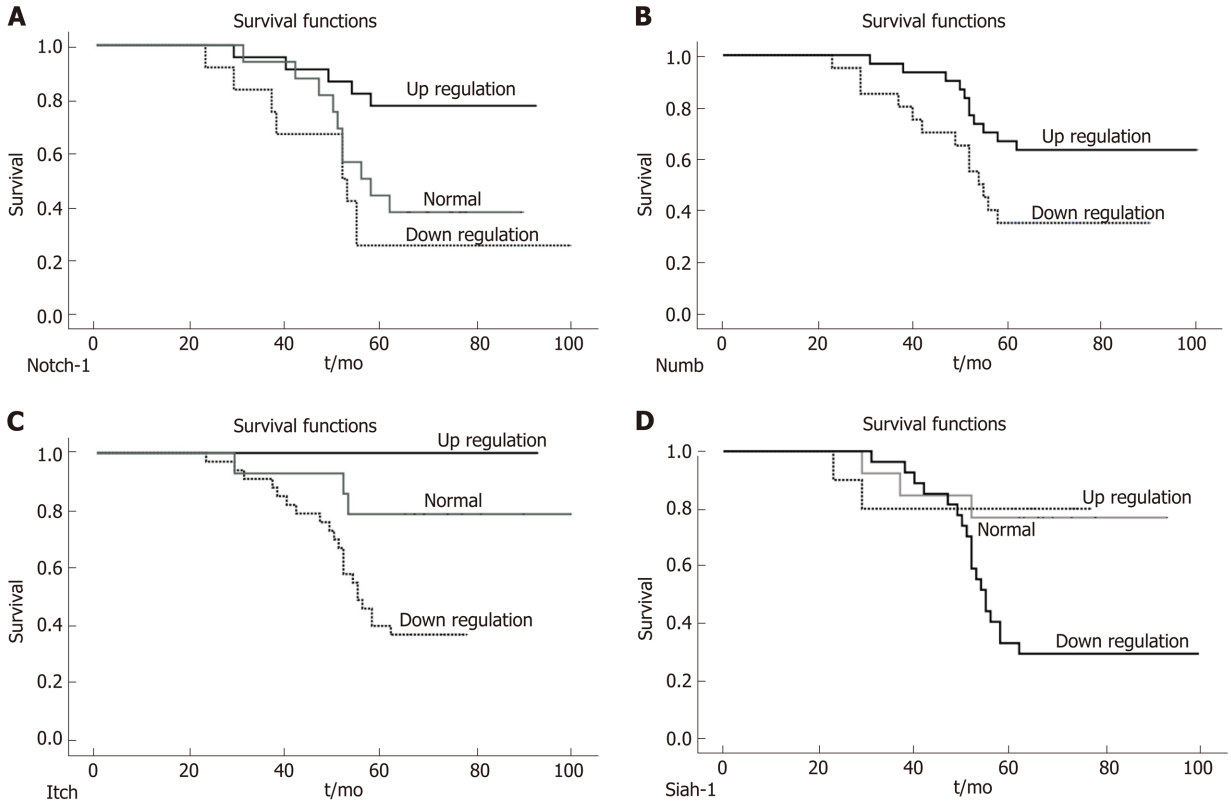

Figure 6 Survival of patients according to expression levels of Notch (A), Numb (B), Itch (C), and Siah-1 (D). Survival of patients with Notch upregulation is shorter than that of patients without Notch upregulation. Conversely, upregulation of Numb, Itch, and Siah-1 is related to better survival.

ARTICLE HIGHLIGHTS

Research background

The advances in immunohistochemical and molecular techniques in recent years, many studies have been carried out, aiming to determine new targets that can be useful in the treatment as well as predicting colorectal carcinoma (CRC) behavior. In this context, the role of Notch-1 in oncogenesis, tumor behavior, and survival have been investigated in recent studies with different results.

Research motivation

The contribution of Numb, Itch and Siah-1 in the Notch pathway is documented. On the other hand, the roles of Numb, Itch and Siah-1 expression in colorectal carcinogenesis and their relationship to tumor behavior, survival, Notch-1 expression have not been evaluated.

Research objectives

In this preliminary study, we aimed to evaluate the expression of Numb, Itch, and Siah-1 in colorectal tumors to clarify their relationship with Notch-1 expression and their role in carcinogenesis and tumor behavior.

Research methods

We retrospectively investigated the expression of Notch, Numb, Itch and Siah-1 in 50 colorectal adenocarcinomas, 30 adenomas, and 10 healthy colon tissue by immunohistochemistry and quantitative real-time PCR analysis. Data were analyzed by the χ^2 test, *t*-test and Spearman's correlation test. Survival probability curves were calculated using the Kaplan-Meier method. A Cox proportional hazards regression model was applied for multivariate analysis. A P value < 0.05 was considered to be significant.

Research results

Notch-1 staining was more frequent in CRC than in adenomas and controls. However, the frequency of Numb, Itch, and Siah-1 staining was higher in controls and adenomas. While the expression of Notch-1 was more frequently observed in tumors with poor histological grade, lymph node metastasis, and an advanced stage, the expression of Numb, Itch, and Siah-1 was more frequent in tumors with well-differentiated morphology, without lymph node metastasis, and at an earlier stage. Although the survival of patients with Notch-1 expression was shorter than that among those without Notch-1 expression, Numb, Itch, and Siah-1 expression was related to better survival. Similarly, it was noted that the gene expression levels of Notch, Numb, Itch and Siah-1 were in line with the results of the immunohistochemical evaluation. The status of Notch-1, Numb, Itch, and Siah-1 expression and their expression levels, as well as lymph node metastasis and stage, were found to be significantly associated with survival. Cox regression analysis revealed that lymph node metastasis, upregulation of Notch, and downregulation of Numb were independent prognostic factors. The Notch-1 expression correlated inversely with the levels of Numb, Itch and Siah-1 expression.

Research conclusions

Our findings support the role of Notch-1 in CRC and indicate that loss of Numb, Itch, and Siah-1 expression is associated with carcinogenesis. Our data also highlight that Numb, Itch, and Siah-1 might contribute to the Notch-1 signaling pathway during CRC progression. Therefore, these three proteins might be key in possible therapies targeting Notch-1 in the treatment of CRC.

Research perspectives

In CRC, Numb, Itch and Siah-1 contribute to carcinogenesis and tumor behavior. In contrast to Notch-1, the relationship of Numb, Itch and Siah-1 expression with better prognostic parameters and improved survival can make them a potential therapeutic target. In this regard, further studies in large patient series and cell cultures can provide comprehensive information on the efficacy of the Notch pathway in therapy.

REFERENCES

1 **Siegel RL**, Miller KD, Jemal A. Cancer statistics, 2019. *CA Cancer J Clin* 2019; **69**: 7-34 [PMID: 30620402 DOI: 10.3322/caac.21551]

2 **Siegel R**, Naishadham D, Jemal A. Cancer statistics, 2012. *CA Cancer J Clin* 2012; **62**: 10-29 [PMID: 22237781 DOI: 10.3322/caac.20138]

3 **Van Cutsem E**, Nordlinger B, Adam R, Köhne CH, Pozzo C, Poston G, Ychou M, Rougier P; European Colorectal Metastases Treatment Group. Towards a pan-European consensus on the treatment of patients with colorectal liver metastases. *Eur J Cancer* 2006; **42**: 2212-2221 [PMID: 16904315 DOI: 10.1016/j.ejca.2006.04.012]

4 **Davies RJ**, Miller R, Coleman N. Colorectal cancer screening: prospects for molecular stool analysis. *Nat Rev Cancer* 2005; **5**: 199-209 [PMID: 15738983 DOI: 10.1038/nrc1569]

5 **Heinemann V**, von Weikersthal LF, Decker T, Kiani A, Vehling-Kaiser U, Al-Batran SE, Heintges T, Lerchenmüller C, Kahl C, Seipelt G, Kullmann F, Stauch M, Scheithauer W, Hielscher J, Scholz M, Müller S, Link H, Niederle N, Rost A, Höffkes HG, Moehler M, Lindig RU, Modest DP, Rossius L, Kirchner T, Jung A, Stintzing S. FOLFIRI plus cetuximab versus FOLFIRI plus bevacizumab as first-line treatment for patients with metastatic colorectal cancer (FIRE-3): a randomised, open-label, phase 3 trial. *Lancet Oncol* 2014; **15**: 1065-1075 [PMID: 25088940 DOI: 10.1016/S1470-2045(14)70330-4]

6 **Spartalis C**, Schmidt EM, Elmasry M, Schulz GB, Kirchner T, Horst D. In vivo effects of chemotherapy on oncogenic pathways in colorectal cancer. *Cancer Sci* 2019; **110**: 2529-2539 [PMID: 31119819 DOI: 10.1111/cas.14077]

7 **Pandurangan AK**, Ismail S, Esa NM, Munusamy MA. Inositol-6 phosphate inhibits the mTOR pathway and induces autophagy-mediated death in HT-29 colon cancer cells. *Arch Med Sci* 2018; **14**: 1281-1288 [PMID: 30393482 DOI: 10.5114/aoms.2018.76935]

8 **Venkatesh V**, Nataraj R, Thangaraj GS, Karthikeyan M, Gnanasekaran A, Kaginelli SB, Kuppanna G, Kallappa CG, Basalingappa KM. Targeting Notch signalling pathway of cancer stem cells. *Stem Cell Investig* 2018; **5**: 5 [PMID: 29682512 DOI: 10.21037/sci.2018.02.02]

9 **Miyamoto S**, Rosenberg DW. Role of Notch signaling in colon homeostasis and carcinogenesis. *Cancer Sci* 2011; **102**: 1938-1942 [PMID: 21801279 DOI: 10.1111/j.1349-7006.2011.02049.x]

10 **Miyamoto S**, Nakanishi M, Rosenberg DW. Suppression of colon carcinogenesis by targeting Notch signaling. *Carcinogenesis* 2013; **34**: 2415-2423 [PMID: 23729655 DOI: 10.1093/carcin/bgt191]

11 **Suman S**, Das TP, Ankem MK, Damodaran C. Targeting Notch Signaling in Colorectal Cancer. *Curr Colorectal Cancer Rep* 2014; **10**: 411-416 [PMID: 25395896 DOI: 10.1007/s11888-014-0252-3]

12 **Mirone G**, Perna S, Shukla A, Marfe G. Involvement of Notch-1 in Resistance to Regorafenib in Colon Cancer Cells. *J Cell Physiol* 2016; **231**: 1097-1105 [PMID: 26419617 DOI: 10.1002/jcp.25206]

13 **Yang Y**, Zhu R, Bai J, Zhang X, Tian Y, Li X, Peng Z, He Y, Chen L, Ji Q, Chen W, Fang D, Wang R. Numb modulates intestinal epithelial cells toward goblet cell phenotype by inhibiting the Notch signaling pathway. *Exp Cell Res* 2011; **317**: 1640-1648 [PMID: 21557937 DOI: 10.1016/j.yexcr.2011.04.008]

14 **Di Marcotullio L**, Greco A, Mazzà D, Canettieri G, Pietrosanti L, Infante P, Coni S, Moretti M, De Smaele E, Ferretti E, Screpanti I, Gulino A. Numb activates the E3 ligase Itch to control Gli1 function through a novel degradation signal. *Oncogene* 2011; **30**: 65-76 [PMID: 20818436 DOI: 10.1038/onc.2010.394]

15 **Jumpertz S**, Hennes T, Asare Y, Vervoorts J, Bernhagen J, Schütz AK. The β-catenin E3 ubiquitin ligase SIAH-1 is regulated by CSN5/JAB1 in CRC cells. *Cell Signal* 2014; **26**: 2051-2059 [PMID: 24882689 DOI: 10.1016/j.cellsig.2014.05.013]

16 **House CM**, Möller A, Bowtell DD. Siah proteins: novel drug targets in the Ras and hypoxia pathways. *Cancer Res* 2009; **69**: 8835-8838 [PMID: 19920190 DOI: 10.1158/0008-5472.CAN-09-1676]

17 **Gulino A**, Di Marcotullio L, Screpanti I. The multiple functions of Numb. *Exp Cell Res* 2010; **316**: 900-906 [PMID: 19944684 DOI: 10.1016/j.yexcr.2009.11.017]

18 **Sun J**, Wang K, Teng J, Yu Y, Hua R, Zhou H, Zhong D, Fan Y. Numb had anti-tumor effects in prostatic cancer. *Biomed Pharmacother* 2017; **92**: 108-115 [PMID: 28531799 DOI: 10.1016/j.biopha.2017.04.134]

19 **Puca F**, Colamaio M, Federico A, Gemei M, Tosti N, Bastos AU, Del Vecchio L, Pece S, Battista S, Fusco A. HMGA1 silencing restores normal stem cell characteristics in colon cancer stem cells by increasing p53 levels. *Oncotarget* 2014; **5**: 3234-3245 [PMID: 24833610 DOI: 10.18632/oncotarget.1914]

20 **Lan L**, Appelman C, Smith AR, Yu J, Larsen S, Marquez RT, Liu H, Wu X, Gao P, Roy A, Anbanandam A, Gowthaman R, Karanicolas J, De Guzman RN, Rogers S, Aubé J, Ji M, Cohen RS, Neufeld KL, Xu L. Natural product (-)-gossypol inhibits colon cancer cell growth by targeting RNA-binding protein Musashi-1. *Mol Oncol* 2015; **9**: 1406-1420 [PMID: 25933687 DOI: 10.1016/j.molonc.2015.03.014]

21 **Prasetyanti PR**, Zimberlin CD, Bots M, Vermeulen L, Melo Fde S, Medema JP. Regulation of stem cell self-renewal and differentiation by Wnt and Notch are conserved throughout the adenoma-carcinoma sequence in the colon. *Mol Cancer* 2013; **12**: 126 [PMID: 24144042 DOI: 10.1186/1476-4598-12-126]

22 **Fre S**, Pallavi SK, Huyghe M, Laé M, Janssen KP, Robine S, Artavanis-Tsakonas S, Louvard D. Notch and Wnt signals cooperatively control cell proliferation and tumorigenesis in the intestine. *Proc Natl Acad Sci U S A* 2009; **106**: 6309-6314 [PMID: 19251639 DOI: 10.1073/pnas.0900427106]

23 **Meng RD**, Shelton CC, Li YM, Qin LX, Notterman D, Paty PB, Schwartz GK. gamma-Secretase inhibitors abrogate oxaliplatin-induced activation of the Notch-1 signaling pathway in colon cancer cells resulting in enhanced chemosensitivity. *Cancer Res* 2009; **69**: 573-582 [PMID: 19147571 DOI: 10.1158/0008-5472.CAN-08-2088]

24 **Gopalakrishnan N**, Saravanakumar M, Madankumar P, Thiyagu M, Devaraj H. Colocalization of β-catenin with Notch intracellular domain in colon cancer: a possible role of Notch1 signaling in activation of CyclinD1-mediated cell proliferation. *Mol Cell Biochem* 2014; **396**: 281-293 [PMID: 25073953 DOI: 10.1007/s11010-014-2163-7]

25 **Gao J**, Liu J, Fan D, Xu H, Xiong Y, Wang Y, Xu W, Wang Y, Cheng Y, Zheng G. Up-regulated expression of Notch1 and Jagged1 in human colon adenocarcinoma. *Pathol Biol (Paris)* 2011; **59**: 298-302 [PMID: 21145176 DOI: 10.1016/j.patbio.2010.11.001]

26 **Qiao L**, Wong BC. Role of Notch signaling in colorectal cancer. *Carcinogenesis* 2009; **30**: 1979-1986 [PMID: 19793799 DOI: 10.1093/carcin/bgp236]

27 **Koch U**, Radtke F. Notch and cancer: a double-edged sword. *Cell Mol Life Sci* 2007; **64**: 2746-2762 [PMID: 17687513 DOI: 10.1007/s00018-007-7164-1]

28 **van Es JH**, van Gijn ME, Riccio O, van den Born M, Vooijs M, Begthel H, Cozijnsen M, Robine S, Winton DJ, Radtke F, Clevers H. Notch/gamma-secretase inhibition turns proliferative cells in intestinal crypts and adenomas into goblet cells. *Nature* 2005; **435**: 959-963 [PMID: 15959515 DOI: 10.1038/nature03659]

29 **Chu D**, Wang W, Xie H, Li Y, Dong G, Xu C, Chen D, Zheng J, Li M, Lu Z, Ji G. Notch1 expression in colorectal carcinoma determines tumor differentiation status. *J Gastrointest Surg* 2009; **13**: 253-260 [PMID: 18777195 DOI: 10.1007/s11605-008-0689-2]

30 **Zhang Y**, Li B, Ji ZZ, Zheng PS. Notch1 regulates the growth of human colon cancers. *Cancer* 2010; **116**: 5207-5218 [PMID: 20665495 DOI: 10.1002/cncr.25449]

31 **Candy PA**, Phillips MR, Redfern AD, Colley SM, Davidson JA, Stuart LM, Wood BA, Zeps N, Leedman PJ. Notch-induced transcription factors are predictive of survival and 5-fluorouracil response in colorectal cancer patients. *Br J Cancer* 2013; **109**: 1023-1030 [PMID: 23900217 DOI: 10.1038/bjc.2013.431]

32 **Schmidt EM**, Lamprecht S, Blaj C, Schaaf C, Krebs S, Blum H, Hermeking H, Jung A, Kirchner T, Horst D. Targeting tumor cell plasticity by combined inhibition of NOTCH and MAPK signaling in colon cancer. *J Exp Med* 2018; **215**: 1693-1708 [PMID: 29769248 DOI: 10.1084/jem.20171455]

33 **Yuan R**, Ke J, Sun L, He Z, Zou Y, He X, Chen Y, Wu X, Cai Z, Wang L, Wang J, Fan X, Wu X, Lan P. HES1 promotes metastasis and predicts poor survival in patients with colorectal cancer. *Clin Exp Metastasis* 2015; **32**: 169-179 [PMID: 25636905]

34 **Sugiyama M**, Oki E, Nakaji Y, Tsutsumi S, Ono N, Nakanishi R, Sugiyama M, Nakashima Y, Sonoda H, Ohgaki K, Yamashita N, Saeki H, Okano S, Kitao H, Morita M, Oda Y, Maehara Y. High expression of the Notch ligand Jagged-1 is associated with poor prognosis after surgery for colorectal cancer. *Cancer Sci* 2016; **107**: 1705-1716 [PMID: 27589478 DOI: 10.1111/cas.13075]

35 **Reedijk M**, Odorcic S, Zhang H, Chetty R, Tennert C, Dickson BC, Lockwood G, Gallinger S, Egan SE. Activation of Notch signaling in human colon adenocarcinoma. *Int J Oncol* 2008; **33**: 1223-1229 [PMID: 19020755 DOI: 10.3892/ijo_00000112]

36 **Ozawa T**, Kazama S, Akiyoshi T, Murono K, Yoneyama S, Tanaka T, Tanaka J, Kiyomatsu T, Kawai K, Nozawa H, Kanazawa T, Yamaguchi H, Ishihara S, Sunami E, Kitayama J, Morikawa T, Fukayama M, Watanabe T. Nuclear Notch3 expression is associated with tumor recurrence in patients with stage II and III colorectal cancer. *Ann Surg Oncol* 2014; **21**: 2650-2658 [PMID: 24728738 DOI: 10.1245/s10434-014-3659-9]

37 **Fender AW**, Nutter JM, Fitzgerald TL, Bertrand FE, Sigounas G. Notch-1 promotes stemness and epithelial to mesenchymal transition in colorectal cancer. *J Cell Biochem* 2015; **116**: 2517-2527 [PMID: 25914224

DOI: 10.1002/jcb.25196]
38 **Arcaroli JJ**, Tai WM, McWilliams R, Bagby S, Blatchford PJ, Varella-Garcia M, Purkey A, Quackenbush KS, Song EK, Pitts TM, Gao D, Lieu C, McManus M, Tan AC, Zheng X, Zhang Q, Ozeck M, Olson P, Jiang ZQ, Kopetz S, Jimeno A, Keysar S, Eckhardt G, Messersmith WA. A NOTCH1 gene copy number gain is a prognostic indicator of worse survival and a predictive biomarker to a Notch1 targeting antibody in colorectal cancer. *Int J Cancer* 2016; **138**: 195-205 [PMID: 26152787 DOI: 10.1002/ijc.29676]
39 **Ishiguro H**, Okubo T, Kuwabara Y, Kimura M, Mitsui A, Sugito N, Ogawa R, Katada T, Tanaka T, Shiozaki M, Mizoguchi K, Samoto Y, Matsuo Y, Takahashi H, Takiguchi S. NOTCH1 activates the Wnt/β-catenin signaling pathway in colon cancer. *Oncotarget* 2017; **8**: 60378-60389 [PMID: 28947978 DOI: 10.18632/oncotarget.19534]
40 **Pece S**, Confalonieri S, R Romano P, Di Fiore PP. NUMB-ing down cancer by more than just a NOTCH. *Biochim Biophys Acta* 2011; **1815**: 26-43 [PMID: 20940030 DOI: 10.1016/j.bbcan.2010.10.001]
41 **Wang L**, Bu P, Shen X. Asymmetric division: An antitumor player? *Mol Cell Oncol* 2016; **3**: e1164279 [PMID: 27652318 DOI: 10.1080/23723556.2016.1164279]
42 **Pastò A**, Serafin V, Pilotto G, Lago C, Bellio C, Trusolino L, Bertotti A, Hoey T, Plateroti M, Esposito G, Pinazza M, Agostini M, Nitti D, Amadori A, Indraccolo S. NOTCH3 signaling regulates MUSASHI-1 expression in metastatic colorectal cancer cells. *Cancer Res* 2014; **74**: 2106-2118 [PMID: 24525742 DOI: 10.1158/0008-5472.CAN-13-2022]
43 **Zhang C**, Kang Y, Ma R, Chen F, Chen F, Dong X. Expression of Numb and Gli1 in malignant pleural mesothelioma and their clinical significance. *J Cancer Res Ther* 2018; **14**: 970-976 [PMID: 30197333 DOI: 10.4103/0973-1482.180614]
44 **Kikuchi H**, Sakakibara-Konishi J, Furuta M, Kikuchi E, Kikuchi J, Oizumi S, Hida Y, Kaga K, Kinoshita I, Dosaka-Akita H, Nishimura M. Numb has distinct function in lung adenocarcinoma and squamous cell carcinoma. *Oncotarget* 2018; **9**: 29379-29391 [PMID: 30034624 DOI: 10.18632/oncotarget.25585]
45 **Wu J**, Shen SL, Chen B, Nie J, Peng BG. Numb promotes cell proliferation and correlates with poor prognosis in hepatocellular carcinoma. *PLoS One* 2014; **9**: e95849 [PMID: 24770339 DOI: 10.1371/journal.pone.0095849]
46 **Li H**, Li F. Exosomes from BM-MSCs increase the population of CSCs via transfer of miR-142-3p. *Br J Cancer* 2018; **119**: 744-755 [PMID: 30220706 DOI: 10.1038/s41416-018-0254-z]
47 **Cheng WC**, Liao TT, Lin CC, Yuan LE, Lan HY, Lin HH, Teng HW, Chang HC, Lin CH, Yang CY, Huang SC, Jiang JK, Yang SH, Yang MH, Hwang WL. RAB27B-activated secretion of stem-like tumor exosomes delivers the biomarker microRNA-146a-5p, which promotes tumorigenesis and associates with an immunosuppressive tumor microenvironment in colorectal cancer. *Int J Cancer* 2019; **145**: 2209-2224 [PMID: 30980673 DOI: 10.1002/ijc.32338]
48 **Zhao YJ**, Han HZ, Liang Y, Shi CZ, Zhu QC, Yang J. Alternative splicing of VEGFA, APP and NUMB genes in colorectal cancer. *World J Gastroenterol* 2015; **21**: 6550-6560 [PMID: 26074693 DOI: 10.3748/wjg.v21.i21.6550]
49 **Hwang WL**, Jiang JK, Yang SH, Huang TS, Lan HY, Teng HW, Yang CY, Tsai YP, Lin CH, Wang HW, Yang MH. MicroRNA-146a directs the symmetric division of Snail-dominant colorectal cancer stem cells. *Nat Cell Biol* 2014; **16**: 268-280 [PMID: 24561623 DOI: 10.1038/ncb2910]
50 **Infante P**, Lospinoso Severini L, Bernardi F, Bufalieri F, Di Marcotullio L. Targeting Hedgehog Signalling through the Ubiquitylation Process: The Multiple Roles of the HECT-E3 Ligase Itch. Cells 2019; 8: pii: E98 [PMID: 0699938 DOI: 10.3390/cells8020098]
51 **Kathania M**, Khare P, Zeng M, Cantarel B, Zhang H, Ueno H, Venuprasad K. Itch inhibits IL-17-mediated colon inflammation and tumorigenesis by ROR-γt ubiquitination. *Nat Immunol* 2016; **17**: 997-1004 [PMID: 27322655 DOI: 10.1038/ni.3488]
52 **Huang G**, Zhu H, Shi Y, Wu W, Cai H, Chen X. cir-ITCH plays an inhibitory role in colorectal cancer by regulating the Wnt/β-catenin pathway. *PLoS One* 2015; **10**: e0131225 [PMID: 26110611 DOI: 10.1371/journal.pone.0131225]
53 **Hansen TM**, Rossi M, Roperch JP, Ansell K, Simpson K, Taylor D, Mathon N, Knight RA, Melino G. Itch inhibition regulates chemosensitivity in vitro. *Biochem Biophys Res Commun* 2007; **361**: 33-36 [PMID: 17640619 DOI: 10.1016/j.bbrc.2007.06.104]
54 **Li F**, Zhang L, Li W, Deng J, Zheng J, An M, Lu J, Zhou Y. Circular RNA ITCH has inhibitory effect on ESCC by suppressing the Wnt/β-catenin pathway. *Oncotarget* 2015; **6**: 6001-6013 [PMID: 25749389 DOI: 10.18632/oncotarget.3469]
55 **Luo L**, Gao Y, Sun X. Circ-ITCH correlates with small tumor size, decreased FIGO stage and prolonged overall survival, and it inhibits cells proliferation while promotes cells apoptosis in epithelial ovarian cancer. *Cancer Biomark* 2018; **23**: 505-513 [PMID: 30347599 DOI: 10.3233/CBM-181609]
56 **Bongiorno-Borbone L**, Giacobbe A, Compagnone M, Eramo A, De Maria R, Peschiaroli A, Melino G. Anti-tumoral effect of desmethylclomipramine in lung cancer stem cells. *Oncotarget* 2015; **6**: 16926-16938 [PMID: 26219257 DOI: 10.18632/oncotarget.4700]
57 **Zhou Y**, Tao F, Cheng Y, Xu F, Yao F, Feng D, Miao L, Xiao W, Ling B. Up-regulation of ITCH is associated with down-regulation of LATS1 during tumorigenesis and progression of cervical squamous cell carcinoma. *Clin Invest Med* 2014; **37**: E384-E394 [PMID: 25618271 DOI: 10.25011/cim.v37i6.22243]
58 **Peng Z**, Ji Z, Mei F, Lu M, Ou Y, Cheng X. Lithium inhibits tumorigenic potential of PDA cells through targeting hedgehog-GLI signaling pathway. *PLoS One* 2013; **8**: e61457 [PMID: 23626687 DOI: 10.1371/journal.pone.0061457]
59 **Choi H**, Gwak J, Cho M, Ryu MJ, Lee JH, Kim SK, Kim YH, Lee GW, Yun MY, Cuong NM, Shin JG, Song GY, Oh S. Murrayafoline A attenuates the Wnt/beta-catenin pathway by promoting the degradation of intracellular beta-catenin proteins. *Biochem Biophys Res Commun* 2010; **391**: 915-920 [PMID: 19962966 DOI: 10.1016/j.bbrc.2009.11.164]
60 **Van Sciver RE**, Lee MP, Lee CD, Lafever AC, Svyatova E, Kanda K, Colliver AL, Siewertsz van Reesema LL, Tang-Tan AM, Zheleva V, Bwayi MN, Bian M, Schmidt RL, Matrisian LM, Petersen GM, Tang AH. A New Strategy to Control and Eradicate "Undruggable" Oncogenic K-RAS-Driven Pancreatic Cancer: Molecular Insights and Core Principles Learned from Developmental and Evolutionary Biology. *Cancers*

(Basel) 2018; **10** [PMID: 29757973 DOI: 10.3390/cancers10050142]

61 **Qi J**, Kim H, Scortegagna M, Ronai ZA. Regulators and effectors of Siah ubiquitin ligases. *Cell Biochem Biophys* 2013; **67**: 15-24 [PMID: 23700162 DOI: 10.1007/s12013-013-9636-2]

62 **Liu J**, Stevens J, Rote CA, Yost HJ, Hu Y, Neufeld KL, White RL, Matsunami N. Siah-1 mediates a novel beta-catenin degradation pathway linking p53 to the adenomatous polyposis coli protein. *Mol Cell* 2001; **7**: 927-936 [PMID: 11389840 DOI: 10.1016/s1097-2765(01)00241-6]

World Journal of Gastroenterology

Submit a Manuscript: https://www.f6publishing.com

World J Gastroenterol 2020 July 14; 26(26): 3834-3850

DOI: 10.3748/wjg.v26.i26.3834

ISSN 1007-9327 (print) ISSN 2219-2840 (online)

ORIGINAL ARTICLE

Observational Study

Helicobacter pylori-induced inflammation masks the underlying presence of low-grade dysplasia on gastric lesions

Alba Panarese, Giovanni Galatola, Raffaele Armentano, Pedro Pimentel-Nunes, Enzo Ierardi, Maria Lucia Caruso, Francesco Pesce, Marco Vincenzo Lenti, Valeria Palmitessa, Sergio Coletta, Endrit Shahini

ORCID number: Alba Panarese 0000-0002-4909-043; Giovanni Galatola 0000-0003-2089-7911; Raffaele Armentano 0000-0003-1661-5504; Pedro Pimentel-Nunes 0000-0002-7308-3295; Enzo Ierardi 0000-0001-7275-5080; Maria Lucia Caruso 0000-0002-2235-5190; Francesco Pesce 0000-0002-2882-4226; Marco Vincenzo Lenti 0000-0002-6654-4911; Valeria Palmitessa 0000-0003-0137-2765; Sergio Coletta 0000-0003-3359-7010; Endrit Shahini 0000-0002-4909-0436.

Author contributions: Panarese A and Shahini E were the guarantor and designed the study; Panarese A, Palmitessa V, Coletta S, and Shahini E participated in the acquisition, analysis, and interpretation of the data; Panarese A and Shahini E drafted the initial manuscript; all authors revised the article critically for important intellectual content.

Institutional review board statement: The study was reviewed and approved by the Committees on Ethics of Italy State National Institute of Gastroenterology "S De Bellis".

Informed consent statement: Patients details have been removed from these case descriptions to ensure anonymity.

Alba Panarese, Endrit Shahini, Department of Gastroenterology and Digestive Endoscopy, National Institute of Gastroenterology "S De Bellis", Research Hospital, Castellana Grotte 70013, Italy

Raffaele Armentano, Maria Lucia Caruso, Sergio Coletta Department of Clinical Pathology, National Institute of Gastroenterology "S De Bellis", Research Hospital, Castellana Grotte 70013, Italy

Pedro Pimentel-Nunes, Center for Research in Health Technologies and Information Systems, Faculty of Medicine, Porto 4200072, Portugal

Pedro Pimentel-Nunes, Surgery and Physiology Department, Faculty of Medicine of the University of Porto, Porto 4200072, Portugal

Enzo Ierardi, Department of Emergency and Organ Transplantation, University of Bari, Bari 70124, Italy

Francesco Pesce, Nephrology Section, Department of Emergency and Organ Transplantation, University of Bari, Bari 70124, Italy

Marco Vincenzo Lenti, First Department of Internal Medicine, San Matteo Hospital Foundation, University of Pavia, Pavia 27100, Italy

Valeria Palmitessa, Laboratory of Microbiology and Virology, National Institute of Gastroenterology "S De Bellis", Research Hospital, Castellana Grotte 70013, Italy

Endrit Shahini, Giovanni Galatola Gastroenterology Unit, Institute for Cancer Research and Treatment, Turin 10121, Italy

Corresponding author: Alba Panarese, MD, Chief Doctor, Research Scientist, Department of Gastroenterology and Digestive Endoscopy, National Institute of Gastroenterology "S De Bellis", Research Hospital, Via Turi n. 27, Castellana Grotte 70013, Italy.
alba.panarese@irccsdebellis.it

Abstract

BACKGROUND

Helicobacter pylori (H. pylori) infection has been associated with a long-term risk of

Conflict-of-interest statement: There are no conflicts of interest to report.

Data sharing statement: No additional data are available.

STROBE statement: The authors have read the STROBE Statement-checklist of items, and the manuscript was prepared and revised according to the STROBE Statement-checklist of items.

Manuscript source: Invited manuscript

Received: March 18, 2020
Peer-review started: March 18, 2020
First decision: May 21, 2020
Revised: June 20, 2020
Accepted: June 30, 2020
Article in press: June 30, 2020
Published online: July 14, 2020

P-Reviewer: Balaban DV, Inal V, Sintusek P
S-Editor: Zhang L
L-Editor: A
E-Editor: Zhang YL

precancerous gastric conditions (PGC) even after *H. pylori* eradication.

AIM
To investigate the efficacy of High-Resolution White-Light Endoscopy with Narrow-Band Imaging in detecting PGC, before/after *H. pylori* eradication.

METHODS
We studied 85 consecutive patients with *H. pylori*-related gastritis with/without PGC before and 6 mo after proven *H. pylori* eradication. Kimura-Takemoto modified and endoscopic grading of gastric intestinal metaplasia classifications, were applied to assess the endoscopic extension of atrophy and intestinal metaplasia. The histological result was considered to be the gold standard. The Sydney System, the Operative-Link on Gastritis-Assessment, and the Operative-Link on Gastric-Intestinal Metaplasia were used for defining histological gastritis, atrophy and intestinal metaplasia, whereas dysplasia was graded according to World Health Organization classification. Serum anti-parietal cell antibody and anti-intrinsic factor were measured when autoimmune atrophic gastritis was suspected.

RESULTS
After *H. pylori* eradication histological signs of mononuclear/polymorphonuclear cell infiltration and Mucosal Associated Lymphoid Tissue-hyperplasia, disappeared or decreased in 100% and 96.5% of patients respectively, whereas the Operative-Link on Gastritis-Assessment and Operative-Link on Gastric-Intestinal Metaplasia stages did not change. Low-Grade Dysplasia prevalence was similar on random biopsies before and after *H. pylori* eradication (17.6% *vs* 10.6%, P = 0.19), but increased in patients with visible lesions (0% *vs* 22.4%, $P < 0.0001$). At a multivariate analysis, the probability for detecting dysplasia after resolution of *H. pylori*-related active inflammation was higher in patients with regression or reduction of Mucosal Associated Lymphoid Tissue hyperplasia, greater alcohol consumption, and anti-parietal cell antibody and/or anti-intrinsic factor positivity [odds ratio (OR) = 3.88, 95% confidence interval (CI): 1.31-11.49, P = 0.01; OR = 3.10, 95%CI: 1.05-9.12, P = 0.04 and OR = 5.47, 95%CI: 1.33-22.39, $P < 0.04$, respectively].

CONCLUSION
High-Resolution White-Light Endoscopy with Narrow-Band Imaging allows an accurate diagnosis of Low-Grade Dysplasia on visible lesions after regression of *H. pylori*-induced chronic gastritis. Patients with an overlap between autoimmune/*H. pylori*-induced gastritis may require more extensive gastric mapping.

Key words: Autoimmune gastritis; Dysplasia; Diagnosis; Malignancy; Gastric cancer; Symptoms; Signs

Core tip: *Helicobacter pylori* (*H. pylori*) infection is commonly responsible for precancerous gastric conditions. Heterogeneous long-term endoscopic follow-up studies (2-16 years), have shown conflicting results on the efficacy of *H. pylori* eradication in reducing the prevalence and histological progression of advanced precancerous gastric conditions. High-Resolution white-light endoscopy combined with narrow-band imaging allows for a more accurate diagnosis of gastric low-grade dysplasia when performed soon after *H. pylori* eradication. Subjects with an overlap between autoimmune and *H. pylori*-induced chronic gastritis should be considered to be at a higher risk for more severe gastric injury and they may require more extensive gastric mapping.

Citation: Panarese A, Galatola G, Armentano R, Pimentel-Nunes P, Ierardi E, Caruso ML, Pesce F, Lenti MV, Palmitessa V, Coletta S, Shahini E. *Helicobacter pylori*-induced inflammation masks the underlying presence of low-grade dysplasia on gastric lesions. *World J Gastroenterol* 2020; 26(26): 3834-3850

URL: https://www.wjgnet.com/1007-9327/full/v26/i26/3834.htm
DOI: https://dx.doi.org/10.3748/wjg.v26.i26.3834

INTRODUCTION

Helicobacter pylori (*H. pylori*) infection has been associated with premalignant gastric conditions (PGC), such as chronic atrophic gastritis and intestinal metaplasia (IM), which are strongly associated with dysplasia and Lauren intestinal-type of gastric carcinoma (GC)[1-7]. Autoimmune atrophic gastritis (AAG) is responsible for progressive mucosal atrophy (antrum-sparing) with or without IM[8]. Many studies have attributed gastric carcinogenesis to both genetic predisposition and *H. pylori*-induced gastric inflammation[9-13]. *H. pylori* strains possessing higher cytotoxicity that infect genetically predisposed subjects have been considered responsible for more severe degrees of inflammation and rapid progression to intestinal-type GC[14-20]. Nowadays, PGC detection and surveillance are considered a cost-effective strategy for the prevention of high-grade dysplasia and GC only in intermediate or high-risk populations[7]. Heterogeneous long-term endoscopic follow-up studies, with a duration of between 2-16 years, have shown conflicting results on the efficacy of *H. pylori* eradication in reducing the prevalence and histological progression of advanced PGC, and in decreasing GC incidence[3,21-25]. The current European guidelines recommend *H. pylori* eradication in high-risk subjects[7,22,26,27]. Nevertheless, even after *H. pylori* eradication, the risk for PGC may remain or even increase in patients undergoing long-term surveillance[3,22].

A high-quality upper endoscopy should include at least five non-targeted biopsies at the lesser and greater curvatures of the antrum-corpus and at the *incisura angularis* for *H. pylori* infection diagnosis and the optimal detection and staging of advanced PGC, which are randomly distributed across the stomach[7,28,29]. Additional targeted biopsies of any visible lesions are recommended, since low-grade dysplasia (LGD) and high-grade dysplasia (HGD) may appear as endoscopically evident, depressed, flat, or raised lesions[7,28,29].

The Sydney System, the Operative-Link on Gastritis-Assessment (OLGA) and the Operative-Link on Gastric-Intestinal Metaplasia (OLGIM) classifications are commonly used to evaluate the histological inflammation and activity due to mononuclear and polymorphonuclear cells infiltration, as well as atrophy and IM, whereas dysplasia is commonly graded according to the World Health Organization classification[30,31]. During white-light endoscopy (WLE), the Kimura-Takemoto modified classification has been used to assess the extension of atrophy[32]. Several studies showed that magnification chromoendoscopy (CE) and narrow-band imaging (NBI) with or without magnification performed by expert endoscopists could be more accurate than WLE alone in diagnosing PGC, although random biopsies may detect PGC otherwise undetectable by NBI targeted biopsies. Thus, a combination of both random-WLE and targeted-NBI biopsies is suggested as the most accurate[29,33-37]. More recent some investigators created and validated a simplified NBI classification, with magnification [(endoscopic grading of gastric intestinal metaplasia (EGGIM)], using reproducible NBI features (based on endoscopic mucosal and vascular patterns)[29] of the whole gastric mucosa, with an accuracy (resulting from a multicentre study) of 73%, 87% and 92%, for *H. pylori*-infection, IM and dysplasia diagnosis, respectively[37].

For patients with an indefinite diagnosis for dysplasia, or with dysplasia resulting from random biopsies without endoscopic evidence of visible lesions, the current guidelines suggest an "immediate" endoscopic reassessment with high-resolution endoscopy with NBI to exclude LGD or HGD on missed visible lesions[7]. This procedure revises what was indicated in previous guidelines[28], which advised, in such an event, a delayed endoscopic follow-up within one year after the diagnosis[7,28].

On these premises, supposing that dysplastic lesions might be missed on the background of an active *H. pylori* related gastritis, we focused on the assessment of the combined diagnostic performance of high-resolution white-light endoscopy (HR-WLE) with NBI in detecting PGC, before and 6 mo after *H. pylori* eradication (primary end-point). As a secondary aim we considered some clinical factors, autoimmune laboratory markers, and histopathological features as potential co-factors for the development of dysplastic lesions.

MATERIALS AND METHODS

Study design, patient selection and endoscopic follow-up

This is an observational, prospective study performed at the tertiary care center of the National Institute of Gastroenterology "S De Bellis" (Castellana Grotte, Bari, Italy). Our research was carried out in compliance with the Declaration of Helsinki and with routine clinical practice (Clinical Trial Gov number NCT03917836). All the procedures received local ethics committee approval (Protocol 67/18/CT, 140/18/CE). All patients gave their written informed consent to take part in the study.

From June 2017 to April 2019, we enrolled 85 consecutive subjects, from a cohort study of 156 outpatients, who underwent high-resolution gastroscopies with/without NBI using the Olympus Evis Exera III processor® and Olympus GIF-HQ190® instruments (Olympus Tokyo, Japan). Figure 1 shows the inclusion and exclusion of enrolment steps.

For patients with suspected AAG, anti-parietal cell antibody (APCA) and anti-intrinsic factor (AIF) were measured in serum using indirect immunofluorescence method and immunoenzimatic assay respectively. APCA antibodies were detected by NOVA Lite® Stomach Kit (Inova Diagnostics, San Diego, CA, United States) and AIF antibodies were detected by an automated assay using a Beckman Coulter Unicel DXI 800 (Beckman Coulter Inc., Fullerton, CA, United States).

The endoscopic procedures were performed by two expert endoscopists (more than 200 HRE-NBI per year), one of whom (AP) was present during all procedures as either operator or supervisor. The statistical review of this study was executed by an experienced biomedical statistician. Based on previously published data[38], we calculated the sample size for the analysis of the primary outcome using the function ss2x2 implemented in the package exact2x2. We examined that 48 patients (24 controls and 24 treated) would yield a power of 0.82 at a significance level of 0.05. Therefore, we aimed at enrolling at least 48 patients. The study was completed when the 85 enrolled subjects had been endoscopically reassessed with HR-WLE and NBI, and with gastric biopsy samples according to the Sydney System[28], 6 mo after *H. pylori* eradication confirmed by ^{13}C-urea breath-test (^{13}C-UBT), in order to identify the diagnostic yield of HR-WLE with NBI in detecting PGC, during this short surveillance time.

^{13}C urea breath test was performed under the following conditions: An 8-h fast, mouth washing before dosing, administration of 75 mg ^{13}C urea in a water solution, collection of breath samples in two 10-mL glass-sample containers, (at baseline and 20 min) and subjects in a sitting position. The breath samples were analyzed by gas-chromatography-mass spectrometry (GC-MS; ABCA Sercon Gateway, United Kingdom). *H. pylori* infection was considered present if the difference in ^{13}C/^{12}C between baseline value and 20-min value exceeded 40/00.

Inclusion criteria were as follows: Patients ≥ 18 years undergoing upper gastrointestinal endoscopy for *H. pylori*-related chronic symptoms (*i.e.*, recurrent abdominal pain, dyspepsia, or unexplained anemia), with positivity to ^{13}C-UBT and with a histological diagnosis of *H. pylori*-related gastritis with/without PGC.

Exclusion criteria were as follows: Past GC or gastric related surgery, impossibility to perform at least five biopsies during endoscopy, relevant comorbidities (cardiac, respiratory, chronic renal insufficiency, chronic liver disease, and psychiatric conditions), anticoagulant therapy/coagulation disorders, non-steroidal anti-inflammatory drugs and/or long-term proton pump inhibitors users, and active smoking habit. Autoimmune co-morbidities were not considered as exclusion criteria.

A history of *H. pylori* infection was investigated on the basis of medical records or a face-to-face clinical examination. During each procedure the qualified endoscopists performed the biopsies according to the study protocol to ascertain or confirm *H. pylori* presence and its related histological alterations. All visible gastric lesions were initially evaluated by HR-WLE with NBI. In detail, we performed at least five random biopsies using HR-WLE with NBI, followed by targeted biopsies on endoscopically evident lesions, suggestive of IM or dysplasia[28]. Furthermore, at least five different images were acquired during gastroscopy by a single expert observer, who was blind to the final histology, and who predicted the diagnosis of normal mucosa, atrophy, IM, or dysplasia using the EGGIM classification according to Pimentel-Nunes *et al*[29].

Histopathological characteristics

The histological result was considered as the gold standard for the diagnosis of dysplasia and IM; all gastric biopsy specimens were independently assessed by two expert gastrointestinal pathologists (MLC and RA). The Sydney System, and the

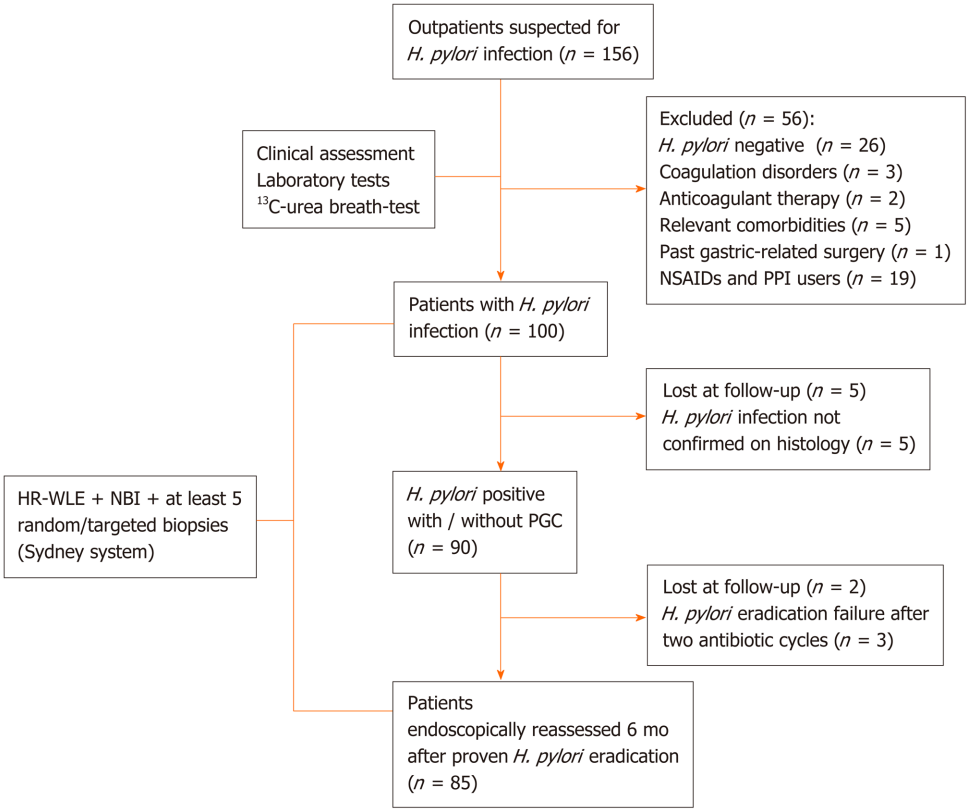

Figure 1 Flow diagram of patient's selection. *H. pylori*: *Helicobacter pylori*; NSAIDs: Non-steroidal anti-inflammatory drugs; PPI: Proton pump inhibitor; HR-WLE: High resolution-white light endoscopy; NBI: Narrow band imaging; PGC: Precancerous gastric conditions.

OLGA and OLGIM systems assessment were used for histological staging of gastritis[30,31,39]; the following diagnostic categories were considered for the evaluation of dysplasia according to the World Health Organization classification: Negative for intraepithelial neoplasia/dysplasia, indefinite for intraepithelial neoplasia/dysplasia, low-grade intraepithelial neoplasia/dysplasia, high-grade intraepithelial neoplasia/dysplasia and intra-mucosal invasive neoplasia/intra-mucosal carcinoma[39]. In all patients, *H. pylori* eradication was assessed by a prior negative result of ^{13}C-UBT and confirmed by histology.

Statistical analysis

Normal distribution of continuous variables was assessed with the Shapiro-Wilk test and data were expressed as mean and ± SD. Categorical variables were reported as percentages and compared using the χ^2 test or Fisher's exact test, when needed. The probability of detecting gastric dysplasia after *H. pylori* eradication was evaluated using univariate and multivariate logistic regression analyses. The association between each explanatory variable and the outcome (detection of dysplasia) was tested using the likelihood ratio test. For each variable included in the multivariate model, we calculated both unadjusted and adjusted odds ratios (OR), with their 95% confidence intervals (CI), and the level of significance (using the likelihood ratio test). Statistical significance was set at $P < 0.05$. All statistical analyses were performed using SPSS 23.0 software (SPSS, Chicago, IL, United States) and R version 3.4.3 (http://www.R-project.org/).

RESULTS

The clinical characteristics of the 85 enrolled patients are described in Table 1. At baseline, the majority of patients (71.8%) had an extensive endoscopic atrophic gastritis (pan-atrophy, corpus-predominant or antrum-predominant atrophy), and the minority (22.4%) had focal antrum atrophy (Table 2)[32]. The patients with a less advanced degree (0-2 and 3-4) of the EGGIM scale were 80%; histological gastritis was

Table 1 Baseline demographic and clinical characteristics of patients who underwent *Helicobacter pylori* eradication

Parameters	Patients (*n* = 85)
Age, mean (SD), yr	56.1 (12.3)
Gender, *n* (%)	
Female	53 (62.4)
BMI, mean (SD), kg/m^2	25.1 (2.2)
Alcohol users (12-24 g/dL /die), *n* (%)	27 (31.8)
Previous smokers, *n* (%)	12 (14.1)
Drug users, *n* (%)	23 (27.1)
Family history of gastric cancer, *n* (%)	4 (4.7)
Family history of other cancer, *n* (%)	9 (10.6)
Autoimmune comorbidity	
Autoimmune atrophic gastritis	12 (14.1)
Autoimmune thyroiditis	6 (7.1)
Type-1/2 diabetes mellitus	3 (3.5)
Skin psoriasis	1 (1.2)
Rheumatoid arthritis	1 (1.2)
Sjögren syndrome	1 (1.2)
A. thyroiditis + vitiligo	1 (1.2)
A. thyroiditis + Crohn's disease	1 (1.2)
A. thyroiditis + Sjögren syndrome	1 (1.2)
APCA and/or AIF antibody positivity	12 (14.1)
Endoscopy indication, *n* (%)	
Gastroesophageal reflux	17 (20)
Recurrent abdominal pain	12 (14.1)
Dyspepsia	41 (48.2)
Unexplained anemia	15 (17.7)
H. pylori eradication scheme, *n* (%)	
Quadruple[1]	53 (62.4)
Modified triple[2]	28 (32.9)
Triple[3]	3 (3.6)
Sequential[4]	1 (1.2)
H. pylori eradication cycles, *n* (%)	
One-cycle	71 (83.5)
Two-cycles	14 (16.5)

Data are expressed as number of patients and percentage (in parenthesis).

[1]Bismuth + Metronidazole + Tetracycline + Proton pump inhibitor.

[2]Amoxicillin + Levofloxacin + Proton pump inhibitor.

[3]Amoxicillin + Clarithromycin + Proton pump inhibitor.

[4]Amoxicillin + Clarithromycin + Proton pump inhibitor Amoxicillin (5 d), then Clarithromycin + Metronidazole (5 d) + Proton pump inhibitor. BMI: Body mass index; SD: Standard deviation; APCA: Anti-parietal cell antibody; AIF: Anti-intrinsic factor; *H. pylori: Helicobacter pylori*; PPI: Proton pump inhibitor.

moderate/severe and mild in 77.6% and 22.4% of the patients respectively; 45.8% of patients also had mucosal associated lymphoid tissue (MALT) hyperplasia (Table 2). Fifteen patients (17.6%) had LGD on random biopsies. Among the 49 patients with

Table 2 Endoscopic and histological characteristics of patients before and after *Helicobacter pylori* eradication

Parameters	Before *H. pylori* eradication (*n* = 85)	After *H. pylori* eradication (*n* = 85)	*P* value
Endoscopic atrophy[1],*n* (%)			
Absent	5 (5.9)	4 (4.7)	1.0
Antrum	19 (22.4)	19 (22.4)	1.0
Antrum-predominant	18 (21.2)	12 (14.1)	0.23
Corpus-predominant	21 (24.7)	23 (27.1)	0.73
Pan-atrophy	22 (25.9)	27 (31.8)	0.40
OLGA-scale, *n* (%)			
Stage 0	4 (4.7)	4 (4.7)	1.0
Stage 1	22 (25.9)	28 (32.9)	0.31
Stage 2	34 (40)	23 (27.1)	0.07
Stage 3	20 (23.5)	25 (29.4)	0.38
Stage 4	5 (5.9)	5 (5.9)	1.0
EGGIM-scale, *n* (%)			
0-2	47 (55.3)	45 (52.9)	0.76
3-4	21 (24.7)	10 (11.8)	0.03[a]
5-6	12 (14.1)	21 (24.7)	0.08
7-8	4 (4.7)	4 (4.7)	1.0
9-10	1 (1.2)	5 (5.9)	0.21
OLGIM-scale, *n* (%)			
Stage 0	40 (47.1)	29 (34.1)	0.08
Stage 1	14 (16.5)	17 (20)	0.55
Stage 2	14 (16.5)	14 (16.5)	1.0
Stage 3	13 (15.3)	18 (21.2)	0.32
Stage 4	4 (4.7)	7 (8.2)	0.53
Gastritis at histology[2],*n* (%)			
Quiescent	0	81 (95.3)	< 0.0001[b]
Mild	19 (22.4)	4 (4.7)	0.001[b]
Moderate	46 (54.1)	0	< 0.0001[b]
Severe	20 (23.5)	0	< 0.0001[b]
MALT-hyperplasia, *n* (%)			
Absent	46 (54.1)	82 (96.5)	< 0.0001[b]
Mild	25 (29.4)	3 (3.5)	< 0.0001[b]
Moderate	11 (12.9)	0	0.007[b]
Severe	3 (3.5)	0	0.24
Histological LGD[3],*n* (%)			
Absent	70 (82.4)	57 (67.1)	0.02[a]
On random biopsies	15 (17.6)	9 (10.6)	0.19
On random + on lesions biopsies	0	6 (7)	0.03[b]
Only on visible lesions	0	13 (15.3)	0.0001[b]

Data are expressed as number of patients and percentage (in parenthesis).

[1]By Kimura and Takemoto[32].

[2]By Sydney System.

[3]LGD: Low-grade dysplasia according to World Health Organization classification.

[a]By χ^2 test.

[b]by Fisher's exact test. *H. pylori*: *Helicobacter pylori*; EGGIM: Endoscopic grading of gastric intestinal metaplasia; MALT: Mucosa-associated lymphoid tissue; OLGA: Operative Link on Gastritis Assessment; OLGIM: Operative Link on Gastric Intestinal Metaplasia.

histological pan-atrophy or corpus-predominant atrophy, 11 (22.4%) tested positive for APCA and/or for AIF antibodies. In 100% of the cases the histological mononuclear and polymorphonuclear cell infiltration disappeared or decreased after *H. pylori* eradication. Additionally, the proportion of patients with mild and moderate/severe grades of MALT hyperplasia significantly decreased after *H. pylori* eradication (29.4% *vs* 3.5%, $P < 0.001$ and 16.4% *vs* 0%, $P < 0.001$, respectively; Table 2). Nevertheless, the proportion of OLGA, OLGIM stages, and that of patients with histological diagnosis of LGD on random biopsies did not significantly change after *H. pylori* eradication (17.6% *vs* 10.6%, $P = 0.19$) (Table 2 and Figure 2). The detection of LGD on visible lesions significantly increased after *H. pylori* eradication (0% *vs* 22.3%, $P < 0.001$; Table 2). Among the 9 patients who showed LGD on random biopsies after *H. pylori* eradication, only 2 (22.2%) had already had a diagnosis of LGD on random biopsies before *H. pylori* eradication. Among the 6 patients with LGD on random and visible lesion biopsies after *H. pylori* eradication, two (33.3%) were negative for LGD before eradication. Furthermore, the proportion of the 13 patients with a new diagnosis of LGD only on visible lesions was significantly higher after *H. pylori* disappearance (0% *vs* 15.3%, $P < 0.001$) and in 6 of them (46.1%) LGD was not detected before *H. pylori* eradication.

The characteristics of the 19 subjects in whom LGD was detected on visible lesions after *H. pylori* eradication are shown in Supplementary Table 1. In details, 11 subjects (57.9%) were male, and in 8 patients (42.1%) LGD was missed before *H. pylori* eradication. Five patients (26.3%) had APCA and/or AIF positivity. Comparison of the patients with or without LGD ($n = 28$ *vs* $n = 57$ respectively) after *H. pylori* eradication is shown in Table 3. In patients with LGD, the age was older (60.9 ± 8.2 *vs* 53.7 ± 13.4 years, $P = 0.01$), there were more alcohol users or past smokers (53.6% *vs* 21.1%, $P = 0.002$ and 35.7% *vs* 3.5%, $P < 0.001$, respectively), there was a higher proportion of APCA and/or AIF antibody positivity (28.6% *vs* 7%, $P = 0.02$), there were more familial cases of GC (14.3% *vs* 0%, $P < 0.001$) and more advanced stages of OLGA and OLGIM, both at the baseline and after *H. pylori* eradication ($P < 0.001$ for both). When we compared the histological characteristics of the 28 patients with LGD after *H. pylori* eradication, we observed that the moderate/severe grades of gastritis and MALT hyperplasia significantly regressed during surveillance ($P < 0.001$ and $P = 0.004$, respectively), whereas OLGA stages were similar ($P = 0.76$; Supplementary Table 2). A higher prevalence of OLGIM stages 3-4 was observed after *H. pylori* eradication, but it did not reach the level of statistical significance (57.1% *vs* 75%, $P = 0.16$).

As shown in Supplementary Table 3, in patients without LGD after *H. pylori* eradication only gastritis significantly improved at the follow-up endoscopy ($P < 0.001$). Table 4 shows the results of the linear regression analysis. According to the multivariate analysis adjusted for age, alcohol use, MALT hyperplasia regression/reduction and for APCA and/or AIF antibody presence, the probability for detecting gastric LGD, randomly or on visible lesions after eradication of *H. pylori*, was significantly higher in patients with regression/reduction of MALT hyperplasia (OR = 3.10, 95%CI: 1.05-9.12, $P = 0.04$), alcohol consumption (OR = 3.88, 95%CI: 1.31-11.49, $P = 0.01$), and APCA and/or AIF antibody positivity (OR = 5.47, 95%CI: 1.33-22.39, $P < 0.04$).

DISCUSSION

Our study shows that HR-WLE in combination with NBI can diagnose gastric LGD on visible lesions with the highest accuracy after regression of *H. pylori*-induced signs of active infection (Figure 3 and 4). This suggests that, in high-risk subjects without alarm features for malignancy, non-invasive tests should be used for prior *H. pylori* identification, and a high-quality upper endoscopy to identify dysplastic lesions should be postponed after *H. pylori* eradication has been achieved. This strategy could

Table 3 Demographic and clinical characteristics of patients with low-grade dysplasia detected on visible gastric lesions or randomly and without low-grade dysplasia, before and after *Helicobacter pylori* eradication

Parameters	With LGD (*n* = 28)	Without LGD (*n* = 57)	*P* value
Age, mean (SD), yr	60.9 (8.2)	53.7 (13.4)	0.01[a]
Gender, *n* (%)			
Female	15 (53.6)	38 (66.7)	0.24
BMI, mean (SD), kg/m^2	25 (2.4)	25 (2.3)	1.0
Alcohol users (12-24 g/dL/die), *n* (%)	15 (53.6)	12 (21.1)	0.002[b]
Previous smokers, *n* (%)	10 (35.7)	2 (3.5)	< 0.0001[c]
Family history of gastric cancer, *n* (%)	4 (14.3)	0	0.001[c]
Family history of other cancer, *n* (%)	6 (21.4)	3 (5.3)	0.001[c]
Autoimmune comorbidity			
Autoimmune atrophic gastritis	8 (28.6)	4 (7)	0.02[c]
Autoimmune thyroiditis	3 (10.7)	3 (5.3)	0.39
A. thyroiditis + vitiligo	1 (3.6)	0	0.33
A. thyroiditis + Crohn's disease	1 (3.6)	0	0.33
A. thyroiditis + Sjögren syndrome	0	1 (1.7)	1.0
Sjögren syndrome	0	1 (1.7)	1.0
Type-1/2 diabetes mellitus	1 (3.6)	2 (3.5)	1.0
Skin psoriasis	1 (3.6)	0	0.33
Rheumatoid arthritis	0	1 (1.7)	1.0
APCA and/or AIF antibody positivity	8 (28.6)	4 (7)	0.02[c]
H. pylori eradication scheme, *n* (%)			
Quadruple[1]	17 (60.7)	36 (63.2)	0.82
Modified triple[2]	9 (32.1)	19 (33.3)	0.91
Triple[3]	1 (3.6)	2 (3.5)	1.0
Sequential[4]	1 (3.6)	0	0.33
H. pylori eradication cycles, *n* (%)			
One cycle	22 (78.6)	46 (86)	0.82
Two cycles	6 (21.4)	8 (14)	0.82
OLGA scale before[5]			
Stage 0	0	4 (7)	0.3
Stage 1-2	8 (28.6)	48 (84.2)	< 0.0001[b]
Stage 3-4	20 (71.4)	5 (8.8)	< 0.0001[c]
OLGA scale after[6]			
Stage 0	0	4 (7)	0.3
Stage 1-2	7 (25)	44 (77.2)	< 0.0001[b]
Stage 3-4	21 (75)	9 (15.8)	< 0.0001[b]
OLGIM scale before			
Stage 0	0	40 (70.1)	< 0.0001[c]
Stage 1-2	12 (42.8)	16 (28.1)	0.17
Stage 3-4	16 (57.1)	1 (1.8)	< 0.0001[c]
OLGIM scale after			

Stage 0	0	29 (50.9)	< 0.0001[c]
Stage 1-2	7 (25)	24 (42.1)	0.12
Stage 3-4	21 (75)	4 (7)	< 0.0001[c]
Gastritis at histology before, *n* (%)			
Quiescent	0	0	1.0
Mild	3 (10.7)	16 (28.1)	0.10
Moderate-severe	25 (89.3)	41 (71.9)	0.10
Gastritis at histology after, *n* (%)			
Quiescent	26 (92.9)	55 (96.5)	0.59
Mild	2 (7.1)	2 (3.5)	0.50
Moderate-severe	0	0	1.0
MALT hyperplasia before, *n* (%)			
Absent	10 (35.7)	36 (63.2)	0.02[b]
Mild	10 (35.7)	15 (26.3)	0.37
Moderate	6 (21.4)	5 (8.8)	0.17
Severe	2 (7.2)	1 (1.8)	0.25
MALT hyperplasia after, *n* (%)			
Absent	10 (35.7)	36 (63.2)	0.02[b]
Mild	18 (64.3)	21 (36.8)	0.02[b]
Moderate	0	0	1.0
Severe	0	0	1.0

Data are expressed as number of patients and percentage (in parenthesis).

[1]Bismuth + Metronidazole + Tetracycline + Proton pump inhibitor.

[2]Amoxicillin + Levofloxacin + Proton pump inhibitor.

[3]Amoxicillin + Clarithromycin + Proton pump inhibitor.

[4]Amoxicillin + Clarithromycin + Proton pump inhibitor Amoxicillin (5 d), then Clarithromycin + Metronidazole (5 d) + Proton pump inhibitor.

[5]Before *Helicobacter pylori* eradication (by Sydney System).

[6]After *Helicobacter pylori* eradication.

[a]By *t*-test.

[b]By χ^2 test.

[c]By Fisher's exact test. BMI: Body mass index; SD: Standard deviation; APCA: Anti-parietal cell antibody; AIF: Anti-intrinsic factor; *H. pylori: Helicobacter pylori*; PPI: Proton pump inhibitor; OLGA: Operative Link on Gastritis Assessment; OLGIM: Operative Link on Gastric Intestinal Metaplasia; MALT: Mucosa-associated lymphoid tissue.

be useful for yielding a higher dysplasia detection rate and for better defining cancer risk and surveillance time.

Despite conflicting evidence, *H. pylori* eradication is presently advised in high-risk subjects for its potential to reduce GC incidence and induce regression of inflammation and atrophic gastritis[7,22-27,40]. Originally, the use of WLE alone provided a weak association between endoscopic and histological findings in diagnosing PGC, probably due to the inefficient technology of endoscopy imaging[41-43]; recent studies have instead shown that the use of HR-WLE allows for a high concordance accuracy for this purpose[7,36]. There is strong evidence that virtual chromoendoscopy should be used for the diagnosis of PGC because of its better performance compared to HR-WLE[34-37,44]. Capelle *et al*[33] studied high-risk patients with IM or dysplasia undergoing endoscopic surveillance 2.0 years (range 0.8–21.1) and 1.9 years (range 0.2–5.2) respectively after the initial diagnosis and showed a slightly better diagnostic yield for the detection of advanced PGC using HRE with NBI *vs* HR-WLE[33]. Conventional CE with the application of dyes has been associated with the highest PGC detection accuracy as compared to virtual chromoendoscopy although procedural time is considerably longer[45-47]. As a result of such evidence, the updated version of the European guidelines suggests that a high-quality endoscopy requires the use of NBI[7].

Table 4 Probability of detecting low-grade dysplasia randomly or on visible lesions after *Helicobacter pylori* eradication

	Univariate		Multivariate	
Variable	**OR (95% CI)**	***P* value**	**OR[1] (95%CI)**	***P* value**
Age, yr	1.05 (1.01-1.11)	< 0.02	1.05 (1.00-1.10)	0.07
Gender				
Female	1.00[2]		-	
Male	1.73 (0.69-4.37)	0.24	-	-
BMI, kg/m^2	0.93 (0.75-1.15)	0.49	-	-
Alcohol use				
No	1.00[2]		1.00[2]	
Yes	4.33 (1.63-11.51)	< 0.01	3.88 (1.31-11.49)	0.01
Drug use				
No	1.00[2]		-	
Yes	1.45 (0.54-3.94)	0.46	-	-
MALT hyperplasia regression/reduction				
No	1.00[2]		-	
Yes	3.90 (1.20-7.91)	< 0.02	3.10 (1.05-9.12)	0.04
APCA and/or AIF antibody positivity				
No	1.00[2]			
Yes	5.30 (1.44-19.56)	0.01	5.47 (1.33-22.39)	< 0.02

[1]Ajusted for age, alcohol use, Mucosa-associated lymphoid tissue hyperplasia reduction/regression and anti-parietal cell antibody and/or anti-intrinsic factor antibody positivity.

[2]Reference group. LGD: Low-grade dysplasia; *H. pylori*: *Helicobacter pylori*; OR: Odds ratio; BMI: Body mass index; MALT: Mucosa-associated lymphoid tissue; APCA: Anti-parietal cell antibody; AIF: Anti-intrinsic factor.

In our study, the histological signs of active gastritis and MALT hyperplasia disappeared or decreased in 100% and 96.5% of patients with or without PGC after *H. pylori* eradication, respectively. The overall prevalence of LGD on random biopsies at a 6-mo interval was similar (17.6% *vs* 10.6%). Nevertheless, among the patients with newly diagnosed LGD on visible lesions, the percentage of endoscopically missed dysplasia was 42.1% before *H. pylori* eradication, when active gastritis was present. Unexpectedly, at the baseline 26.3% of such patients (5/19) had an overlapping AAG with APCA and/or AIF positivity. This prevalence rose to 28.6% (8/28 patients) when we considered the total patients with dysplasia, and the percentage of this positivity did not change after *H. pylori* eradication (P = 1.0, data not shown). We observed an almost doubled prevalence of gastric LGD on biopsies performed randomly or on visible lesions before and after *H. pylori* disappearance (17.6% *vs* 32.9% respectively). A similar prevalence was found in another study from two referral centers using NBI endoscopy, in which dysplasia was detected in 28/85 (33%) and 38/85 *H. pylori* positive patients (45%)[37].

Patients with LGD were older and showed more advanced OLGA and OLGIM stages as compared to those without LGD, at baseline as well as after *H. pylori* eradication. The prevalence of OLGIM stages 3-4 showed a tendency to increase after *H. pylori* eradication only in patients with dysplasia, from 57.1% to 75%.

The higher prevalence of LGD after *H. pylori* eradication could depend on the presence of more severe and extensive mucosal atrophy and IM at baseline in our high-risk subgroup of patients rather than disease progression itself, considering the short interval of endoscopic surveillance of our study. In this scenario, the background of active *H. pylori* inflammation is likely to play a confounding role that may have hampered the accurate detection of gastric dysplasia. Nevertheless, the unexpected high baseline prevalence of dysplasia may be partially justified by the concomitant presence of AAG in a considerable number of our patients, in accordance with results from a recent study showing that in the presence of AAG the risk of developing more

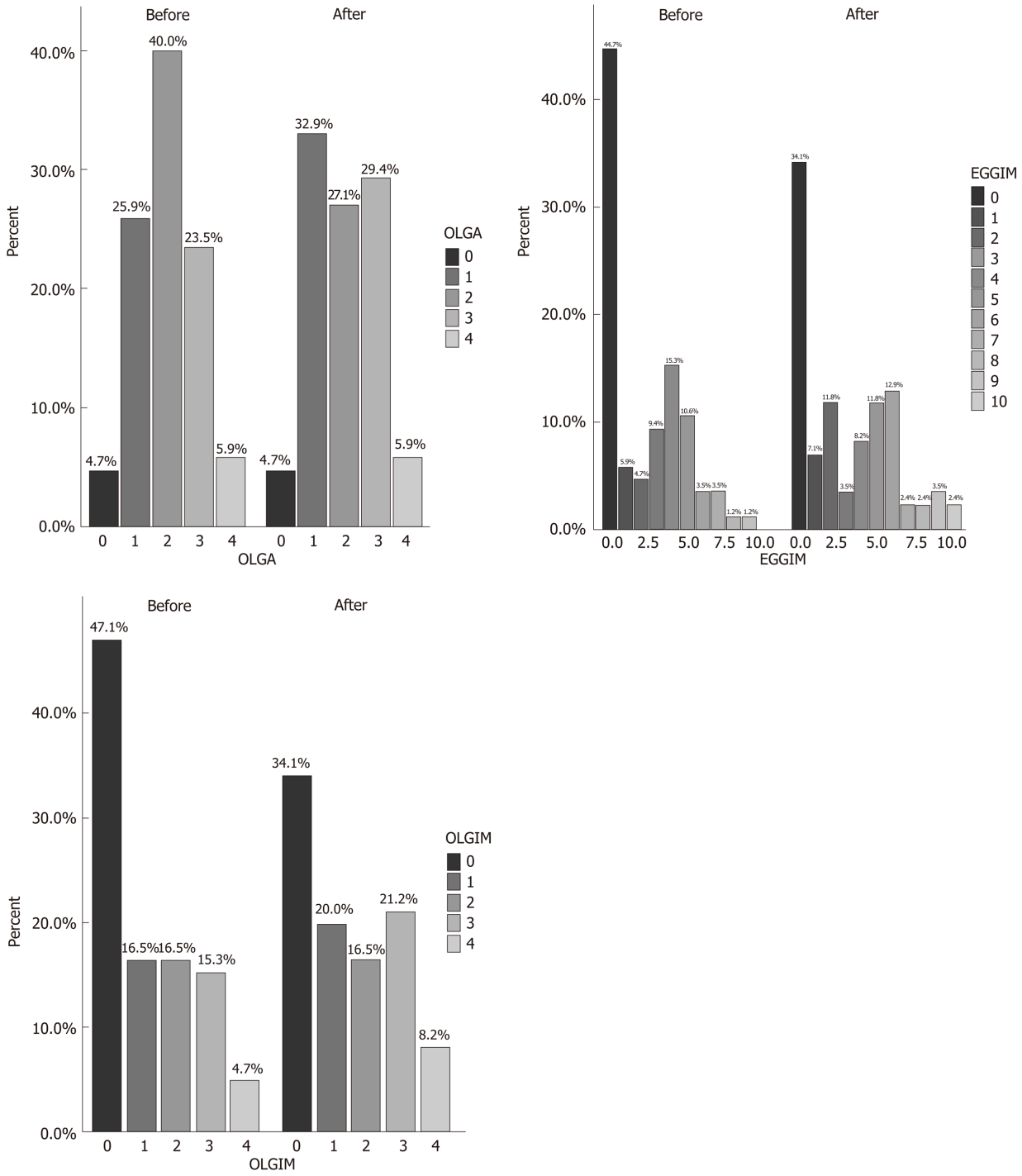

Figure 2 Prevalence of Operative Link on Gastritis Assessment, endoscopic grading of gastric intestinal metaplasia, and Operative Link on Gastric Intestinal Metaplasia scores, respectively in the 85 patients before and after *Helicobacter pylori* eradication. OLGA: Operative Link on Gastritis Assessment; EGGIM: Endoscopic grading of gastric intestinal metaplasia; OLGIM: Operative Link on Gastric Intestinal Metaplasia.

advanced stages on long-term follow-up is greater in patients with more severe gastric lesions[8]. The overlap between autoimmune and *H. pylori*-induced chronic gastritis may presumably be associated with a more severe gastric injury, especially in older subjects.

At a multivariate analysis, the probability for detecting gastric dysplasia after resolution of *H. pylori*-related active inflammation was significantly higher in older patients with regression or reduction of MALT hyperplasia, greater alcohol consumption, and APCA and/or AIF positivity. Therefore, MALT hyperplasia with active gastritis, whether induced or not by *H. pylori*, could be an additional confounding factor influencing the detection of PGC, and, particularly, LGD in high-risk patients (Table 4).

Figure 3 Gastric white-light endoscopy, narrow band imaging and histological evaluation before *Helicobacter pylori* eradication. A, B: Gastritis during white-light endoscopy and narrow band imaging assessment of corpus before *Helicobacter pylori* eradication; and C: Histological evaluation: moderately atrophic chronically active gastritis with lymphoplasmacellular infiltration of the lamina propria and foveolar epithelium hyperplasia (fundus before *Helicobacter pylori* eradication. Sections of 3 microns colored with Hematoxylin Eosin and Giemsa respectively. Magnifications: × 10).

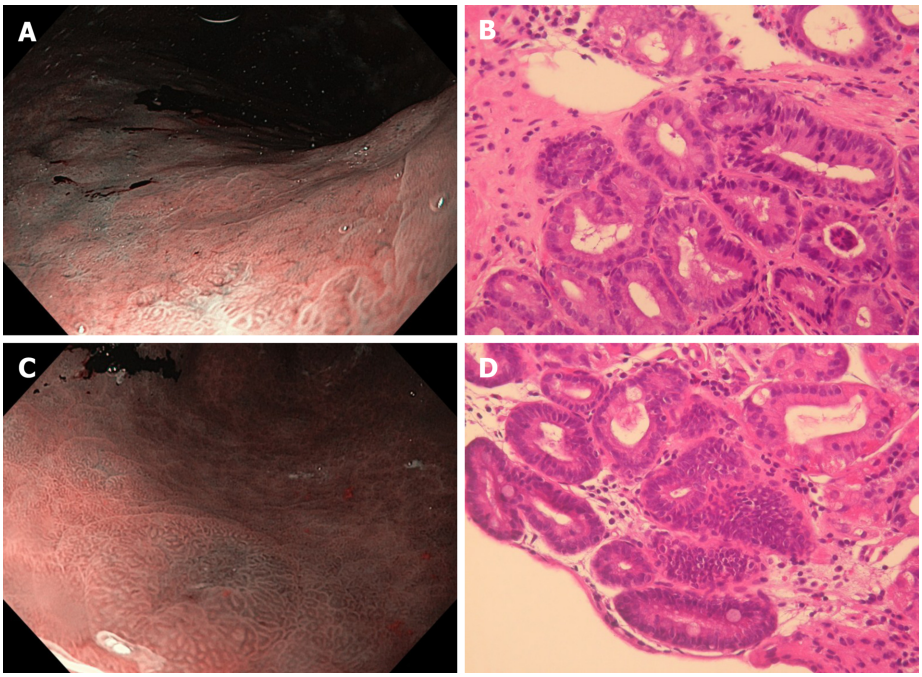

Figure 4 Gastric narrow band imaging and histological evaluation after *Helicobacter pylori* eradication. A: Low-grade dysplasia on flat lesion during narrow band imaging assessment of corpus after *Helicobacter pylori* eradication; B: Histological appearance: inactive chronically mild atrophic gastritis with intestinal metaplasia and low-grade dysplasia on intestinal metaplastic epithelium (fundus after *Helicobacter pylori* eradication); C: Low-grade dysplasia aspect of antrum on visible lesion during narrow band imaging assessment after *Helicobacter pylori* eradication; and D: Histological appearance: inactive chronically moderate atrophic gastritis with intestinal metaplasia and low-grade dysplasia on intestinal metaplastic epithelium (antrum after *Helicobacter pylori* eradication). Hematoxylin Eosin. Sections of 3 microns. Magnification: × 10.

The prevalence of autoimmune diseases (24.7%) in our patients showed a tendency to increase among patients with LGD (35.7% *vs* 17.5% in those without LGD, $P = 0.06$ by χ^2 test). Since autoimmune disorders are linked to the presence of DRB1 and DQB1 haplotypes our finding may suggest a reciprocal role between the genetics of immune response and *H. pylori* chronic infection.

Our results are in full accordance with the current European recommendations, which suggest to perform an endoscopic reassessment with HRE-NBI as soon as possible after dysplasia is diagnosed in the "apparent" absence of endoscopically visible lesions, to search for malignancy on misdiagnosed lesions[7,27,48]. Where the presence of *H. pylori* active gastritis without alarming features for malignancy is suspected, considering the present lack of clinical recommendations on the diagnosis and surveillance of PGC[7], our study suggests that the best diagnostic workout in symptomatic patients should entail performing prior *H. pylori* non-invasive tests, thus increasing the probability of detecting LGD on visible lesions at an endoscopy carried

out soon after *H. pylori* eradication has been achieved.

There are some limitations to our study. The sample size is relatively small, although all endoscopies were performed in a standardized way by using the same biopsy protocol and technical procedures and with the presence of the same endoscopist throughout the study. The hypothesis that LGD could have progressed into visible lesions is unlikely due to our short 6-mo follow-up interval[7]: The risk of PGC progression has indeed been demonstrated to increase only on long-term follow-up (2-16 years), after eradication of *H. pylori*[22-25,40]. Our results may help explain the heterogeneous findings of a possible increased PGC prevalence after *H. pylori* eradication in long-term surveillance studies, as this might be due to a misdiagnosis at initial endoscopic examination.

In conclusion, HR-WLE with NBI can be more accurate in diagnosing LGD on visible lesions after *H. pylori* eradication has been achieved, probably due to the disappearance of the underlying confounding effects of inflammatory and mucosal lymphoproliferative changes induced by *H. pylori* chronic active infection. Elderly patients and those with autoimmune diseases could be at higher risk for *H. pylori* chronic infection. An effective and cost-effective strategy to diagnose LGD with the highest accuracy should entail a high-quality upper endoscopy performed soon after eradication of *H. pylori* infection, detected by prior non-invasive tests.

ARTICLE HIGHLIGHTS

Research background

Helicobacter pylori (H. pylori) infection is frequently responsible for precancerous gastric conditions (PGC) and the long-term risk of PGC may even progress after *H. pylori* eradication.

Research motivation

Heterogeneous long-term endoscopic follow-up studies (2-16 years) have shown conflicting results on the efficacy of *H. pylori* eradication in reducing the prevalence and histological progression of advanced PGC. Moreover, High-Resolution White-Light Endoscopy (HR-WLE) in combination with narrow-band imaging (NBI) is effective in detecting PGC and determines the timing and mode of endoscopic surveillance.

Research objectives

To assess the efficacy of HR-WLE with NBI in detecting PGC, before and after *H. pylori* eradication at a short-term interval.

Research methods

We evaluated 85 consecutive patients with *H. pylori*-related gastritis with/without PGC at baseline and 6 mo after proven *H. pylori* eradication. The Operative-Link on Gastritis-Assessment and Operative-Link on Gastric-Intestinal Metaplasia have been used as gold standards for histological definition of gastritis, atrophy and intestinal metaplasia. Serum anti-parietal cell antibody and anti-intrinsic factor were measured when autoimmune atrophic gastritis was suspected.

Research results

HR-WLE in combination with NBI allows for a more accurate diagnosis of gastric low-grade dysplasia (LGD) when performed soon after *H. pylori* eradication, due to regression of *H. pylori*-induced signs of inflammation. Furthermore, we observed an unexpected high prevalence of autoimmune disorders, suggesting an interaction between the genetics of immune response and *H. pylori* chronic infection, especially in relation to the risk of LGD development.

Research conclusions

HR-WLE with NBI allows an accurate diagnosis of gastric LGD on visible lesions after regression of *H. pylori*-induced signs of active infection, especially in high-risk subjects. Patients with overlap between autoimmune and *H. pylori*-induced chronic gastritis may require more extensive gastric mapping.

Research perspectives

Our findings will appeal to both clinical gastroenterologists and endoscopists, and stimulate the development of more accurate and cost-effective strategies for identifying patients with *H. pylori* infection who are at risk of gastric cancer. Subjects with an overlap between autoimmune and *H. pylori*-induced chronic gastritis should be considered to be at a higher risk of more severe gastric injury.

REFERENCES

1 **Correa P**. Human gastric carcinogenesis: a multistep and multifactorial process--First American Cancer Society Award Lecture on Cancer Epidemiology and Prevention. *Cancer Res* 1992; **52**: 6735-6740 [PMID: 1458460]

2 **Correa P**, Haenszel W, Cuello C, Tannenbaum S, Archer M. A model for gastric cancer epidemiology. *Lancet* 1975; **2**: 58-60 [PMID: 49653 DOI: 10.1016/s0140-6736(75)90498-5]

3 **Mera RM**, Bravo LE, Camargo MC, Bravo JC, Delgado AG, Romero-Gallo J, Yepez MC, Realpe JL, Schneider BG, Morgan DR, Peek RM Jr, Correa P, Wilson KT, Piazuelo MB. Dynamics of *Helicobacter pylori* infection as a determinant of progression of gastric precancerous lesions: 16-year follow-up of an eradication trial. *Gut* 2018; **67**: 1239-1246 [PMID: 28647684 DOI: 10.1136/gutjnl-2016-311685]

4 **Ihamäki T**, Saukkonen M, Siurala M. Long-term observation of subjects with normal mucosa and with superficial gastritis: results of 23--27 years' follow-up examinations. *Scand J Gastroenterol* 1978; **13**: 771-775 [PMID: 725497 DOI: 10.3109/00365527809182189]

5 **Carneiro F**, Machado JC, David L, Reis C, Nogueira AM, Sobrinho-Simões M. Current thoughts on the histopathogenesis of gastric cancer. *Eur J Cancer Prev* 2001; **10**: 101-102 [PMID: 11263582 DOI: 10.1097/00008469-200102000-00013]

6 **de Vries AC**, van Grieken NC, Looman CW, Casparie MK, de Vries E, Meijer GA, Kuipers EJ. Gastric cancer risk in patients with premalignant gastric lesions: a nationwide cohort study in the Netherlands. *Gastroenterology* 2008; **134**: 945-952 [PMID: 18395075 DOI: 10.1053/j.gastro.2008.01.071]

7 **Pimentel-Nunes P**, Libânio D, Marcos-Pinto R, Areia M, Leja M, Esposito G, Garrido M, Kikuste I, Megraud F, Matysiak-Budnik T, Annibale B, Dumonceau JM, Barros R, Fléjou JF, Carneiro F, van Hooft JE, Kuipers EJ, Dinis-Ribeiro M. Management of epithelial precancerous conditions and lesions in the stomach (MAPS II): European Society of Gastrointestinal Endoscopy (ESGE), European Helicobacter and Microbiota Study Group (EHMSG), European Society of Pathology (ESP), and Sociedade Portuguesa de Endoscopia Digestiva (SPED) guideline update 2019. *Endoscopy* 2019; **51**: 365-388 [PMID: 30841008 DOI: 10.1055/a-0859-1883]

8 **Miceli E**, Vanoli A, Lenti MV, Klersy C, Di Stefano M, Luinetti O, Caccia Dominioni C, Pisati M, Staiani M, Gentile A, Capuano F, Arpa G, Paulli M, Corazza GR, Di Sabatino A. Natural history of autoimmune atrophic gastritis: a prospective, single centre, long-term experience. *Aliment Pharmacol Ther* 2019; **50**: 1172-1180 [PMID: 31621927 DOI: 10.1111/apt.15540]

9 **Wang P**, Xia HH, Zhang JY, Dai LP, Xu XQ, Wang KJ. Association of interleukin-1 gene polymorphisms with gastric cancer: a meta-analysis. *Int J Cancer* 2007; **120**: 552-562 [PMID: 17096351 DOI: 10.1002/ijc.22353]

10 **Camargo MC**, Mera R, Correa P, Peek RM Jr, Fontham ET, Goodman KJ, Piazuelo MB, Sicinschi L, Zabaleta J, Schneider BG. Interleukin-1beta and interleukin-1 receptor antagonist gene polymorphisms and gastric cancer: a meta-analysis. *Cancer Epidemiol Biomarkers Prev* 2006; **15**: 1674-1687 [PMID: 16985030 DOI: 10.1158/1055-9965.EPI-06-0189]

11 **Hnatyszyn A**, Wielgus K, Kaczmarek-Rys M, Skrzypczak-Zielinska M, Szalata M, Mikolajczyk-Stecyna J, Stanczyk J, Dziuba I, Mikstacki A, Slomski R. Interleukin-1 gene polymorphisms in chronic gastritis patients infected with Helicobacter pylori as risk factors of gastric cancer development. *Arch Immunol Ther Exp (Warsz)* 2013; **61**: 503-512 [PMID: 23995914 DOI: 10.1007/s00005-013-0245-y]

12 **Xue H**, Lin B, Ni P, Xu H, Huang G. Interleukin-1B and interleukin-1 RN polymorphisms and gastric carcinoma risk: a meta-analysis. *J Gastroenterol Hepatol* 2010; **25**: 1604-1617 [PMID: 20880168 DOI: 10.1111/j.1440-1746.2010.06428.x]

13 **Loh M**, Koh KX, Yeo BH, Song CM, Chia KS, Zhu F, Yeoh KG, Hill J, Iacopetta B, Soong R. Meta-analysis of genetic polymorphisms and gastric cancer risk: variability in associations according to race. *Eur J Cancer* 2009; **45**: 2562-2568 [PMID: 19375306 DOI: 10.1016/j.ejca.2009.03.017]

14 **Figueiredo C**, Machado JC, Pharoah P, Seruca R, Sousa S, Carvalho R, Capelinha AF, Quint W, Caldas C, van Doorn LJ, Carneiro F, Sobrinho-Simões M. Helicobacter pylori and interleukin 1 genotyping: an opportunity to identify high-risk individuals for gastric carcinoma. *J Natl Cancer Inst* 2002; **94**: 1680-1687 [PMID: 12441323 DOI: 10.1093/jnci/94.22.1680]

15 **Amieva MR**, El-Omar EM. Host-bacterial interactions in Helicobacter pylori infection. *Gastroenterology* 2008; **134**: 306-323 [PMID: 18166359 DOI: 10.1053/j.gastro.2007.11.009]

16 **Machado JC**, Figueiredo C, Canedo P, Pharoah P, Carvalho R, Nabais S, Castro Alves C, Campos ML, Van Doorn LJ, Caldas C, Seruca R, Carneiro F, Sobrinho-Simões M. A proinflammatory genetic profile increases the risk for chronic atrophic gastritis and gastric carcinoma. *Gastroenterology* 2003; **125**: 364-371 [PMID: 12891537 DOI: 10.1016/s0016-5085(03)00899-0]

17 **Huang JQ**, Zheng GF, Sumanac K, Irvine EJ, Hunt RH. Meta-analysis of the relationship between cagA seropositivity and gastric cancer. *Gastroenterology* 2003; **125**: 1636-1644 [PMID: 14724815 DOI: 10.1053/j.gastro.2003.08.033]

18 **Palli D**, Masala G, Del Giudice G, Plebani M, Basso D, Berti D, Numans ME, Ceroti M, Peeters PH, Bueno de Mesquita HB, Buchner FL, Clavel-Chapelon F, Boutron-Ruault MC, Krogh V, Saieva C, Vineis P, Panico S, Tumino R, Nyrén O, Simán H, Berglund G, Hallmans G, Sanchez MJ, Larrãnaga N, Barricarte A,

Navarro C, Quiros JR, Key T, Allen N, Bingham S, Khaw KT, Boeing H, Weikert C, Linseisen J, Nagel G, Overvad K, Thomsen RW, Tjonneland A, Olsen A, Trichoupoulou A, Trichopoulos D, Arvaniti A, Pera G, Kaaks R, Jenab M, Ferrari P, Nesi G, Carneiro F, Riboli E, Gonzalez CA. CagA+ Helicobacter pylori infection and gastric cancer risk in the EPIC-EURGAST study. *Int J Cancer* 2007; **120**: 859-867 [PMID: 17131317 DOI: 10.1002/ijc.22435]

19 **Basso D**, Zambon CF, Letley DP, Stranges A, Marchet A, Rhead JL, Schiavon S, Guariso G, Ceroti M, Nitti D, Rugge M, Plebani M, Atherton JC. Clinical relevance of Helicobacter pylori cagA and vacA gene polymorphisms. *Gastroenterology* 2008; **135**: 91-99 [PMID: 18474244 DOI: 10.1053/j.gastro.2008.03.041]

20 **Rizzato C**, Kato I, Plummer M, Muñoz N, Stein A, Jan van Doorn L, Franceschi S, Canzian F. Risk of advanced gastric precancerous lesions in Helicobacter pylori infected subjects is influenced by ABO blood group and cagA status. *Int J Cancer* 2013; **133**: 315-322 [PMID: 23319424 DOI: 10.1002/ijc.28019]

21 **Lee YC**, Chen TH, Chiu HM, Shun CT, Chiang H, Liu TY, Wu MS, Lin JT. The benefit of mass eradication of Helicobacter pylori infection: a community-based study of gastric cancer prevention. *Gut* 2013; **62**: 676-682 [PMID: 22698649 DOI: 10.1136/gutjnl-2012-302240]

22 **Leung WK**, Lin SR, Ching JY, To KF, Ng EK, Chan FK, Lau JY, Sung JJ. Factors predicting progression of gastric intestinal metaplasia: results of a randomised trial on Helicobacter pylori eradication. *Gut* 2004; **53**: 1244-1249 [PMID: 15306578 DOI: 10.1136/gut.2003.034629]

23 **You WC**, Brown LM, Zhang L, Li JY, Jin ML, Chang YS, Ma JL, Pan KF, Liu WD, Hu Y, Crystal-Mansour S, Pee D, Blot WJ, Fraumeni JF Jr, Xu GW, Gail MH. Randomized double-blind factorial trial of three treatments to reduce the prevalence of precancerous gastric lesions. *J Natl Cancer Inst* 2006; **98**: 974-983 [PMID: 16849680 DOI: 10.1093/jnci/djj264]

24 **Wong BC**, Lam SK, Wong WM, Chen JS, Zheng TT, Feng RE, Lai KC, Hu WH, Yuen ST, Leung SY, Fong DY, Ho J, Ching CK, Chen JS; China Gastric Cancer Study Group. Helicobacter pylori eradication to prevent gastric cancer in a high-risk region of China: a randomized controlled trial. *JAMA* 2004; **291**: 187-194 [PMID: 14722144 DOI: 10.1001/jama.291.2.187]

25 **Chen HN**, Wang Z, Li X, Zhou ZG. Helicobacter pylori eradication cannot reduce the risk of gastric cancer in patients with intestinal metaplasia and dysplasia: evidence from a meta-analysis. *Gastric Cancer* 2016; **19**: 166-175 [PMID: 25609452 DOI: 10.1007/s10120-015-0462-7]

26 **Chey WD**, Wong BC; Practice Parameters Committee of the American College of Gastroenterology. American College of Gastroenterology guideline on the management of Helicobacter pylori infection. *Am J Gastroenterol* 2007; **102**: 1808-1825 [PMID: 17608775 DOI: 10.1111/j.1572-0241.2007.01393.x]

27 **Malfertheiner P**, Megraud F, O'Morain CA, Gisbert JP, Kuipers EJ, Axon AT, Bazzoli F, Gasbarrini A, Atherton J, Graham DY, Hunt R, Moayyedi P, Rokkas T, Rugge M, Selgrad M, Suerbaum S, Sugano K, El-Omar EM; European Helicobacter and Microbiota Study Group and Consensus panel. Management of Helicobacter pylori infection-the Maastricht V/Florence Consensus Report. *Gut* 2017; **66**: 6-30 [PMID: 27707777 DOI: 10.1136/gutjnl-2016-312288]

28 **Dinis-Ribeiro M**, Areia M, de Vries AC, Marcos-Pinto R, Monteiro-Soares M, O'Connor A, Pereira C, Pimentel-Nunes P, Correia R, Ensari A, Dumonceau JM, Machado JC, Macedo G, Malfertheiner P, Matysiak-Budnik T, Megraud F, Miki K, O'Morain C, Peek RM, Ponchon T, Ristimaki A, Rembacken B, Carneiro F, Kuipers EJ; European Society of Gastrointestinal Endoscopy; European Helicobacter Study Group; European Society of Pathology; Sociedade Portuguesa de Endoscopia Digestiva. Management of precancerous conditions and lesions in the stomach (MAPS): guideline from the European Society of Gastrointestinal Endoscopy (ESGE), European Helicobacter Study Group (EHSG), European Society of Pathology (ESP), and the Sociedade Portuguesa de Endoscopia Digestiva (SPED). *Endoscopy* 2012; **44**: 74-94 [PMID: 22198778 DOI: 10.1055/s-0031-1291491]

29 **Pimentel-Nunes P**, Libânio D, Lage J, Abrantes D, Coimbra M, Esposito G, Hormozdi D, Pepper M, Drasovean S, White JR, Dobru D, Buxbaum J, Ragunath K, Annibale B, Dinis-Ribeiro M. A multicenter prospective study of the real-time use of narrow-band imaging in the diagnosis of premalignant gastric conditions and lesions. *Endoscopy* 2016; **48**: 723-730 [PMID: 27280384 DOI: 10.1055/s-0042-108435]

30 **Dixon MF**, Genta RM, Yardley JH, Correa P. Classification and grading of gastritis. The updated Sydney System. International Workshop on the Histopathology of Gastritis, Houston 1994. *Am J Surg Pathol* 1996; **20**: 1161-1181 [PMID: 8827022 DOI: 10.1097/00000478-199610000-00001]

31 **Lahner E**, Zagari RM, Zullo A, Di Sabatino A, Meggio A, Cesaro P, Lenti MV, Annibale B, Corazza GR. Chronic atrophic gastritis: Natural history, diagnosis and therapeutic management. A position paper by the Italian Society of Hospital Gastroenterologists and Digestive Endoscopists [AIGO], the Italian Society of Digestive Endoscopy [SIED], the Italian Society of Gastroenterology [SIGE], and the Italian Society of Internal Medicine [SIMI]. *Dig Liver Dis* 2019; **51**: 1621-1632 [PMID: 31635944 DOI: 10.1016/j.dld.2019.09.016]

32 **Kimura K**, Takemoto T. An Endoscopic Recognition of the Atrophic Border and its Significance in Chronic Gastritis. *Endoscopy* 1969; **1**: 87-97 [DOI: 10.1055/s-0028-1098086]

33 **Capelle LG**, Haringsma J, de Vries AC, Steyerberg EW, Biermann K, van Dekken H, Kuipers EJ. Narrow band imaging for the detection of gastric intestinal metaplasia and dysplasia during surveillance endoscopy. *Dig Dis Sci* 2010; **55**: 3442-3448 [PMID: 20393882 DOI: 10.1007/s10620-010-1189-2]

34 **Panteris V**, Nikolopoulou S, Lountou A, Triantafillidis JK. Diagnostic capabilities of high-definition white light endoscopy for the diagnosis of gastric intestinal metaplasia and correlation with histologic and clinical data. *Eur J Gastroenterol Hepatol* 2014; **26**: 594-601 [PMID: 24743505 DOI: 10.1097/MEG.0000000000000097]

35 **Ezoe Y**, Muto M, Uedo N, Doyama H, Yao K, Oda I, Kaneko K, Kawahara Y, Yokoi C, Sugiura Y, Ishikawa H, Takeuchi Y, Kaneko Y, Saito Y. Magnifying narrowband imaging is more accurate than conventional white-light imaging in diagnosis of gastric mucosal cancer. *Gastroenterology* 2011; **141**: 2017-2025.e3 [PMID: 21856268 DOI: 10.1053/j.gastro.2011.08.007]

36 **Ang TL**, Pittayanon R, Lau JY, Rerknimitr R, Ho SH, Singh R, Kwek AB, Ang DS, Chiu PW, Luk S, Goh KL, Ong JP, Tan JY, Teo EK, Fock KM. A multicenter randomized comparison between high-definition white light endoscopy and narrow band imaging for detection of gastric lesions. *Eur J Gastroenterol*

Hepatol 2015; **27**: 1473-1478 [PMID: 26426836 DOI: 10.1097/MEG.0000000000000478]
37 **Pimentel-Nunes P**, Dinis-Ribeiro M, Soares JB, Marcos-Pinto R, Santos C, Rolanda C, Bastos RP, Areia M, Afonso L, Bergman J, Sharma P, Gotoda T, Henrique R, Moreira-Dias L. A multicenter validation of an endoscopic classification with narrow band imaging for gastric precancerous and cancerous lesions. *Endoscopy* 2012; **44**: 236-246 [PMID: 22294194 DOI: 10.1055/s-0031-1291537]
38 **Panarese A**, Shahini E, Pesce F, Caruso ML. Detection of lesions in Helicobacter Pylori gastritis before and after eradication by expert endoscopists. *UEG J* 2018; **6**: A734
39 **Yue H**, Shan L, Bin L. The significance of OLGA and OLGIM staging systems in the risk assessment of gastric cancer: a systematic review and meta-analysis. *Gastric Cancer* 2018; **21**: 579-587 [PMID: 29460004 DOI: 10.1007/s10120-018-0812-3]
40 **Kapadia CR**. Gastric atrophy, metaplasia, and dysplasia: a clinical perspective. *J Clin Gastroenterol* 2003; **36**: S29-36; discussion S61-2 [PMID: 12702963 DOI: 10.1097/00004836-200305001-00006]
41 **Carpenter HA**, Talley NJ. Gastroscopy is incomplete without biopsy: clinical relevance of distinguishing gastropathy from gastritis. *Gastroenterology* 1995; **108**: 917-924 [PMID: 7875496 DOI: 10.1016/0016-5085(95)90468-9]
42 **Redéen S**, Petersson F, Jönsson KA, Borch K. Relationship of gastroscopic features to histological findings in gastritis and Helicobacter pylori infection in a general population sample. *Endoscopy* 2003; **35**: 946-950 [PMID: 14606018 DOI: 10.1055/s-2003-43479]
43 **Eshmuratov A**, Nah JC, Kim N, Lee HS, Lee HE, Lee BH, Uhm MS, Park YS, Lee DH, Jung HC, Song IS. The correlation of endoscopic and histological diagnosis of gastric atrophy. *Dig Dis Sci* 2010; **55**: 1364-1375 [PMID: 19629687 DOI: 10.1007/s10620-009-0891-4]
44 **Buxbaum JL**, Hormozdi D, Dinis-Ribeiro M, Lane C, Dias-Silva D, Sahakian A, Jayaram P, Pimentel-Nunes P, Shue D, Pepper M, Cho D, Laine L. Narrow-band imaging versus white light versus mapping biopsy for gastric intestinal metaplasia: a prospective blinded trial. *Gastrointest Endosc* 2017; **86**: 857-865 [PMID: 28366441 DOI: 10.1016/j.gie.2017.03.1528]
45 **Areia M**, Amaro P, Dinis-Ribeiro M, Cipriano MA, Marinho C, Costa-Pereira A, Lopes C, Moreira-Dias L, Romãozinho JM, Gouveia H, Freitas D, Leitão MC. External validation of a classification for methylene blue magnification chromoendoscopy in premalignant gastric lesions. *Gastrointest Endosc* 2008; **67**: 1011-1018 [PMID: 18178207 DOI: 10.1016/j.gie.2007.08.044]
46 **Tanaka K**, Toyoda H, Kadowaki S, Hamada Y, Kosaka R, Matsuzaki S, Shiraishi T, Imoto I, Takei Y. Surface pattern classification by enhanced-magnification endoscopy for identifying early gastric cancers. *Gastrointest Endosc* 2008; **67**: 430-437 [PMID: 18294504 DOI: 10.1016/j.gie.2007.10.042]
47 **Zhao Z**, Yin Z, Wang S, Wang J, Bai B, Qiu Z, Zhao Q. Meta-analysis: The diagnostic efficacy of chromoendoscopy for early gastric cancer and premalignant gastric lesions. *J Gastroenterol Hepatol* 2016; **31**: 1539-1545 [PMID: 26860924 DOI: 10.1111/jgh.13313]
48 **Lim H**, Jung HY, Park YS, Na HK, Ahn JY, Choi JY, Lee JH, Kim MY, Choi KS, Kim DH, Choi KD, Song HJ, Lee GH, Kim JH. Discrepancy between endoscopic forceps biopsy and endoscopic resection in gastric epithelial neoplasia. *Surg Endosc* 2014; **28**: 1256-1262 [PMID: 24310738 DOI: 10.1007/s00464-013-3316-6]

Published by **Baishideng Publishing Group Inc**
7041 Koll Center Parkway, Suite 160, Pleasanton, CA 94566, USA
Telephone: +1-925-3991568
E-mail: bpgoffice@wjgnet.com
Help Desk: https://www.f6publishing.com/helpdesk
https://www.wjgnet.com